

**Optimisation of the Hoechst 33342 Dye
Efflux Assay for Small Cell Number
Microarray Profiling of the Prostate**

A thesis submitted to

The University of Manchester

for the degree of Doctor of Medicine MD

in the

Faculty of Medical and Human Sciences

2009

Benjamin R. Grey

School of Medicine

ProQuest Number: 10997047

All rights reserved

INFORMATION TO ALL USERS

The quality of this reproduction is dependent upon the quality of the copy submitted.

In the unlikely event that the author did not send a complete manuscript and there are missing pages, these will be noted. Also, if material had to be removed, a note will indicate the deletion.



ProQuest 10997047

Published by ProQuest LLC (2018). Copyright of the Dissertation is held by the Author.

All rights reserved.

This work is protected against unauthorized copying under Title 17, United States Code
Microform Edition © ProQuest LLC.

ProQuest LLC.
789 East Eisenhower Parkway
P.O. Box 1346
Ann Arbor, MI 48106 – 1346

(EURQ9)

✕
Th32609

- THE
JOHN RYLANDS
UNIVERSITY
LIBRARY

List of Contents

Chapter 1	Introduction	Page
1.1	The Prostate	45
1.1.1	General Morphology	45
1.1.2	Anatomical Relations	45
1.1.3	Anatomical Structure	46
1.1.4	Vascular Supply	50
1.1.4.1	Arterial Supply	50
1.1.4.2	Venous Drainage	52
1.1.5	Lymphatic Drainage	52
1.1.6	Nerve Supply	53
1.1.7	Histology	53
1.1.8	Embryology	54
1.1.9	Physiology	55
1.2	Carcinoma of the Prostate	56
1.2.1	Epidemiology	56
1.2.1.1	United Kingdom	56
1.2.1.2	United States of America	59
1.2.1.3	Worldwide	59
1.2.1.4	Effect of Prostate Specific Antigen on Epidemiology	60
1.2.2	Demographics	61
1.2.3	Aetiology	62
1.2.3.1	Familial / Hereditary	63

1.2.3.2	Androgens	63
1.2.3.3	Genetic Polymorphisms	64
1.2.3.4	Vitamin D	64
1.2.3.5	Insulin-like Growth Factor	65
1.2.3.6	Diet	65
1.2.3.6.1	Fat	65
1.2.3.6.2	Calcium	66
1.2.3.6.3	Lycopene	66
1.2.3.6.4	Selenium	67
1.2.3.6.5	Vitamin E	67
1.2.3.6.6	Vasectomy	68
1.2.3.6.7	Sexual Activity	68
1.2.3.6.8	Smoking	69
1.2.3.6.9	Alcohol Consumption	69
1.2.3.6.10	Height	69
1.2.3.6.11	Weight	69
1.2.3.6.12	Occupation	70
1.2.4	Natural History	70
1.2.5	Pathology	73
1.2.5.1	Adenocarcinoma	73
1.2.5.2	Prostatic Intraepithelial Neoplasia	75
1.2.5.3	Histological Grading	76
1.2.5.4	Staging of Disease	79
1.2.6	Clinical Features and Diagnosis	79
1.2.6.1	Symptoms and Signs	79

1.2.6.2	Mode of Presentation	81
1.2.6.3	Screening for Prostate Cancer	81
1.2.6.4	Diagnosis	83
1.2.6.4.1	Prostate Specific Antigen	84
1.2.6.4.2	Prostate Specific Antigen Threshold	85
1.2.6.4.3	Prostate Specific Antigen Density	86
1.2.6.4.4	Prostate Specific Antigen Velocity	87
1.2.6.4.5	Free: Complexed Prostate Specific Antigen Ratio	88
1.2.6.4.6	Digital Rectal Examination	88
1.2.6.4.7	Needle Core Biopsy	89
1.2.6.4.8	Radiological Imaging	89
1.2.7	Prostate Cancer Treatment	90
1.2.7.1	Active Surveillance	90
1.2.7.1.1	Active Surveillance in Localised Prostate Cancer (T1-T2, Nx-N0, M0)	91
1.2.7.1.2	Active Surveillance in Locally Advanced Prostate Cancer (T3-T4, Nx-N0, M0)	92
1.2.7.1.3	Active Surveillance in Metastatic Prostate Cancer (M1)	93
1.2.7.2	Radical Prostatectomy	93
1.2.7.2.1	Radical Prostatectomy in Stage T1a-T1b Prostate Cancer	94
1.2.7.2.2	Radical Prostatectomy in Stage T1c Prostate Cancer	94

1.2.7.2.3	Radical Prostatectomy in Stage T2 Prostate Cancer	95
1.2.7.2.4	Radical Prostatectomy in Stage T3 Prostate Cancer	95
1.2.7.2.5	Nodal Disease	96
1.2.7.2.6	Radical Prostatectomy Complications and Functional Outcome	97
1.2.7.3	Definitive Radiotherapy	98
1.2.7.3.1	External Beam Radiotherapy in Localised Prostate Cancer (T1-T2c, N0 M0)	98
1.2.7.3.2	New techniques in Radiotherapy Administration	100
1.2.7.3.3	Brachytherapy	100
1.2.7.3.4	Toxicity	101
1.2.7.3.5	Immediate versus Delayed Postoperative Radiotherapy for Pathological T3 N0 M0	102
1.2.7.4	Experimental Treatments in Prostate Cancer	103
1.2.7.4.1	Cryosurgery of the Prostate	103
1.2.7.4.2	High-Intensity Focused Ultrasound of the Prostate	104
1.2.7.5	Hormone Manipulation Therapy	105
1.2.7.5.1	Bilateral Subcapsular Orchiectomy	106
1.2.7.5.2	Oestrogens	106

1.2.7.5.3	Luteinizing Hormone-Releasing Hormone Agonists	107
1.2.7.5.4	Luteinizing Hormone-Releasing Hormone Antagonists	107
1.2.7.5.5	Antiandrogens	108
1.2.7.5.6	Outcome	109
1.2.7.5.7	Chemotherapy	109
1.3	The Stem Cell	109
1.3.1	General	109
1.3.2	Definition of the Stem Cell	110
1.3.3	Cancer Stem Cells and the Cancer Stem Cell Theory of Cancer	113
1.3.4	The Stem Cell Niche	114
1.3.5	Cell Division and the Cell Cycle	115
1.3.6	Evidence for Adult Stem and Cancer Stem Cells	117
1.3.6.1	Non-Epithelial Stem Cells	117
1.3.6.1.1	Haemopoietic Stem Cells	118
1.3.6.1.2	Haemopoietic Cancer Stem Cells	119
1.3.6.1.3	Central Nervous System Stem Cells	121
1.3.6.1.4	Central Nervous System Cancer Stem Cells	123
1.3.6.2	Epithelial Stem Cells	125
1.3.6.2.1	Breast Stem Cells	126
1.3.6.2.2	Breast Cancer Stem Cells	127

1.3.6.2.3	Epidermal Stem Cells	128
1.3.6.2.4	Gastro-Intestinal Stem Cells	129
1.3.7	Prostate Stem Cells	131
1.3.7.1	Normal Prostate Morphology and Physiology	131
1.3.7.2	Rationale for the Cancer Stem Cell Theory in the Prostate	132
1.3.7.3	Experimental Evidence for the Prostate Stem Cell	134
1.3.7.3.1	Differential Androgen Sensitivity of Basal and Luminal Epithelia	134
1.3.7.3.2	Cytokeratin Expression	135
1.3.7.3.3	Histological Location of the Stem Cell Niche	138
1.3.7.3.4	Clonogenic Sphere Formation	138
1.3.7.4	Methods Used in the Isolation of Putative Stem Cell Populations from the Prostate	140
1.3.7.4.1	Putative Prostate Stem Cell Surface Markers	140
1.3.7.4.1.1	CD44 ^{+ve} / $\alpha 2\beta 1^{\text{hi}}$ Phenotype Selection	140
1.3.7.4.1.2	CD133 Enrichment of CD44 ^{+ve} / $\alpha 2\beta 1^{\text{hi}}$ Phenotype	141
1.3.7.4.2	CSC Surface Markers	142
1.3.7.4.2.1	CD44 ^{+ve} Cell Selection	142

1.3.7.4.2.2	CD133 Selection and the Putative Prostate CSC	143
1.3.7.4.3	Side population Analysis	144
1.3.8	Summary of Experimental Evidence for Prostate Stem Cells	150
1.3.9	Epithelial Stem Cell Regulation	151
1.3.9.1	Integrins	151
1.3.9.2	Notch Signalling	152
1.3.9.3	Hedgehog Signaling	153
1.3.9.4	The Wnt Pathway, Beta Catenin and c-Myc	153
1.3.9.5	The Cyclin Dependent Kinase Inhibitors p21 ^{WAF/Cip1} and p27 ^{Kip1}	155
1.3.9.6	Musashi-1	156
1.3.9.7	TGF- β	157
1.3.9.8	CD133	158
1.3.9.9	PTEN	160
1.3.9.10	p63	160
1.3.9.11	Steroids	161
1.3.9.12	Non-Steroidal Factors	161
1.4	Molecular Biology Techniques	162
1.4.1	Principles of Gene Expression Analysis	162
1.4.2	Affymetrix [®] GeneChip [®] Technology	165

1.4.3	Gene Expression Analysis	167
1.4.4	Microarray Analysis of the Prostate	169
1.4.5	Microarray Analysis of Putative Stem and Cancer Stem Cell Populations in the Prostate	170
1.4.6	Microarray Analysis of Side Populations	172
1.4.7	Experimental Limitations to the Study of Prostate Microarrays	173
1.5	Clinical Challenges Posed by Prostate Cancer	174
1.6	Aims of Research	176
1.6.1	General Aims	176
1.6.2	Specific Aims	176
1.7	Rationale for Aims	177
Chapter 2	Materials and Methods	179
2.1	Materials	179
2.1.1	General Materials	179
2.1.2	Antibodies for Hoechst 33342 Dye Efflux Assay	179
2.1.3	Adjuncts to the RNase-Free Hoechst 33342 Dye Efflux Assay	180
2.1.4	Antibodies for Immunocytochemistry	180
2.1.5	Flow Cytometry Equipment	181
2.2	Media Recipes	184
2.2.1	Growth Media	184

2.2.2	PC-3 Media	184
2.2.3	STO Media	185
2.3	Buffers	185
2.3.1	Wash Buffer	185
2.3.2	Optiprep	185
2.4	Cell Lines	186
2.5	Processing of Primary Prostate Specimens	187
2.6	Standard Hoechst 33342 Dye Efflux Assay for Isolation of the CD133^{+ve}/CD45^{-ve} Side Population	189
2.7	Fluorescent-Activated Cell Sorting (FACS) Analysis of the CD133^{+ve}/CD45^{-ve} Hoechst 33342 Dye Efflux Assay	193
2.8	Adaptation of the Hoechst 33342 Dye Efflux Assay to Minimise the Effects of RNases	195
2.9	Modification of the Hoechst 33342 Dye Efflux Assay to Enable Analysis of the Subfractionated Side Population	196

2.10	Determination of the Relative CD133 Staining of BPH Epithelial Cells with PE-Cy5 and PE-Cy7 Secondary Conjugate Antibodies	201
2.11	Determination of the Functional and Phenotypic Characteristics of the Prostate Epithelial Cell Subpopulations	204
2.11.1	Primary Monolayer Cell Culture and Colony-Forming Ability	24
2.11.2	Microscopy - Entire Flask Image Capture	205
2.11.3	Protocol for Repeat Flow Cytometric Analysis of Cultured Cells	206
2.11.4	Immunocytochemistry	210
2.11.4.1	Citric Acid Buffer Manufacture	210
2.11.4.2	Slide Preparation, Cell Fixation, Permeabilisation and Antigen Retrieval	210
2.11.4.3	Antibody Staining	211
2.11.4.4	Staining Optimisation Pilot	213
2.11.4.5	Microscopy - Immunocytochemical Image Capture	213
2.12	Epistem Ltd Small Cell Number Affymetrix® Microarray Study	215

2.12.1	Epistem Ltd Protocol for Sample Processing, RNA Isolation, cDNA Manufacture, Labelling and Affymetrix® Microarray Hybridisation	215
2.12.2	Affymetrix® GeneChip® Microarray Data Analysis	217
2.12.3	Identification of Probesets for Validation by Real-Time PCR	217
2.13	Revised Small Cell Number Affymetrix® Microarray Protocol	218
2.13.1	RNA Extraction Protocol	218
2.13.2	Assessment of RNA Purity	221
2.13.2.1	Assessment of RNA Degradation	221
2.13.2.2	Ribosomal Band 28S/18S Ratio	221
2.13.2.3	RNA Integrity Number	222
2.13.2.4	Additional Peaks in the Analysis or an Increase in Baseline Fluorescence	222
2.13.2.5	The 260/280nm Ratio	222
2.13.3	Revised Protocol for cDNA Manufacture, Labelling and Affymetrix® Microarray Hybridisation	223
2.13.4	Affymetrix® GeneChip® Microarray Data Analysis	223
2.13.5	Identification of Probesets for Validation by Real-Time PCR	224

2.14	Statistical Analysis	224
Chapter 3	Analysis of the CD133⁺ve/CD45⁻ve Hoechst 33342 SP and CD133⁺ve/CD45⁻ve Hoechst 33342 NSP Affymetrix[®] Microarray Data	225
3.1	Sample Identification	225
3.2	Analysis of Extracted RNA to Determine Quantity and Quality	225
3.3	Affymetrix Genechip Quality Control Data	228
3.4	Array Normalisation	232
3.5	Biological Comparability of Array Data	232
3.6	Identification of Appropriate Affymetrix[®] Probesets for Subsequent qRT-PCR Validation of the Microarray Data	236
3.7	Correlation Between MAS5.0 Generated Detection Calls and Raw Expression Values	240
3.8	Summary of Chapter Results	243
Chapter 4	Results of Introducing RNase-Free Adjuncts to the Hoechst 33342 Dye Efflux Assay Protocol	245
4.1	Initial Pilot Experiment	245

4.1.1	DNase Treatment	246
4.1.2	Volumes of RNase-free Water for Elution	250
4.1.3	Concentration of Elution Volumes	253
4.1.4	RNAlater [®]	257
4.2	Definitive Attempt at Determination of the Effect of RNase-free Adjuncts on RNA Quality	258
4.3	Summary of Chapter Results	265
Chapter 5	Characterisation of the Hoechst 33342 Dye Efflux Assay	266
5.1	Analysis of CD133^{+ve}/CD45^{-ve} Hoechst 33342 Profiles	266
5.2	Relative CD133 Staining of BPH Epithelial Cells with PE-Cy5 and PE- Cy7 Conjugates	271
5.3	Identification of a CD133^{-ve}/CD45^{-ve} Hoechst^{lo} Subfraction of the SP	274
5.4	Enhanced Cell Number Yield Using the Hoechst 33342^{lo} DSP	276
5.4.1.1	Primary Monolayer Cell Culture and Colony-Forming Ability	279
5.4.1.2	Repeat Flow Cytometric Analysis of Cultured Cells	295

5.5	Determination of the Immunocytochemical Phenotype of the DSP and PSP	299
5.6	Summary of Chapter Results	304
Chapter 6	Analysis of the Affymetrix® Microarray Data for the CD45^{-ve} DSP, PSP and NSP Isolated from Normal, Benign Prostatic Hyperplasia and Carcinoma of the Prostate Samples	308
6.1	Sample Identification	308
6.2	Analysis of Extracted RNA to Determine Quantity and Quality	313
6.3	Clinical Data for the Patient Samples Utilised	316
6.4	Affymetrix Genechip Quality Control Data	320
6.5	Array Normalisation	331
6.6	Biological Comparability of Arrays	331
6.7	Correlation between MAS5.0 Generated Detection Calls and Raw Expression Values	346
6.8	Determination of the Differentially Expressed Affymetrix Probesets	349

6.9	Correlation Between Array Expression Data and Immunocytochemistry Phenotype	353
6.10	Identification of Appropriate Affymetrix® Probesets for Subsequent qRT-PCR Validation of the Microarray Data	355
6.11	Summary of Chapter Results	355
Chapter 7	Discussion	357
7.1	Overview	357
7.2	The Epistem Ltd Microarray Dataset	360
7.3	Steps Taken to Optimise the Affymetrix Microarray Data	363
7.3.1	Minimisation of the Effect of RNase Degradation of Transcripts	363
7.3.2	Subfraction of the SP Tail into the Distal (DSP) and Proximal (PSP) Subpopulations	366
7.3.3	Cellular Amplification Versus Amplification of the Transcriptome	367
7.4	The Molecular Biology Core Facility Microarray Dataset	373
7.4.1	Improvement in Data Quality	373
7.4.2	Limitations to the Dataset	378

7.5	Refinement of the Hoechst 33342 Dye Efflux Assay	382
7.5.1	Overview	382
7.5.2	Demonstration of a Conserved Population of Hoechst 33342 ^{lo} Cells Towards the Distal Tip of the Side Population (DSP)	388
7.5.3	Functional Characteristics	390
7.5.3.1	Differential Colony-Forming Ability and Proliferation Capacity of the DSP and PSP	390
7.5.3.2	FACS Analysis of Cultured Cells Suggests Preservation of the DSP in Cultured DSP Cells and Evidence of Lineage Differentiation	392
7.5.4	Immunocytochemical Phenotype of the DSP and PSP	395
7.6	Realisation of Original Aims and Objectives	397
7.7	Conclusions	398
7.8	Future Direction	399
	Bibliography	401
<u>Word Count</u>	71,161 Words	

List of Tables

Table		Page
1.1	The 2002 Tumour Node Metastasis (TNM) classification of CaP	80
2.1	Details of the primary antibodies used for immunocytochemical analysis of the DSP and PSP	182
2.2	Details of the secondary antibodies used for immunocytochemical analysis of the DSP and PSP	183
2.3	Constituents of each of the control and sort tubes used in the CD133 ^{+ve} /CD45 ^{-ve} Hoechst 33342 dye efflux assay	192
2.4	Constituents of each of the control and sort tubes used in the isolation of the CD133 ^{-ve} /CD45 ^{-ve} DSP, CD133 ^{+ve} /CD45 ^{-ve} PSP and the NSP during the Hoechst 33342 dye efflux assay	200
2.5	Constituents of each of the control and sort tubes used to enable modification of the Hoechst 33342 dye efflux assay for further flow cytometric analysis of passaged prostate epithelial cells	209

2.6	Combinations of slide preparation and secondary antibody concentration applied to each of the eight primary antibody panel replicates	214
3.1	Cell number isolated by FACS and the amount of RNA extracted by Epistem Ltd	227
3.2	Amount of RNA extracted per cell by Epistem Ltd from each of the populations (SP and NSP)	229
3.3	Epistem Ltd microarray quality control statistics	231
3.4	The degree of biological correlation between the Epistem Ltd arrays	237
3.5	The final stages of identifying probesets that were suitable for use in an experiment to validate the fold changes seen on the Epistem Ltd arrays by qRT-PCR	239
3.6	The gene calls generated by MAS5.0 for the 10 probesets that were previously identified as being suitable for qRT-PCR validation of the Epistem Ltd arrays	241
4.1	RNA Integrity Number (RIN) for each of the samples isolated by both RNase-free and standard FACS protocols	249

4.2	RNA Integrity Number (RIN) following DNase treatment for each of the samples isolated by both RNase-free and standard FACS protocols	252
4.3	RNA Integrity Number (RIN) following DNase treatment and vacuum concentration for each of the samples isolated by both RNase-free and standard FACS protocols	255
4.4	Amount of RNA extracted per cell after both the initial and DNase-treated stages of analysis for each of the SP and NSP samples processed by the standard and RNase-free protocols	256
4.5	RNA Integrity Number (RIN) and the 28S/18S rRNA ratio for each of the samples processed by both RNase-free and standard protocols	262
4.6	Cell numbers isolated by FACS and the amount of RNA isolated per cell	263
4.7	Comparison of the RNA yield per cell for the SP and NSP processed by either standard or RNase-free protocols	264

5.1	Percentage of SP and NSP cells in the total live prostate epithelial cell population and the live CD133 ^{+ve} /CD45 ^{-ve} gated population	268
5.2	Percentage of CD133 ^{+ve} /CD45 ^{-ve} cells occupying the SP and NSP regions gated for total live prostate epithelial cells and the CD133 ^{+ve} /CD45 phenotype	270
5.3	Percentage of live epithelial cells residing in region R2 when the IgG-FITC control and three increasing amounts of the fluorochromes PE-Cy5 and PE-Cy7 conjugated to the CD133 secondary antibody were analysed	273
5.4	Percentage of cells in the DSP (R6) from both BPH and CaP patient samples	278
5.5	Comparative cell yields for BPH and CaP patients using the CD133 ^{+ve} /CD45 ^{-ve} and subfractionated Hoechst dye efflux assay techniques	280
5.6	Immunocytochemical assessment of the CD133 status of cells from the DSP and PSP	282
5.7	Colony forming ability of BPH DSP and PSP populations	283

5.8	Proliferation of the DSP and PSP sample wells that successfully reached passage	286
5.9	Second attempt at assessing the colony forming ability of BPH DSP and PSP populations	288
5.10	Number of colonies formed from the BPH DSP and PSP	289
5.11	Cell numbers isolated and seeded from the BPH DSP and PSP for the initial attempt at immunocytochemical assessment	300
5.12	Results of the staining optimisation pilot study	301
5.13	Differential expression of a panel of lineage-specific and putative stem cell markers between the CD45 ^{-ve} BPH DSP and PSP	305
6.1	mRNA recovery details for the normal samples	309
6.2	mRNA recovery details for the BPH samples	310
6.3	mRNA recovery details for the CaP samples	311

6.4	Details of the amount and quality of RNA extracted for the MBCF microarray series	312
6.5	Mean cell number yielded for the DSP, PSP and NSP from normal, BPH and CaP patient samples	314
6.6	RNA yield per cell for the DSP, PSP and NSP from normal, BPH and CaP patient samples	315
6.7	The available clinical details for the normal patient samples	317
6.8	The available clinical details for the BPH patient samples	319
6.9	The available clinical details for the CaP patient samples	321
6.10	The overall MBCF microarray quality control statistics for the 60 arrays	323
6.11	Comparison of the overall quality control statistics from the Epistem Ltd and MBCF microarray series	324
6.12	The overall MBCF microarray quality control statistics for the normal patient sample arrays	325

6.13	The overall MBCF microarray quality control statistics for the BPH patient sample arrays	327
6.14	The overall MBCF microarray quality control statistics for the CaP patient sample arrays	329
6.15	Differential expression of the Affymetrix probesets between each of the DSP, PSP and NSP subpopulations and each of the tissue types	351
6.16	Comparison of the microarray and immunocytochemical log2 fold changes between the DSP and PSP for lineage-specific and stem cell markers	354
6.17	The Affymetrix probesets chosen for subsequent qRT-PCR validation of the microarray data	356

List of Figures

Figure		Page
1.1	McNeal's zonal anatomy of the prostate	49
1.2	Sagittal section of the human male pelvis	51
1.3	Cancer Research UK 2005 male cancer incidence pie chart	57
1.4	Cancer Research UK 2005 age-specific graphical statistics for prostate cancer incidence	58
1.5	Gleason grading of prostate cancer	77
1.6	Schematic diagram of the proposed stem cell hierarchy	112
1.7	The eukaryotic cell cycle	116
1.8	Cartoon depicting the response of a prostatic tubule to castration and androgen replacement	133
2.1	Flow cytometry analysis of the CD133 ⁺ ^{ve} /CD45 ⁻ ^{ve} Hoechst 33342 dye efflux assay prior to FACS	194
2.2	Flow cytometry analysis of the CD45 ⁻ ^{ve} Hoechst 33342 dye efflux assay prior to FACS	197

2.3	Flow cytometry analysis of the subfractionated Hoechst 33342 dye efflux assay side population prior to FACS	202
2.4	Miami Vice schematic illustrating the Epistem Ltd small cell number microarray protocol	216
3.1	Agarose gel (1%) analysis of post amplification cDNA quality	226
3.2	Chart summarising the Qc statistics generated by MAS5.0 for the Epistem Ltd microarray	230
3.3	Boxplots demonstrating the spread of data before and after MAS5.0 normalisation	233
3.4	Scatter plot of the mean log ₂ expression SP vs. NSP	234
3.5	Scatter plots showing the differential gene expression of the SP and NSP for each of the four Epistem Ltd array comparisons	235

3.6	Cluster dendrogram illustrating the hierarchical clustering of data from the eight Epistem Ltd arrays	238
3.7	Graphical comparison of expression values with the MAS5.0 gene detection calls using an example from the Epistem Ltd array data against an example of a sound dataset obtained from the MCF7 cell line	242
4.1	Electrophoretic output for the first set of five live CD45 ^{-ve} epithelial SP and NSP patient samples analysed	247
4.2	An example of the initial electrophoretic output using patient GU18	248
4.3	An example of the electrophoretic output using patient GU18 following on-column DNase treatment	251
4.4	An example of the electrophoretic output using patient GU18 after DNase treatment and vacuum concentration	254

4.5	A simulation of the traditional electrophoretic gels demonstrating the bands of ribosomal RNA detected for each of the samples from the standard and RNase-free FACS protocols	259
4.6	Electrophoretic output for the second set of five BPH patient samples analysed after DNase treatment and volume concentration	261
5.1	Density plot of the CD133 ^{+ve} /CD45 ^{-ve} Hoechst 33342 Red/Blue Profile	269
5.2	Relative fluorescence of secondary antibodies (PE-Cy5 and PE-Cy7) to CD133	272
5.3	Density plots (gated for live cells only) of FL-1 vs. FL-3 for the 5µL and 7.5µL amounts of both PE-Cy5 and PE-Cy7	275
5.4	Dot plots of Hoechst 33342 Red/Blue prostate epithelial cell profiles demonstrating the presence of a CD133 ⁺ /CD45 ^{-ve} subpopulation of the SP	277
5.5A	Number of colonies counted from the DSP	284
5.5B	Number of colonies counted from the PSP	284

5.6	Number of colonies counted from both the DSP and the PSP during the second attempt at colony-forming assays	290
5.7	Photomicrograph of the entire 25cm ² flask containing the cultures for GU59 PSP	291
5.8	Photomicrograph of the entire 25cm ² flask containing the cultures for GU61 PSP	292
5.9	Photomicrograph of the entire 25cm ² flask containing the cultures for GU59 DSP	293
5.10	Photomicrograph of the entire 25cm ² flask containing the cultures for GU61 DSP	294
5.11	Flow cytometric analysis of cells after passage	297
5.12	Representative images depicting differential CD133 expression	302
5.13	Images representative of the observed staining for the lineage-specific and putative stem cell immunocytochemical markers	303

6.1	Chart summarising the Qc statistics generated by MAS5.0 for the MBCF microarray series in normal patients	326
6.2	Chart summarising the Qc statistics generated by MAS5.0 for the MBCF microarray series in BPH patients	328
6.3	Chart summarising the Qc statistics generated by MAS5.0 for the MBCF microarray series in CaP patients	330
6.4	Graph showing the percentage of gene probesets called present for each of the DSP, PSP and NSP arrays from normal, BPH and CaP samples	332
6.5	Boxplot demonstrating the spread of raw data for all microarrays before normalisation	333
6.6	Boxplot demonstrating the spread of data after the process of MAS5.0 normalisation	334
6.7	Boxplot demonstrating the spread of data after the process of RMA normalisation	335

6.8	Scatter plots showing the differential mean log ₂ expression of probesets from all normal samples between the DSP and PSP, DSP and NSP and the PSP and NSP arrays	336
6.9	Scatter plots showing the differential mean log ₂ expression of probesets from all BPH samples between the DSP and PSP, DSP and NSP and the PSP and NSP arrays	337
6.10	Scatter plots showing the differential mean log ₂ expression of probesets from all CaP samples between the DSP and PSP, DSP and NSP and the PSP and NSP arrays	338
6.11	Heatmap demonstrating the comparability of all 60 arrays	340
6.12	Heatmap demonstrating the comparability of those arrays with a satisfactory RIN value (≥ 6.3)	341
6.13	Heatmap demonstrating the comparability of all 18 CaP arrays	343

6.14	Cluster dendrogram indicating the clustering pattern for all 60 arrays	345
6.15	Principal component analysis (PCA) mapping showing the three largest degrees of separation between the DSP, PSP and NSP arrays for each of the patient samples	347
6.16	Plots from both the second (MBCF) and first (Epistem Ltd) rounds of microarrays showing the frequency of probesets called "Absent" by the MAS5.0 software and their corresponding log2 expression summaries	348
6.17	The perfect match and mismatch expression data for three arrays representative of the MBCF microarray data are compared to that of the cell lines MCF7 and MCF10a and the first set of data from Epistem Ltd	350
6.18	Venn diagrams illustrating the number of Affymetrix probesets that were differentially expressed by a log2 fold change of greater than +1 or -1	352

7.1	Flow diagram illustrating the proposed hierarchy for the CD133 phenotype within the prostate epithelial population	386
-----	--	-----

Abbreviations

3-D	Three dimensional
ABC	ATP-Binding Cassette
ACT	Alpha ₁ -antichymotrypsin
ADT	Androgen Deprivation Therapy
ALL	Acute Lymphoblastic Leukaemia
AML	Acute Myelogenous Leukaemia
APC	Adenomatosis Polyposis Coli
AR	Androgen Receptor
AS	Active Surveillance
AUA	American Urological Association
β-actin	Beta Actin
BPH	Benign prostatic hyperplasia
BrdU	Bromodeoxyuridine
BSA	Bovine Serum Albumin
BSCO	Bilateral Subcapsular Orchidectomy
CAB	Complete Androgen Blockade
CaP	Carcinoma of the Prostate
CDKI	Cyclin Dependant Kinase Inhibitor
cDNA	Complementary DNA
CK	Cytokeratin
CML	Chronic Myelogenous Leukaemia
CNS	Central Nervous System
CRUK	Cancer Research UK

CSC	Cancer Stem Cell
CT	Computed Tomography
DEPC	Diethyl Pyrocarbonate
DHH	Desert Hedgehog
DHT	Dihydrotestosterone
DMEM	Dulbecco's Modified Eagle's Medium
DMSO	Dimethyl-Sulfoxide
DNA	Deoxyribonucleic Acid
DRE	Digital Rectal Examination
DSP	Distal Side Population
EAU	European Association of Urology
EBR	External Beam Radiotherapy
EGF	Epidermal Growth Factor
ENU	N-ethyl-N-nitrosourea
EORTC	European Organisation for Research and Treatment of Cancer
ERSPC	European Randomised Screening for Prostate Cancer
ESTRO	European Society for Therapeutic Radiology and Oncology
FACS	Fluorescence-Activated Cell Sorting
Fc	Fold Change
FCS	Foetal Calf Serum
FDR	False Discovery Rate
FGF	Fibroblast Growth Factor

FSH	Follicle-Stimulating Hormone
GAPDH	Glyceraldehyde 3-Phosphate Dehydrogenase
GSK3	Glycogen Synthase Kinase 3
GUCR	Genito-Urinary Cancer Research Group
HBSS	Hanks' Balanced Salt Solution
HES	Hairy/enhancer of split 1 and 5
HIFU	High-Intensity Focused Ultrasound
HPV	Human papilloma virus
HRPC	Hormone-Refractory Prostate Cancer
HSC	Haemopoietic Stem Cell
IGF-1	Insulin-like Growth Factor 1
IgG	Immunoglobulin
IHH	Indian Hedgehog
IPSS	International Prostatic Symptom Score
KSFM	Keratinocyte Serum-Free Media
LH	Luteinising Hormone
LHRH	Luteinising Hormone-Releasing Hormone
MAP	Mitogen Activation Protein
MBCF	Molecular Biology Core Facility
MDR	Multidrug Resistance
MG	Alpha ₂ -macroglobulin
MR	Magnetic Resonance
MRC	Medical Research Council
mRNA	Messenger RNA
MRU	Mammary Repopulating Unit

MSC	Microbiological Safety Cabinet
Msi-1	Musashi-1
NF- κB	Nuclear Factor- κ B
NGF	Nerve Growth Factor
NOD/SCID	Non-Obese Diabetic Severe Combined Immunodeficient
NSC	Neurological Stem Cell
NSP	Non-Side Population
PAP	Prostatic Acid Phosphatase
PBS	Phosphate Buffered Saline
PCA	Principle Component Analysis
PCR	Polymerase-Chain Reaction
PI3	Phosphatidylinositol 3'
PICR	Paterson Institute for Cancer Research
PIN	Prostatic Intraepithelial Neoplasia
PLCO	Prostate, Lung, Colorectal and Ovary
PSA	Prostate Specific Antigen
PSP	Proximal Side Population
PTEN	Phosphatase and Tensin homologue
qRT-PCR	Real-Time Reverse-Transcription Polymerase Chain Reaction
RBP	Retinol Binding Protein
RIN	RNA Integrity Number
RMA	Robust Multiarray Averaging
RNA	Ribonucleic Acid

RNase	Ribonuclease
RNAF	Ribonuclease-Free
RP	Radical Prostatectomy
RRP	Radical Retropubic Prostatectomy
rRNA	Ribosomal RNA
RTOG	Radiation Therapy Oncology Group
SC	Stem Cell
SCC	Squamous Cell Carcinoma
SCID	Severe Combined Immunodeficiency
SEER	Surveillance, Epidemiology, and End Results
SHH	Sonic Hedgehog
SP	Side Population
SuH	Suppressor of Hairless
TAP	Transit-Amplifying Population
TCC	Transitional Cell Carcinoma
TCF	T-Cell Factor
TNM	Tumour Node Metastasis
tRNA	Transfer RNA
TRUS	Trans-Rectal Ultrasound
TURP	Trans-Urethral Resection of the Prostate
UESCD	Urologic Epithelial Stem Cell Database
UK	United Kingdom
US	United States
USA	United States of America
USS	Ultrasound

The University of Manchester

Abstract of Thesis submitted by Benjamin Robin Grey for the Degree of Doctor of Medicine MD and entitled "Optimisation of the Hoechst 33342 Dye Efflux Assay for Small Cell Number Microarray Profiling of the Prostate." January 2009.

Both Benign Prostatic Hyperplasia (BPH) and Carcinoma of the Prostate (CaP) are characterised by the loss of cell growth regulation. There is gathering evidence that this is secondary to disordered control of the stem cell (SC) compartment. SCs are rare, quiescent cells defined by their properties of self renewal, clonogenicity and pluripotentiality. It has been reported that both normal and cancer SCs (CSCs) could be isolated by α -2 integrin^{hi}/CD133^{ve} selection. However, these prostate epithelial cell (PEC) populations had undergone clonal expansion with the potential for genetic drift prior to functional and genetic analysis. To date, the physical isolation of a pure unexpanded primary PEC SC population has proven elusive and remains limited by small cell numbers. Genetic analysis of the prostate SC population is required to identify novel markers to facilitate SC isolation as well as to provide additional information about SC regulatory pathways and how genetic changes in the SC compartment lead to the development of BPH and CaP. Knowledge of such behaviour would address current diagnostic and prognostic pitfalls as well as providing novel therapeutic targets.

The Hoechst 33342 "side population" (SP) is an alternative method for isolating SC-enriched populations. The PEC SP has been shown to be highly enriched for SC characteristics. However, an initial attempt at the microarray analysis of the SP and non-SP (NSP) was unsuccessful and ultimately unsatisfactory for biological datamining, due to the low cell numbers isolated and poor Ribonucleic Acid (RNA) quality.

Subsequently, standardised fluorescence-activated cell sorting (FACS) protocols were successfully optimised to reduce the degradation of RNA transcripts. Improvement in the RNA amplification chemistries that complement the microarray analysis of small cell number samples afforded the opportunity to amplify very small quantities of this good quality RNA and succeed in creating sufficient cDNA for hybridisation to Affymetrix HG-U133_Plus 2 arrays. The literature has suggested that cells residing in the distal SP (DSP), which are the most efficient at effluxing the Hoechst 33342 dye, represent further SC population enrichment. A discrete CD45^{-ve}/CD133^{-ve/low} DSP comprising 0.116% (BPH) and 0.025% (CaP) of the total PEC populations has been successfully isolated. Compared with the proximal SP (PSP), the DSP had significantly enhanced clonogenicity. Immunocytochemistry confirmed significant enrichment for the putative SC markers Beta Catenin, p27 and Notch-1 in the DSP. Repeat FACS analysis of the DSP after passage suggested properties of self renewal and pluripotentiality. Ultimately, microarray quality control data has confirmed the improved quality of extracted RNA and gene calls were equivalent to those seen in cell line experiments (mean 50.19%). Pearson correlation has revealed good intra-population array correlation.

Further enrichment for SC characteristics has been achieved using the Hoechst 33342 functional assay. Despite the low cell numbers seen in a SC-enriched population, this unique study has generated differential gene expression data for the DSP, PSP and NSP from normal, BPH and CaP tissue and is now available for interrogation to determine genes of biological interest.

Declaration

I declare that no portion of the work referred to in the thesis has been submitted in support of an application for another degree or qualification of this or any other university or other institute of learning.

Benjamin R. Grey MB.ChB. MRCS (Eng)

Copyright Statement

The author of this thesis (including any appendices and/or schedules to this thesis) owns any copyright in it (the "Copyright") and s/he has given The University of Manchester the right to use such Copyright for any administrative, promotional, educational and/or teaching purposes.

Copies of this thesis, either in full or in extracts, may be made **only** in accordance with the regulations of the John Rylands University Library of Manchester. Details of these regulations may be obtained from the Librarian. This page must form part of any such copies made.

The ownership of any patents, designs, trade marks and any and all intellectual property rights except for the Copyright (the "Intellectual Property Rights") and any reproductions of copyright works, for example graphs and tables ("Reproductions"), which may be described in this thesis, may not be owned by the author and may be owned by third parties. Such Intellectual Property Rights and Reproductions cannot and must not be made available for use without the prior written permission

of the owner(s) of the relevant Intellectual Property Rights and/or Reproductions.

Further information on the conditions under which disclosure, publication and exploitation of this thesis, the Copyright and any Intellectual Property Rights and/or Reproductions described in it may take place is available from the Head of School of Medicine (or the Vice-President).

Dedicated to Amber

For understanding, loving and supporting me

Acknowledgements

Overall, this period of research has been both extremely rewarding and enjoyable. I feel that I have developed as an individual, clinician and researcher as a consequence. However, I am very aware that I could not have succeeded in completing this body of work without the inspiration, guidance and support of some key individuals along the way.

I thank Professor Noel Clarke for giving me with the opportunity to join the Genito-Urinary Cancer Research Group as Clinical Research Fellow. He has provided support and encouragement throughout this research project and continues to be source of great inspiration to me.

I thank Dr Mick Brown for his supervision and his ability to guide myself and other clinicians before, safely through the challenges posed by working in scientific research. In addition, I am grateful for his time and comments when reviewing my numerous manuscripts, grant applications and abstracts over the last three years.

Claire Hart has patiently taught me all the techniques I used and been an invaluable source of advice throughout my time in laboratory research.

I am grateful to the Consultant staff at Salford Royal Hospitals NHS Foundation Trust, Christie Hospital NHS Foundation Trust and the University Hospitals of South Manchester NHS Foundation Trust for kindly recruiting the patients and providing the tissue samples.

The members of staff in the Molecular Biology Core Facility (Dr Stuart Pepper, Yvonne Hey, Gill Newton, Sian Dibben and Emma Saunders) have been instrumental in my understanding of microarray techniques and analysis and have expertly overseen the chemistries which have proved key to the project's success. Mike Hughes, Jeff Barry and Dr Morgan Blaylock have spent countless hours in the Flow Cytometry facility diligently helping to sort my cell populations as well as offering advice as to how to maximise the protocols. Dr Steve Bagley from the Advanced Imaging facility taught me how to use a microscope properly and has steered me through the more complex techniques of image capture. These individuals at the Paterson Institute for Cancer Research have all spared their valuable time to support this body of work and without them this project would not have been possible.

My colleague, Mr Jeremy Oates, has provided great camaraderie over the last three years and as become a good friend.

I am greatly indebted to the patients who consented to providing tissue samples for research use. I am impressed by their willingness to take part in research which is unlikely to benefit them personally. Their desire to try and help others even during their own times of stress is commendable.

Finally, most importantly, I thank Amber, my Mum and Dad and all my family and friends for their love and support throughout this project and my career thus far. The pressures that the work has brought at times were only withstood because of their understanding and encouragement. "It was worth it in the end!"

Chapter 1: Introduction

1.1 The Prostate

1.1.1 General Morphology

The prostate is an organ unique to the male. The paraurethral glands of Skene are the equivalent structure in the female ¹. On average it measures three centimetres (cm) in length, four cm in width, and two cm in depth ^{1,2}.

1.1.2 Anatomical Relations

Described as walnut-shaped ¹, the prostate has anterior, posterior, and lateral surfaces. The lower pole is termed the apex and sits above the uro-genital diaphragm. Superiorly the broader base is fused with the bladder. The proximal urethra (prostatic urethra) traverses the longitudinal length of the prostate gland.

Denonvilliers' fascia is a condensation of fascia which is believed to be a fusion of the layers of pelvic peritoneum that forms the rectovesical pouch above ¹ and is connected with the posterior surface of the prostatic capsule. Further posteriorly, loose areolar tissue separates the thin plane between Denonvilliers' fascia and the rectum. The seminal vesicles sit behind the prostate and below the rectovesical peritoneal reflection. They join with the ampullae of the vas deferens from each side to form the two ejaculatory ducts. The ejaculatory ducts pierce the

prostate obliquely and open on the verumontanum in the prostatic urethra.

Anteriorly, condensations of the visceral endopelvic fascia form the pubo-prostatic ligaments and extend from either side of the prostatic apex to insert on the posterior aspect of the pubic bones' body. The antero-lateral surfaces of the prostate are supported by the pubococcygeal portions of levator ani, of which, the most medial fibres merge with the prostatic visceral endopelvic fascia as the levator prostatae. The endopelvic fascial layers separate from the prostate's capsule antero-laterally. The space between them is filled by fatty areolar tissue and the dorsal vein complex. The superficial branch of the dorsal vein lies outside this fascia in the retropubic fat but subsequently pierces the fascial layers and ultimately drains into the dorsal vein complex.

1.1.3 Anatomical Structure

The prostate is composed of approximately 70% glandular elements and 30% fibromuscular stroma. The capsule, composed of collagen and abundant smooth muscle, encases the fibromuscular and glandular tissue of the prostate. It is the coordinated contraction of the capsule that expels prostatic secretions into the urethra during the process of ejaculation. Peripheral to the true capsule lies the loose areolar connective tissue of the endopelvic fascia forming the "false capsule". The prostatic plexus of veins runs between these two capsules.

Histologically no intervening fibromuscular stroma can be seen at the apex or base and prostatic glands extend directly into the muscle. The apex of the prostate is continuous with the striated urethral sphincter (sphincter urethrae) which is responsible for continence and the prostatic base is invaded by the middle circular and inner longitudinal fibres of the bladder detrusor to form the pre-prostatic sphincter responsible for antegrade ejaculation.

The prostatic urethra commences at the internal meatus running closest to the anterior border of the prostate. It consists of a transitional cell epithelium surrounded by a coat of inner longitudinal and outer circular smooth muscle. A posterior midline ridge projects into the prostatic urethra throughout its length. This urethral crest forms grooves either side known as the prostatic sinuses.

At the prostatic urethra's midpoint, approximately two centimetres from the bladder neck, the urethra turns anteriorly. This angulation, typically 35° , divides the prostatic urethra into proximal and distal segments. In addition to the preprostatic sphincter's role, the proximal segment contributes approximately one percent of the ejaculate volume via small peri-urethral glands extending between the smooth muscle fibres. The distal segment is primarily involved with receiving the vast majority of the ejaculate. The urethral crest widens at its approximate midpoint to form a rounded eminence termed the seminal colliculus or verumontanum. The prostatic utricle, formed from the fused paramesonephric (Müllerian) ducts, opens at the apex of the verumontanum. In turn the ejaculatory

ducts open either side of the utricle's orifice. Finally the glands of the peripheral zone empty into the prostatic sinuses.

Previously, the prostate was described as consisting of a middle lobe and two lateral lobes separated by a central sulcus. The preferred classification currently involves its glandular elements being divided into histologically and functionally discrete zones (Figure 1.1³). The transitional zone's ducts drain at the urethral angle. The transition zone itself constitutes up to 10% of the prostatic glandular tissue and is compartmentalised by a fibromuscular band clearly visualised by transrectal ultrasonography. Enlargement of the transitional zone is the main contributor to benign prostatic hyperplasia (BPH). However, it is estimated that 20% of prostatic adenocarcinomas can arise there.

The caudal limit of the central zone's glandular ducts are circularly arranged around the orifices of the ejaculatory ducts and course cranially into the wedge-shaped central zone which itself forms the base of the prostate. The central zone encompasses approximately 20% of the glandular tissue and again contributes to BPH. Its glands are histologically distinct from the remainder of the prostate and are believed to be of Wolffian origin. This perhaps explains the low incidence of carcinoma in this zone of less than five percent.

The peripheral zone sits below and behind the central zone and incorporates 70% of the prostate gland's volume. The majority (70%) of carcinoma of the prostate (CaP) develops in the peripheral zone. Unless replaced by adenomatous tissue, as in BPH, the anterior portion is made

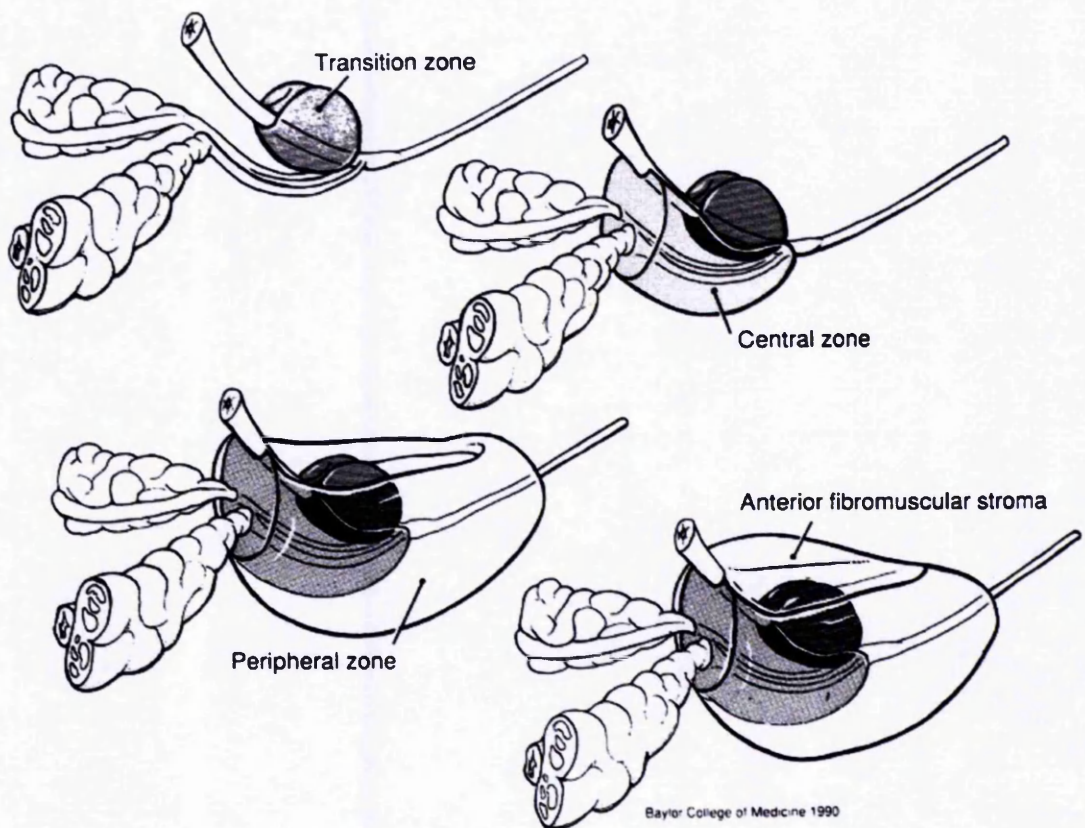


Figure 1.1: McNeal's zonal anatomy of the prostate (Am J Surg Pathol 1988;12:619–633).

up of very little glandular tissue but instead consists of fibromuscular stroma.

1.1.4 Vascular Supply

1.1.4.1 Arterial Supply

The common iliac artery bifurcates at the level of the pelvic brim anterior to the sacro-iliac joint to form the external and internal iliac arteries. The internal iliac, or hypogastric artery, is the main artery to the pelvic viscera. Soon after the common iliac artery bifurcation the internal iliac divides into a short posterior and longer anterior division. The anterior division's anatomy can be varied particularly between the male and female sexes. The precise order that arteries arise can vary and some arteries may arise via common stems (Figure 1.2⁴).

The prostatic branch of the inferior vesical artery is the prostate's principal supply however additional collaterals from the middle rectal and internal pudendal branches of the internal iliac may also contribute¹. The prostatic artery branches into two forming; urethral and capsular groups of arteries.

The urethral artery branches enter the prostate postero-laterally (between the one and five o'clock and seven and 11 o'clock positions) taking a perpendicular course inwards towards the urethra. On reaching the urethra they turn to run parallel to the urethra supplying it and its associated peri-urethral glands. In addition it supplies the transitional zone and can therefore be implicated in supplying adenomas as well as

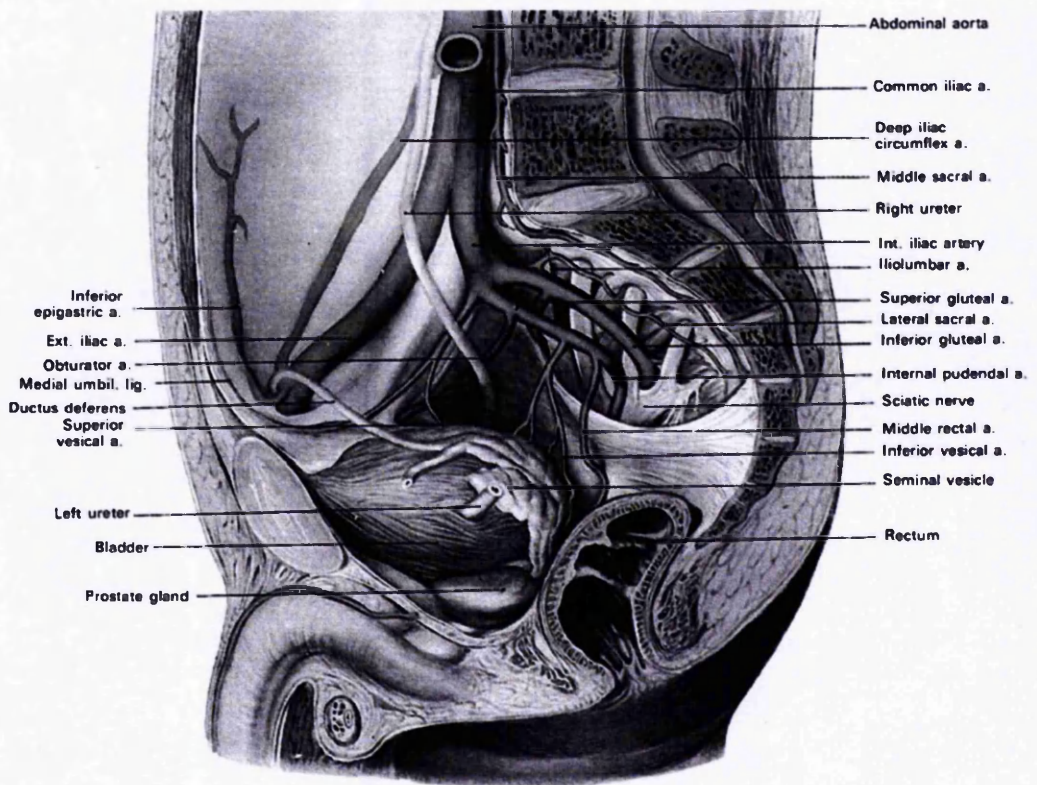


Figure 1.2: Sagittal section of the human male pelvis illustrating the pelvic viscera and arterial vasculature, the ureter and vas deferens pass medial to the vessels (from Clemente CD: Gray's Anatomy, 30th American ed. Philadelphia, Lea & Febiger, 1985, p 750.)

conversely being the source of haemorrhage after trans-urethral resection of the prostate (TURP).

The capsular branches reach the prostate's postero-lateral surface with the cavernous nerves as part of the neurovascular bundle. They then course anteriorly and ramify over the prostatic capsular surface before entering the gland at right angles and supplying the underlying glandular stroma. Finally the distal branches pierce the urogenital diaphragm to enter the perineum.

1.1.4.2 Venous Drainage

Between the true and false capsules run the peri-prostatic plexus of veins. This plexus receives the dorsal vein complex and anastomoses with the vesical plexus to form a series of inferior vesical veins. In turn, these ultimately drain back to the internal iliac vein and the systemic circulation. The veins of the pelvis are without valves and therefore retrograde flow of blood can occur during episodes of raised intra-abdominal pressure, from the pelvis to the lumbar vertebrae via the posterior branch of the internal iliac vein. This phenomenon has been suggested as an explanation for the high incidence of metastatic deposits to the lumbo-sacral spine in CaP ⁵.

1.1.5 Lymphatic Drainage

Lymphatic drainage of the prostate is primarily across the pelvic floor to the internal iliac (hypogastric) and obturator nodes however, more rarely, the external iliac and presacral groups of nodes may be involved ^{1, 2}.

1.1.6 Nerve Supply

The inferior hypogastric plexus provides the autonomic nervous supply of the prostate. It is composed of sympathetic innervation, provided via the superior hypogastric plexus and the visceral branches of the sacral sympathetic trunks, and cholinergic innervation via the parasympathetic fibres of the pelvic splanchnic nerves (S2, S3 and S4). The plexus is a network of nerve fibres that, in the male, lays lateral to the rectum, prostate, seminal vesicle and posterior aspect of the bladder. Visceral branches from the plexus travel to the prostate with the cavernous nerves and capsular vasculature. The smooth muscle fibres of the fibromuscular stroma and capsule are under the α -adrenergic control of these sympathetic nerves. Conversely therefore pharmacological α_1 -adrenergic blockade may be therapeutic in BPH by helping to increase urinary flow rates. Peptidergic and nitric oxide synthase-containing neurons may also be implicated in smooth muscle relaxation having been isolated from the prostate. The parasympathetic nerves supply the acini and promote glandular secretions. Afferent sensory neurons from the prostate terminate in the pelvic and thoracolumbar spinal centres.

1.1.7 Histology

The glands of the prostate are tubuloalveolar and are lined with a pseudo-stratified columnar epithelium with basally located nuclei and foamy cytoplasm ⁶. The epithelium is thrown into a series of folds with a central core of supporting lamina propria. Cells of the central zone are large and “squared-off” with the compact stroma closely related to the

epithelium. Glands of the peripheral zone are smaller and rounder. The peripheral zone luminal borders appear to be smoother and straighter and the epithelium is surrounded by a looser arrangement of muscle fibres. Finally the transitional zone has glands similar to the peripheral zone but the stroma is more compact, as is the case in the central zone. Biopsy cores cannot distinguish between the zones reliably. However, whole section can do on the basis of microanatomical assessment ⁷.

The prostatic epithelium consists of three main cell types; secretory luminal cells, basal cells and scattered neuroendocrine cells. Luminal cells typically express high levels of cytokeratin (CK)8 and CK18 as well as prostate specific antigen (PSA) and androgen receptor (AR). In contrast the basal layer consists of cells with preferential expression of the higher molecular weight keratins CK5 and CK14 as well as p63 ⁸.

1.1.8 Embryology

Initially all embryos are ambisexual and possess a pair of undifferentiated gonads and two sets of ducts (Müllerian and Wolffian ducts). Between the 4th and 7th week of embryonic development the urorectal septum divides the endodermal cloaca into the primitive urogenital sinus anteriorly and the anorectal canal posteriorly. The cloacal membrane then forms the urogenital and anal membranes respectively. The gonadal primordia differentiate into the testes which in turn produce testosterone and Müllerian inhibiting substance with consequent maintenance of the Wolffian duct system and regression of the Müllerian ducts. Further testosterone stimulation induces formation

of the epididymis, ductus deferens and seminal vesicles from the Wolffian ducts ⁹. The remainder of the lower urinary tract develops from the urogenital sinus. The upper and largest part forms the urinary bladder. Below this, the pelvic part of the sinus gives rise to the prostatic and membranous parts of the urethra ¹⁰.

The prostate develops as direct outward growths of the urogenital sinus at the level of the prostatic urethra, again under testosterone stimulation ¹¹. The complex processes of epithelial budding, branching and canalisation stimulates the mesenchyme to differentiate into its smooth muscle and fibroblast constituent parts ¹¹.

1.1.9 Physiology

The function of the prostate is to secrete semen, a thin and milky fluid that acts as a vehicle for transporting sperm, to facilitate successful fertilisation of the female ovum. Semen contains citrate and phosphate ions, calcium, profibrinolysin and a clotting enzyme. In response to parasympathetic stimulation the glandular acini secrete their fluids into the ductal system. Subsequently sympathetic stimulation causes contraction of the smooth muscle of the stroma and capsule. Ductal contents empty to the prostatic urethra (emission), allowing mixture with the sperm delivered by the ejaculatory ducts. Further sympathetic stimulation of the smooth muscle leads to ejaculation.

The fluid of the vas deferens is slightly acidic secondary to the presence of citric acid and the metabolic by-products of sperm metabolism. Acid

pH decreases sperm motility. The alkaline property of semen (pH~7.5) helps to overcome both the inherent acidity of the sperm and the acidic environment of the vagina. Neutralisation of the acid pH by the prostatic fluid may therefore promote sperm motility and successful fertilisation.

Sperm and fluid from the vas deferens contributes approximately 10% of the seminal fluid. The majority (60%) is from the seminal vesicles and the remaining 30% is formed from the secretions of the prostate and peri-urethral glands ¹².

1.2 Carcinoma of the Prostate

1.2.1 Epidemiology

1.2.1.1 United Kingdom

In the United Kingdom (UK), Cancer Research UK (CRUK) placed CaP as the commonest male malignancy in 2005 with 34,302 new cases registered (24% of the total number of registered malignancies). The crude incidence rate was high at 116.3 cases per 100,000 of the population for all ages (Figure 1.3)¹³. The Office for National Statistics reports the 2003 incidence rates by age, with the incidence per 100,000 population being 8.5 for ages 45-49 years and 740.7 for ages 75-79 years (Figure 1.4) ¹⁴. CaP is the second commonest cause of cancer death in men and accounted for 10,038 deaths in 2006. This equates a crude death rate of 34.0 deaths per 100,000 population ¹³.

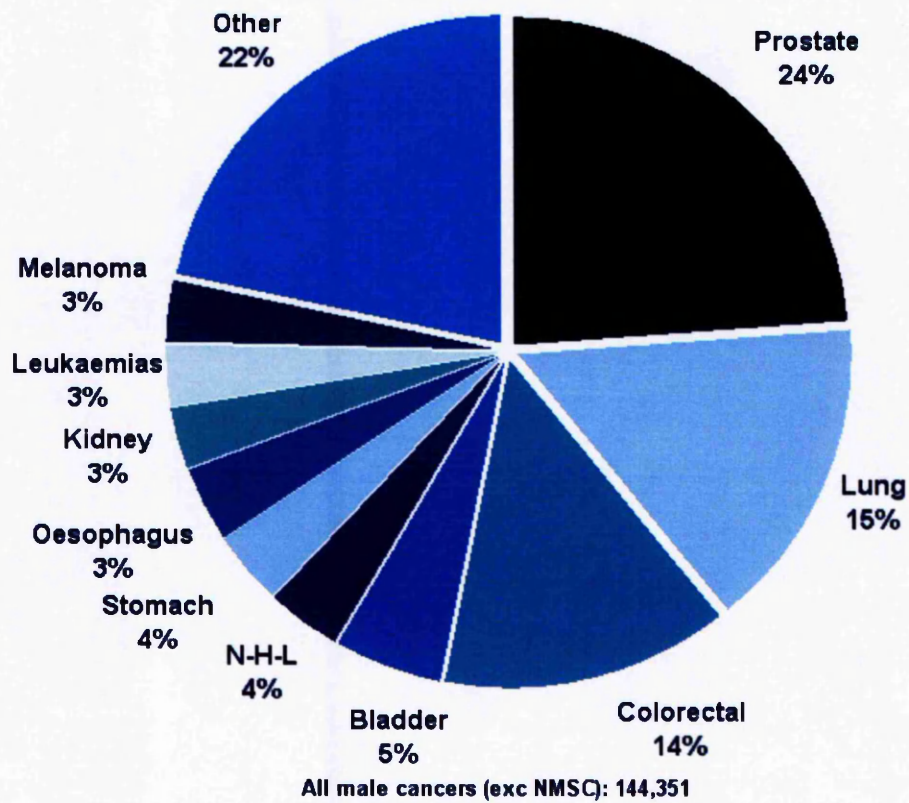


Figure 1.3: Cancer Research UK pie chart demonstrating the 2005 UK incidence for the commonest male cancers.

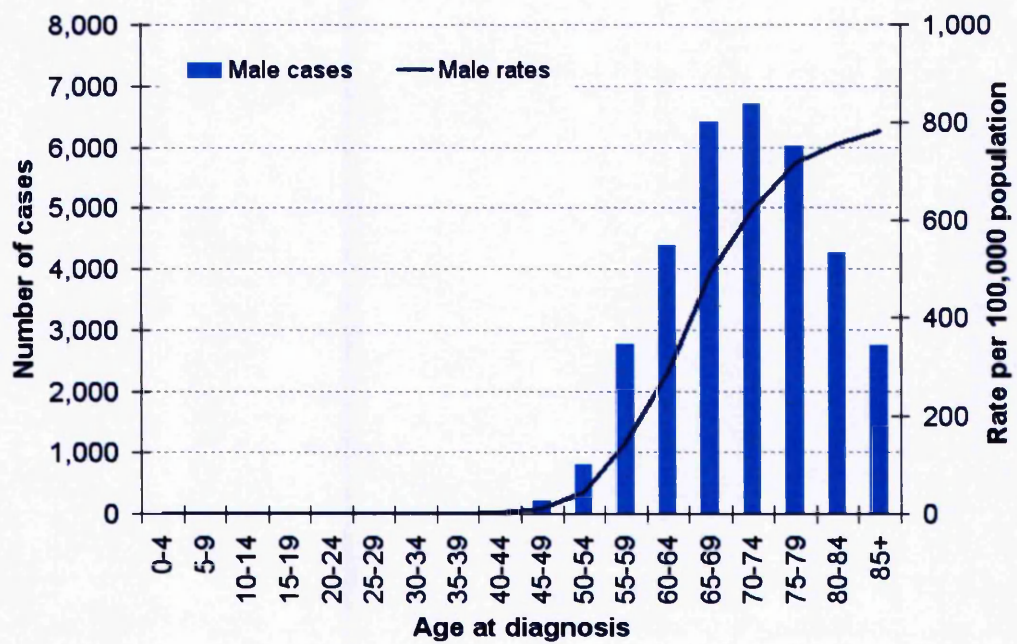


Figure 1.4: Graph illustrating the age-specific Cancer Research UK statistics for numbers of new CaP diagnoses and the rate of diagnoses per 100,000 UK population in 2005.

1.2.1.2 United States of America

The Surveillance, Epidemiology, and End Results (SEER) programme in the United States (US) is the most complete epidemiological record of CaP incidence in the US provided by the National Cancer Institute. It has demonstrated that incidence rates have increased dramatically since the late 1980s. US incidence rates increased steadily by 2.3% per annum in the decade between 1975 and 1985 before climbing to 6% per annum (1985-1989) and 18.4% annually thereafter until 1992. The annual incidence rates have fallen from 1992 to 1995 and appear now to be reaching a plateau. The changes are consistent with the widespread adoption of PSA as a screening tool in the US and the consequent improvement in detecting previously sub-clinical cancers ¹⁵. Whilst such explosive increases are likely to be secondary to PSA screening, there is evidence to suggest a steady increase in the incidence of clinically-detected CaP to a lesser degree, prior to its introduction. Post *et al* ¹⁶ observed that the rate increased from 36 to 55/100,000 between 1971 and 1989 in the Southern Netherlands before PSA was introduced in 1990.

1.2.1.3 Worldwide

Globally, overall incidence rates for CaP are comparatively lower than those of the UK and US with it being the fourth most common male malignancy. Whilst incidence and mortality rates are generally lower in the developing countries than the developed countries of the Western world, the complex interplay of genetic and environmental factors causes

marked variation amongst different countries. This is illustrated by the Scandinavians' comparatively high rates (31.5% of all new Swedish cancer cases in 1999)¹⁷. Norway has approximately 24 cases per 100,000 compared with those of Spain (13/100,000). These remain low when the US rates are taken into consideration but are still markedly higher than those of the Far-East where the lowest worldwide rates are recorded (Japan 4/100,000 for 1992-1995)¹⁸.

1.2.1.4 Effect of PSA on Epidemiology

Incidence rates have increased for CaP since the introduction of PSA testing. Overall there appears to have been down-staging and earlier diagnosis of new tumours. The incidence of local and regional disease appears to have proportionally increased, whilst the rate of metastatic disease has decreased^{19, 20}. In a series that pre-dated PSA, George reported that 58% of patients from a study cohort had presented with metastatic disease²¹. A study from 1997, following PSA introduction, showed that less than half this number (25% of the cohort) were presenting with metastases²². Further evidence to support the higher incidence of early disease (organ-confined) is illustrated by the experience of Stamey *et al*. The group reported that a significantly larger proportion of patients (73% in 1996 vs 10% in 1988) were undergoing prostatectomy for stage T1c disease. Higher rates of pathologically confirmed cancer (40 to 75% between 1988 and 1996) with a parallel fall in positive margin and seminal vesicle invasion rates were observed in a significantly younger population²³.

Since 1992, with the widespread introduction of PSA screening, US mortality rates for CaP have been decreasing. This is despite the highest incidence of CaP being in the elderly age groups and that the elderly population is expanding ^{19, 24, 25}. Mortality rates appear to have increased in other populations but at a much slower rate than the incidence ²⁶. With respect to PSA, these encouraging results from the US have not been replicated across the globe. The group of patients studied by Post *et al* ¹⁶ showed a continued rise in mortality whilst a Swedish study showed no downward trend ^{27, 28}.

1.2.2 Demographics

Within the Western population the Afro-American men clearly have the highest incidence of CaP. In the USA, Afro-American incidence rates increased 102% from 124 to 250 per 100,000 between 1986 and 1993. Rates increased by a similar rate (86 to 179 per 100,000) for white Americans for a similar period ¹⁹. This rate, like that of white Americans, is likely to continue to fall and reach a baseline. However, the Afro-Americans continued to have the highest incidence rates (approximately 170/100,000), ahead of the white (110/100,000), Hispanic (104/100,000) and Asian (82/100,000) populations of the US in 1995.

Shared environmental risk factors may be responsible for the high incidence rates in Afro-American men, though an underlying genetic predisposition is more likely given that Osegbe showed similar rates in a male Nigerian population ²⁹. However, the western environment does seem to play a role. This is demonstrated by the raised incidence and

mortality rates seen in the Japanese and Chinese residents of the USA compared with their indigenous populations³⁰ and furthermore, by the rising rates in the native inhabitants as these nations become more westernised. Studies have verified that migrating populations appear to develop an altered CaP incidence proportional to the changes in patterns of incidence between their original population and that of their new residence^{31, 32}.

The incidence of CaP is greatest in the more elderly populations as is often the case for all cancers. In CaP the effect appears to be more striking with 75% of new diagnoses being in those over 65 years of age. Men of 75-79 years are 100-times more at risk than those in the 40-49 years group³³.

1.2.3 Aetiology

No clear aetiology has yet been defined for CaP. Studies have investigated the role of various risk factors but the majority of evidence appears to be equivocal. Further study may reveal one of the exogenous risk factors as an explanation for the geographical variation in clinically significant CaP. The strongest current evidence is supportive of hereditary factors. Diets which are high in animal fat may be important in increasing the risk of CaP development³⁴. However, the question of whether the strength of this evidence is sufficient to implicate changes in lifestyle in CaP patients and their relatives remains as yet unanswered.

1.2.3.1 Familial / Hereditary

Studies have suggested that CaP incidence is higher in men with a positive family history in a first-degree relative ³⁵. It appears that the risk increases two, five and eleven-fold for patients with one, two and three affected first-degree relatives respectively ³⁵⁻³⁸. Furthermore a younger age of onset in the relative appears to increase the subsequent rate of familial incidence ³⁷. Carter *et al* ³⁷ proposed that hereditary cases were secondary to autosomal dominant inheritance of a rare allele and may explain 9% of cases of CaP and up to 43% of the cases occurring in the under-55 year old age group. The majority of evidence suggests that hereditary and sporadic cancers are indistinct in their pathological behaviour ³⁹.

1.2.3.2 Androgens

The role of endogenous androgens in the aetiology of CaP remains a contentious issue ¹⁵ despite antiandrogen therapy being one of the mainstays of treatment of established disease. Studies have provided arguments both for ^{40, 41} and against ^{42, 43} a link between CaP and high levels of testosterone and its metabolites. A meta-analysis by Shaneyfelt *et al* in 2000 ⁴⁴ suggested that men with testosterone concentrations in the upper quartile had a 2.34-fold increase in CaP. The difference in design of the studies has lead to some problems in comparing the data and as yet the hypothesis that androgens initiate cancer rather than promote it is unanswered.

1.2.3.3 Genetic Polymorphisms

As mentioned previously, Carter *et al*³⁷ suggested that up to 9% of CaP may be familial and secondary to a rare allele that is highly penetrant (i.e. high lifetime risk), inherited in an autosomal dominant fashion. Other less penetrant mutations may well occur and the combination of this with environmental factors may also contribute to the aetiology.

Specific mutations include; 5 α -Reductase Type 2 and Type 2 3 β -Hydroxysteroid Dehydrogenase genes. Both work to raise the concentration of the potent testosterone metabolite dihydrotestosterone (DHT). Studies have shown evidence to suggest that mutations that raise the DHT concentration have caused a greater incidence of CaP⁴⁵,⁴⁶ whereas those that cause a less effective conversion have conveyed a lower risk⁴⁷. Mutations in the allele repeat sequences of the AR may too cause CaP and worsen the prognosis of established disease.

Correlations of these genetic changes have been made with the known epidemiological observations that Afro-Americans are at highest risk and Asians at lowest risk⁴⁸. Overall it appears that CaP may be more heterogenous than other cancers making specific gene mapping more difficult⁴⁹.

1.2.3.4 Vitamin D

Vitamin D is a steroid hormone that has shown to convey anti-tumour activity in preliminary clinical trials⁵⁰⁻⁵². It has been suggested that lower vitamin D levels in Northern countries with fewer hours of daylight may

be an explanatory mechanism for the higher incidence of CaP in Scandinavia ⁵³.

1.2.3.5 Insulin-like Growth Factor

A number of studies have shown the mitogenetic and anti-apoptotic effect of Insulin-like Growth Factor (IGF-1) on prostate epithelial cells and Chan *et al* have provided the most conclusive evidence of its role in CaP via a prospective trial. Men with IGF-1 levels in the highest quartile had a 4.3-fold increased incidence of CaP when compared with those men in the lowest quartile ⁵⁴.

1.2.3.6 Diet

As previously mentioned, environmental factors are considered important in the development of clinical CaP particularly as the prevalence post-mortem is relatively constant across the world. Specifically this helps explain why individuals' incidence rates alter with a change in country of residence. Diet may not truly initiate cancers but may be involved in the promotion of histological cancers to clinically manifest ones ¹⁵.

1.2.3.6.1 Fat

Evidence to suggest a causative role for dietary fat in CaP has been shown by studies highlighting both that high-fat diet promoted growth ⁵⁵, ⁵⁶ and that fat-free diets reduced growth of androgen-dependent tumours ⁵⁷.

The greater the proportion of fat making up the calorie intake in the diet the higher the androgen levels ⁵⁸⁻⁶⁰. Furthermore, fat may be responsible for free radical formation ⁶¹ and the manufacture of proinflammatory fatty acid metabolites such as arachidonic acid that may promote CaP *in vivo* ⁶²⁻⁶⁵. Epidemiological evidence for an association between high dietary fat intake and CaP has reached no firm conclusions. However, a review by Kolonel *et al* ⁶¹ did tentatively suggest a link, particularly with diets high in red meat. Whether it is the meat intake itself, or that such diets may be low in other constituents such as vegetables, is yet to be decided upon.

1.2.3.6.2 Calcium

High calcium intake in the diet has been associated with a raised incidence of CaP ⁵⁴, possibly related to inhibition of vitamin D production, and consequently promotion of cell proliferation ⁶⁶.

1.2.3.6.3 Lycopene

Lycopene is present in high concentrations in tomatoes. It is a carotenoid and a powerful antioxidant. It is believed to be a negative risk factor for CaP ⁶⁷ with as much as a 36% reduction in incidence rates being seen in those with high dietary intakes ^{68, 69}. Such beneficial effects are only seen if the tomatoes are cooked. DeMarzo *et al* ⁷⁰ suggested that chronic prostatitis is a precursor for CaP and that lycopene protected the prostatic epithelium from reactive oxygen species produced by such inflammation. No epidemiological data is available to

support this, with no evidence of a raised incidence of prostatitis in cancer patients. A further explanation extrapolated from work in mammary cells by Karas *et al*⁷¹ suggests lycopene may inhibit IGF-mediated cell proliferation.

1.2.3.6.4 Selenium

Selenium is a trace mineral that forms a component of the antioxidant glutathione peroxidase. Van den Brandt *et al* demonstrated lower cancer mortality rates from certain cancers in areas with high soil selenium concentrations⁷². Although Clark *et al*⁷³ found no reduction in risk for skin cancer, which was their primary study area; they did find an incidental decrease in CaP risk. Yoshizawa *et al*⁷⁴ reproduced this finding as part of the Health Professionals Follow-Up Study. They demonstrated a 50% reduction in CaP risk for those patients with the highest levels of selenium in their toenails pre-diagnosis versus those with the lowest.

1.2.3.6.5 Vitamin E

A further antioxidant, Vitamin E (α -tocopherol), protects cell membranes from free-radicals. The proapoptotic and antiproliferative effects seen with *in vitro* studies⁷⁵ have been further demonstrated *in vivo* by a prospective trial from Finland. Investigating the role of Vitamin E supplements on lung cancer incidence, the investigators showed a 32% decrease in CaP incidence and a 41% decrease in CaP mortality versus placebo⁷⁶. Heinonen *et al* were looking at a population of smokers and

other groups studying non-smokers have failed to show any benefit to Vitamin E supplementation ⁷⁷ suggesting further studies are required.

1.2.3.6.6 Vasectomy

Studies have not led to any final conclusions about the risks related to vasectomy. Giovannucci *et al* reported an increased relative risk of 1.6 of CaP in men who had undergone a vasectomy ⁷⁸. Stanford *et al* ⁷⁹ failed to demonstrate such a relationship. Once more, further studies are required to firm up the debate. Postulated hypotheses for mechanisms via which vasectomy confers a raised CaP risk include; the presence of antisperm antibodies, decreased prostatic secretions and decreased androgen concentrations within the semen.

1.2.3.6.7 Sexual Activity

Honda *et al* ⁸⁰ suggested that those with a greater number of sexual partners, or those who had become sexually active earlier in life, had a greater risk of CaP because of the greater risk of exposure to infectious agents. Human papilloma virus (HPV) is linked with cervical cancer in females. However, Wideroff *et al* ⁸¹ found no evidence of HPV or Chlamydia in CaP specimens. Compared with controls, studies have suggested those individuals with; greater sexual drive yet lower actual sexual activity ^{82, 83}; earlier age of puberty and later age of first intercourse ⁸³ have higher incidence rates of CaP. Married men appear to have lower mortality rates.

1.2.3.6.8 Smoking

Whilst cigarette smoking is a risk factor in other epithelial cancers such as lung or bladder cancer, arguments have been proposed for⁸⁴ and against^{85, 86} its role in CaP.

1.2.3.6.9 Alcohol Consumption

Breslow's hypothesis⁸⁷ that heavy alcohol intake decreased CaP incidence was based on the theory alcohol would raise the oestrogen, and decrease the testosterone levels circulating. However, as discussed previously, the evidence for androgens initiating cancer is limited and, once more, the experimental data has not supported the hypothesis.

1.2.3.6.10 Height

Chan *et al*⁵⁴ have demonstrated an initiating role for IGF-1 in CaP and, as IGF-1 correlates with height, it has been proposed that taller men are at higher risk. Once again data is mixed with both positive⁸⁸ and negative⁸⁹ studies reported.

1.2.3.6.11 Weight

Snowden *et al*⁹⁰ found CaP mortality was 2.5 times greater in overweight men. Other studies, as with many of the risk factors discussed, have provided a counterargument though disputing this^{91, 92}.

1.2.3.6.12 Occupation

Finally, studies have attempted to examine the relationship between CaP risk and french polishers, engine drivers, river workers, coal miners and chemists. However, the only occupation with any form of consistency was agriculture ⁹³. A Canadian study ⁹⁴ showed this correlated with the number of acres sprayed with herbicides.

1.2.4 Natural History

Some tumours are clinically evident, producing lower urinary tract symptoms, complications of metastatic disease or death. Others remain clinically latent and are only detected at post mortem or after histological examination of specimens resected for apparent benign disease ^{95, 96}.

Autopsy studies have revealed the high incidence of CaP in asymptomatic individuals who had died from other causes ^{97, 98}. Latent disease has been reported as being present in as many as 30% of the prostates of 50 year old men and 75% of individuals over 80 years of age ⁹⁹. Whilst it has been suggested that this latent disease actually represents a less aggressive sub-type of CaP ¹⁰⁰, this is not currently known and authors have warned of the malignant potential of such tumours ^{101, 102}. It could be argued that the finding of undiagnosed disease at autopsy is infact merely an artefact and that those individuals would have developed clinically significant disease if they had lived long enough.

Series from the era before PSA testing have provided valuable data on the natural history of CaP in populations treated expectantly by active surveillance. George ²¹ prospectively observed a group of 120 CaP patients (mean age 74.8 years) with no evidence of bone metastases on isotope bone scan at diagnosis. All were treated conservatively. A disease-specific survival of 80% and 75% at five and seven years respectively was reported and this corresponded to a rate of 13% at five years for those with metastases at diagnosis. Eighty-four percent had palpable local disease progression and this high rate has been corroborated by other investigators. Adolfsson *et al* ¹⁰³ also looked at patients with no evidence of metastases managed by active surveillance and showed 67% disease progression at five years. McLaren *et al* ¹⁰² also reported such stage progression with 40% of patients with stage one (T1) and 51% with stage two (T2) demonstrating palpable local disease progression. Importantly, although local progression rates are high, these studies provide evidence to demonstrate that not all prostatic carcinomas need treatment. George suggested a positive bone scan at diagnosis provided the most reliable predictor of cancer-related death.

In a large study of 11,500 cases of localised CaP reported to the Finnish Cancer Registry, Adolfsson ¹⁰⁴ reported that the disease-specific survival rate reached a plateau at 30% after 23 years follow up. Of those patients with localised disease that did die, more than 50% died from other causes. The proportion of patients dying from CaP decreased with time and was only 5% in the group that survived 10 years or more. Johansson *et al* looked at all cases of localised CaP in one county in

Sweden over a 15 year period. This study revealed lower rates of local disease progression (33%) but strikingly similar rates of metastasis (13%) and disease-specific mortality (11%) to previous series. Interestingly, compared with 80 year olds, men younger than 61 years had a higher metastasis rate (36% vs. 5%) and mortality (44% vs. 25%).

Less favourable outcomes were seen in the study by Aus *et al*¹⁰⁵. Aus studied 514 patients from diagnosis until death and revealed that the mortality rate in those patients with no metastases at diagnosis and those surviving greater than ten years was surprisingly high at 50% and 63% respectively. However, once adjusted for the grade of tumour, only those cases with high grade CaP had poor survival rates. A meta analysis of 828 conservatively treated patients with localised disease again highlighted the importance of tumour grade and patient age in determining outcome¹⁰⁶. A Cox regression analysis found that an age of less than 61 years and poorly differentiated tumour at histological diagnosis had a significant negative impact on disease-specific survival. The ten year disease-specific survival was lower for those with high grade tumours (34%) compared with those individuals with well and moderately differentiated disease (87%). Furthermore, metastasis-free survival was worse in those with high grade disease (26%) compared with the well differentiated group (81%). Subsequently, interrogation of the SEER database of 19,898 cases of CaP treated conservatively for ten years, has consolidated these results with disease-specific survival clearly being inversely linked to tumour grade¹⁰⁷.

The majority of these studies are from the period prior to the widespread adoption of PSA testing and as a consequence the contemporary natural history of CaP remains unclear. Deciding on which tumours will become significant, and potentially dangerous as a consequence, remains one of the diagnostic challenges facing clinicians. The aforementioned studies have demonstrated that young age, high stage disease, high grade tumours and the presence of metastases at diagnosis all have a negative impact on CaP survival. However, it has become increasingly clear that the use of PSA has not helped address this problem. PSA testing is believed to have increased the lead time of up to 14 years^{108, 109}. This creates an additional dilemma for clinicians. Despite the potential advantage conferred by an early CaP diagnosis, the situation is complicated by decisions about which of these early cancers require aggressive radical treatment rather than active surveillance and consequently which cases are deemed sufficiently high risk to warrant exposure to the potential side effects associated with radical treatments.

1.2.5 Pathology

1.2.5.1 Adenocarcinoma

Adenocarcinoma is the major histological subtype seen in CaP. The epithelial cells form a single layer, unlike the double layer seen in BPH. Macroscopically tumours are yellow or grey coloured and are firm or gritty to palpation⁹⁹. Microscopic examination of the cells reveals the presence of cytoplasmic lipid, which accounts for the yellow colouring, and may often show evidence of mucin production. Seventy percent of

CaP develops in the peripheral zone ¹¹⁰. As a precursor for invasive adenocarcinomas, this is consequently also where high grade prostatic intraepithelial neoplasia (PIN) tends to be found. Twenty-five percent of tumours arise in the transitional zone ¹¹⁰. High grade PIN can be seen in the transitional zone but much less frequently ¹¹¹. Unilateral tumours detected by digital rectal examination (DRE) are actually subsequently found to be bilateral when examined histologically in 70% of cases. Eighty-five percent of adenocarcinomas diagnosed are actually multifocal although the other tumours tend to be small, low grade and clinically insignificant ^{112, 113}. Spread of CaP may be direct to the surrounding stroma and involve the bladder base and urethra. Extra-prostatic extension can involve the seminal vesicles and pelvic sidewalls. The rectum can also be invaded but Denonvillier's fascia provides some degree of protection from this.

Lymphatic metastasis usually involves the internal iliac, obturator and para-aortic lymph nodes, though external iliac, presacral and even inguinal groups may also more rarely be affected. Haematogenous metastatic spread can involve the lungs (usually asymptomatic) and liver but, most commonly, spread is to the skeleton, due to predilection for red marrow ¹¹⁴. The lumbosacral spine and pelvis are the most common anatomical regions for skeletal metastasis and may, occur from retrograde flow through the lumbosacral and pelvic venous systems.

1.2.5.2 Prostatic Intraepithelial Neoplasia

The term PIN describes prostatic acini or ducts that appear architecturally benign but contain cytologically atypical cells ¹¹⁵. The expression of various biochemical markers in high grade PIN has been shown to be either the same as in invasive cancer, or to lie somewhere between benign and malignant tissue ^{116, 117}. PIN has been suggested as a precursor of invasive prostatic adenocarcinomas ¹¹⁸. Despite this there is little data on the natural history of high grade PIN. Unlike in other organ models, the prostate does not lend itself well for determining whether there is invasive cancer at the site of high grade dysplasia, or whether carcinoma has developed in its immediate vicinity. As a consequence there is a reluctance to apply the term "carcinoma in situ" to PIN. Instead it may be more appropriate to state there is an association between the cytological and invasive phenotypes. This may not be entirely causative but induced by a common pathological field change to the gland. This association appears stronger in intermediate to high grade peripheral zone cancers.

Currently, PIN detection within a specimen has no prognostic implications. When pre-invasive disease is noted in other solid tumours, such as Ductal Carcinoma in Situ in breast malignancy, clinicians ask the question; "when shall invasive disease develop?" Evidence of isolated PIN should instead raise the question; "is invasive disease already present and have sampling techniques so far just failed to prove it?" ⁷. Studies have suggested that, in patients diagnosed with high

grade PIN alone at their initial biopsy, 23% to 50% were found to have concomitant invasive disease on re-biopsy ¹¹⁸⁻¹²¹. Monitoring of disease with PSA is not a viable option as PSA is not raised by high grade PIN ¹²².

No additional risk of invasive cancer detection has been proven when patients with low grade PIN were compared with controls matched for age and serum PSA concentration ^{123, 124}.

1.2.5.3 Histological Grading

Grading systems are used as a tool for assessing tumour aggression and prognosis. The Gleason grading system and score have been widely adopted in the assessment of CaP (Figure 1.5) ¹²⁵. Assessed at relatively low magnification, the pathologist reviews the glandular architecture of the specimen and scores the prostatic tissue between one (most differentiated) and five (least differentiated). Gleason patterns one and two are characterised by well-defined uniform nodules containing single glands of medium size in close approximation. In Gleason grade three disease, glands are usually smaller and their shape is more variable. At this level glands start to invade surrounding non-neoplastic tissue. Gleason pattern four glands are no longer single but instead are large, irregular and cribriform. It is particularly important to recognise Gleason pattern four as it is associated with a significantly poorer prognosis than Gleason pattern three ¹²⁶. Glands in Gleason pattern five disease demonstrate no differentiation and instead, solid sheets, nests or cords of tumour with central comedonecrosis are seen.

PROSTATIC ADENOCARCINOMA (Histological Patterns)

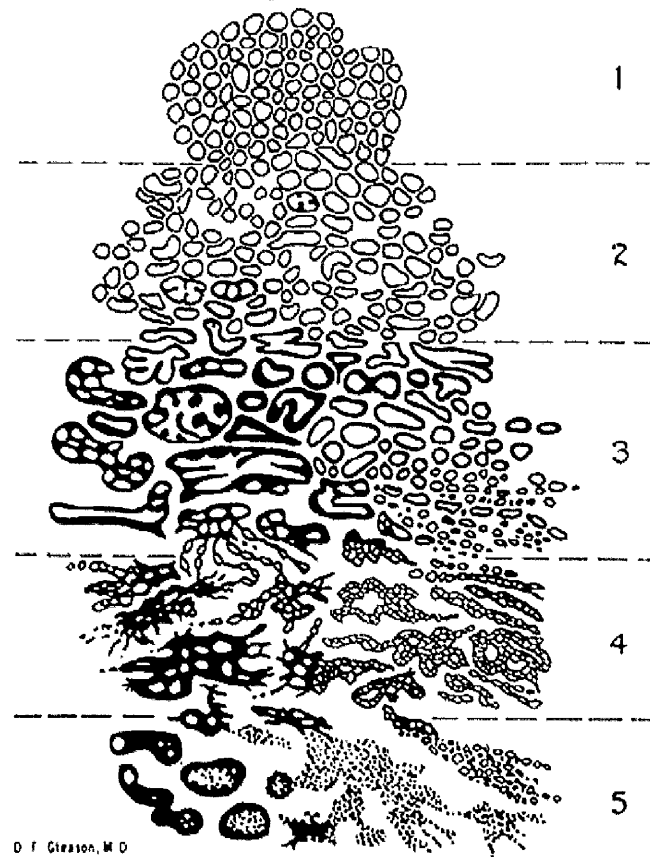


Figure 1.5: Dr D.F. Gleason's original diagram demonstrating the histological pattern to each of the five Gleason grades.

To be counted, the Gleason pattern must occupy at least five percent of the biopsy tissue. The Gleason score is the sum of the first and second most prevalent grades by area. For example, a Gleason score of 4+3=7 indicates that the most dominant grade is four, and that the second commonest is three. If the tumour is homogeneous then the score is the product of the grade being doubled, for example 3+3=6. In tumours made up of two different tissue grades, Gleason showed that the prognosis fell between that of each grade individually. Rather than attribute an incorrect prognosis to the tumour, the Gleason score was developed. Gleason scores can range from two (1+1) to ten (5+5). Long term follow-up studies have demonstrated that Gleason scores offer an effective means of prognostic assessment ^{125, 127}.

Interobserver variability is generally at an acceptable level for the Gleason grading system. Although biopsy-defined grades have been shown to correlate well with histology reports post radical prostatectomy (RP) ¹²⁸⁻¹³⁰, problems can arise with the interpretation of needle biopsy material. Sampling error may induce erroneous assessment of grade. Under-grading of a specimen has a greater potential for clinical impact. It has been suggested that combined Gleason scores between two and four should be avoided for biopsy specimens as; firstly many are incorrectly low and are actually five or six when reviewed by a pathologist specialising in urological oncology and secondly; combined scores of between two and four are not reproducible. Abandoning their use prevents clinicians making the false assumption of a tumour being low grade and treating inappropriately ¹¹².

1.2.5.4 Staging of Disease

The 2002 Tumour Node Metastasis (TNM) classification of CaP is the most commonly utilised system of staging in clinical practice (Table 1.1)

131

1.2.6 Clinical Features and Diagnosis

1.2.6.1 Symptoms and Signs

As the peripheral zone of the prostate is most commonly affected by neoplasia, patients may have no significant lower urinary tract symptoms at all. If the tumour is sufficiently large, or if it is directly invading the urethra, patients may develop haematuria or symptoms suggestive of bladder outflow obstruction. Invasion of the ejaculatory ducts may cause symptoms such as haemospermia or decreased ejaculate volume. Locally advanced tumours may invade the periprostatic neurovascular bundles causing impotence.

Alternatively, patients may present with advanced disease and symptoms of metastasis such as bone pain, pathological fracture or lower limb oedema. Leucoerythroblastic anaemia can develop in cases where extensive infiltration of the bone marrow with tumour replacing the normal haemopoietic tissue. Furthermore, tumour-induced fibrinolysis may cause patients to develop bleeding tendencies.

Stage	Definition
Primary Tumour	
Tx	Primary tumour cannot be assessed
T0	No evidence of primary tumour
T1	Clinically, the tumour is neither palpable nor visible with imaging
T1a	Tumour is an incidental histologic finding in 5% or less of tissue resected
T1b	Tumour is an incidental histologic finding in more than 5% of tissue resected
T1c	Tumour identified with needle biopsy (eg, because of an elevated PSA level)
T2	Tumour confined within the prostate
T2a	Tumour involves one half of one lobe or less
T2b	Tumour involves more than one-half of one lobe but not both lobes
T2c	Tumour involves both lobes
T3	Tumour extends through the prostate capsule
T3a	Extracapsular extension (unilateral or bilateral)
T3b	Tumour invades seminal vesicle(s)
T4	Tumour is fixed or invades adjacent structures other than seminal vesicles
Regional Lymph Nodes	
Nx	Regional lymph nodes were not assessed
N0	No regional lymph node metastasis
N1	Metastasis in regional lymph node(s)
Distant Metastasis	
Mx	Distant metastasis cannot be assessed (not evaluated with any modality)
M0	No distant metastasis
M1	Distant metastasis
M1a	Nonregional lymph node(s)
M1b	Bone(s)
M1c	Other site(s) with or without bone disease

Table 1.1: The 2002 Tumour Node Metastasis (TNM) classification of CaP (Sobin 2002).

1.2.6.2 Mode of Presentation

Until the late 1980s, the majority of cases of CaP were diagnosed following investigation for symptoms of bladder outflow obstruction ²¹. Contemporary practice has been changed by the introduction of widespread serum PSA testing. Although no formal screening programme has as yet been introduced in the UK, patients often present as a consequence of finding a raised serum PSA concentration or as an incidental finding on DRE.

1.2.6.3 Screening for Prostate Cancer

Some observers have attributed the fall in CaP mortality to the introduction of widespread serum PSA testing in the early-1990s ¹³². Utilising PSA testing, regional screening programmes have shown substantial decreases in mortality compared with national trends. Bartsch *et al* showed a significantly higher fall in CaP mortality in Tyrol, where PSA screening was freely available and encouraged, compared to the rest of Austria which did not employ the test ¹³³. The Olmsted County study from Minnesota, USA, showed a 22% reduction in CaP mortality for the period 1993-1997 compared with the period prior to widespread PSA testing (1980-1992) ¹³⁴. The only randomised prospective study of CaP screening thus far has been the Quebec study which aimed to assess the impact of screening on cause-specific death in 46,193 men between 1989 and 1996. The group reported a 69% reduction in CaP mortality amongst the screened population. However, the study has since been criticised for not analysing the data on an intention to screen

basis thus reporting mortality rates in those that received screening rather than those that had initially been assigned to the screening group ¹³⁵.

Whilst PSA screening may increase the proportion of newly-diagnosed disease that is localised and thus amenable to definitive treatment ¹³⁶, the argument against the adoption of widespread PSA screening is that a greater number of indolent localised low grade tumours would be detected. In turn, this would lead to an unnecessary psychological burden for some patients and the potential for over treatment of low risk cancers with the additional co-morbidity this would confer ¹³⁷. In a retrospective population-based cohort study, Albertsen *et al* ¹³⁸ reported on the 20-year survival of 767 men with localised CaP treated with active surveillance or androgen withdrawal therapy alone. They showed a minimal risk of dying from low risk CaP (Gleason score two to four) and an intermediate risk with Gleason scores of five or six over a period of 20 years follow up. They highlighted that mortality rates remained stable 15 years on from diagnosis and proposed the notion that localised low risk CaP did not warrant aggressive treatment.

The current recommendations from the various worldwide representative organisations are divided. The US Preventative Services Taskforce ¹³⁹ has stated that it does not recommend the routine use of DRE, PSA and biopsy as screening methods. The American Urological Association (AUA) acknowledge the current air of uncertainty surrounding widespread screening but recommend an annual serum PSA and DRE for men over 50 years of age (over 40 years if deemed high risk) with a

life expectancy of more than ten years ¹⁴⁰. The European Association of Urology (EAU) state that men over 50 years of age have the right to know about screening but at the “present time, there is a lack of evidence to support or disregard widely adopted, population-based screening programmes for early detection of CaP aimed at all men in a given population” ¹⁴¹. In the UK, the National Screening Committee, working on behalf of the National Health Service, decree that “prostate cancer screening should not be introduced” but that “prostate cancer screening can be provided on request, provided that the man fully understands the lack of good quality evidence about the benefits and risks of testing” ¹⁴².

The reports of large randomised studies from both sides of the Atlantic are eagerly awaited. The ProtecT study from the UK, the Prostate, Lung, Colorectal and Ovary (PLCO) study from America and the European Randomised Screening for Prostate Cancer (ERSPC) study, will hopefully address the current controversies and provide definitive guidance as to the most appropriate usage of serum PSA in CaP screening.

1.2.6.4 Diagnosis

Clearly, histological confirmation is required to secure a diagnosis of CaP and this is usually achieved by transrectal ultrasound (TRUS) guided biopsy of the prostate. Currently, the commonest indication for proceeding to TRUS and biopsy of the prostate is either an abnormal finding on DRE or a raised serum PSA or both. As yet, no accurate form

of radiological imaging is available to reliably detect the presence of extraprostatic spread. As a consequence, nomograms that utilise the combination of DRE, PSA and biopsy histology (Gleason score) are relied upon to calculate the likelihood of patients being amenable to definitive therapies for localised disease for example Partin's tables ¹⁴³. The common tools utilised in the diagnosis and investigation of CaP are discussed in this section.

1.2.6.4.1 Prostate Specific Antigen

PSA is a 33kD protein which is a member of the kallikrein serine protease family. Its physiological role is to liquefy the seminal coagulum ¹⁴⁴. It is secreted almost exclusively by the prostatic epithelium. There is significant debate surrounding which scientist can be credited with its introduction ¹⁴⁵. PSA is detectable at relatively high concentrations in the semen (mg/ml) but to a much lesser degree in the serum (ng/ml).

Conventional testing methods relate to the serum concentration where PSA circulates as both free PSA and bound forms complexed with the antiproteases alpha₁-antichymotrypsin (ACT) and alpha₂-macroglobulin (MG). Free PSA is inactive in the serum and contributes 10%-35% of the immunodetectable PSA load. The remainder detectable by conventional assays is bound to ACT (65%-90%). Free PSA is thought to be renally excreted ¹⁴⁶ and has a shorter half-life of 2 to 3 hours ¹⁴⁷ compared to the hepatic clearance ¹⁴⁸ of complexed PSA which is longer at 2 to 3 days ¹⁴⁹.

PSA is organ-specific, not disease-specific. It is by no means diagnostic of cancer and may be raised in non-cancerous disease states such as BPH, prostatitis and urinary tract infection as well as following prostatic manipulation or instrumentation. Ideally patients should be free from active urinary tract infection, have refrained from ejaculation and vigorous exercise for 48 hours and not undergone TRUS and biopsy for 6 weeks prior to testing. DRE does not appear to significantly raise the PSA ^{150, 151}. Androgens strongly influence PSA expression ^{152, 153} and indeed the use of 5 α -reductase inhibitors in the treatment of benign prostatic hypertrophy can reduce PSA levels to 50% of the pre-treatment level within the first 12 months of therapy ¹⁵⁴.

A normal PSA does not exclude CaP. Large studies have suggested that up to 18% of patients with CaP would have been missed if PSA detection alone was used ^{155, 156}. However, the positive predictive value of PSA is superior to that of DRE alone ¹⁵⁵. It is therefore accepted practice that both modalities are used for detection.

1.2.6.4.2 Prostate Specific Antigen Threshold

The precise threshold at which a prostatic biopsy should be recommended is controversial. PSA testing is further complicated by the difficulty in defining an acceptable normal range. Oesterling *et al* suggested an age-specific reference range for PSA in 1993 of 0-2.5ng/mL for men aged 40-49 years, 0-3.5ng/mL for 50-59 year olds, 0-4.5ng/mL for those aged 60-69 years and 0-6.5ng/mL for 70-79 year olds ¹⁵⁷. This recommendation has become widely adopted in the UK

though interim guidance from the National Health Service's CaP Risk Management Programme is that patients should be offered further investigation of a PSA greater than or equal to 3.0 if aged 50-59 years; greater than or equal to 4.0 if aged 60-69 years and greater than or equal to 5.0 if aged 70 years or more ^{158, 159}.

A caveat to the application of a limit at which biopsy is recommended, is that those individuals below the limit may still have cancers. Many studies have used a PSA limit of greater than or equal to 4.0ng/ml. A US prevention study ¹⁶⁰ defined the risks of cancer as being from 6.6% for PSA values between 0 and 0.5ng/ml and 26.9% for values between 3.1 and 4.0ng/ml in a patient cohort of 2950 men aged 62-91 years.

Lowering the cut-off for biopsy may not increase the detection of clinically significant cancers though ¹⁶¹. Long term data is still required to determine the PSA threshold for biopsy required to identify non-palpable but clinically significant CaP. To this end, a number of modifications of the serum PSA value have been proposed to aid PSA specificity in the diagnosis of early and clinically important CaP from benign disorders.

1.2.6.4.3 Prostate Specific Antigen Density

A large proportion of individuals have a moderately raised PSA between 4ng/ml and 10ng/ml and this probably relates to the high incidence of BPH in the population. In patients where DRE or TRUS fails to provide any indication for further investigation, PSA density may help delineate between those patients with large prostates and thus higher PSA levels

and those with a high PSA because of a malignant process. In 1992, Benson *et al*¹⁶² introduced the idea of PSA density, which is calculated by dividing the PSA reading by the prostatic volume defined by TRUS. Several studies have now documented predictive relationships between the risk of cancer and a PSA density of 0.15 or greater¹⁶³⁻¹⁶⁵. Such thresholds may still not be absolute but help with the risk assessment of patients regarding the indication for proceeding to biopsy and indeed re-biopsy.

1.2.6.4.4 Prostate Specific Antigen Velocity

Changes in PSA between measurements are usually physiological. The rate of change of PSA is the change in PSA per unit time and is known as the PSA velocity. Described by Carter *et al*¹⁶⁶ in 1992, an increase of 0.75ng/ml per year was associated with a higher risk of CaP. Secondly, in the five years prior to a diagnosis of prostate disease, when PSA levels were normal, PSA rises were greater in those who subsequently developed cancer.

In a large prospective screening study, Smith and Catalona¹⁶⁷ demonstrated that the cancer detection rate was 11% if the PSA velocity was less than 0.75ng/mL/year but 47% if more than 0.75ng/mL/year. Furthermore the specificity of PSA velocity was reported as high, with less than 5% of men without CaP having a PSA velocity more than 0.75ng/mL/year. A cut-off for performing a biopsy of 0.75ng/mL/year was again shown by Carter and colleagues to be sensitive and specific for CaP. However, sensitivity decreased to only 11% at PSA concentrations

less than 4ng/ml compared with 79% between 4ng/ml and 10ng/ml. At least 3 separate measurements over 18 months have been suggested as the time period over which PSA velocity should be calculated to optimise cancer detection accuracy rates ¹⁶⁶⁻¹⁶⁹.

1.2.6.4.5 Free: Complexed Prostate Specific Antigen Ratio

It has been demonstrated that the constituent parts of a CaP patient's circulating PSA are made up of a greater proportion of PSA bound to the protein ACT. Low free to bound serum PSA levels are therefore seen in CaP ^{155, 170, 171}. Studies have proposed many different ratio levels from their individual study cohorts. Variation amongst these populations has hampered the definition of a consensus for a single recommended threshold ratio for subsequently proceeding to biopsy.

1.2.6.4.6 Digital Rectal Examination

The majority of cancers are situated in the peripheral zone and may therefore be palpable rectally. The positive predictive value of DRE is low in those individuals with PSA values of less than 4.0ng/mL ¹⁶⁰.

Elgamal *et al* reviewed 100 Radical Prostatectomy (RP) specimens and suggested that between 11% and 26% of patients with T1c disease had insignificant cancers. The reliability of DRE is called into question by the finding from the same study that between 18% and 49% of the tumours staged as T1c pre-operatively actually had evidence of locally advanced disease on final histology ¹⁷².

1.2.6.4.7 Needle Core Biopsy

Initial studies suggested it was acceptable to perform limited biopsies of palpable nodules in patients with a PSA of greater than 10ng/ml ¹⁷³ but that detection rates were increased with a more extensive biopsy.

Sextant biopsies were introduced by Hodge *et al* as a method for achieving this ¹⁷⁴. Laterally-directed biopsies have optimised the cancer detection rate by targeting the peripheral zone where the majority of cancers are harboured ¹⁷⁵. The cancer detection rates at primary biopsy appear to increase with a larger number of biopsies ¹⁷⁶. Whilst the precise number of biopsies to be performed remains a controversial issue it appears that systematic biopsy of the peripheral zone, at least initially, is of the most importance. Usually patients undergo twelve biopsies, taken under ultrasound guidance in a bilateral para-sagittal distribution from the base, mid-gland and apex laterally and then more medially ⁷.

If primary biopsies demonstrate benign histology but an indication for biopsy persists, many clinicians offer a second biopsy. Djavan *et al* found that the majority of clinically significant cancers were detected with two sets of biopsies ¹⁷⁷. Again no agreement exists as to when no further biopsies are required despite a persistent indication ¹⁷⁸.

1.2.6.4.8 Radiological Imaging

Diagnostic imaging by ultrasound (USS) or computed tomography (CT) scanning helps to identify upper urinary tract obstruction secondary to

bladder outflow obstruction or extensive retroperitoneal lymphadenopathy. TRUS helps quantify the gland size as well as identify any hypoechoic areas suggestive of neoplasia.

Metastatic bone disease often appears as osteosclerotic lesions on plain radiographs. Radiological appearances can be similar to those of Paget's disease. An isotope bone scan is useful in determining the nature of bone disease and helps identify subclinical lesions.

Standard CT or magnetic resonance (MR) cross-sectional imaging have no advantage over TRUS in the staging of CaP and specifically in the determination of whether disease is localised and therefore amenable to curative treatment^{179, 180}.

1.2.7 Prostate Cancer Treatment

The available treatments for localised CaP have not all been subjected to randomised clinical trials. The optimal treatment is therefore still unknown. Considerations to be made during the decision making process include the likely natural history of the individual cancer after risk stratification, patient factors such as age, comorbidity and life expectancy and patients' expectations and desired outcomes.

1.2.7.1 Active Surveillance

Active Surveillance (AS) of CaP as a treatment strategy has also been termed watchful waiting and active monitoring. It encompasses the careful follow up of patients with close disease monitoring with

postponement of treatment until there is sufficient evidence that treatment is required.

1.2.7.1.1 Active Surveillance in Localised Prostate Cancer (T1-T2, Nx-N0, M0)

In patients with localised CaP amenable to curative therapy (T1-T2, Nx-N0, M0), there may be a desire to defer curative treatments, with their risk of comorbidity, until there is a clearer indication that the disease is likely to be clinically significant (either rising PSA, deteriorating histopathological or DRE findings). Clearly this has a risk of missing the time window whereby curative therapy is possible. Many papers have examined data in an attempt to stratify this risk. Albertson *et al*¹⁸¹ re-evaluated biopsy specimens and defined the risk of death from CaP. Their findings agreed with those on stage T1a disease by other authors¹⁰⁶ that cancer specific mortality increased with higher tumour grades and was very high at Gleason scores seven to ten, intermediate in Gleason 6 scores and low in Gleason scores two to five. The 15-year risk of dying in this cohort of patients aged 55 to 74 years of age was defined. The cancer-specific mortality compensates for differences in competing mortality and therefore indicates the outcome if the patient lived 15 years. The rates increased with grade and were 8% for Gleason scores of between two and four; 14% for Gleason scores of five; 44% for Gleason scores of six; 76% for Gleason scores of seven and 93% for Gleason scores of between eight and ten¹⁸¹.

Clearly, if this treatment option is going to be used in younger patients, with an otherwise good life expectancy, accurate initial staging and grading must be performed to ensure that more advanced or more poorly differentiated disease has not been missed. Griebeling and Williams¹⁸² have advocated the re-evaluation of patients, particularly the younger ones, with PSA examination, TRUS and biopsy. Moreover, those with otherwise good life expectancies (of greater than 10 years) appear to have a higher mortality without intervention^{105, 183, 184}. Despite having well and moderately differentiated localised CaP, the patients in the study by Johansson *et al*¹⁸⁵ had a worse mortality rate if left untreated.

A prospective randomised controlled trial comparing RP with AS demonstrated an improved disease-specific mortality for patients assigned to the RP treatment arm¹⁸⁶. In terms of hormonal therapy it appears satisfactory to withhold treatment until disease progression occurs, despite one study¹⁸⁷ suggesting some improvement in early institution of hormonal manipulation.

1.2.7.1.2 Active Surveillance in Locally Advanced Prostate Cancer (T3-T4, Nx-N0, M0)

There is little data available on this patient group. A study of 50 patients with well and moderately differentiated T3 tumours concluded that, with five and ten year survival rates of 90% and 74% respectively, watchful waiting may still be a viable option for those patients without aggressive disease (poorly differentiated) and life expectancies of less than 10

years ¹⁸⁸. Some authors have demonstrated that there is no survival advantage in instituting hormones prior to development of metastases ^{189, 190} however, a large randomised Medical Research Council (MRC) trial ¹⁹¹ did suggest a survival benefit after immediate institution and this was reinforced by a trial comparing bicalutamide 150mg with placebo which also suggested early treatment had an improved progression free survival ¹⁹².

1.2.7.1.3 Active Surveillance in Metastatic Prostate Cancer (M1)

The consensus is that AS should only be pursued in such patients when there is an asymptomatic patient with a specific desire to avoid the potential side effects of treatment and then close observation for deterioration should be ensured ¹⁹³. The term “watchful waiting” is often used in these circumstances.

1.2.7.2 Radical Prostatectomy

Radical prostatectomy involves the excision of the entire prostate gland with the adjacent seminal vesicles between the urethra and base of the bladder. The two classical procedures are the retropubic prostatectomy (RRP), first performed by Memmelaar and Millin ¹⁹⁴, and the transperineal prostatectomy described by Young ¹⁹⁵. Increasingly, experience is being gained in laparoscopic approaches. RP is the only curative treatment modality for localised CaP that has been demonstrated to have an improved survival benefit compared with AS

alone ¹⁸⁶. The RRP is more popular than the perineal approach because of the lower complication rates ¹⁹⁶.

1.2.7.2.1 Radical Prostatectomy in Stage T1a-T1b Prostate Cancer

Although the risk of progression in these stage tumours is low, even stage T1a tumours can progress in 50% of patients after 10-13 years ¹⁹⁷. If the patient is younger, with an expected life expectancy in this region, careful consideration should be given to offering curative treatment.

T1b have >5% of the sampled histological specimen involved with cancer or less with a poorly differentiated tumour. Most patients in this group will show disease progression after five years and therefore should be treated more aggressively. It is therefore of extreme importance to delineate between these two groups and repeat biopsies may be required three months after the original TURP. Whilst definitive treatment in those with greater than 10 years life expectancy is warranted, RP may be too challenging after a thorough TURP ¹⁹⁸, and radiotherapy in such patients may be indicated.

1.2.7.2.2 Radical Prostatectomy in Stage T1c Prostate Cancer

This encompasses the majority of patients undergoing RP. The therapeutic challenge in such patients is to avoid subjecting them to an unnecessary surgical intervention for a lesion that will ultimately be clinically insignificant. The Partin tables may help predict the final stage and thus indicate whether surgical intervention is required ^{143, 199}.

1.2.7.2.3 Radical Prostatectomy in Stage T2 Prostate Cancer

Once disease has reached stage T2a, progression can be expected in 35-55% of patients after five years if no treatment is offered. Stage T2b is still organ-confined but is of greater volume and its five-year progression rate is higher at 70% ²⁰⁰.

RP for stage T2 CaP has a good prognosis in the hands of an experienced operator. Despite the many high grade tumours being found to extend beyond the capsule, and therefore upstaged to T3, after post operative histological examination, those that do remain confined to the prostate have a good prognosis ²⁰¹⁻²⁰³.

In young individuals with a life expectancy greater than 10 years and no significant medical comorbidity, a RP is an excellent option and has been shown to have superior disease-specific mortality rates than watchful waiting.

1.2.7.2.4 Radical Prostatectomy in Stage T3 Prostate Cancer

With the introduction of PSA the proportion of tumours presenting as stage T3 has fallen. The question of whether stage T3 patients should be offered a RP is controversial as such cases are associated with increased rates of incomplete excision, a higher risk of a positive nodal status and higher rates of failure to achieve a curative resection ^{204, 205}.

However, the data studying such groups is somewhat limited ²⁰⁶⁻²¹².

Accuracy in pre-operative determination of clinical stage further complicates decision making with 15% of stage T3 tumours being over

staged (actually stage T2) and 8% being under staged (actually stage T4) ²⁰⁷. The prognosis of the two distinct groups is understandably markedly different.

For stage T3 tumours, 20% will be free of biochemical relapse at five years. Progression is more likely the higher the Gleason score. Seminal vesicle invasion (stage T3b), lymph node involvement, positive resection margins and a high PSA are all independent predictors of a poorer prognosis. As with stage T2 disease Partin nomograms may help the surgeon define the likelihood of the clinical stage and thus the predicted success of surgical intervention ¹⁹⁹.

1.2.7.2.5 Nodal Disease

The previous section regarding RP assumes a negative node status of patients. Those with positive nodes are likely to progress systemically and resection will therefore ultimately fail. Eighty percent 10-year survival rates with simultaneous hormonal therapy have been reported ²¹³ but with disease suitable for RP these rates may actually only signify the effect of the hormones alone. Messing *et al* reported that those patients with nodal metastases who had undergone RP and lymphadenectomy had improved overall survival, CaP-specific survival and progression-free survival when given immediate androgen deprivation therapy compared to those who received treatment only when disease progression had occurred ²¹⁴.

Many surgeons would abort RP if a patient was found to have node involvement macroscopically or on frozen section. If node involvement is only established at histological examination of the specimen, then the fewer positive nodes there are and the presence of microscopic involvement only confer a more favourable impact on prognosis. The timing of adjuvant treatment with hormonal manipulation is determined by the balance of expected side effects associated with long term therapy and the risk of waiting until PSA relapse before instituting treatment ²¹⁵.

1.2.7.2.6 Radical Prostatectomy Complications and Functional Outcome

Davidson *et al* ²¹⁶ quoted a peri-operative mortality rate of 0-1.5%. In terms of morbidity, the rates of urinary incontinence persisting for more than a year postoperatively are 7.7% ²¹⁷. Erectile dysfunction rates have fallen with the introduction of nerve sparing techniques which are available to those patients who are potent pre-operatively and have low-stage, low grade (Gleason score <7 and PSA <10ng/mL) disease. The drawback with such a technique is the potentially increased risk of local recurrence. This risk may be limited by the avoidance of such nerve-sparing procedures in patients with high grade disease, with disease involving the apex and with tumour palpable intra-operatively ²¹⁸⁻²²⁰. For stage T2 disease however, a unilateral procedure sparing the nerve bundle on the contralateral side could be considered ²²¹.

1.2.7.3 Definitive Radiotherapy

Whilst there are no randomised controlled trials comparing external beam radiotherapy (EBR) and RP, the National Institutes of Health's data suggests that EBR offers the same long term survival rates with quality of life levels no worse than surgery^{222, 223}. Technology such as intensity modulated radiotherapy has further advanced three-dimensional (3D) conformal radiotherapy which was introduced in the 1990s. Anatomical data is acquired from the patient whilst in the treatment position. Sophisticated three-dimensional mapping of the targeted volume is then achieved and real-time portal imaging verifies the irradiation field during treatment. Such improvements in accuracy of dose delivery with a surrounding safety zone have allowed for higher doses to be administered without increasing the side effects.

1.2.7.3.1 External Beam Radiotherapy in Localised Prostate Cancer (T1-T2c, N0 M0)

This group of patients can be further sub-divided into low, intermediate and high risk. The low risk group comprises patients with stage T1a-T2a, N0, M0 disease with a Gleason score of less than or equal to six and a PSA of less than or equal to 10ng / mL. A study by Hanks *et al* was unable to demonstrate a statistical advantage in escalating the dose from the recommended 70Gy-72Gy²²⁴.

Patients with stage T2b disease, PSA between 10 and 20ng / mL or a Gleason score of 7 fall into the intermediate risk group. Defining their

intermediate risk group by a PSA range of 10.0-19.9 ng / mL, Hank *et al* showed significant improvements in the proportion of patients that were free of clinical or biochemical evidence of disease at five years. Treated with 76Gy, 75% of patients were relapse-free at five years compared with only 35% at a dose of 70Gy ($p=0.0049$)²²⁴. The MD Anderson Cancer Centre randomized study compared the escalated dose of 78Gy delivered by the 3D conformal radiotherapy unit with 70Gy of the standard radiotherapy. Three hundred and five patients with pre-treatment PSA of greater than 10 ng/mL and stage T1-T3 were followed up for median of 40 months and were demonstrated to have a significantly improved freedom from failure rate at five years when they received 78Gy instead of 70Gy (75% versus 48% $p=0.01$)²²⁵. Although a greater proportion of the patient group had lower stage disease (T1b-T2b) and lower PSA levels (<15 ng / mL) than the study by Pollack *et al*, the interim analysis of 393 patients by Zietman *et al* also suggested a significantly lower ($p=0.00001$) biochemical failure rate with dose escalation from 70.2Gy to 79.2Gy²²⁶. A dose escalation to 78Gy in this group is recommended by the EAU²²⁷.

For the high risk patient group (T2c, Gleason score >7 or PSA >20 ng /mL), five year biochemical relapse rates are improved by dose escalation and Pollack again demonstrated this. However, it appears that dose escalation is insufficient alone to prevent relapse outside of the pelvis. Studies have looked at the use of adjuvant hormone manipulation to try and redress this. A prospective randomised trial by D'Amico *et al* in 2004 demonstrated that, in a patient group of 206 patients with similar

high risk characteristics; rates of survival; cancer-specific mortality and survival without the need for salvage androgen deprivation were all significantly improved if patients received adjuvant hormone manipulation with the radiotherapy ²²⁸. Prophylactic irradiation of pelvic lymph node chains has not gained widespread popularity after the randomized controlled trials held in the 1970s and 1980s. The Radiation Therapy Oncology Group (RTOG) study ²²⁹ and the Stanford study ²³⁰ showed that no improvement in survival or local recurrence was achieved with irradiation of the pelvic nodes.

1.2.7.3.2 New techniques in Radiotherapy Administration

Intensity modulated radiotherapy allows for increased doses to be applied to the target volume. Excellent relapse-free survival rates have been reported with acceptable toxicity rates ²³¹. This technology has led the movement towards hypofractionated therapy. More targeted treatment with lower doses is delivered over shorter treatment times ²³².

Bolla et al conducted a randomised prospective trial to compare EBR alone and EBR and adjuvant goserelin in patients with locally advanced CaP. Overall 5-year survival (79% vs. 62%) and disease-free survival (85% vs. 48%) were both significantly improved in the cohort receiving adjuvant hormones ²³³.

1.2.7.3.3 Brachytherapy

The joint consensus of the European Society for Therapeutic Radiology and Oncology (ESTRO), the EAU and the European Organisation for

Research and Treatment of Cancer (EORTC) is that trans-perineal brachytherapy is a safe and efficient technique for patients with localised low volume disease, an initial PSA less than or equal to 10 ng / mL, a Gleason score of less than 7, a prostatic volume of 50cm³ or less and a good international prostatic symptom score (IPSS) ²³⁴. The brachytherapy seeds are introduced under rectal sonographic guidance. For permanent implants, Iodine-125 granules (160Gy) are usually implanted though Palladium-103 may be used for more aggressive, more poorly differentiated tumours (120Gy). In a study of 2991 consecutive patients with localised (T1-T2) CaP similar 5 year biochemical failure rates were seen for RP, high-dose EBR and permanent brachytherapy seed implantation ²³⁵.

1.2.7.3.4 Toxicity

The pelvic irradiation required to treat the prostate can potentially be complicated by toxicity to adjacent organs, namely bladder and rectum. A large randomized prospective EORTC trial (22863) ²³⁶ looked at the long term toxicity from irradiation in 377 patients with T3-4 CaPs. Eighty-six of them (22.8%) had greater than or equal to grade-two toxicity relating to urinary, rectal or leg oedema complications (72 (19.1%) grade-two, ten (2.7%) grade-three, four (1.1%) grade-four (fatal)). Overall, genitourinary toxicity was more prevalent than gastrointestinal (12.4% vs 9.5% at grade-two, 2.3% vs 0.2% at grade-three, 0% vs 1% at grade-four). A meta-analysis by Robinson *et al* ²³⁷ has calculated the probability of developing erectile dysfunction, the other major

complication following radiotherapy. After cryotherapy (0.13), RP was shown to be the most likely to induce such problems with a probability of 0.25 via a standard approach and 0.32 using a nerve-sparing technique. External radiotherapy had rates of 0.55 and 0.60 when used in addition to brachytherapy. Finally, brachytherapy alone had a rate of 0.76. When longer (\geq two years) follow-up rates were calculated (excluding brachytherapy), these fell further to 0.25 for standard RP, 0.25 for nerve sparing RP and 0.52 for external beam radiotherapy. Of note, after two years, this meta-analysis demonstrated no difference in the likelihood of erectile dysfunction between nerve-sparing and standard RP techniques.

1.2.7.3.5 Immediate versus Delayed Postoperative Radiotherapy for Pathological T3 N0 M0

EORTC trial 22911 looked at patients diagnosed with stage T3 disease post RP. They showed that five-year clinical or biochemical survival rates were significantly better if radiation was administered in the immediate post-operative period rather waiting for local recurrence (72.2% vs 51.8% $p < 0.0001$)²³⁸. This was without any appreciable compromise in terms of toxicity. Less than 3.5% of patients had grade 3 or 4 urinary toxicity²³⁹ and no adverse effects were seen in incontinence or anastomosis stricture rates²⁴⁰. Radiation should be administered before biochemical relapse escapes a PSA level of 1.0 ng/mL as thereafter local control is vastly reduced²⁴¹.

1.2.7.4 Experimental Treatments in Prostate Cancer

1.2.7.4.1 Cryosurgery of the Prostate

TRUS scanning guides the placement of 12-15 cryotherapy needles, a urethral warmer, and thermal sensors at the level of the bladder neck and external sphincter. Two freeze-thaw cycles induce cell death by; protein denaturation from dehydration; cell membrane disruption from ice crystals; microvascular stasis, ischaemia and apoptosis²⁴²⁻²⁴⁵.

Characteristics suitable for cryotherapy include; low and intermediate risk patients with localised CaP in a prostate of 40ml or less in volume. The serum PSA should be less than 20ng/mL and Gleason score less than seven. Patients with life expectancies of greater than ten years must be counselled that there is sparse data on the technique's efficacy out to ten to 15 years.

Comparison of cryosurgical results is difficult as different definitions of PSA failure are used in different studies. An example of progression-free rates for cryosurgery patients is illustrated by the study by Long *et al* of 975 patients. Progression-free rates were found to be inferior to RP. Specifically, biochemical free survival was defined as 76% and 60% (low risk), 71% and 45% (intermediate risk) and 61% and 36% (high risk) for PSA nadirs of 1.0ng/mL and <0.5ng/mL respectively²⁴⁶.

Irrespective of the generation of machine, erectile dysfunction remains a complication affecting approximately 80% of men. However, 37% of men are able to have sufficient function to enable sexual intercourse at three

years²⁴⁷. Other complications include; tissue sloughing (3%), pelvic pain (1.4%), incontinence (4%), urinary retention (2%), fistula development (<0.2%) and bladder outlet obstruction requiring TURP (5%)^{246, 248-252}.

The EAU states that cryotherapy may have a place in treating those individuals unfit for radical surgery or with life expectancies less than 10 years but suggests that the technique would benefit from the publication of further data²⁵³.

1.2.7.4.2 High-Intensity Focused Ultrasound of the Prostate

High-Intensity Focused Ultrasound (HIFU) is performed with the patient in the left lateral position using general or spinal anaesthesia. A probe, positioned rectally, delivers focused ultrasound waves which induce heat (>65°C) and subsequently coagulative necrosis.

As with the interpretation of the cryotherapy data, varying PSA nadirs make the comparison of results difficult. Thüroff *et al*²⁵⁴ reported a European multicentre study of 559 patients and demonstrated a negative biopsy rate of 87.2% after at least six months follow up. PSA nadir at this time was as high as 1.8ng/mL, though subsequently Blana has suggested the true nadir may only be reached 12-18 months post procedure²⁵⁵.

Bladder outflow obstruction is much more prevalent in HIFU than cryosurgery such that many operators perform a prophylactic TURP pre-HIFU. Impotence rates are still high at 50-70% and grade one and two urinary incontinence rates are in the region of 12%.

The precise role that HIFU has to play in the treatment of CaP is yet to be clearly defined. This may be best reserved for those patients with localised recurrence following radiation therapy. Guidelines from the EAU again state that HIFU would benefit from the publication of further data to clarify its role ²⁵³.

1.2.7.5 Hormone Manipulation Therapy

Androgen deprivation therapy (ADT) in the form of surgical castration and oestrogen administration was demonstrated to have a positive effect on advanced CaP in seminal studies performed by Huggins and Hodges ^{256, 257}. Whilst it remains the mainstay of treatment in such disease, more recently, there has been a shift towards its use in younger males with non-metastatic disease or as a salvage therapy after a failed attempt at definitive treatment.

Ninety to ninety-five percent of testosterone is manufactured by the testis, therefore medical or surgical castration can successfully induce androgen deprivation and thus remove the essential fuel to tumour cell growth and maintenance ²⁵⁸. Alternatively androgens may be blocked by anti-androgen medications at the receptor level. The combination of both strategies is known as complete androgen blockade (CAB).

Cancer-specific mortality is usually a consequence of the development of hormone-escaped disease. Hormone-refractory prostate cancer (HRPC) occurs when disease progression is evident despite CAB and patients have a median survival in the region of 18 months ²¹.

1.2.7.5.1 Bilateral Subcapsular Orchiectomy

Surgical castration in the form of total or subcapsular techniques (subcapsular techniques preserve the tunica albuginea and epididymis) is still considered the gold standard for ADT. Despite the ease with which the procedure can be performed, the vast improvement in the efficacy of medications has meant that increasingly patients and surgeons are finding the surgical option an unacceptable or unnecessary psychological burden.

1.2.7.5.2 Oestrogens

The effects of oestrogens have been reported as multiple and include; down-regulation of luteinising hormone (LH)-releasing hormone (LHRH) secretion; androgen inactivation; Leydig cell function suppression and, *in vitro*, direct cytotoxicity of the prostatic epithelium²⁵⁹. Initially the clinical use of oestrogen therapy fell out of favour because of the associated cardiovascular morbidity and mortality. Oestrogen therapy does not appear to have the same severity of bone loss and cognitive decline though as seen in long term ADT²⁶⁰. Although it remains excluded from first-line hormonal manipulation therapy, its use in hormone-escaped disease is now commonplace in the UK. The reports from the randomised Scandinavian Prostatic Cancer Group Study of over 900 patients with metastatic disease demonstrated no significant differences in both disease-specific and overall survival between those receiving CAB and those receiving parenteral oestrogen. Importantly whilst it did

show increased rates of cardiovascular morbidity with oestrogen therapy there was no increase in mortality ²⁶¹.

1.2.7.5.3 Luteinizing Hormone-Releasing Hormone Agonists

Long acting LHRH agonists are the mainstay of ADT and common forms of the therapeutic synthetic analogues include buserelin, goserelin, triptorelin and leuprorelin. Ninety percent of individuals reach castration levels of testosterone ²⁶² within two to four weeks ^{263, 264} of instituting treatment. Before the down regulation of LHRH receptors can occur, the analogues do actually transiently stimulate LH and follicle-stimulating hormone (FSH) secretion after two to three days ²⁶⁵. This can last up to a week and must therefore be covered with antiandrogen therapy co-administered during this period. This is the main drawback of LHRH agonists and has been shown to be more likely in those symptomatic individuals with high volume metastatic disease of the bone ²⁶⁶. More rapid suppression of testosterone may need to be achieved in those patients with impending spinal cord compression where surgical castration or the use of LHRH-antagonists may be particularly indicated.

1.2.7.5.4 Luteinizing Hormone-Releasing Hormone Antagonists

LHRH antagonists compete with LHRH binding sites and achieve rapid decreases in LH and FSH without an associated flare phenomenon. Phase III trials have demonstrated that the LHRH antagonist Abarelix has a similar efficacy to both an LHRH agonist ²⁶⁷ and CAB ²⁶⁸, using PSA control and castrate testosterone levels as endpoints.

1.2.7.5.5 Antiandrogens

Antiandrogens come in steroidal (cyproterone acetate, megestrol acetate and medroxyprogesterone acetate) and non-steroidal (nilutamide, flutamide and bicalutamide) forms. Both act at the nuclear receptor level to inhibit CaP growth and induce apoptosis²⁶⁹. The progestational effects of the steroid hormones act centrally to actually decrease pituitary and adrenal-driven testosterone production as well as peripherally blocking receptors. The non-steroidal forms block the action of testosterone without lowering circulating levels, which may conversely become raised.

Androgens of adrenal origin are converted to 5- α -dihydrotestosterone in the prostate. In addition to decreasing the circulating testosterone concentration with castration, the peripheral action may also be blocked by the antiandrogens and 5- α -reductase inhibitors. The peripheral action alone can be blocked to help decrease the impact such therapies have on quality of life and particularly sexual function. However, long term data on its oncological efficacy is awaited.

CAB does not eliminate all cells in the malignant population. After an average of 24 months, such cells can initiate replication independent of androgens. The theory behind the use of intermittent CAB is that ADT will be withdrawn before the step to hormone-insensitive disease is made by the tumour. When reinstituted, the ADT will again be acting upon a hormone sensitive cancer. As yet data does not support its widespread usage²⁷⁰.

1.2.7.5.6 Outcome

In patients with metastatic disease only 7% of patients treated by hormonal manipulation survive at least ten years ²⁷¹. The median survival being 28 to 53 months ²⁷².

1.2.7.5.7 Chemotherapy

The use of chemotherapy in HRPC has gained some popularity in the last few years though its use is only advised in carefully selected patients with a suitable performance status. Two studies have looked at the use of the Taxane agent Docetaxel given in combination with estramustine (SWOG 99-16 trial) ²⁷³ and prednisolone (TAX 327 study) ²⁷⁴. Compared with the standard treatment of mitoxantrone and prednisolone, a survival advantage of 2 months was demonstrated in the SWOG trial and 2.4 months in the TAX 327 study. The TAX 327 study also reported an improvement in biochemical control, symptom measures and quality of life though unfortunately, only around one third of patients responded ²⁷⁴.

1.3 The Stem Cell

1.3.1 General

The abundance of stem cell (SC) research is driven by the unified aim of researchers to solve the problems conferred by damaged or diseased tissues. It is hoped that further study of the normal SC will in turn allow a

better understanding of the mechanisms surrounding the development of important diseases that are increasingly facing the modern world.

It is known that SCs have varying potential. The fertilised oocyte is not only the most primitive of SCs but also has the most potential (totipotent), being able to form both embryo and placenta. The pluripotent SCs of the inner cell mass of the blastocyst are the source of embryonic SCs and are usually harvested from embryos not utilised during the in-vitro fertilisation process. They may develop into almost all specialised cell types but not the placenta. At a tissue level, the multipotentiality of tissue-specific adult SCs means that they are able to repopulate individual organ systems and their various tissue types by producing eight to ten distinct lineages of mature cells. In less diverse tissues, such as the epidermis, unipotential SCs produce cells of one particular type ²⁷⁵. The ethical implication of embryonic SC use has led to an increased focus being placed on the study of adult tissue-specific SCs.

1.3.2 Definition of the Stem Cell

Although difficult to prove *in vivo*, adult SCs are defined by their specific properties of self renewal, clonogenicity and pluripotentiality ²⁷⁶⁻²⁷⁸.

Despite their great proliferative potential, the SCs do not possess the functional properties of their differentiated progeny that constitute mature tissue but instead they usually remain quiescent within their microenvironment or “niche”. SCs are able to make identical copies of themselves for long periods of time (long-term self renewal). By a

process known as asymmetrical division, one copy maintains the SC population in the quiescent state and preserves the original genotype whilst the other proceeds to delineate and form the fully-differentiated cell types of the tissue with their mature phenotypes (pluripotentiality). Known as the immortal strand hypothesis²⁷⁹, label-retaining studies have shown that the SC appears to retain the original copy of the genome and the newly synthesised deoxyribonucleic acid (DNA) strand is transferred to the committed progenitor²⁸⁰⁻²⁸². This SC often generates an intermediate cell type that then continues to divide into the differentiated cells of the mature tissue. These cells are known as committed progenitors or a transit-amplifying population (TAP) and, whilst having a limited phenotypic potential, are able to proliferate more quickly. This expands the numbers of cells, whose differentiation pathway is by now already determined (Figure 1.6). SCs may divide symmetrically though this is less common. The resultant cells have the same potential in that both may be SCs or committed progenitor cells. The requirements of the tissue and the homeostatic balance between numbers of stem and differentiated cells govern whether symmetrical or asymmetrical division occurs. This is known as the “population mechanism”²⁸³. It is argued by many investigators that unipotential SCs are in fact not SCs at all but are instead committed progenitors. Terminal differentiation of cells is generally associated with reproductive sterility (reviewed in²⁷⁵).

Adult tissue-specific SCs appear to be located in most tissues of the human body. In addition to their defining features, as previously

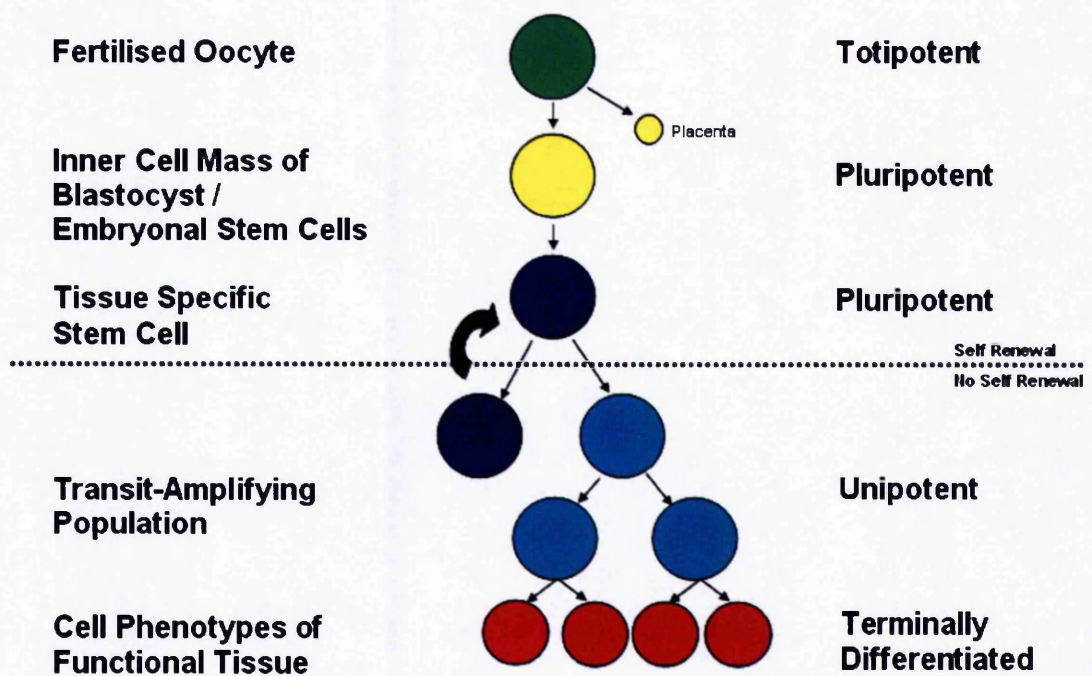


Figure 1.6: Schematic diagram showing the proposed stem cell hierarchy from the most primitive cell to the differentiated cell phenotypes of the mature tissue. For the purposes of clarity, only the process of asymmetrical division of the tissue specific stem cell is shown. Asymmetrical division results in a transit-amplification cell, which proceeds to populate the tissue with the differentiated cell phenotypes, and self renewal, which results in preservation of the original DNA in the stem cell compartment. Symmetrical division occurs when the tissue specific stem cell divides into two cells with the same potential, both being either transit amplifying cells or stem cells.

described, SCs constitute only a small fraction of the total cellularity of a tissue and are rare. The rarity of SCs complicates their successful isolation for further study and characterisation. Furthermore, they are likely to be positioned at the beginning of the flux of cells. For example, in the hair follicle, SCs appear to nest in the bulge region of the hair follicle²⁸⁴.

1.3.3 Cancer Stem Cells and the Cancer Stem Cell Theory of Cancer

The stochastic model of carcinogenesis implies that any cell (including terminally differentiated cells) can potentially be tumourigenic and result in a homogenous phenotype^{285, 286}. However, it is more likely that a small fraction of primitive cells within the tumour are actually responsible for tumour initiation as this would explain the observed tumour heterogeneity and apparent hierarchical epithelial arrangement.

The SC attributes of self renewal, in combination with their intrinsic growth potential, make SCs relevant to oncogenesis^{286, 287}. It may be that such Cancer Stem Cells (CSCs) arise from the direct mutation of normal SCs. It appears that several genetic mutations are required to initiate invasive cancer and it is hypothesised that this occurs at the most primitive cellular level to allow the necessary time for this process which could not be afforded by the relative short life span of the terminally-differentiated population.

Furthermore, evidence has suggested that the TAP may also gain mutations and contribute significantly to raise the malignant cell numbers

via their enhanced replication potential^{288, 289}. The process of de-differentiation, where TAP's regain properties of self-renewal has been postulated as a further mechanism for CSC development^{290, 291}.

1.3.4 The Stem Cell Niche

The cellular and structural microenvironment in which a SC resides is termed its niche. It is believed that the SC niche is able to function independently of the SC though the SC itself is dependent on its microenvironment²⁹².

A "lineage" niche determines the fate of each of the daughter cells of the SC division and it does this by the relation of the cell to the basement membrane. If the daughter cells remain in contact with the basement membrane then they remain under the influence of the adjacent stroma and therefore a SC. A "population" niche occurs when the progeny become dissociated from this regulatory supporting stroma and are thus stimulated to differentiate. A combination of the two niches is most common and is representative of asymmetrical division²⁹³.

Signalling by the niche is believed to determine the precise configuration of the SC hierarchy within a particular organ system. Tissues with a high turnover of their differentiated population such as the skin, eyes and gut will have a predominance of the TAP and actively proliferating cells whilst maintaining only small numbers of SCs in quiescence. Examples of defined SC niches include the gastrointestinal SCs, which are believed to reside towards the base of the intestinal crypts and be under

the influence of growth factors from surrounding Paneth cells^{294, 295} and the follicular SCs, which have been localised to the apical portion of the bulge region of the hair follicle²⁹⁶. It has become apparent from studies of the bone marrow in the haemopoietic²⁹⁷ breast²⁹⁸ and neurological systems²⁹⁹ that it is probably the entire microenvironment or niche in which the SC resides rather than just the individual cells themselves which are important.

Similar to the niche described in normal SCs, exogenous stimulation by the surrounding tissues may be important in the control of CSCs. Kiaris and colleagues provided data to suggest the role of p53 in such control with the revelation of reduced tumour latency in the MCF-7 cell line when injected subcutaneously into the knockout p53 severe combined immunodeficiency (SCID) mouse compared with the heterozygote or p53⁺/p53⁺ phenotype³⁰⁰. Conversely though it may be the ability of a CSC to escape the regulation of the niche microenvironment and still thrive that characterises it as carcinogenic. An example of this process would be the development of distant metastasis.

1.3.5 Cell Division and the Cell Cycle

The cell cycle regulates the duplication of DNA and its passage on to the progeny resulting from cell division. The cell cycle is divided into four phases; G₁ (Gap 1), S (Synthesis), G₂ (Gap 2) and M (Mitosis) (Figure 1.7³⁰¹). G₁ is the rest period for the cell immediately following mitosis. The S phase is when the DNA is duplicated so that there are sufficient

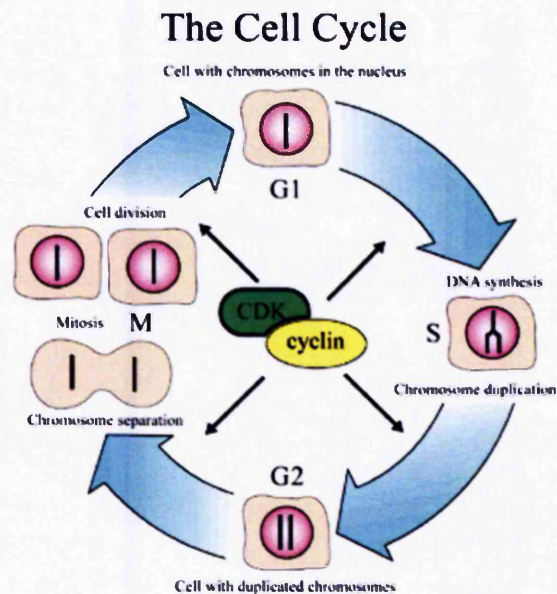


Figure 1.7: The eukaryotic cell cycle. The cell moves through G1 to ultimately divide at mitosis. The cell grows during G1. S phase is when the DNA is duplicated providing sufficient chromosomes for the two daughter cells. G2 follows S phase and precedes the final process of mitosis. G0 is an optional phase which follows mitosis. This quiescent resting phase is favoured by the stem cell whilst the committed progenitor continues into G1 and actively cycles through the standard four phases (The Nobel Foundation) ³⁰¹.

chromosomes for the two new cells. G_2 follows S phase and precedes the final process of mitosis and formation of two daughter cells. All cells have a further optional phase (G_0) which follows mitosis. This quiescent resting phase is favoured by SCs and is entered whilst the committed progenitor continues into G_1 and actively cycles through the standard four phases³⁰².

Extracellular factors such as growth factors regulate cell movement between G_0 and G_1 . The progression of a cell through the stages of the cell cycle is determined by the levels of intracellular cyclin. In turn, the cyclins are controlled by the upregulation of the cyclin dependent kinases by the extracellular growth factors. Restriction points at the start of the cell cycle (G_1/S) and towards the end of G_2 phase (restriction point R) serve as quality control mechanisms to ensure that firstly; the cell is actually required to enter the cycle and that secondly; any serious mutations incurred during DNA synthesis do not get passed on to the daughter cells. Instead any mutated cells are committed to apoptosis.

1.3.6 Evidence for Adult Stem and Cancer Stem Cells

1.3.6.1 Non-Epithelial Stem Cells

The haematological system has the most studied and best characterised SC biology followed by the SC biology of the central nervous system.

1.3.6.1.1 Haemopoietic Stem Cells

Human haemopoietic cells have been successfully engrafted into non-obese diabetic severe combined immunodeficient (NOD/SCID) mice and pre-immune foetal sheep. Notably in the foetal sheep model, CD34^{+ve} and CD38^{-ve} cells exhibited properties of long term persistence within the host ³⁰³. Vascular growth factor receptor-2 positive cells (KDR^{+ve}) are seen to coexist in cell populations enriched for SCs ³⁰⁴. CD34^{+ve} and KDR^{+ve} cells have been shown to have enhanced self renewal capability whereas the subfraction that are CD34^{+ve} and KDR^{-ve} have no self renewal capability at all ³⁰³.

As with many marker studies in the SC field, there has still not been a single marker identified that encompasses the gold standard for SC identification. Zanjani *et al* used sheep xenograft models to demonstrate the heterogeneity of the SC population. They showed that a lineage negative (Lin^{-ve}) CD34^{-ve} subpopulation had the properties of long term repopulation and multilineage differentiation *in vivo* ³⁰⁵. Functional investigation of the subpopulation demonstrated that Lin^{-ve} CD34^{-ve} cells had a poorer response to growth factors and were less clonogenic than Lin^{-ve} CD34^{+ve} cells. The conclusion is that this cell phenotype may be more primitive than its CD34^{+ve} counterpart and that it is a long term repopulating cell that does not preferentially differentiate but is instead responsible for self renewal ³⁰³. Specifically, the CD34 status of a cell may determine whether a cell is quiescent in G₀ (CD34^{-ve}) or actively cycling (CD34^{+ve}) ³⁰⁶.

The determination of the haemopoietic cell lineage occurs at a transcription level which may in turn be influenced by either intrinsic or extrinsic factors or indeed both. The dynamic process by which differential expression of various transcription factors occurs determines the proliferation, commitment, differentiation and ultimate survival of the cell lineage. Evidence suggests that transcription genes encode the coordinated development and maintenance of haemopoietic SCs (HSCs)³⁰⁷ and that their loss may induce leukaemic proliferation. Important transcription factors identified within the haemopoietic system include; GATA and SCL/tal-1³⁰⁸⁻³¹⁰, PU.1 and WT-1^{311, 312} and Hox B4^{313, 314}.

In addition to the many different chromosomal translocations that usually encode transcription factors, the HSC experience has also identified a number of other proteins that regulate HSCs. An example is the mammalian Notch molecules with their ligands Delta-like, Jagged family and the fringe family of signalling modifiers as well as their numerous downstream regulators^{303, 315}. Notch itself can regulate transcription by association with nuclear factors. Cells incubated with Jagged 1 have been shown to control the HSC self renewal process *in vitro*³¹⁶. TGF- β appears to keep HSCs in the quiescent state by blocking entry to the cell cycle at G₁³¹⁷ and has been shown to be a potent inhibitor of murine SCs.

1.3.6.1.2 Haemopoietic Cancer Stem Cells

CSCs have been identified in acute myelogenous leukaemia (AML)^{318, 319} and chronic myelogenous leukaemia (CML)³²⁰, and have been

implicated in acute lymphoblastic leukaemia (ALL)^{321, 322}. The quiescent cell cycle status of normal SCs has been demonstrated in the CSCs implicated in CML and the majority of CSCs in AML. If such CSCs are not actively cycling it makes it unlikely that antiproliferative cytotoxics will be effective. Cell surface markers specific to CSCs have been identified, such as the interleukin-3-receptor α -chain which is present on the CSC but not the normal SC in AML³²³. This represents the potential for exciting immunotherapeutic possibilities. Indeed the use of antibodies to another marker (CD33 antigen) has shown some benefit in AML^{324, 325}. Furthermore, CD33 is expressed on some leukaemic CSCs³²⁶. Again this suggests a potential mechanism for therapeutic targeting of the CSC itself. It is hoped that treatment of the CSC should remove the risk of remission and metastasis from that particular tumour. Immunotherapy against stem-cell specific antigens is likely to continue.

The ABL kinase inhibitor, imatinib mesylate, has been used as a targeting agent to modulate leukaemic cell growth and it achieved good clinical responses in CML patients³²⁷. Interestingly, whilst it manages to eradicate most, if not all, leukaemic cells it appears to do so by acting on the TAPs rather than the CSC itself. Thus, on withdrawal of the treatment, disease recurrence occurs. This adds further weight to the theory that CSC treatment alone will truly lead to cure^{328, 329}.

Activation of nuclear factor- κ B (NF- κ B) and phosphatidylinositol 3' (PI3) kinase signalling pathways have been detected in AML CSCs.

Furthermore they appear to be cancer-specific as they are undetectable

in normal quiescent SCs^{330, 331}. Guzman *et al* recognised the specific eradication of AML CSCs and the sparing of normal HSCs when NF- κ B was pharmacologically inhibited *in vitro*³³². AML cell growth was reduced by inhibition of PI3 kinase directly³³¹ and the chemosensitivity of AML to etoposide was increased by inhibition of one of PI3 kinase's downstream targets³³³.

1.3.6.1.3 Central Nervous System Stem Cells

Adult neurological SCs have been found to reside in two regions of the central nervous system (CNS); the hippocampus and subventricular zones as well as the spinal cord. Though limited in their differentiation potential compared to embryonic SCs, the neurological SC (NSC) has the ability to differentiate into all the principal cell types of the CNS including neurones, oligodendrocytes and astrocytes³³⁴. Totipotent embryonic SCs from the inner cell mass of the blastocyst have been used to create embryoid bodies and from their three constituent germ layers, cells could be encouraged to differentiate into primitive neural cells with their characteristic marker nestin³³⁵.

Normal NSCs have been cultured *in vivo* and, on nonadherent surfaces, they form neurospheres^{336, 337}. These neurospheres can be dissociated into single cells from which NSCs can be re-isolated and used to form new neurospheres, thus demonstrating self renewal. Transplantation of foetal NSCs into animal models has also demonstrated neuronal and glial differentiation and offers exciting potential for the treatment of neurodegenerative disorders and neurological injury^{338, 339}.

Surface markers are being developed but this is often done retrospectively after the isolated cells' functional behaviour has been determined. NSCs have been shown to be CD133^{+ve} ³⁴⁰ in concordance with the SCs and progenitors of other tissues ³⁴¹.

Many studies have investigated neurodevelopmental biology and specifically the role of various transcription factors during embryogenesis. Neuronal development appears to precede the glial support tissues. The two distinct lineages arise from common stem progenitors but it is the homeodomain (eg NKx2.2 ³⁴²) and basic helix-loop-helix (eg Olig 1 and Olig 2 ^{343, 344}) families of transcription factors that induce the final fate decisions. In turn, the gliogenic transcription factors may be under the control of Notch ³⁴⁵. It has been postulated that the Notch ligand jagged 1 suppresses the formation of oligodendrocytes ³⁴⁶. On completion of the neuron, downregulation of jagged 1 allows uninhibited development and growth of oligodendrocytes and thus the process of myelination occurs ³⁴⁷. As with HSCs, the TGF- β superfamily plays a role in the regulation of transcription, cell fate and maturation ³⁴⁸. An example being BMP-2 regulated induction of Mash-1, a basic helix-loop-helix transcription factor ³⁴⁹. NCAM, N-cadherin and cadherin 6-b are key neural adhesion molecules that are down regulated in the migration of neural crest tissue long distances away from the neural tube to form the peripheral nervous system in a process known as delamination ^{350, 351}. In the adult subventricular zone, antagonism of BMP by noggin drives neurogenesis yet when BMP levels are allowed to rise, cells undergo gliogenesis ³⁵².

The improved knowledge about NSCs may help our understanding of degenerative neurological disorders and why the mature brain has a very limited response to injury. Interestingly, subventricular zone cells that were originally astrocytes were subsequently demonstrated as having neuronal phenotypes after stroke-induced injury³⁵³. Despite the limited reparative capability of the adult brain, evidence to suggest NSCs exist and that they may respond to injury has led to exciting hypotheses about SC replacement therapy being generated. These remain a focus for research attention within the NSC field. Studies are examining the role of foetal neural tissue, embryonic SCs and immortalised SC cell lines as replacement therapies³⁴⁸. It has been postulated that, although SC progenitors have been identified, the cellular environment is such that it restricts their proliferation and thus the ability to repair³⁴⁸.

1.3.6.1.4 Central Nervous System Cancer Stem Cells

As with NSCs, the development of cell surface antigens for use as CSC markers has been slow and the primary method of isolation of putative neural CSCs has been by the neurosphere assay. The first evidence of cells with stem properties being isolated from CNS cancer was reported by Ignatova *et al* who isolated clonogenic cells that formed neurospheres from operative specimens of glioblastoma multiforme. On differentiation, the cells expressed neuronal and astroglial markers³⁵⁴. These findings were confirmed and extended to medulloblastoma^{355, 356} and ependymoma³⁵⁷. Hemmati *et al* showed that medulloblastoma neurosphere-forming cells gave rise to dysplastic tissue when

transplanted into neonatal rat brains³⁵⁶. These studies appeared to suggest that neural CSCs had similar molecular properties to NSCs and that CD133 may again be a suitable marker for the subpopulation^{355, 358} (reviewed in³⁵⁹).

The gold-standard determinant of a CSC is serial transplantation. Galli *et al* offered the optimal evidence available thus far by successfully demonstrating cancer initiation in the striatum of immunodeficient mice on transplantation of glioblastoma multiforme cells²⁹⁹. The tumours that developed had the morphological and histological properties of glioblastoma multiforme. The proposed CSC could again be harvested from the tumours and used to re-establish a secondary cell line with functional characteristics akin to the primary cultures. Most importantly, the secondary brain tumour cells again induced new tumour formation on further transplantation, thus demonstrating the cell population's ability to self renew²⁹⁹. The precise phenotype of the cells is still not clear though it appears that the CSC does indeed exist. Singh *et al* have demonstrated the differential ability to induce CNS tumours *in vivo* based on CD133 selection. Transplantation of 100 CD133^{+ve} human glioma cells initiated glioma in mice whereas 10⁵ CD133^{-ve} cells from the same tumour failed³⁵⁸.

Characterisation of the CSC is important to help understand the underlying biology and therefore identify potential therapeutic targets. Whilst it still remains to be fully established whether the neural CSC is a direct transformation of the NSC, various signalling pathways have been

discovered that are common to both normal and malignant SC processes (reviewed in ³⁶⁰). These include the Wnt, Sonic Hedgehog (SHH) in both medulloblastoma and glioma as well as phosphatase and tensin homologue (PTEN) and possibly the Notch pathway in glioma ^{286, 290}. In addition to CD133, many potential SC antigens evident in normal NSCs have been seen in malignancy. Nestin has been identified in early undifferentiated neoplastic cell populations induced by the potent neurocarcinogen N-ethyl-N-nitrosourea (ENU) ³⁶¹ as well as in paediatric brain tumours ³⁶². Uchida *et al* have suggested that Msi-1 may also select for paediatric CNS tumours from the subventricular zone ³⁶³, echoing the experience with normal NSCs ³⁶⁴.

1.3.6.2 Epithelial Stem Cells

The breast SC is probably one of the most studied epithelial tissue specific SCs thus far and is of additional interest as, like the prostate, it is composed of glandular subunits that are influenced by sex hormones. They have an outer layer of myoepithelial basal cells supporting a luminal secretory epithelium. The breast SC is believed to be instrumental in the development of the breast at puberty and enables the enlargement and remodelling seen in response to the raised oestrogen levels of pregnancy and the cyclical changes evident in the menstrual cycle. Furthermore, there is a degree of involution in response to weaning but the same enlargement and induction of lactation is seen with each subsequent pregnancy.

1.3.6.2.1 Breast Stem Cells

DeOme *et al* first suggested the presence of a breast SC by demonstrating that cells from mouse epithelium were able to produce a fully functional mature mammary gland with ducts, lobules and myoepithelial cells on transplantation³⁶⁵. More importantly, the confirmation of a SC was subsequently demonstrated with successful serial transplantation³⁶⁶. The functional potential of the normal breast SC has been demonstrated by their ability to regenerate a mammary gland in a suitable host^{367, 368}. Using retroviral tagging, Kordon and Smith demonstrated that the progeny of a single multipotent SC could repopulate an entire mammary gland³⁶⁹.

There have been a number of methods used to isolate and characterise the breast SC. Label-retaining studies using two molecules, 3H-thymidine and bromodeoxyuridine (BrdU) revealed that, not only did label-retaining cells undergo asymmetric division but that they were able to selectively retain the original template DNA strand and only pass on the newly synthesised strand to the daughter cell and therefore their progeny²⁸¹. The Hoechst dye efflux assay will be discussed in more detail in section 1.3.7.4.3. Suffice to say, a side population has been isolated from breast epithelia³⁷⁰, and has been shown to give rise to all three mammary epithelial lineages^{371, 372} and form mammospheres in non-adherent culture³⁷³.

The mammary repopulating unit (MRU) has been demonstrated to be a rare subpopulation of cells able to repopulate the breast whilst also

showing evidence of self renewal^{367, 368}. This subpopulation of mammary epithelial cells was analysed and enrichment for the CD24^{+ve}/CD29^{hi} or CD24^{+ve}/CD49^{hi}/Sca-1^{lo} phenotype was detected. Single cells from each of the two phenotypes have repopulated cleared mammary fat pads and have therefore been shown to have properties of self renewal. Independent study of MRUs has shown a greater enrichment in the CD24^{low} population. Determination of the lineage phenotype in CD24^{-ve}, CD24^{low} and CD24^{hi} cells has shown them to be non-epithelial, basal/myoepithelial and luminal epithelial cells respectively³⁷⁴. Essentially, it appears that these markers probably only serve to enrich for the SC population rather than provide direct identification³⁷⁵.

1.3.6.2.2 Breast Cancer Stem Cells

Al Hajj *et al*²⁹⁸ demonstrated that only a minority of tumour cells were able to initiate new tumour formation. This cellular subpopulation possessed the CD44^{+ve}/CD24^{-ve} cell surface antigen profile and formed tumours in immunodeficient mice whereas those outside this subgroup from the remainder of the tumour did not. Furthermore, the CD44^{+ve}/CD24^{-ve} subpopulation could be serially isolated following passage, and has been shown to differentiate and subsequently reconstitute a heterogeneous phenotype similar to that of the original tumour.

The ability to grow mammospheres from single cell suspensions in anchorage-independent culture is believed to be a sign of stem activity.

Ponti *et al*/ were able to produce mammospheres after the dissociation of primary breast tumours. The predominant CD44^{+ve} / CD24^{-ve} phenotype contained a subpopulation of 10-20% which were able to undergo self renewal. They could be seeded at a 1000-fold greater dilution than established breast cancer cell lines and still initiate tumours in immunodeficient mice ³⁷⁶. CD44^{+ve}/CD24^{-ve/low} subpopulations from MCF-7 and MDA-MB-231 breast cancer cell lines have attributes of importance to clinical practice, showing greater resistance to radiation ³⁷⁷. Finally, translational studies have shown that whilst there was no significant correlation between the CD44^{+ve}/CD24^{-ve} phenotype and overall survival of patients with breast cancer, a significant proportion (80%) of the 15 patients in the cohort with more than 10% CD44^{+ve}/CD24^{-ve} tumour cells and recurrent disease, had distant metastases only (p=0.04) and all five of the patients with greater than 20% CD44^{+ve}/CD24^{-ve} tumour cells had bone metastases (p=0.02) ³⁷⁸, ³⁷⁹.

1.3.6.2.3 Epidermal Stem Cells

The skin comprises a mesenchymal dermal layer separated from the rapidly-dividing superficial epidermal layer of stratified squamous epithelium by a basement membrane. The cellular hierarchy of a SC, a TAP and terminally differentiated cells has been demonstrated *in vitro*. SCs have enhanced proliferative potential and form larger colonies than those seen from the TAP. Whilst the TAP cells can form colonies more quickly, they lack the ability to self renew and their replicative potential is

therefore exhaustable. Jones *et al* reported that keratinocytes with stem characteristics expressed high surface levels of beta-1 integrin and rapidly adhered to extracellular matrix proteins whereas TAP cells adhered more slowly and reached reproductive sterility after one to five divisions. The authors suggested that the differential adherence of cells to extracellular matrix proteins could serve as a method of SC isolation and purification ³⁸⁰.

Slow-cycling, label-retaining cells have been shown to remain in the basal layer of the epithelium after three months of growth *in vivo* whereas the TAP and terminally differentiated cells were located more superficially and had diluted their dye content such that it was no longer detectable ^{381, 382}.

1.3.6.2.4 Gastro-Intestinal Stem Cells

The gastro-intestinal tract comprises abundant columnar epithelial cells, neuroendocrine cells, mucin-secreting goblet cells and Paneth cells. Paneth cells are located at the base of the intestinal crypts of Lieberkuhn. The epithelium is supported by myofibroblasts which act on the epithelial cells in a paracrine fashion by secreting growth factors such as TGF- β , and platelet-derived growth factor-A ^{383, 384}. The combination of the epithelial cells and their supporting myofibroblasts form the gut SC niche. As in the skin, cell turnover in the gut is massive at 10^{10} cells per day and the SCs are required to maintain tissue homeostasis ³⁸⁵. Bjerknes *et al* subdivided these SCs into multipotent (10-20%) and unipotent (80-90%) SCs ²⁹⁵. The gut SC niche provides an

excellent example of SCs being situated near the beginning of the flux of cells, forming an annular ring of cells at the base of the crypt just above the Paneth cells from which cells ascend the “escalator” towards the luminal extent of the crypt (reviewed by Marshman *et al*³⁸⁶). The notion of the presence of a cell with stem properties was strengthened by the demonstration that the intestinal crypt could be reconstituted by small numbers of radio-resistant cells after radiation-induced DNA damage³⁸⁷.

As with the keratinocytes of the skin, a number of extracellular matrix proteins and growth factors have been put forward as being contributory to mechanisms for maintaining the SC niche³⁸⁶. Despite the fact that no single factor has currently been identified, the T-cell factor (TCF) family may be implicated, especially TCF-4 as the crypt SCs appear to be lost in TCF-4 knockout mice³⁸⁸.

Isolating single gastro-intestinal SCs has been hampered by the lack of markers and the majority of study has therefore come from their study *in situ* within the crypts both *in vivo* and *in vitro*. Booth *et al*³⁸⁹ took freshly isolated cells and cultured small and large intestinal crypts which grew subcutaneously in immunocompromised mice. The cultures formed cysts lined by a simple epithelium initially. These subsequently developed into multicellular invaginations composed of many mitotic and apoptotic cells. Mucin production by goblet cells was evident and signified epithelial cell differentiation. The recognised flux of cells within the crypt was reproduced such that the grafts displayed zones of proliferation at their

bases and areas of specialist function (mucin production) at the luminal end.

1.3.7 Prostate Stem Cells

1.3.7.1 Normal Prostate Morphology and Physiology

The prostate is a hormonally regulated organ and its growth in the male adult human responds to the increased androgen levels present from puberty. There are three cellular phenotypes present (reviewed by Foster *et al.* ²⁹³). The most common is the secretory luminal epithelium which has the characteristic markers of CD57 ³⁹⁰, PSA and the cytokeratin profile of CK8 and CK18 ³⁹¹⁻³⁹⁴. Luminal cells are androgen dependent terminally differentiated cells with a low proliferative capacity and a high apoptotic index. The second cell type is the basal epithelial cells which express CD44 ³⁹⁰ and the cytokeratins CK5 and CK14, which anchor the epithelium to the surrounding stroma ³⁹¹⁻³⁹⁴. Basal cells tend to be less well differentiated and androgen independent, with a high proliferative capacity and a low apoptotic index. The least common phenotype is the neuroendocrine cell which is positive for chromogranins. The true role of these cells is unknown but they appear to be critical for growth stimulation ³⁹⁵⁻³⁹⁷. Compared with the luminal compartment the majority of the proliferating cells (approximately 70%) are basal. The neuroendocrine cells are entirely post-mitotic ^{398, 399}.

1.3.7.2 Rationale for the Cancer Stem Cell Theory in the Prostate

In terms of the prostate, the origin of the CSC has been studied by many groups. Bonkhoff and Remberger suggested that the CSC arose from direct mutation of the normal SC ⁴⁰⁰. Others prefer the theory that the CSC is actually a product of dedifferentiation of either the TAP ^{401, 402} or luminal phenotypes ^{403, 404}.

The major cellular component of a prostate tumour appears to be the secretory luminal epithelium on the basis that they express luminal markers such as CK8/18 and AR but not p63 and CD44. As a consequence many have previously suggested that these luminal cells are responsible for the initiation of tumourigenesis. Whilst many animal models have used luminal cell-specific probasin promoters to drive oncogene expression or delete tumour suppressors, this does not provide satisfactory evidence that the luminal cells are the primary oncogenic cell.

CaP is heterogeneous at a genetic ⁴⁰⁵, chromosomal ⁴⁰⁶ and histopathological level ⁴⁰⁷ (reviewed by Maitland and Collins ⁴⁰⁸). Both BPH and CaP are diseases characterised by loss of regulation of cell growth in the prostate. There is gathering evidence that this arises because of disordered cellular control in the SC compartment of the prostate. Prostatic SCs are vital for normal tissue homeostasis, as illustrated by studies of androgen withdrawal and replacement, whereby the withdrawal precipitates prostate cellular regression to the basal layer of the prostatic acinus and subsequent replacement stimulates regrowth

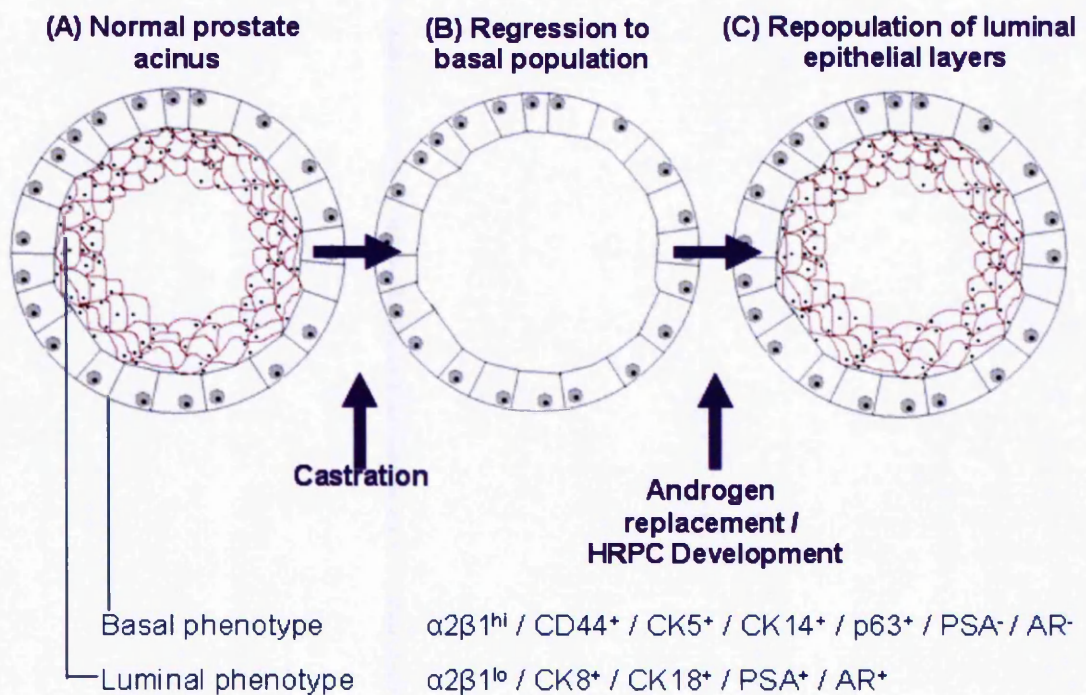


Figure 1.8: Cartoon depicting (A) a cross sectional view of a prostatic tubule and (B) regression of the luminal epithelium in response to castration followed by (C) repopulation of the luminal epithelial layer in response to androgen replacement or, in the case of hormone-refractory disease, repopulation with a hormone-insensitive epithelial phenotype.

from that same stem rich compartment ⁴⁰⁹, even if re-institution of androgens is delayed for a year ⁴¹⁰ (Figure 1.8). This phenomenon, also seen in HRPC, suggests the persistence of a SC which subsequently gains the necessary mutations for repopulation and tumour maintenance from a treatment refractory phenotype.

1.3.7.3 Experimental Evidence for the Prostate Stem Cell

Experimental support for the existence of general SC behaviour within the prostate will first be reported before specific prostate SC and CSC regulatory pathways and markers are detailed.

1.3.7.3.1 Differential Androgen Sensitivity of Basal and Luminal Epithelia

As mentioned previously, initial support for a prostatic SC population came from experiments in rodents and to date these and subsequent series of similar experiments still provide the strongest evidence for a prostatic SC ⁴¹⁰. The prostatic secretory epithelium has been shown to serially undergo apoptosis and regress back to leave just the AR^{-ve} basal population after castration, with subsequent repopulation of all the epithelial layers with an AR^{+ve} secretory luminal phenotype ⁴⁰⁹ in response to testosterone replacement ⁴¹⁰⁻⁴¹³. The seminal work by Isaacs and Coffey demonstrated a reduction of prostate epithelial cell number to 25% of that seen in six month old controls one week after castration. Histologically this regression was characterised by loss of the normal secretory luminal epithelium and reduction in the volume of

residual glands. After restoration of pre-castrate serum testosterone levels (2-3ng/mL) with subcutaneous testosterone implants, the prostate population size had returned to normal after just one week. This involution / restoration cycle was continued up to 30 cycles whereby again the prostate was shown to be able to entirely repopulate itself. More mature one-year old rats had their prostate epithelial populations reduced to less than 50% within one month of castration but cell numbers were again fully replenished within one month of exogenous testosterone administration despite a full year of being castrate. This suggests the persistence of an androgen-independent cell able to repopulate the entire epithelium and thus the property of long-term self renewal characteristic of a SC population ⁴¹⁰.

1.3.7.3.2 Cytokeratin Expression

Basal cells strongly express CK5 and are only weakly positive for CK18 whereas luminal cells possess no CK5 immunoreactivity and are strongly positive for CK18 ⁴¹⁴. Rather than a SC dividing exponentially and populating a tissue, it is proposed that the SC initially undergoes an asymmetric division and the resultant early progenitor is then responsible for expansion of the tissue through a TAP. Hudson *et al* provided evidence for such a cellular hierarchy based on cytokeratin expression, suggesting the prostate SC expressed CK5 and CK14, the TAP CK5, CK17 and CK19 and the fully differentiated secretory cells of the luminal population were positive for CK8 and CK18 ⁴¹⁵. Further evidence for a phenotypically intermediate transit-amplifying population

between the SC and luminal cells has been demonstrated at an immunocytochemical level by the recognition of cells sharing the common surface markers CK5 and CK18⁴¹⁴ or CK5 and CK8 without CK14^{394, 402}. A SC should be able to populate an entire tissue with its constituent phenotypes and further evidence for the role of the TAP in this process is suggested by the cytokeratin profile of the neuroendocrine cells being the same as the intermediate cell population⁴¹⁶. Further verification of this was provided by Wang and colleagues who postulated that the entire prostate could be generated from the urogenital sinus and that the majority of its constituent cells dual-stained for both basal and secretory epithelial markers including CK19. This phenotype was then shown to occupy a small fraction of the adult basal population and was able to differentiate into mature differentiated basal and secretory populations⁴¹⁷. More recently, Schalken *et al* reported a cell culture system which demonstrated glandular budding from single cells and that cells at a particular level were CK5^{+ve} and those higher were CK18^{+ve} and expressed PSA⁴¹⁸. Collins and Maitland point out that the use of transfected markers or single cell clonal assays are required to track the progeny of a known cell and thereby cement the hierarchical relationship between basal and luminal phenotypes⁴¹⁹.

Following culture, the morphology, size and density of the resultant colonies may indicate the phenotype of the initiating cell. Hudson describes two types of colony. Type 1 colonies were more common and constituted up to 8500 irregular-shaped cells after 14 days culture. In contrast the type 2 colonies were larger (up to 40,000 cells) and of

higher cell density. The immunocytochemical profile of the colony types lead to the conclusion that type 2 colonies (comprising CK14^{+ve} and only rarely CK8^{+ve} cells) were the product of an undifferentiated SC and the mixed profile of CK14, CK8 or both evident in type 1 colonies was indicative of a TAP⁴¹⁵. The rarity of the postulated SCs and the morphology of the colonies was recapitulated in mice by Sawicki and Rothman⁴²⁰.

The ability of cells in monolayer culture to differentiate into their terminally-differentiated progeny may be lost *in vitro* and the demonstration of true pluripotentiality is best achieved by growing out the cells in 3-D culture models. Hudson harvested cells from the aforementioned type 2 colonies and, using conditioned media and Matrigel, was able to grow spherical structures akin to the prostatic acinus after 3-17 days. Subsequent histological analysis confirmed the previous keratin hierarchy with CK14^{+ve}/CK5^{+ve} basal cells in the outside layer, cells with a TAP phenotype inside this and finally some androgen receptor positive cells shed within the spheroid lumen.

In cancer, the predominant phenotype is luminal (CK8^{+ve}/CK18^{+ve}). This has previously led to the belief that malignant transformation occurred within the secretory compartment. Small populations of CK5^{+ve} cells have however been confirmed in malignancy and the importance of the basal population in tumour-initiation was again inferred by the finding that the proportion of CK5^{+ve} cells increased to 75% following the induction of disease control by androgen deprivation therapy⁴²¹.

1.3.7.3.3 Histological Location of the Stem Cell Niche

The precise location of the SC niche in the prostate remains unclear with evidence providing support for it being at opposite ends of the prostatic duct. The majority of evidence that is currently available is from work in rodent models. The precise organization of the rodent prostate differs from that of the human gland. Successful xenotransplantation of prostate epithelial cells with mesenchymal remnants of the urogenital sinus within the renal capsule has led to prostatic gland generation ⁴²² and work by Kinbara *et al* localised these proliferating cells to the distal tip of the adult rat dorsal and lateral prostatic ducts ⁴²³. The murine prostatic duct consists of a proximal region attached to the urethra, an intermediate region, and a distal tip ⁴²⁴. Whilst Tsujimura *et al* acknowledged previous work that had shown proliferating cells to be located at the tips of the ducts ⁴²⁵, they proposed that these rapidly-cycling cells were from the TAP rather than being prostatic SCs as previously suggested. BrdU labelling studies identified cells undergoing asymmetric division, which is a feature of long term cell renewal, and showed that slow cycling label-retaining cells with a high proliferative capacity were localised to the basal layer of the proximal prostatic tubules ⁴²⁶.

1.3.7.3.4 Clonogenic Sphere Formation

Assays have identified cells able to generate spherical clones in 3D culture. Studies using primary CNS ³⁵⁸ and melanoma ⁴²⁷ cells have demonstrated the successful engraftment of such spheres in murine recipients. Two distinct cell types have been isolated from the normal

prostate cell line RWPE-1. WPE-stem and WPE-int cells were proposed as the SC and TAP cells respectively. WPE-stem cells had a 4.5-fold enhancement in colony-forming ability and were able to form spheroid structures termed prostaspheres ⁴²⁸. Purified single cell suspensions of LAPC-4 and LAPC-9 prostate cancer metastasis cell lines have been shown to develop distinct spheres after only two weeks, the latter aided by a fibroblast feeder layer, and continue to enlarge until four weeks when the rate of apoptosis within the lumen outweighed the proliferative function of the peripheral cells. The sphere-forming fraction of the primary seeded cells was small (0.7% and 0.2% respectively) but increased after serial passage of the resultant spheres. Injection of 10 LAPC-4 spheres into the NOD/SCID mouse initiated the generation of three tumours suggesting the presence of a CSC within the sphere population ⁴²⁹.

Lang *et al* reported the initial experience in spheroid culture and suggested that the co-culture system could be utilised as an *in vitro* demonstration of SC properties in primary prostate cells. The spheroids formed were composed of a 34 β E12^{+ve} outer basal layer that enclosed an inner layer of PSA^{+ve}/AR^{+ve} luminal cells ⁴³⁰. Subsequently, Brown *et al* successfully grew spheroids cultured from the SC enriched side population isolated from primary benign prostatic tissue (see section 1.3.7.4.3) ⁴³¹. Richardson *et al* did not produce spheroids but did manage to generate prostate-like acini *in vivo* from their putative CD133^{+ve}/ α 2 β 1^{hi} SC population ⁴³².

1.3.7.4 Methods Used in the Isolation of Putative Stem Cell

Populations from the Prostate

1.3.7.4.1 Putative Prostate Stem Cell Surface Markers

Cell surface antigens represent one method of detection and isolation of SCs. Often these markers are identified retrospectively from cells shown to have functional characteristics akin to a stem population. Studies have suggested a number of candidate populations as enriched for prostatic SC and progenitor cells.

Tang *et al*/report in their review that all primary populations of normal human prostate stem-like cells were positive for the cell surface markers; $\alpha 2\beta 1$, CD44, CK5/CK14, p63 and hTERT but negative for luminal markers such as; AR, PSA, CD57, prostate acid phosphatase (PAP) and 15-LOX2. This seems to confirm the SC phenotype as predominantly basal ⁴²⁹.

1.3.7.4.1.1 CD44^{+ve}/ $\alpha 2\beta 1$ ^{hi} Phenotype Selection

Markers that appear to have gained most popularity include CD44 ⁴³³, CD133 ⁴³² and $\alpha 2\beta 1$ ⁴³⁴. CD44 is a cell surface glycoprotein involved in cell adhesion, cell to cell interaction and migration with specific cellular functions including homing, haematopoiesis, and tumor metastasis (reviewed by Naor *et al* ⁴³⁵).

The integrins are cellular receptors that mediate both attachment to the surrounding extracellular matrix and cell to cell adhesion. Enrichment for

cells with SC characteristics has been demonstrated within prostatic epithelial populations. Hudson *et al*⁴³⁶ showed a five-fold enrichment compared to the differentiated population but found no differences in adherence between those cells forming type 1 or type 2 colonies.

Collins *et al*⁴³⁴ showed that $\alpha 2$ integrin conferred the most rapid adherence and that such cells were present in an isolated manner within the prostate basal layer. The $\alpha 2\beta 1^{\text{hi}}$ cells represent approximately 1% of the basal population and additional rapid-adherence purification of CD44^{+ve} cells with $\alpha 2\beta 1^{\text{hi}}$ selection demonstrated a higher colony forming ability. Questions have been raised as to whether the observed increased clonogenicity was directly related to the $\alpha 2\beta 1^{\text{hi}}$ selection or whether the increased proliferation on type-1 collagen was actually a product of the increased adhesive properties of the CD44^{+ve}/ $\alpha 2\beta 1^{\text{hi}}$ population^{429, 434}. This population of cells was successfully xenografted in 8 out of 30 athymic nude mice, forming recognisable prostatic glandular structures within 6 weeks⁴³⁴.

1.3.7.4.1.2 CD133 Enrichment of CD44^{+ve}/ $\alpha 2\beta 1^{\text{hi}}$ Phenotype

More recently, further purification has been demonstrated with a concomitantly higher *in vitro* proliferative capacity with the addition of CD133^{+ve} selection. This population represents 0.75% of the benign prostate basal cell population⁴³². A limitation of this study was that the CD133^{-ve} population also contained clonogenic cells (albeit a lower proportion) and the study failed to determine whether CD133^{+ve}/ $\alpha 2\beta 1^{\text{hi}}$ cells could in turn produce CD133^{-ve}/ $\alpha 2\beta 1^{\text{hi}}$ or CD133^{-ve}/ $\alpha 2\beta 1^{\text{lo}}$ cells.

Interestingly, the majority of the actively cycling cells (as determined by the cell proliferation marker Ki-67) were found in the CD133^{-ve} population (Ki-67^{+ve}) whereas the CD133^{+ve} cells were more quiescent (Ki-67^{-ve}).

Richardson *et al* showed that, although colonies (>32 cells) were slower to form by 5+/-1.5 days, the colony forming efficiency of CD133^{+ve} cells was greater than the CD133^{-ve} cells (87.5% vs 36%).

Miki *et al* also demonstrated enhanced stem cell characteristics in cells with the CD133^{+ve}/CD44^{+ve}/α2β1^{+ve}/34βE12^{+ve}/CK18^{+ve}/p63^{-ve}/AR^{-ve}/PSA^{-ve} phenotype ⁴³⁷.

1.3.7.4.2 CSC Surface Markers

1.3.7.4.2.1 CD44^{+ve} Cell Selection

CD44 positivity appears to delineate a population that is approximately 100 times more proliferative, tumourigenic and aggressive than the corresponding CD44^{-ve} population. Patrawala *et al* demonstrated this fact, with only 1000 CD44^{+ve} LAP-9 cells needed to successfully induce a tumour orthotopically whereas 100,000 CD44^{-ve} cells were required ⁴³⁸. This mirrors the experience with CD44 in normal prostate populations as well as those of the HSCs ⁴³⁹, mesenchymal SCs ⁴⁴⁰, NSCs ⁴⁴¹ and mammary SCs ^{298, 442}. Sub analysis of the CD44^{+ve} population demonstrated that they were not actively cycling ⁴³⁸ and were relatively quiescent within their holoclones or spheroids. These holoclones and spheroids were confirmed as epithelial, with all cells staining for CK18 and Ber-EP4 ⁴³⁸. Gene expression analysis of the CD44^{+ve} cells

demonstrated raised expression of several SC associated genes like Bmi, smoothened (SMO), β -catenin and Oct-3/4. Bmi has been implicated as being responsible for the long-term self renewal and proliferative capacities of stem-like cells in normal and malignant (leukaemic) HSCs and normal NSCs⁴⁴³. It inhibits differentiation and apoptosis when overexpressed. Oct-4 is responsible for self renewal in teratocarcinoma and embryonic SCs⁴⁴⁴. β -catenin is a mediator of the Wnt pathway and SMO is the activating receptor in the sonic hedgehog signalling pathway. Increased activation of both pathways has been proposed in carcinogenesis of the prostate⁴⁴⁵.

Whilst this evidence suggests “stemness”, sub analysis of the CD44^{+ve} population suggests only approximately 1% can undergo asymmetric division. It may therefore be that the CD44^{+ve} cells actually contain a more primitive cell population that behave as true SCs and that infact the previously reported studies actually applied to a TAP⁴³⁸. The CD44^{+ve} clones have however been shown to differentiate into CD44^{-ve} cells.

1.3.7.4.2.2 CD133 Selection and the Putative Prostate CSC

Collins *et al*/ have translated their experience with benign prostate tissue to malignant prostate samples⁴⁴⁶. These studies involved primary CaP tissue, with isolated cells being put into supplemented long term culture. Clonal expansion of the population was performed to expand the size of the cell population for experimentation. As in the benign population, a CD44^{+ve}/ α 2 β 1^{hi}/CD133^{+ve} population was isolated from 40 cancer patients irrespective of the tumour grade. This represented only a small

proportion of the cell population (0.1%-0.3%). The clonogenicity of the CD44^{+ve}/α2β1^{hi}/CD133^{+ve} population was 3.7-fold greater than the total population and significantly (P<0.05) better than the CD133^{-ve} and α2β1^{lo} populations. The secondary colony-forming ability of the re-plated CD133^{+ve} clones was significantly (P<0.005) better than that of the CD133^{-ve} clones. This was suggested to demonstrate enhancement of the stem-like property of self renewal in the CD133^{+ve} population compared with the proposed CD133^{-ve} TAP⁴⁴⁶. Few colonies were formed by the CD44^{+ve}/α2β1^{lo} populations and none from the cells displaying a luminal phenotype (CD44^{-ve}/CD57^{+ve}). The CD133^{+ve} cells had a greater proliferative capacity than the starting population and the previously studied benign prostate populations.

To ensure the results were not related to contamination by normal prostate cell populations invasion assays were performed and demonstrated that the CD44^{+ve}/α2β1^{hi}/CD133^{+ve} population were more (n=4) or similarly (n=2) invasive as PC-3 and MCF-7 cancer cell lines. Immunocytochemically the CD44^{+ve}/α2β1^{hi}/CD133^{+ve} population had a basal phenotype (CK5^{+ve}/CK14^{+ve}/CK19^{+ve}). Markers of the TAP (c-MET) and differentiated cell populations were negative (AR^{-ve}/PAP^{-ve}).

1.3.7.4.3 Side population Analysis

As yet, no single marker has as yet proved to be entirely tissue or location specific. It is arguable that the primitive nature of SCs would actually mean they do not express cell surface markers thus inferring that the use of cell surface markers for identification and isolation is

inappropriate and instead only useful for downstream derivatives of the SC compartment. An alternative method has therefore been developed that exploits a cyto-protective mechanism possessed by many non-committed SCs and thereby uses SC functionality for isolation and identification.

Hoechst 33342 is a fluorescent dye that binds to the DNA of all live cells (except erythrocytes, which do not contain DNA) and is effluxed by primitive cells. The degree of Hoechst 33342 fluorescence is proportional to the cellular DNA content and therefore it is also useful as an indicator of cell cycle. Following uptake it binds to the DNA except in the case of primitive SCs which possess the ability to actively efflux the dye via the MDR1 gene product (p-glycoprotein) ⁴⁴⁷. The basis of the identification technique and its application to the study of primitive SCs is that the Hoechst^{lo} cells (as detected by dual parameter fluorescence-activated cell sorting (FACS) analysis) represent the primitive SC and may be isolated for further study. Hoechst^{lo} cells sit to the bottom left of a tail known as the side population (SP) on a FACS plot of Hoechst Blue dye on the vertical axis and Hoechst Red dye on the horizontal axis. Definitive determination of the Hoechst^{lo} cells that truly possess the MDR1 efflux pump is possible with a Verapamil control. The SP is lost on the addition of Verapamil which is a potent inhibitor of MDR1 mediated transport and therefore Hoechst efflux ⁴⁴⁸.

Goodell *et al* ⁴⁴⁷ first described the SP technique of enriching for HSCs in 1996. At that time their experience was in a murine model but since then

the same group have recapitulated their findings in the rhesus monkey⁴⁴⁹. Subsequently many groups have developed the technique (reviewed by Challen and Little⁴⁵⁰) and applied it to various human cell types including brain⁴⁵¹, breast³⁷⁰, intestinal tract⁴⁵², liver⁴⁵³, skeletal muscle^{454, 455}, kidney⁴⁵⁶, bladder⁴⁵⁷ and prostate^{431, 458}. Kondo *et al* were the first group to use the SP principle for isolation of a CSC and not only demonstrated CSCs in the C6 glioma cell line but also revealed that the isolated SP cells were capable of regenerating murine tumours⁴⁵⁹.

Primitive SCs express the ATP-binding cassette (ABC)⁴⁶⁰ and multidrug resistance (MDR)⁴⁶¹ efflux pumps and thus are able to remove toxic metabolites and xenobiotics from the interior of the cell. Interestingly, despite the SP phenotype in mice being mediated by the ABCG2 transporter, Patrawala *et al* noticed a similar tumourigenicity with both ABCG2^{+ve} and ABCG2^{-ve} populations isolated prospectively from human CaP cell lines⁴⁶². They concluded that this may reflect that the MDR proteins play a more significant role in human cells than the ABC family.

SP cells from both primary cancers and cell lines have been shown to be able to efflux cytotoxic agents. Not only would this potentially select for SCs and CSCs, or at least “cancer-initiating cells”, but more importantly, the cells are “treatment-resistant” and thus important clinically. The isolated SP from primary neuroblastoma and a variety of cancer cell lines (bone, brain, breast, kidney, lung and ovary) was shown to efflux the chemotherapy agent Mitoxantrone and ultimately survive whereas the NSP cells were unable to proliferate and form colonies following

treatment⁴⁶³. Similar findings were demonstrated by the SP from gastro-intestinal cell lines, these being more resistant to three chemotherapy agents; 5-Fluorouracil; Doxorubicin and Gemcitabine⁴⁶⁴. Indeed, evidence is available to demonstrating the relative chemoresistance of SCs compared with the differentiated cellular populations⁴⁶⁵. This survival advantage is clearly beneficial to the organ or tissue as it is the SC that would survive and be able to repair and repopulate an injured tissue. Furthermore, this would explain the mechanism surrounding disease remission, relapse, treatment resistance and ultimately progression discussed earlier.

The Genito-Urinary Cancer Research Group (GUCR) at the Paterson Institute for Cancer Research (PICR) now has extensive experience of the Hoechst 33342 dye efflux technique in determination of the SP of both normal and malignant prostate epithelial populations. This functional determination of the SC population follows on from the haematological experience of SP characterisation⁴⁴⁷. Bhatt *et al* successfully applied the technique to solid tumours by investigating the prostate⁴⁵⁸. On average the prostatic SP accounted for 1.38+/-0.07% of the total prostate epithelial population and this was significantly reduced by the addition of Verapamil⁴⁵⁸. Cells with a basal phenotype were enriched in the SP (mean 218% P<0.005). Cell cycle analysis was determined by plotting Hoechst 33342 (DNA) content on the x-axis and Pyronin Y (ribonucleic acid (RNA)) staining on the y-axis. Cells in G₀ were defined as having no more than 2n DNA and a low RNA content determined by Pyronin Y fluorescence. Results were comparable to

those reported from the study of CD34⁺ve HSCs⁴⁶⁶. The prostatic SP was composed of 12.38 \pm 0.31% G₀ cells and 63.19 \pm 2.12% G₁ cells (higher RNA content)⁴⁵⁸.

Brown and Gilmore *et al* modified the Hoechst protocol from that of Bhatt *et al* by limiting Hoechst 33342 staining to 5 μ M per 1 \times 10⁶ prostate epithelial cells/mL for 90 minutes at 37°C with continuous agitation. Bhatt *et al* had pre-labelled the SP population with Ber-EP4 and α 2 integrin which precluded further phenotyping. Cells excluded from these plots were noted to have forward and side scatter plots similar to CD45⁺ve lymphocytes. Similar Verapamil-sensitive SP populations were then defined for both the benign and malignant patient samples with additional CD45⁻ve selection. The SP populations comprised 0.93 \pm 0.12% and 0.57 \pm 0.11% of the total epithelial populations respectively⁴³¹. Phenotypic analysis with Ber-EP4-FITC confirmed epithelial cells.

Characterisation of the prostate SP supports findings in the HSCs. The SP cells were demonstrated to be significantly smaller than the cells from the main body of the sample (NSP) by 3-D thresholding. Notably the SP cells had little cytoplasm. The benign SP was shown to be enriched for cells with a basal cytokeratin phenotype (CK5⁺ve/CK14⁺ve) compared with the benign NSP. This was further supported by the enhanced expression of p63 in the SP population and decreased expression of PSA. The SC markers p21^{WAF1/Cip1}, p27^{kip1} and Msi-1 were preferentially expressed in the SP population compared with the NSP

but there was no significant differences identified for Notch1, β -catenin and Cleaved Notch ⁴³¹.

The malignant SP demonstrated an increased expression of luminal markers CK8 and CK18 and the interesting finding of decreased AR expression. The malignant SP cells were noticeably different and a lower proportion expressed p21^{WAF1/Cip1}.

Tissue marker localisation was performed to determine the histological location of SP and NSP cells within the prostate acinus. Unlike the staining of the benign tissue, malignant acini were primarily composed of PSA-expressing luminal cells. The basal layer also appeared breached or indeed absent. This may complement the decreased integrity of the basal layer in CaP ⁴⁶⁷. Furthermore this may represent a shift of the SC population to a strongly proliferative TAP ^{394, 402, 468, 469} or a more primitive undifferentiated phenotype ⁴³¹.

Brown *et al* also showed that the benign SP was enriched for the RNA binding protein Musashi, which is a marker of both colonic and neural SCs ^{470, 471} and is required for asymmetric division. Furthermore higher expression of the cyclin dependant kinase inhibitor (CDKI) p21^{WAF1/Cip1} was present in the benign SP and co-localised to the basal layers of the acinus where it constituted less than 1% of the total population. The authors postulated that such findings are in keeping with a population (SP) enriched for cells with SC characteristics. Interestingly and somewhat surprisingly the markers were not detectable in the histological sections of malignant prostate. The loss of such regulatory

markers in the SP population may highlight the presence of CSCs which have gained the ability to cycle, differentiate, proliferate and self-renew and thus behave like a multipotent SC²⁹⁰. Finally p27^{kip1} is believed to prevent progression of the cell cycle through to S-phase and thus its expression signifies the quiescent population shown by Bhatt *et al*⁴⁵⁸. Increased expression was demonstrated in the benign SP compared with the benign NSP however a lower proportion was seen in malignant samples, where SP and NSP proportions were similar.

Following the protocol devised by Lang *et al*⁴³⁰, 1-4x10³ SP or NSP cells were placed into long term culture suspended in Matrigel in addition to DHT, oestrogen and a STO feeder layer. Both populations generated spheroids after 2 or 3 weeks in culture. Although not significant (p=0.34) the efficiency appeared to be greater in the SP and only the SP cells generated branching, hollow spheroids akin to the acinus morphology or the prostate (23+/-12%).

1.3.8 Summary of Experimental Evidence for Prostate Stem Cells

In summary, experimental evidence confirms the identification of cell populations with stem-like features but it is likely that these individual subsets of either label-retaining, CD44^{+ve}, CD133^{+ve} or SP cells actually overlap and merely offer methods for SC and CSC purification rather than their absolute determination⁸. They are likely to consist of tumour progenitors as well as a fraction of the more primitive CSCs. Despite this, such AR^{-ve} populations are inherently more tumourigenic than the bulk of the prostate tumour which is made up of more differentiated

luminal cells that are CD57^{+ve} and AR^{+ve} ⁴⁴⁶. Ultimately, *in vivo* serial transplantation data is still required to be able to confirm secondary tumour initiation and thus inexorably that a given cell population has the requisite properties of self renewal required to be labelled a SC or CSC ⁴⁷².

1.3.9 Epithelial Stem Cell Regulation

In order that the normal tissue homeostasis is preserved, careful coordinated control of the SC hierarchy must be ensured with the rates of apoptosis being matched by the proliferation of the SC and TAP compartments. Control is influenced by cellular interactions with the extracellular matrix, adjacent cells and soluble factors in the SC niche. Constituent parts of some of these regulatory pathways have been proposed as putative markers for SC identification.

1.3.9.1 Integrins

The integrins are involved in cell to cell adhesion and adhesion of the cell to the basement membrane. Study of other epithelial systems has revealed enrichment for SC characteristics in cell populations that preferentially adhere to type I collagen or other extracellular matrices via the functional $\alpha 2$ and $\beta 1$ integrins ³⁸⁰. Loss of these integrins signifies the passage of the cell from the SC niche to a differentiating pathway ⁴⁷³, ⁴⁷⁴.

$\alpha 2\beta 1$, also known as CD49b, acts as a type IV collagen cell membrane receptor in both epithelial tissues ⁴⁷⁵ and the haemopoietic system ⁴⁷⁶.

Jones *et al* used the differential binding capacity of the $\beta 1$ -integrin to type IV collagen to differentiate between SCs and the TAP. SCs expressed high levels of $\beta 1$ -integrin, rapidly adhered to collagen and had functional properties characteristic of SCs whereas cells adhering more slowly behaved like the TAP ³⁸⁰.

In addition to the belief that $\beta 1$ -integrin maintains the SC in its quiescent state by its adherence to the basement membrane, it also controls the cell phenotype and proliferative potential by stimulating the mitogen activation protein (MAP) kinase cascade which keeps the cell in quiescence. Low $\alpha 2\beta 1$ expression down regulates the MAP kinase cascade and initiates the cell to re-enter the cell cycle and potentially differentiate down a specific lineage ⁴⁷⁷.

1.3.9.2 Notch Signalling

Partial loss of the Notch gene causes notch formation in the wings of flies ⁴⁷⁸. The gene codes for four transmembrane proteins and is responsible for normal development. These proteins interact with ligands of the Notch receptor on adjacent cells. Activation of the ligands (Delta and Jagged) induces the intracellular domain (Cleaved Notch) to move to the nucleus where it activates the transcription factor Suppressor of Hairless (SuH). The combined action of SuH and the DNA binding protein retinol binding protein (RBP-1) leads to upregulation of Hairy/enhancer of split 1 and 5 (HES). These downstream genes are responsible for inducing adjacent cells to enter the differentiation pathway ^{479, 480}.

In normal murine prostate tissue, Wang *et al*/ demonstrated that inhibition of Notch prevented branching morphogenesis, growth and differentiation in the developing organ as well as preventing recapitulation of the castrated mouse epithelium after re-instituting androgens ⁴⁸¹.

Upregulation of Notch 1 was also seen in the TRAMP mouse model during tumourigenesis ⁴⁸² suggesting that disruption of the normal Notch-mediated SC niche may precipitate the increased proliferation seen in carcinogenesis.

1.3.9.3 Hedgehog Signaling

The human Hedgehog gene encodes a protein essential for the *in utero* development of the orbital structures with loss leading to cyclopia ⁴⁸³.

There are three Hedgehog genes in mammals termed Sonic (SHH), Indian (IHH) and Desert (DHH). Hedgehog and its transmembrane receptors Patched and Smoothened signal ultimately to the Gli transcription factor and it has been suggested that they play an important role in SC self renewal. Experiments to block the Hedgehog pathway both *in vitro* and *in vivo* led to inhibition of cell growth ⁴⁸⁴.

1.3.9.4 The Wnt Pathway, Beta Catenin and c-Myc

Beta Catenin is a subunit of the cadherin family of transmembrane proteins and has been implicated as having a role in cell to cell adhesion as well as playing an integral part of the Wnt signalling pathway which controls cellular self renewal, proliferation and differentiation ⁴⁸⁵. Beta Catenin has an associated scaffolding protein called Axin and when this

complexes with glycogen synthase kinase 3 (GSK3) and the adenomatosis polyposis coli (APC) gene product, a substantial increase in the phosphorylation of Beta Catenin occurs. Phosphorylated Beta Catenin degrades. When Wnt binds to its receptor (Frizzled), the effector protein (Dishevelled) is recruited to the membrane and inactivates GSK3 and thus phosphorylation of Beta Catenin. Consequently, Beta Catenin is allowed to build up in the cytosol and translocate to the nucleus⁴⁸⁶. Once inside the nucleus, Beta Catenin activates the transcription factors lymphoid enhancing factor (Lef-1) and T-cell factor 1 (Tcf-1)⁴⁸⁷.

Loss of GSK-3 regulated phosphorylation of Beta Catenin in mouse basal epidermal cells induced keratinocytes to undergo a process resembling *de novo* hair morphogenesis. The new follicles formed dermal papilla and sebaceous glands which usually only occurs during embryogenesis⁴⁸⁸. Beta Catenin has been proposed as a putative SC marker as its expression has been shown to correlate with SC density in keratinocytes. In this study, the authors concluded that Beta Catenin functioned through its stimulation of the transcription factors Tcf-1 and Lef-1 rather than by effecting cell cycle kinetics or cell to cell adhesion.

Beta Catenin also regulates the DNA binding protein c-myc, part of the basic helix-loop-helix family. c-myc regulates transcription to suppress differentiation of cell lineages and stimulate cell proliferation. c-myc is down-regulated in cells when they differentiate thus it has been suggested as a possible marker of more primitive cells^{489, 490}.

Dysfunction of the Wnt pathway has been linked to the development of murine breast tumours³⁶⁷, but its strongest links are to colon cancer development secondary to the down regulation of the tumour suppressor gene product APC. Abnormal phosphorylation of Beta Catenin allows it to accumulate and increase Tcf mediated transcription⁴⁹¹. Finally, putative mouse prostate CSCs have been demonstrated to express Beta Catenin⁴⁶² and Wnt signalling has been implicated with enhanced tumourigenicity in human CaP^{492, 493}.

1.3.9.5 The Cyclin Dependent Kinase Inhibitors p21^{WAF/Cip1} and p27^{Kip1}

As their name suggests, the cyclin dependent kinase inhibitors p21^{WAF/Cip1} and p27^{Kip1} interrupt cyclin and cyclin dependent kinase complex formation and thus act as cell cycle regulators. Both cause G₁ cell cycle arrest allowing time for DNA repair in damaged cells³⁰². p21^{WAF/Cip1} is upregulated by the tumour suppressor gene p53 in response to stress stimuli. It has been proposed as a putative SC marker and is believed to hold the SC in G₀ preventing uncontrolled differentiation of the SC compartment down the cellular hierarchy until mitogenic stimuli dictate otherwise (reviewed by Ezoe *et al*⁴⁹⁴). Indeed loss of p21^{WAF/Cip1} in the primitive bone marrow cells of the haemopoietic system was shown to encourage cells down a path of terminal differentiation. In addition, lack of self renewal caused exhaustion of the SC compartment⁴⁹⁵. Di Cunto *et al* reported that p21^{WAF/Cip1} expression reduced as a cell's pluripotency decreased⁴⁹⁶.

Down regulation of p27^{Kip1} expression by mitogenic stimuli allows the cell to progress through the G₁/S restriction point ⁴⁹⁷. In contrast to p21 knockout mice, p27-null mice had normal numbers of haemopoietic SCs which were able to self renew but had an decreased number of early progenitors. The p27 knockout mice were able to regenerate on serial transplantation whereas p21 deficient mice were not suggesting that p27^{Kip1} is a marker of the TAP and important for proliferation of the early progenitors. De Marzo *et al* concluded that p27 expression correlated with the TAP and that loss of the normal p27 regulation of this compartment may be critical to the development of carcinogenesis in CaP ⁴⁰¹. The degree of p27 loss has since been shown to correlate with advanced tumour grade in CaP ⁴⁹⁸.

1.3.9.6 Musashi-1

Musashi-1 (Msi-1) is a member of the Musashi RNA binding protein family and is expressed in the nucleus or cytoplasm of neural multipotent progenitor cells that differentiate into the functional neural tissue (neurons and glia). Such expression decreases as the neurogenic process matures from foetus to adult ^{499, 500}.

Numb mRNA encodes a membrane associated antagonist of Notch signalling and is therefore believed to be involved in the determination of cell fate. By blocking Numb, Msi-1 allows Notch-1 to maintain cells in a primitive undifferentiated state ⁵⁰¹.

The nuclear activation of Notch signalling and suppression of malignant cell apoptosis is seen in glioblastomas and corresponds with a high nuclear staining for Msi-1⁴⁷⁹. In a panel of RNA from 32 cancers and cell lines, increased expression of Msi-1 correlated with CNS malignancies in contrast to low levels of expression in prostate cancer and melanoma. Not only did expression appear specific to the CNS but was increased compared to non-neoplastic CNS tissue and the highest expression was evident in Glioblastoma, the most malignant tumour. Indeed, Msi-1 has been suggested as a diagnostic and prognostic tool in neurological tumours that contain primitive cell types⁴⁷¹.

As in the CNS, Msi-1 expression appears to also be downregulated as gut epithelial cells mature and more towards the villus. Potten *et al* reported that the Msi-1^{hi} cells were not only relatively radiation-resistant compared to other gut epithelial cells but appeared to be responsible for repopulation of the damaged tissue⁴⁷⁰.

1.3.9.7 TGF- β

TGF- β appears to play a role in maintaining such cells within the quiescent state by limiting SC proliferation^{426, 502}. Lack of TGF- β signalling from the stroma induces marked epithelial proliferation⁵⁰³ and indeed carcinogenesis (TGF- β type 2)^{504, 505}. Bcl-2 is believed to antagonise the effects of TGF- β mediated apoptosis⁵⁰⁶.

1.3.9.8 CD133

In 1997, Yin *et al* produced a monoclonal antibody to the murine AC133 antigen which is a glycosylation-dependent epitope of human CD133 (prominin-1), a five transmembrane domain glycoprotein and cell surface protein. Demonstration of its exclusive expression in CD34⁺⁵⁰⁶ haemopoietic progenitor cells and the ability of these cells to repopulate xenografted animals led to its implication as a cell surface marker for a stem population ⁵⁰⁷.

CD133 has been reported to enrich for SC characteristics in the neural ³⁴⁰ and endothelial populations ⁵⁰⁸. Furthermore it has been suggested as a marker of cancer stem cell populations in brain tumours ³⁵⁸, prostatic malignancy ⁴⁴⁶, adenocarcinoma of the pancreas ⁵⁰⁹, carcinoma of the colon ^{510, 511}, hepatocellular carcinoma ⁵¹² and renal tumours ⁵¹³.

Unlike the reported observations using the AC133 epitope, CD133 mRNA has been shown to be strongly expressed in several tissues including adult kidney: the authors concluded that AC133 expression was restricted to undifferentiated cells whereas CD133 expression was maintained throughout the process of cell differentiation (reviewed by Florek *et al.* ⁵¹⁴). In an attempt to resolve any uncertainties about CD133 expression, Shmelkov *et al* developed a transgenic mouse model with endogenous promoters of CD133 which, in turn, drive the expression of the promoter gene *lacZ* and demonstrated that both undifferentiated and differentiated colonic epithelial cells in mice and humans expressed CD133 ³⁴¹. The demonstration that virtually the entire tumour cell

population were CD133⁺ve provides further evidence to suggest that CD133 is not a marker of organ-specific SC's in the colon and indeed the CD133⁻ve phenotype was associated with a more aggressive phenotype in metastatic tumours ³⁴¹.

Beier *et al* studied the role of CD133 in Glioblastoma-derived CSC's ⁵¹⁵. The authors demonstrated that four out of the 15 tumours examined were composed of cells with a CD133⁻ve phenotype and that these still had SC characteristics. Whilst the CD133⁻ve cells had a lower proliferative index, this evidence supported the theory that in neural CSC's (and potentially also in other tissue-specific SC's), CD133 status is not the determinant of the SC compartment.

Evidence for a more primitive lineage negative population has been strengthened by the experience of Wang *et al* ⁵¹⁶ who have suggested that CD133 expression is not required for a brain tumour's initiation but may be involved in its progression. Brain tumours initiated directly from biopsy material expressed little or no CD133. Following passage, these CD133⁻ve tumours gradually started to display increasing levels of CD133 which coincided with a shorter survival, a finding more characteristic of an amplifying / differentiating population than a stem one. Subsequent implantation of CD133⁻ve cells into the brains of six nude rats led to the confirmation of tumourigenesis in three cases. Interestingly, CD133⁺ve cells were ultimately harvested from the tumour populations that had been originally initiated by the CD133⁻ve cells. It is therefore arguable that the most likely hierarchy in relation to CD133 is

that the CD133^{-ve} population represents either the SC or terminally differentiated populations and that the TAP has a CD133^{+ve} phenotype.

1.3.9.9 PTEN

The tumour suppressor cytoplasmic phosphatase PTEN negatively regulates signalling via the phospho-inositide 3-kinase (PI3K) pathway and keeps proliferation in check and the SC compartment in a quiescent state. Loss of PTEN has been shown to be directly linked to the activation of cancer-initiating cells in leukaemia and the development of myeloproliferative disease and leukaemia itself^{517, 518}. The causal relationship between PTEN deletion and leukaemia-initiating cells was confirmed by the rescue of the disease with the mTOR inhibitor rapamycin which acts on the downstream products of the PI3K pathway⁵¹⁹. An observational study of PTEN deletion in the murine prostate revealed the development of localised CaP over a period of months before subsequently transforming into invasive luminal adenocarcinoma accompanied by occasional micrometastatic deposits in the lymph nodes, liver and lungs⁵²⁰. One study has suggested PTEN as having a role in the control of prostate cancer-initiating cells⁵²¹ but further study is required⁵¹⁹

1.3.9.10 p63

p63 is a homologue of the tumour suppressor gene p53. It is also a lineage marker, specifically being a marker of basal epithelial cells. The precise mechanism for p63 is as yet not entirely defined. Genetic studies

have suggested that p63 is essential for the preservation of the epithelial ability to regenerate. p63^{-/-} mice developed with truncated or absent limbs and without epithelial structures such as mammary glands (reviewed by Finlan and Hupp⁵²²). Loss of p63 would encourage cellular differentiation and mice that over express p63 were shown to have accelerated ageing of the skin with deficiencies in wound healing capability, decreased skin thickness and hair loss^{523, 524}.

Using p63-null mice, Signoretti *et al* demonstrated failure of prostate development and concluded that the p63^{+ve} basal layer of the prostate must contain the SC compartment. The same group also showed that 97% of CaP did not express p63⁵²⁵.

1.3.9.11 Steroids

Whereas the luminal secretory epithelium is dependent on androgens, the majority of cells within the basal population are not. Androgens appears important for control of differentiation from a basal to luminal phenotype and mediate this via the stromal cells (reviewed by Ware⁵²⁶). Oestrogen and progesterone receptors have been demonstrated in the basal layer and oestrogens have been shown to cause basal cell hyperplasia suggesting they counteract the androgen-driven differentiation to luminal cells^{293, 526}.

1.3.9.12 Non-Steroidal Factors

In addition to this hormonal control, a feedback loop involving non-steroidal growth factors exists between the luminal (factor positive) and

basal (receptor positive) populations. These non-steroidal factors may in turn be controlled by androgens. An example is epidermal growth factor (EGF), produced by the secretory epithelial layer, which is not only required for *in vitro* proliferation of prostate epithelial cells but is likely to also play an important role *in vivo* with basal cells expressing the EGF receptor ^{293, 526}. Other suggested growth factors include Fibroblast Growth Factor (FGF) ⁵²⁷, Insulin-like Growth Factor-1 (IGF-1) and Nerve Growth Factor (NGF) ²⁹³.

1.4 Molecular Biology Techniques

1.4.1 Principles of Gene Expression Analysis

Gene expression is the process whereby the DNA sequence of a gene can potentially be used to make a functional protein. Transcription involves the formation of messenger RNA (mRNA) complementary to the base sequence on the template DNA strand under the control of the enzyme RNA polymerase. The mRNA carries the genetic code to the ribosomes in the cytoplasm. RNA differs from DNA in that it contains a uracil base instead of thymine. On reaching the ribosome, the process of translation leads to the synthesis of polypeptide chains. Amino acids attached to transfer RNA (tRNA) are brought into sequence by the binding of the tRNA codons to the complementary base sequences on the mRNA strand and protein synthesis occurs (reviewed by Allen *et al* ⁵²⁸). However, not all genes encode proteins and not all mRNA transcripts result in a protein formation.

Whilst the genome across all of an organism's cells is identical, the organism controls the degree to which different genes are actively expressed. Only those genes that are required at that given time are switched on. The mRNA from such "active" genes is termed the transcriptome and its cellular concentration can be measured to determine the gene expression profile of a cell. The measurement of a transcriptome can indicate the function and phenotype of a particular cell at a particular time point. Studying the transcriptome of a particular cell phenotype (expression profiling) allows a better understanding of its function and provides the opportunity for comparison with other phenotypes. For example, the differential expression of genes between cancerous and non-cancerous cell populations may elucidate the dysfunctional processes that initiate carcinogenesis.

Copies of known DNA sequences (probes) are hybridised with the RNA extracted from the cells being studied after the RNA has been converted to complementary DNA (cDNA). If hybridisation occurs, a fluorescent signal will be released and can be detected. In order to assess the entire transcriptome of a cell this hybridisation process must be repeated for each gene expressed. This is achieved by the use of a microarray of DNA sequences.

In an early experiment, all 6000 genes of *Saccharomyces cerevisiae* were immobilised on an 80 by 80 array placed on an 18mm² glass slide. The differential gene expression that was associated with the switch from aerobic to anaerobic respiration was assayed. Hybridisation of

labelled cDNA to the DNA probes of the array was detected by confocal microscopy and revealed that 1740 genes showed two-fold or greater changes in expression either up or down ⁵²⁹. Applying such techniques to the larger human transcriptome has brought its own challenges. The earliest DNA chips used to be manufactured on glass slides or a nylon membrane which meant that only a relatively low probe density could be achieved.

Potential weaknesses to gene expression profiling are that not all transcribed mRNAs will be translated into proteins. Arguably, proteomics affords a more reliable study of a cell's functional state. Furthermore, in a process known as alternative splicing, it has become apparent that identical mRNA sequences may in fact result in different protein products. This is a mechanism whereby eukaryotic cells can store their genetic code economically yet remain phenotypically diverse. Sequences known as exons are separated from the remainder of the original mRNA sequence (pre-mRNA) and reconnected in such a way as to produce alternative ribonucleotide sequences and, after translation, different protein isoforms ⁵³⁰. More intense scrutinisation of the mRNA sequences is possible with exon arrays. These report the presence of individual exons and thus determine the precise splice variant expressed. Finally, important genes may be missed due to their production of low levels of transcript. Improved chemistries are now available which maximise the ability of arrays to detect such transcripts.

1.4.2 Affymetrix® GeneChip® Technology

High density microarray technology is designed to measure gene expression at a transcriptional level. Different sets of probes are used to scrutinise the large transcriptomes from mammalian cells in relation to different cell characteristics. The Affymetrix® system uses photolithography to chemically synthesise oligonucleotide probes *in situ* at specific locations (features) on the quartz-coated surface of the chip. The quartz wafer possesses a compound that only allows formation of a bond between itself and the first nucleotide of the probe sequence in the presence of light. Lithographic masks either block or transmit light onto specific locations of the wafer surface corresponding to the different probes. Adenine, thymine, cytosine or guanine bases are then introduced to the wafer and coupling is allowed to occur in the illuminated regions that have been unprotected from the light. In turn, the coupled nucleotide also bonds with the next nucleotide in the presence of light and thus, with the introduction of the various bases and the cyclical masking and unmasking of light, the probes are manufactured

531, 532 .

Each probe is 25 base pairs long (25-mer) and is designed to hybridise to a particular complementary sequence towards the 3' end of the known biological transcript. An advantage with the Affymetrix® GeneChip® technology is the ability of the array to quantify non-specific hybridisation. This is achieved because each probe is represented on the GeneChip® by a perfect match to the transcript as well as by a

'mismatch' probe which has a single base change half way along its 25-mer length. This 'mismatch' probe allows the researcher to quantify the degree of background non-specific binding for each probeset.

Depending on the specific GeneChip[®] used, each transcript is targeted by 11-20 probe pairs (perfect match and mismatch) and these interrogate different regions within the same sequence. Together such a collection of probes are known as a probeset. Each array constitutes thousands of probe cells which in turn are composed of millions of identical base sequences.

Following cellular extraction, mRNA is converted to complementary DNA (cDNA). This provides increased stability. The cDNA is labelled with a fluorescent tag and presented to the array. Wherever the transcript finds a complementary probe sequence on the array chip, hybridisation and consequently fluorescence will occur. The GeneChip[®] consists of millions of probes for each probe-sequence therefore the array is able to determine a quantitative measure of the amount of transcript in solution. The degree of fluorescence detected by the laser on scanning is proportional to the degree of hybridisation, the brighter the fluorescent signal the greater the transcriptional product. A camera calculates the average intensity of each spot. As the perfect match and mismatch pairs are placed next to each other the true expression values above background can be calculated for each probe pair representing a gene. Ultimately the signal from these multiple probes in each probeset must be combined into a single value called the expression summary.

1.4.3 Gene Expression Analysis

In order to compare expression data from different samples, any differences between arrays must first be corrected for. The process, termed normalisation, allows the biological data from different chips to be compared by smoothing any variation induced by upstream experimental factors (eg efficiency of the hybridisation process). A number of normalisation techniques are available, but the most common ones rely on applying a set of computed global statistics to the data to align it. The MAS5.0 algorithm (Affymetrix[®] proprietary software Microarray Suite Version 5.0) makes the assumption that the majority of transcripts isolated and hybridised to the arrays in a particular experiment do not change and therefore each array should have the same (trimmed) mean expression level⁵³³. The scale factor is then indicative of the degree to which a particular array has been altered to bring it into line with the others in the series.

In order to counteract background noise, the MAS5.0 algorithm adjusts the intensities for each region of the chip (probe cell) using the lowest spot intensity values for comparison. The next step is to account for non-specific hybridisation. Expression values for the mismatch probes may simply be subtracted from those of the perfect matches to indicate the true quantitative expression of the transcript. If the product of this intensity value calculation is negative an alternative formula may be employed by MAS5.0. The Tukey Biweight algorithm calculates the mean of the data for each probeset and uses the distance of each

individual intensity value from this mean to determine the weight each point should carry towards the calculation of the final average⁵³³.

MAS5.0 normalisation results in the assignment of a \log_2 expression value for each probeset and provides an indication as to whether a probeset is 'present' (P), 'marginal' (M) or 'absent' (A). Not only does such a 'detection call' provide an additional determinant of confidence, it also allows data to be filtered (for example, by removing all probesets called 'A' on all arrays) to reduce the dataset and remove background⁵³⁴.

The collection of expression summaries for each sample can now be examined and those with significant changes that could contribute to the sample's genetic signature identified. Two sets of microarrays from an experiment (eg stem cell and non-stem cell enriched populations) can be compared by calculating the differences between the expression values for each gene from the two individual arrays. In order to focus the process of analysis, gene lists may be refined by applying a filter to obtain a list of genes with the largest increase or decrease in one group compared to the other. In applying such a filter, a threshold level of fold change must be assigned. Those genes with fold changes of a magnitude greater than this threshold can then be considered important and worthy of further investigation. The determination of such 'genes of interest' is aided by the assignment of statistical significance. In a simple pairwise comparison, with appropriate replicates from each experimental group, a p-value from a t-test is sufficient. Such filters usually focus on

the largest fold changes, it should not be forgotten that genes may still have great biological significance despite exhibiting only minor fold changes between the two samples. In addition, whilst a fold change may be high and therefore infer differential expression of a transcript, it is important to review the individual raw expression values and ensure that at least one value is indeed significant.

1.4.4 Microarray Analysis of the Prostate

The majority of microarray studies in the prostate field have so far focused on genome-wide changes evident in BPH and CaP. The availability of larger arrays has removed the potential bias of smaller spotted membrane arrays which limited the number of genes that could be simultaneously studied and were relatively insensitive at detecting low levels of expression. Despite this differential expression was seen with both increased⁵³⁵ and decreased⁵³⁶ transcript expression detected in CaP. Numerous studies have now used larger arrays to simultaneously examine the expression of thousands of genes in normal prostatic, BPH and CaP tissues using hierarchical clustering which groups samples based on the similarity of their expression profiles. Using such analytical techniques many lists of differentially expressed genes have been published. Using spotted arrays, CaP samples have been discriminated from BPH samples⁵³⁷ and 76 genes were shown to be differentially expressed between normal prostate tissue derived from radical prostatectomy specimens and BPH tissue derived from open prostatectomy and TURP⁵³⁸. Normal prostate, BPH, localised CaP and

metastatic CaP have all been shown to cluster separately⁵³⁹.

Differences between normal prostatic and CaP tissue have been demonstrated using Affymetrix array technology⁵⁴⁰. All three groups identified increased expression of the transmembrane serine protease hepsin in CaP. Dhanasekaran *et al*⁵³⁹ reported the paradox that lower levels of hepsin in CaP predicted a worse prognosis (reviewed by Brooks⁵⁴¹). Many potential biomarkers have been identified by such genome-wide expression analysis and collaborative projects such as that coordinated by the US National Cancer Institute hope to provide the numbers required to allow subclasses of gene expression signatures to discriminate clinical prognosis regardless of histological appearance. Singh *et al* have already reported a correlation between Gleason score and their expression data⁵⁴². The urologic epithelial stem cell database (UESC)⁵⁴³ has collated data into an archive which includes details of transcript abundance from DNA microarray analysis.

1.4.5 Microarray Analysis of Putative Stem and Cancer Stem Cell Populations in the Prostate

Historically microarray analysis of the prostate has focused its attention on the search for genome-wide diagnostic markers in the hope that early diagnosis may improve survival. Furthermore, determination of prognosis markers and the likely natural history for a given patient may help determine those cancers that are at a high risk of progression and metastasis within the expected lifetime of the patient, thus alerting the clinician to those patients that are in need of treatment⁵⁴⁴.

The SC theory of cancer has gained new popularity recently and targetted gene expression mapping may help yield more biologically useful information about the SC and CSC phenotypes and thereby retrospectively delineate new markers. Not surprisingly, the majority of the research has been done in the haemopoietic system and this has provided the majority of information about the putative regulatory pathways seen in the SC population ⁵⁴⁵.

Recently, Birnie *et al* have reported on differential gene expression between 12 CaP samples compared to seven BPH controls and by combination of the lists of genes differentially expressed between the proposed SC (CD133^{+ve}/α2β1^{hi}) and differentiated (CD133^{-ve}/α2β1^{low}) populations with those differentially expressed between the normal and malignant SC populations, have proposed a list of 581 differentially expressed genes with functional association with inflammation, cellular adhesion and metastasis. Using hierarchical clustering, their proposed CSC gene signature was able to distinguish between different differentiation states as well as between benign and malignant phenotypes, providing those tumours which had been hormone-manipulated or whose Gleason score was less than seven were excluded. Furthermore, they have suggested focal adhesion signalling and the JAK-STAT pathway as key processes specific to the prostate CSC phenotype ⁵⁴⁶.

Shepherd *et al* have also recently reported further microarray examination of the CD133^{+ve} prostate epithelial cell phenotype using

both primary BPH and HRPC needle core biopsies expanded by culture⁵⁴⁷. They compared the expression profiles of the CD133⁺ and CD133⁻ population both within and between the two tissue types. They reported that conserved differentially expressed genes in the BPH CD133⁺ population fell into the functional subgroups of development, responsiveness to chemical and biotic stimuli, cell proliferation, cell communication and ion homeostasis whereas those in the BPH CD133⁻ fraction were indicative of a TAP, evidenced by the upregulation of genes involved with cell cycle and proliferation, transcription of RNA and protein manufacture. Unlike the CD133⁻ populations in BPH and HRPC, segregation of the CD133⁺ populations between disease groups was less clear with only four of the seven CaP samples forming a separate group and the remaining three samples being insignificantly distinguishable from BPH. Evaluation of the differential expression of genes between benign and malignant CD133⁺ populations therefore only utilised those four populations, but managed to demonstrate a list of 627 up-regulated and 658 down-regulated genes. Application of biological significance to the lists suggested the most significant findings associated with the HRPC CD133⁺ population to be involved in RNA metabolism and processing, cell cycle and small GTPase signal transduction.

1.4.6 Microarray Analysis of Side Populations

The microarray analysis of the Hoechst 33342 SP has been examined in primary haemopoietic⁵⁴⁸ and mammary SC⁵⁴⁹ populations as well as

human breast (MCF-7) ⁵⁵⁰, oesophageal (EC9706 and EC109) ⁵⁵¹, thyroid (ARO, FRO, NPA, and WRO) ⁵⁵², hepatocellular (Huh7 and PLC/PRF/5) ⁵⁵³ and gastrointestinal cancer cell lines ⁴⁶⁴.

The SP from some of these studies was shown to be enriched for “stemness genes” that confer the properties of cell cycle and development regulation. Upregulation of aspects of the Wnt pathway appeared to be a recurring theme across many of the studies in both SCs ⁵⁴⁹ and CSCs ^{551, 553}. Upregulation of members of the ABC transporter family was a consistent finding in the SP though this was not necessarily ABCG2. Other genes enriched in the oesophageal cancer cell line SP were Oct4, SOX2, Bmi-1 and 2FX ⁵⁵¹.

1.4.7 Experimental Limitations to the Study of Prostate Microarrays

It is a commonly held belief that immortalised cell lines are not ideal for gene expression analysis and instead primary tissue should ideally be used. Whichever cell type is used, expression analysis must be interpreted in the context of the *in vitro* experimental conditions used, as a certain percentage of genes may or may not be expressed despite being significant *in vivo*. Particular attention needs to be paid to the hormonal milieu ⁵⁴⁴.

The advantage of cell lines is that cell number does not limit the amount of RNA that is potentially extractable. Prostate tumours are often small and may provide insufficient RNA for microarray analysis. A technique used by some investigators is to place samples into culture and thereby

achieve sufficient cell numbers for further analysis at passage ⁵⁵⁴. This has the propensity for genetic drift of the cellular phenotype.

Not only are cell numbers obtained from the prostate often low but there is a propensity for contamination of the tissue with other cell types. For example epithelial cells may be analysed alongside cells from their supporting stroma. This may not be of biological importance if entire tissue populations are being compared but the relative stromal composition of each tissue should be considered in data interpretation ⁵³⁸. Furthermore, the gene signature for a given phenotype may be influenced by contamination from other pathologies. In the prostate this is a common problem. Both BPH and CaP are often interspersed amongst normal prostatic tissue or each other. Determining that a prostate sample is truly normal is difficult as subtle nuclear changes have been reported in morphologically normal prostate tissue taken from radical prostatectomy specimens, suggesting a possible global epithelial “field change” in CaP ⁵⁵⁵. Finally, the data analysis for genes of significance may be further complicated by signal noise secondary to contaminants that make identification of low levels of differentially expressed genes more difficult and often requires large numbers of sample replicates ⁵⁴¹.

1.5 Clinical Challenges Posed by Prostate Cancer

1) The natural history of CaP is unclear and remains difficult to predict for an individual patient. Current diagnostic tools are limited by their lack of sensitivity and specificity for malignant disease and have a

limited role in determining prognosis. As a consequence, not only are cases of CaP being missed but also, more commonly, there is a potential for over diagnosis and the ensuing diagnostic dilemma of which cancers require definitive treatment and which should be deemed clinically indolent and safely observed. The challenge is to predict the natural history of disease accurately.

2) All radical, and therefore potentially curative, treatments bring the risk of side effects. Currently, RP for truly organ-confined disease affords a good chance of cure for CaP as the SC will be removed. If there is already micrometastatic disease at the time of RP there is the potential for SC survival and consequently the development of recurrent disease. Despite treatment with curative intent, recurrent disease is unfortunately still seen and again suggests the presence of a therapy-resistant SC. The challenge is to identify and characterise this SC or therapy-resistant cell further so that novel targets can be found to directly target and eradicate it.

3) Patients with locally advanced or metastatic spread at presentation are not amenable to curative treatment and their disease is largely controlled by hormone manipulative therapies. Those patients who subsequently develop HRPc with bone metastases have an average life expectancy of only 18 months. The challenge is to identify markers that are more specific for CaP which also provide prognostic stratification of patients. This would improve the screening process and prevent patients presenting with advanced disease. Novel therapeutic

targets against the SC should, in theory, eradicate HRPC as a clinical entity.

1.6 Aims of Research

1.6.1 General Aims

The goal of this project is to fully characterise the phenotype, functionality and genetic signature of the unexpanded SP and NSP isolated from benign and malignant prostate epithelial cells. The SP and NSP gene expression profiles for BPH tissue will be compared with those for CaP to determine the expression profile associated with malignancy.

1.6.2 Specific Aims

1. To analyse existing CD133⁺ SP and NSP Affymetrix microarray data from BPH tissue:

- i) To determine the quality of the microarray data.
- ii) To datamine the microarray data to determine the gene expression profile of the CD133⁺ SP and NSP or, if the microarray quality is poor and unsuitable for further analysis, define protocols for the isolation of mRNA from small cell number populations isolated by FACS.

2. To isolate and characterise subpopulations of the benign and malignant SP using Hoechst 33342 dye efflux protocols:

- i) To determine the immunocytochemical phenotype of such subpopulations for lineage-specific and putative SC markers and to define the differential expression of such markers between the different subpopulations and for each tissue type.
- ii) To characterise the functionality of such subpopulations by the assessment of colony forming efficiency, proliferative capacity, long term self renewal and asymmetric division.
- iii) To use Affymetrix microarrays to determine the differential gene expression profile for each of these subpopulations in both benign and malignant prostatic disease.

1.7 Rationale for Aims

The SC compartments in the prostate are not essential for life and so successful targeting of such a tissue specific SC affords a real therapeutic benefit which is not possible in leukaemias and brain tumours⁵⁵⁶. It appears that the prostatic SC and CSC occupy the basal epithelial population. Whilst there has been excitement about certain SC and CSC markers, no definitive cellular antigen or combination of antigens has yet been reported.

Rather than concentrating on the SC compartment, it is more important to focus attention on the cells that confer cancer initiation or treatment resistance properties. It may be that cancer-initiating or treatment resistant cells are synonymous with the stem population. Either way,

functional assays such as the SP definition afford a highly effective method for isolation and identification of such cellular populations.

The array-based comparison of the putative SC population transcriptome in benign and malignant prostates with each other, and with that of the corresponding differentiated population, will hopefully illuminate the processes that underpin the hierarchical relationship between SCs and the bulk of the differentiated tumour progeny as well as helping to define the key genetic pathways important in carcinogenesis. Determination of new markers that are specific to the SC enriched population will afford researchers with the opportunity to identify and isolate SCs prospectively, determine the molecular pathways specific to SC homeostasis and the changes that confer a phenotype consistent with BPH and CaP. Identification of such pathways would then allow better understanding of the causes of prostate SC dysfunction and utilisation of genetic markers will hopefully allow the development of improved diagnostic and prognostic markers as well as novel therapeutic targets to eliminate the root cause of disease.

Chapter 2: Materials and Methods

2.1 Materials

2.1.1 General Materials

All materials for general use that are mentioned in this chapter were sourced from Sigma-Aldrich (Poole, UK) apart from; RPMI1640 and foetal calf serum (FCS) (Cambrex BioSciences, Verviers, Belgium), collagenase type-1 and trypsin (Lorne Laboratories, Twyford, UK), Hanks' balanced salt solution (HBSS), HEPES, Keratinocyte Serum-Free Media (KSFM), Dulbecco's Modified Eagle's Medium (DMEM), Hoechst 33342, Prolong Gold antifade reagent with DAPI (Invitrogen, Paisley, UK) and Optiprep (Axis – Shield Diagnostics Limited, Dundee, UK).

2.1.2 Antibodies for Hoechst 33342 Dye Efflux Assay

Antibodies used in the FACS analysis of the Hoechst 33342 dye efflux assay included: Mouse Immunoglobulin (IgG)1 (50µg/ml)(Clone X40, Cat #: 345815) and CD45-FITC (Clone 2D1, Cat #: 345808) which were both manufactured by BD Biosciences (San Jose, California, USA); CD133/2-Biotin (50µg/ml)(Clone 293C3) (Miltenyi Biotec, Bergisch Gladbach, Germany), Streptavidin PE-Cy7 (Invitrogen/Caltag™, Paisley, UK Cat #: SA1012) and Streptavidin PE-Cy5 (Sigma-Aldrich, Poole, UK Cat #: S2899). Not all manufacturers supplied information about the type of clone and stock concentration. In these cases the suggested dilution

of the antibody was used and the catalogue numbers have been supplied.

2.1.3 Adjuncts to the RNase-Free Hoechst 33342 Dye Efflux Assay

As described in section 2.8, 0.5% 6.9M Diethyl Pyrocarbonate (DEPC) (Sigma-Aldrich, Poole, UK) was added to the standard PBS carriage buffer. Both Ribonuclease (RNase) Inhibitors used in the adapted protocol (RNaseSecure and SUPERase-In (20u/μL) were manufactured by Ambion (Foster City, California, USA). RNAlater[®] was also acquired from Ambion (Foster City, California, USA).

2.1.4 Antibodies for Immunocytochemistry

The primary antibodies were manufactured by the following companies: mouse IgG1 anti-cytokeratin-8 and mouse IgG2a anti-human p63 from Sigma-Aldrich (Poole, UK); monoclonal mouse IgG1 anti-human p21^{waf1/cip1}, mouse IgG1 anti-human p27^{kip1}, mouse IgG1 anti-human PSA from DAKO (Glostrup, Denmark); mouse IgG1 anti-cytokeratin-5 from BD Biosciences (San Jose, California, USA); normal mouse IgG1, normal mouse IgG2a, normal goat IgG and normal rabbit IgG from R&D systems (Abingdon, UK); polyclonal rabbit anti-Musashi-1 from Abcam (Cambridge, Massachusetts, USA); mouse IgG1 anti-Androgen Receptor from Novocastra (Newcastle-Upon-Tyne, UK); goat polyclonal IgG anti-Notch-1, mouse IgG1 anti-human c-myc and goat polyclonal IgG anti-SHH from Santa Cruz Biotechnology (Santa Cruz, California,

USA), polyclonal rabbit anti-Cleaved Notch and polyclonal rabbit anti-Beta-Catenin from Cell Signalling (Danvers, Massachusetts, USA).

The Alexafluor secondary antibodies comprised a goat anti-mouse IgG 555nm, a goat anti-mouse IgG 488nm, a goat anti-rabbit IgG 488nm, a rabbit anti-goat IgG 488nm and a streptavidin 488nm species. All secondary antibodies and Prolong Gold antifade reagent with DAPI were acquired from Invitrogen-Molecular Probes (Paisley, UK). Information regarding the type of clone, catalogue number and stock concentration of the primary and secondary antibodies are detailed in Table 2.1 and 2.2. Not all manufacturers supplied information about the type of clone and stock concentration. In these cases the suggested dilution of the antibody was used and the catalogue numbers have been supplied.

2.1.5 Flow Cytometry Equipment

All samples were analysed and sorted using a Becton Dickinson (Franklin Lakes, NJ, USA) FACSVantage SE Flow Cytometer. A BroadPass 424/44 filter was used to measure Hoechst red along with a 675/20 BroadPass filter to measure Hoechst Blue (Omega Optical, Brattleboro, VT, USA).

Antibody	Abbreviation	Clone	Immunoglobulin	Species	Manufacturer	Catalogue Number	Stock Concentration	Working Dilution	Secondary Antibody	Blocking Agent
Beta Catenin	Beta Catenin	p21	Polyclonal	Rabbit	Cell Signaling	9562	n/a	1:50	Goat anti-Rabbit IgG	Goat
p21	p21	SK118	IgG1	Mouse	DAKO	M7202	n/a	1:10	Goat anti-Mouse IgG	Goat
Cleaved Notch	Cleaved Notch	VAL1744	Polyclonal	Rabbit	Cell Signaling	2421	n/a	1:50	Goat anti-Rabbit IgG	Goat
p27	p27	SK53G8	IgG1	Mouse	DAKO	M7203	n/a	1:40	Goat anti-Mouse IgG	Goat
Sonic Hedgehog	SHH	N-19	Polyclonal	Goat	Santa Cruz Biotechnology	Sc1194	200µg/mL	1:50	Rabbit anti-Goat IgG	Rabbit
c-myc	c-myc	20329	IgG1	Mouse	Santa Cruz Biotechnology	Sc70464	200µg/mL	1:100	Goat anti-Mouse IgG	Goat
Prostate Specific Antigen	PSA	ER-PR8	IgG1	Mouse	DAKO	M0750	600mg/L	1:25	Goat anti-Mouse IgG	Goat
p63	p63	4A4	IgG2A	Mouse	Sigma-Aldrich	P3737	2mg/mL	1:500	Goat anti-Mouse IgG	Goat
Androgen Receptor	AR	AR27	IgG1	Mouse	Novocastra	NCL-AR-2F12	n/a	1:20	Goat anti-Mouse IgG	Goat
Notch 1	Notch 1	M-20	Polyclonal	Goat	Santa Cruz Biotechnology	Sc8015	200µg/mL	1:50	Rabbit anti-Goat IgG	Rabbit
Cytokeratin 5	CK5	n/a	IgG1	Mouse	BD Biosciences	55506	50µg/100µL	1:75	Goat anti-Mouse IgG	Goat
Cytokeratin 8	CK8	M20	IgG1	Mouse	Sigma-Aldrich	C8301	n/a	1:200	Goat anti-Mouse IgG	Goat
CD133	CD133	293C3	Biotin	Mouse	Millipore Biotech	130-090-852	50µg/mL	1:10	Streptavidin anti-Biotin	Goat
Musashi-1	Msi-1	n/a	Polyclonal	Rabbit	Abcam	33251	1mg/mL	1:1000	Goat anti-Rabbit IgG	Goat
Mouse IgG1 Control	Mouse IgG1	11711	IgG1	Mouse	R+D Systems	MAB002	1µg/µL	1:10	Goat anti-Mouse IgG	Goat
Mouse IgG2A Control	Mouse IgG2A	21102	IgG2A	Mouse	R+D Systems	MAB003	1µg/µL	1:500	Goat anti-Mouse IgG	Goat
Goat IgG Control	Goat IgG	ES30	Polyclonal	Goat	R+D Systems	AB-108-C	1µg/µL	1:50	Rabbit anti-Goat IgG	Rabbit
Rabbit IgG Control	Rabbit IgG	ER11	Polyclonal	Rabbit	R+D Systems	AB-105-C	1µg/µL	1:1000	Goat anti-Rabbit IgG	Goat

Table 2.1: Table showing the details of the primary antibodies used for immunocytochemical analysis of the DSP and PSP isolated from prostate epithelial cells. When available, details of the clone, host species, immunoglobulin isotype, manufacturer, catalogue number, stock concentration and working dilution are shown. The required secondary antibody and blocking agent are then reported for each of the primary antibodies. Not all manufacturers supplied information about the type of clone and stock concentration. In these cases the suggested dilution of the antibody was used and the catalogue numbers have been supplied.

Antibody	Immunoglobulin	Species	Manufacturer	Catalogue Number	Stock Concentration	Working Dilution
Streptavidin Alexafluor 488nm	Biotin		Invitrogen-Molecular Probes	S-32354	2mg/mL	1:100
Goat anti Mouse IgG Alexafluor 488nm	Polyclonal	Goat		A11001	2mg/mL	1:200
Goat anti Rabbit IgG Alexafluor 488nm	Polyclonal	Goat		A11008	2mg/mL	1:200
Rabbit anti Goat IgG Alexafluor 488nm	Polyclonal	Rabbit		A11078	2mg/mL	1:200
Goat anti Mouse IgG Alexafluor 555nm	Polyclonal	Goat		A21127	2mg/mL	1:200

Table 2.2: Table showing the details of the secondary antibodies used for immunocytochemical analysis of the DSP and PSP isolated from prostate epithelial cells. When available, details of the host species, immunoglobulin isotype, manufacturer, catalogue number, stock concentration and working dilution are shown.

2.2 Media Recipes

2.2.1 Growth Media

The culture medium used to demonstrate the SC features of asymmetrical division and long term self renewal in primary prostate epithelial cultures was termed growth media and prepared using the following recipe ⁴⁴⁶: Cholera toxin (100ng/ml) (Sigma-Aldrich, Poole, UK), leucocyte inhibitory factor (2ng/ml)(StemCell Technology, Vancouver, Canada), GM-CSF (1µg/ml) and stem cell factor (20mg/ml) (R+D systems, Abingdon, UK), added to KSFM treated with 0.005µg/ml of human epithelial growth factor, 0.05mg/ml of bovine pituitary extract, antibiotics and antimycotics (100iu/ml Penicillin G sodium, 100µg/ml Streptomycin sulphate and 0.25µg/ml Amphotericin B in 0.85%saline). The addition of 2% FCS modified the recipe to allow differentiation of the cell populations.

2.2.2 PC-3 Media

PC-3 cells were cultured in PC-3 media which was prepared by the addition of 7% FCS and 2mM L-glutamine to Ham's F12. The media was stored at 4°C until required for use at which point it was warmed to 37°C in a waterbath.

2.2.3 STO Media

STO cells were cultured in STO media prepared by the addition of 10% FCS to DMEM. The media was stored at 4°C until required for use at which point it was warmed to 37°C in a waterbath.

2.3 Buffers

2.3.1 Wash Buffer

Wash buffer was made from phosphate buffered saline (PBS) with 1mM EDTA and 1% bovine serum albumin. Hoechst buffer consisted of HBSS with 10% FCS, 2% 1M HEPES and 1% D-glucose.

2.3.2 Optiprep

Optiprep solution is supplied at a stock concentration of 60% (w/v) iodixanol in double distilled water. The working concentration is achieved by mixing two iodixanol solutions of different density. Solution A (20% iodixanol) is high density and is prepared by adding 33.3ml of optiprep to 50ml DMEM. Solution B (10% iodixanol) is low density and prepared by the addition of 16.7ml optiprep to 66ml DMEM. The osmolarity of both solutions A and B was measured and adjusted to 300mOsm by adding double distilled water, the volume of which was calculated by the equation: additional volume of double distilled water required = (measured osmolarity (mOsm) of solution x volume of solution)/300. HEPES (1ml) was added to both solutions followed by the appropriate volume of DMEM to make both solutions up to 100ml total volume. The

solutions were sterilised by filtration and 3ml aliquots of solution A and B were placed into two separate universal tubes. Solutions A and B and their aliquots, double distilled water and some 2ml syringes were stored at 4°C overnight. The required final density of optiprep was 1.080 g/cm³. The density of the aliquots was measured and the required ratio of solution A to B calculated using the equation: $x \text{ ml} = 10(1.080 - \text{Solution B})/(\text{Solution A} - 1.080)$ where x is the volume of solution A that should be added to 10ml solution B. The density of the prepared optiprep was checked and aliquots were stored at -20°C until required.

2.4 Cell Lines

The PC-3 human adenocarcinoma of the prostate epithelial cell line is derived from bone metastases⁵⁵⁷. Mouse STO fibroblasts were routinely used as feeder layers for maintenance of SCs in the undifferentiated state. Their usage was first documented with teratocarcinoma SCs⁵⁵⁸,
559.

Cell line cultures were incubated in T-25 flasks in their appropriate culture media at 37°C in 5%CO₂ in air. Cells were passaged approximately once every three days or immediately on reaching confluence. Passage was performed in a laminar flow Level 2 microbiological safety cabinet (MSC). First the culture media was removed and the monolayer washed twice with PBS. Trypsin/EDTA (1x 0.5g porcine trypsin and 0.2g EDTA in 1 litre HBSS with phenol red, Sigma-Aldrich, Poole, UK Cat #: T3924) was added for two minutes. During this time flasks were returned to 37°C in 5%CO₂ in air. Five

millilitres of appropriate culture media was added to the flask thereby halting the action of the trypsin. A single cell suspension was ensured before cells were split one in six and added to a fresh flask. The cell concentration was diluted by the addition of further culture media which served to ensure the bottom of the flask was adequately covered.

2.5 Processing of Primary Prostate Specimens

Patients were recruited from three teaching hospitals (Salford Royal Hospitals NHS Foundation Trust, Salford, UK; University Hospital of South Manchester NHS Foundation Trust and Christie Hospital NHS Foundation Trust, Manchester, UK) according to the ethics agreements in place. Samples were obtained from consenting individuals undergoing TURP after sufficient tissue had been sent to the pathology department at the original institution in order to secure a clinical diagnosis. The remainder of the sample was placed in 0.9% Normal Saline and sent to the GUCR Group laboratories at the PICR. Normal tissue was retrieved from the prostates of patients undergoing cystoprostatectomy for malignancy of the bladder. Such tissue appeared macroscopically normal.

On arrival at the laboratory, the specimens were appropriately recorded according to the regulations laid down by the Human Tissue Act 2004. Throughout processing a laminar flow Level 2 MSC was used. The TURP chips were bisected with sterile scissors and forceps and half of each chip was placed in 4% Formalin/PBS and sent for further histological analysis so that a diagnosis representative of this sample

could be achieved. A representative sample of the cystoprostatectomy specimen was also sent for histological analysis. Along with the detailed histological report of the main operative specimens from the originating institutions, these reports were checked to confirm the overall histological diagnosis.

A small portion of the samples was placed in a universal tube with 4% Formalin/PBS and a paraffin-embedded slide was subsequently made. A further portion was snap frozen in isopentane methyl-2-butane cooled in a bath of liquid nitrogen. The remaining tissue was diced into pieces approximately 1mm³, suspended in 15ml type 1 collagenase (200U/ml in RPMI 1640 media with 2% foetal calf serum) and incubated in a T-75 flask on a shaking platform at 37°C for at least six hours, preferably overnight.

Following collagenase digestion, cells were centrifuged to pellet the cells (800g/5 minutes/Brake 3) and the supernatant discarded. The cell pellet was resuspended in 10 ml of 0.1% trypsin / wash buffer and incubated for 15 minutes in the same T-75 flask at 37°C on the shaking platform.

The sample was again centrifuged to pellet the cells (800g/5 minutes/Brake 3) and washed twice with wash buffer. The cell population was resuspended in 20ml RPMI 1640 and differential centrifugation (360g/1 minute/Brake Zero) was used to separate the fibroblasts (supernatant) and epithelia (pellet). The fibroblasts were added to a fresh tube and spun down (800g/ 5 minutes/Brake 3). The epithelial cells

were passed through a 100µm cell strainer (BD Biosciences, Bedford, USA) and were then ready for use as a fresh experimental sample.

If there was no immediate need for the epithelia, or fibroblasts, they were spun down (800g/5 minutes/Brake 3) and both the epithelial and fibroblast samples were resuspended in at least 1ml 10% Dimethyl-Sulfoxide (DMSO) in FCS at a concentration less than 2×10^7 cells/ml. The labelled cryovials were frozen slowly by using a freezing head overnight and placed in designated storage positions in liquid nitrogen the following day.

2.6 Standard Hoechst 33342 Dye Efflux Assay for Isolation of the CD133^{+ve}/CD45^{-ve} Side Population

An appropriate sample was identified from the database and removed from the liquid Nitrogen storage. Defrosting was performed by leaving it at room temperature for 30 seconds and then agitating it in a 37°C waterbath for 60 seconds. Pressure was released by partially undoing the cryovial top before resealing again and continuing with agitation until fully defrosted. The remainder of the protocol was undertaken in a laminar flow MSC.

Without delay the sample was then added dropwise to 45ml PBS in a 50ml tube. Two rinses of the cryovial with PBS were performed and also added to the tube before centrifugation at 400g/5 minutes/Brake 3. The supernatant was discarded promptly and the pellet was re-suspended in 5ml Hoechst Buffer and passed through a 40µm cell sieve (BD

Biosciences, Bedford, USA) into a fresh 50ml tube. A further 5ml rinse of the tube was also passed through the filter. After centrifugation (800g/5 minutes/Brake 3), the pellet was resuspended in 1.5ml ice cold Hoechst Buffer and 750µl each was gently pipetted on top of 1.5ml of optiprep that had been pre-cooled to 4°C in two pop-top tubes (Falcon BD, Franklin Lakes, NJ, USA). A further 1.5ml ice cold Hoechst Buffer was used to wash out any remaining cells in the tube and again 750µl was added to each of the two optiprep vials. Cold centrifugation was performed (800g/15 minutes/4°C/Brake 3). The interface layer of live epithelial cells was carefully removed and added to a fresh 50ml tube. The volume was made up to 20ml with Hoechst buffer. If the interface layer was particularly thick then this step was repeated with larger volumes of optiprep (3ml per tube). A further spin was performed (800g/5 minutes/Brake 3). Following resuspension in 1ml Hoechst buffer, a cell count was performed using a haemocytometer. A further centrifuge spin was performed (800g/5 min/Brake 3) and the pellet was resuspended in 100µl Hoechst buffer.

The Verapamil control sample was prepared by removing 10µl of cell suspension and adding it to a pop-top tube labelled 'Hoechst + Verapamil + IgG FITC'. The volume was made up with 490µl (or an appropriate volume such that cellular concentration remained less than 1×10^6 cells/ml) Hoechst buffer and placed on ice. The CD45 control sample was prepared by removing 10µl of the cell suspension and adding it to a pop-top tube labelled 'Hoechst + CD45 FITC'. The volume was again made up with 490µl (or an appropriate volume such that

cellular concentration remained less than 1×10^6 cells/ml) Hoechst buffer and placed on ice. Ten microlitres of Hoechst buffer and 10 μ l CD133/2-Biotin (stock concentration 50 μ g/ml) were added to the remaining 'sort' sample. This was incubated in the dark for 30 minutes at 4°C. A wash with 3ml Hoechst buffer was performed and, following pellet formation (400g/5 minutes/Brake 3), the cells were resuspended in 195 μ l Hoechst buffer and 5 μ l of the secondary antibody Streptavidin-PE-Cy7 was added. Again cells were incubated in the dark for 30 minutes at 4°C. A further wash with 3ml Hoechst buffer was then performed (400g/5 minutes/Brake 3) before the pellet was resuspended in appropriate volumes of Hoechst buffer for Hoechst 33342 dye staining. Cellular concentrations had to be less than or equal to 1×10^6 cells/ml and only a 1ml volume of cell suspension was placed in each pop top tube. On occasion, multiple 'sort' tubes were therefore used.

With the laminar flow hood lights switched off, the remaining antibodies were added to the appropriate tubes (IgG-FITC: 10 μ L/ml of stock concentration 50 μ g/ml and CD45: 10 μ L/ml). The amount of each antibody required had been optimised previously^{431, 458}(Table 2.3). Verapamil (Verapamil V106, Sigma Aldrich, Poole, UK stock concentration 50mM) was then added (4 μ L/ml) to the 'Hoechst + Verapamil + IgG FITC' tube cell suspension. Two minutes later, 5 μ L/ml Hoechst 33342 dye (stock concentration 1mM) was then added to all the tubes. The tubes were wrapped in foil and incubated for 90 minutes on a shaking platform at 37°C.

Tube Constituents	Stock Concentration	Control Tubes		Sort Tube
		Hoechst + Verapamil + IgG-FITC	Hoechst + CD45-FITC	CD45 + CD133 SORT
Verapamil	50mM	4µl/ml		
IgG-FITC	50µg/ml	10µl/ml		
CD45-FITC	n/a		10µl/ml	10µl/ml
CD133/2 Biotin	50µg/ml			100µl/ml
Streptavidin PE-Cy7	n/a			25µl/ml
Hoechst 33342	1mM	5µl/ml	5µl/ml	5µl/ml

Table 2.3: Constituents of each of the control and sort tubes used in the CD133⁺/CD45⁻ Hoechst 33342 Dye Efflux Assay. The stock concentration is shown when available from the manufacturer.

To terminate the reaction, 3ml of ice cold Hoechst buffer was added to each tube. The cells were pelleted and the control tubes were each resuspended in 0.5ml of Hoechst buffer and the sort tube in appropriate volumes for a concentration of less than or equal to 2×10^6 cells/ml. Tubes were placed on ice and taken immediately for FACS.

2.7 Fluorescent-Activated Cell Sorting (FACS) Analysis of the CD133^{+ve}/CD45^{-ve} Hoechst 33342 Dye Efflux Assay

The 'sort' cell sample was sorted using a series of gates applied using the information gained by the preliminary analysis of the cellular population (Figure 2.1). Firstly, the samples were gated for 'live cells' (R1). Dead cells to the left of a forward scatter (cell size, x) against side scatter (cell granularity, y) plot were excluded from further analysis. Next the degree of background fluorescence was defined by the 'Hoechst + CD45 FITC' sample and gate R2 was constructed using a plot of FL-1 (FITC channel) versus FL-3 (Strep-PE-Cy7 channel). On running the 'sort' sample the CD133^{+ve} fluorescence was evident in gate R2 above the level of background fluorescence provided by the CD45 control. The SP tail was defined by the use of the 'Hoechst + Verapamil + IgG FITC' and 'Hoechst + CD45 FITC' controls run on a plot of FL-4 (Hoechst Red) versus FL-5 (Hoechst Blue). The main body of the epithelial population, the NSP, was encompassed by gate R4 on the same plot and selected the main Hoechst 33342 population.

The combination of gates was then defined to collect the SP and NSP populations into pre-labelled sterile tubes containing 1.5ml Hoechst

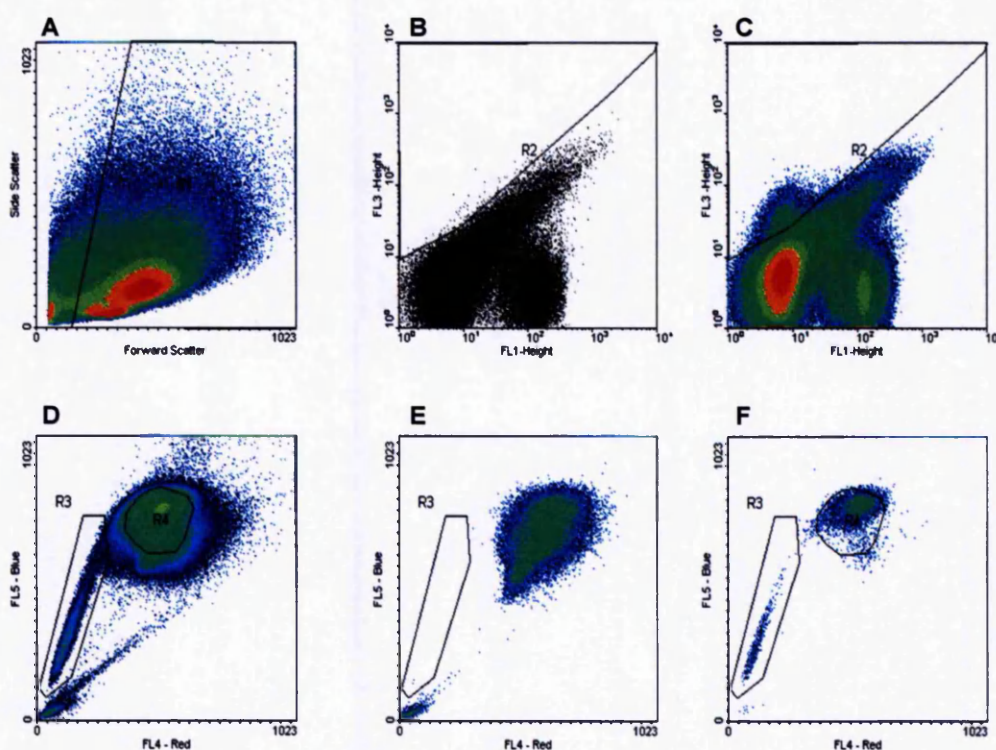


Figure 2.1: Flow Cytometry analysis prior to FACS. (A) Live cells only were included by gate R1. (B) Gate R2 defined the background fluorescence in the 'Hoechst and CD45' control sample so that, when using the 'sort' sample, cells with fluorescence above this control level on the FL-3 axis could be defined as CD133⁺ (C). (D) The SP cells (R3) are low in Hoechst 33342 compared to the main body of the sample, the NSP (R4), because the MDR proteins efflux the toxic dye out of the cell. These cells sit to the bottom left of the Hoechst 33342 Red/Blue plot as a tail with decreasing concentration of Hoechst 33342. (E) The precise location of such cells possessing this capability is defined by the Verapamil control. By blocking the MDR efflux mechanism all cells retain the dye and therefore appear in the main body of the sample. Different combinations of gates can be applied to sort for cells with particular phenotypes. (F) Both a CD133⁺/CD45⁻ live Side Population (SP) (R1+R2+R3) and a CD133⁺/CD45⁻ live non-SP (NSP) (R1+R2+R4) are shown.

buffer. After the necessary processing, these samples could then be used in a variety of further experiments including functional assays of colony-forming efficiency or proliferative capacity, immunocytochemical analysis or Affymetrix® differential gene expression analysis.

2.8 Adaptation of the Hoechst 33342 Dye Efflux Assay to Minimise the Effects of RNases

Four modifications to the Hoechst 33342 dye efflux assay were made to minimise the effect of RNases. Firstly, the standard carrier buffer used by the Flow Cytometry cell sorter was sterile PBS. The sterile PBS was changed to sterile PBS treated with 0.5% 6.9M DEPC. This was prepared the day before a sort by adding DEPC to PBS at the required concentration in a laminar flow hood. After thorough mixing, four litres of solution were left at room temperature for at least 12 hours and then autoclaved before use.

Secondly, prior to transporting the samples for FACS, standard procedure was to resuspend the cells in Hoechst buffer. The modified protocol used ice cold Hoechst buffer that had been pre-treated with 4% RNasecure. The RNasecure had been added to Hoechst buffer at the correct concentration and subsequently warmed to 45 °C for 15 minutes before being cooled again to 4 °C prior to use.

Thirdly, once resuspended in the correct volumes of RNasecure Hoechst buffer, 50µl/ml of SUPERase-In RNase Inhibitor (stock concentration 20u/ml) was added to each of the 'sort' and control tubes.

Fourthly, sorted SP and NSP samples had initially been collected into Hoechst buffer. After a centrifuge step (800g/5 minutes/Brake 3), the cells were then resuspended in RNAlater[®] for stabilisation and storage at -20 °C. A later adaptation to the protocol saw a move towards initial collection in DEPC treated PBS, immediate RNA extraction and storage of the isolated RNA in RNase-free water at -80 °C until required.

A pilot study was performed to assess the effect of the RNase-free modifications to the Hoechst 33342 dye efflux assay. Samples were divided equally into two prior to FACS. One set of samples were sorted using the standard protocol. Immediately after completion of this sort, the FACS carriage buffer was exchanged to the DEPC-treated PBS and the samples that had already been treated with the remaining RNase-free adjuncts were then sorted.

Cells were sorted by gates constructed for the CD45^{-ve} SP (R3) and CD45^{-ve} NSP (R4). No labelling with, or selection for, CD133 was undertaken. An alternative R2 gate was therefore constructed to that previously described. This was now concerned with definition of the CD45^{-ve} population rather than the combined CD133^{+ve}/CD45^{-ve} population (Figure 2.2).

2.9 Modification of the Hoechst 33342 Dye Efflux Assay to Enable Analysis of the Subfractionated Side Population

The standard protocol for determination of the CD133^{+ve}/CD45^{-ve} prostate epithelial cell SP and NSP (described in section 2.6 and 2.7)

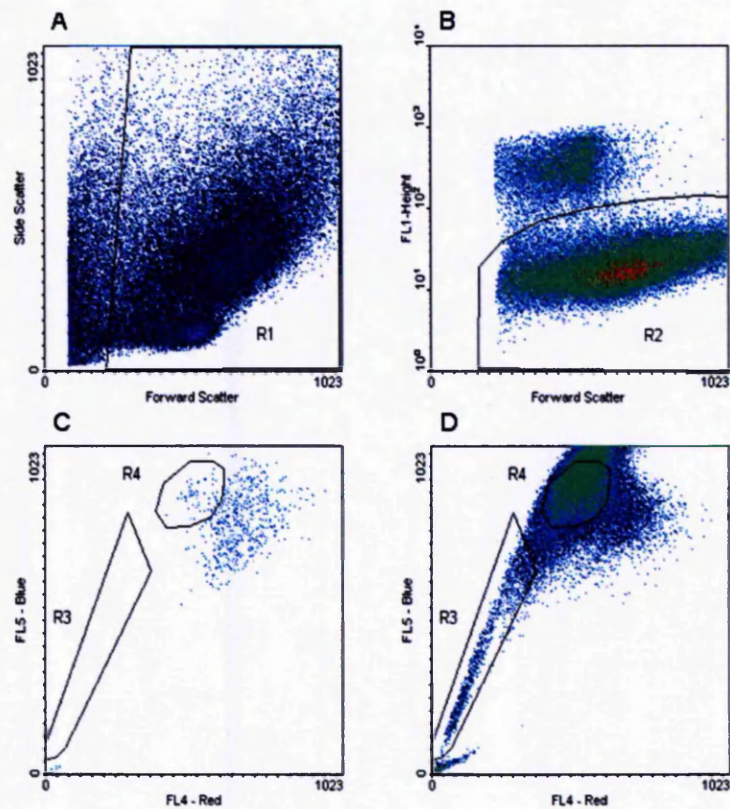


Figure 2.2: Flow Cytometry Analysis prior to FACS. (A) Live cells only were included by gate R1. (B) Using the 'Hoechst and CD45' control sample, gate R2 and the CD45^{-ve} population were defined. (C) The SP cells (R3) were defined by their sensitivity to Verapamil and sit to the bottom left of the Hoechst 33342 Red/Blue plot. (D) A CD45^{-ve} live Side Population (SP) (R1+R2+R3) and a CD45^{-ve} live non-SP (NSP) (R1+R2+R4) are shown.

was followed until the cell count had been performed and the pelleted sample resuspended in 100µl of Hoechst buffer. The Verapamil control sample was prepared by removing 5µl of cell suspension and adding it to a pop-top tube labelled 'Hoechst + Verapamil + IgG FITC'. The volume was made up with 495µl (or an appropriate volume such that cellular concentration remained less than 1×10^6 cells/ml) Hoechst buffer and placed on ice. The CD45 control sample was prepared by removing 5µl of the cell suspension and adding it to a pop-top tube labelled 'Hoechst + CD45 FITC'. The volume was again made up with 495µl (or an appropriate volume such that cellular concentration remained less than 1×10^6 cells/ml) Hoechst buffer and placed on ice. Twenty microlitres of the cell suspension was removed and added to a pop-top tube labelled 'Hoechst + CD45 FITC + CD133'. Seventy microlitres of Hoechst buffer and 10µl CD133/2-Biotin (stock concentration 50µg/ml) were added and the tube incubated in the dark for 30 minutes at 4°C. The remaining 'sort' sample was diluted with Hoechst buffer so that there were 10^6 cells/ml. The sort sample was divided into 1ml aliquots and placed on ice. After 30 minutes the CD133 control was washed with 3ml of Hoechst buffer and centrifuged at 800g/ 5 minutes/ Brake 3. The pellet was resuspended in 195µl of Hoechst buffer before 5µl of Streptavidin-PE-Cy7 was added. Again cells were incubated in the dark for 30 minutes at 4°C. A further wash with 3ml Hoechst buffer and centrifugation (800g/5 minutes/Brake 3) was then performed before the pellet was resuspended in appropriate volumes of Hoechst buffer for Hoechst 33342 dye staining ($<10^6$ cells/ml).

With the laminar flow hood lights switched off, the remaining antibodies were added to the appropriate tubes (IgG-FITC: 10 μ L/ml of stock concentration 50 μ g/ml and CD45: 10 μ L/ml). The amount of each antibody required had been optimised previously^{431, 458}(Table 2.4). Verapamil (Verapamil V106, Sigma Aldrich, Poole, UK stock concentration 50mM) was then added (4 μ L/ml) to the 'Hoechst + Verapamil + IgG FITC' tube cell suspension. Two minutes later, 5 μ L/ml Hoechst 33342 dye (stock concentration 1mM) was then added to all the tubes. The tubes were wrapped in foil and incubated for 90 minutes on a shaking platform at 37°C.

To terminate the reaction, 3ml of ice cold Hoechst buffer was added to each tube. The cells were pelleted and the control tubes were each resuspended in 0.5ml of Hoechst buffer and the sort tube in appropriate volumes for a concentration of less than or equal to 2×10^6 cells/ml. Tubes were placed on ice and taken immediately for FACS.

The flow cytometric analysis for isolation of the subfractionated SP was initially similar to that previous described for the CD133^{+ve}/CD45^{-ve} and CD45^{-ve} Hoechst 33342 dye efflux assays (section 2.6 and 2.7). Again, live cells only were included by gate R1 on a plot of forward against side scatter. Gate R2 defined the background fluorescence in the 'Hoechst and CD45' control sample so that, when using the CD133 control sample, cells with fluorescence above this control level on the FL-3 axis could be defined as CD133^{+ve}. The well-defined CD45^{+ve} population on a plot of forward scatter against FL-1 was excluded and on this occasion

Tube Constituents	Stock Concentration	Control Tubes			Sort Tube
		Hoechst + Verapamil + IgG-FITC	Hoechst + CD45-FITC	Hoechst + CD45-FITC + CD133	CD45-ve SORT
Verapamil	50mM	4µl/ml			
IgG-FITC	50µg/ml	10µl/ml			
CD45-FITC	n/a		10µl/ml	10µl/ml	10µl/ml
CD133/2 Biotin	50µg/ml			100µl/ml	
Streptavidin PE-Cy7	n/a			25µl/ml	
Hoechst 33342	1mM	5µl/ml	5µl/ml	5µl/ml	5µl/ml

Table 2.4: Constituents of each of the control and sort tubes used in the isolation of the CD133^{-ve}/CD45^{-ve} DSP, CD133^{+ve}/CD45^{-ve} PSP and the NSP during the Hoechst 33342 Dye Efflux Assay with subfractionation of the SP. The stock concentration is shown when available from the manufacturer.

this was termed the R3 gate. The IgG-FITC control was used to define the verapamil-sensitive cells (R4) of the SP on a plot of Hoechst red against Hoechst blue. The main body of the sample, the NSP (R5), was then defined on the same axes. The subfractionation of the SP was determined by the CD133 status of its component cells. Using the CD133 control, the same R4 and R5 gates were applied. R6 intersects the CD133^{-ve} low tail (DSP) and CD133^{+ve} high tail (PSP) and was drawn at the level of the CD133^{+ve} cell with the lowest Hoechst 33342 fluorescence. When applied to the main 'sort' sample, the three populations (DSP, PSP & NSP) could be identified and collected for further investigation (Figure 2.3).

2.10 Determination of the Relative CD133 Staining of BPH Epithelial Cells with PE-Cy5 and PE-Cy7 Secondary Conjugate Antibodies

A pilot study was performed to validate the degree of CD133 staining with two different fluorescent conjugates; Streptavidin PE-Cy5 and Streptavidin PE-Cy7. This served to ensure that any CD133 fluorescence observed was a consequence of the cellular phenotype rather than the degree of CD133 staining. Furthermore, the optimal amount of conjugate antibody was checked. The manufacturers did not provide information on concentrations of the conjugate antibodies therefore the volumes added are reported.

An epithelial sample from a patient with BPH was defrosted, added dropwise to PBS and centrifuged (800g/5 min/brake 3). The pellet was resuspended in 5ml Hoechst buffer and this volume was added to 10ml

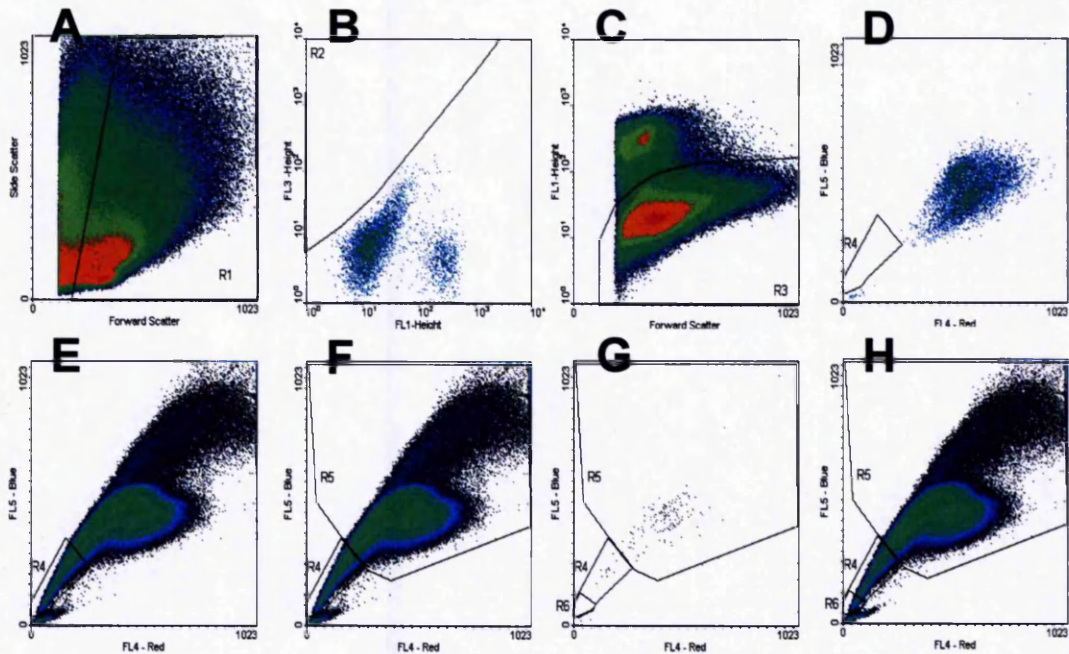


Figure 2.3: Flow Cytometry analysis prior to FACS of the subfractionated Hoechst 33342 dye efflux assay SP. (A) Live cells only were included by gate R1 on a plot of forward against side scatter. (B) Gate R2 defined the background fluorescence in the 'Hoechst and CD45' control sample so that, when using the CD133 sample, cells with fluorescence above this control level on the FL-3 axis could be defined as CD133⁺. (C) The well-defined CD45⁺ population on a plot of forward scatter against FL-1 was excluded by the R3 gate. (D) The IgG-FITC control was used to define the verapamil-sensitive cells of the SP on a plot of Hoechst red against Hoechst blue (R4) (E). (F) The main body of the sample, the NSP (R5), was then defined on the same axes. The subfractionation of the SP was determined by the CD133 status of its component cells. (G) Using the CD133 control, the same R4 and R5 gates were applied. R6 intersects the CD133⁻ low tail (DSP) and CD133⁺ high tail (PSP) and is drawn at the level of the CD133⁺ cell with the lowest Hoechst 33342 fluorescence. (H) When applied to the main 'sort' sample, the three populations (DSP, PSP & NSP) could be identified and collected.

of optiprep. The tube was washed out with a further 5ml volume of Hoechst buffer and added to the optiprep. Centrifugation was then performed in a pre-cooled centrifuge (4°C/15 min/ 800g/Brake 3). The resultant cellular interface was carefully aspirated and added to a tube containing Hoechst buffer. Following a further centrifugation step (800g/5 min/brake 3), the pellet was resuspended in 1ml of Hoechst buffer and a cell count was performed using a haemocytometer. The cells were pelleted (800g/5 min/brake 3) and resuspended in 100µl of Hoechst buffer. Ten microlitres were removed for use as an IgG-FITC control and placed on ice in a pop-top sample tube containing 490µl Hoechst buffer (or an appropriate volume such that cellular concentration remained less than 1×10^6 cells/ml). Ten microlitres of CD133/2 Biotin (stock concentration 50µg/ml) were added to the remaining 90µl of cell suspension and incubated in the dark at 4°C. After 30 minutes, the cells were washed with Hoechst buffer and centrifuged at 800g/ 5 min/ Brake 3. The resultant pellet was resuspended in 1170µl of Hoechst buffer and divided in to six pop-top tubes with aliquots of 195µl in each. Volumes of 2.5µl, 5µl and 7.5µl of Streptavidin PE-Cy5 were added to three separate tubes and 2.5µl, 5µl and 7.5µl of Streptavidin PE-Cy7 were added to the remaining three. The total volume of all the tubes were made up to 200µl by the addition of the required volume of Hoechst buffer where necessary. All six tubes were incubated in the dark at 4°C for 30 minutes. The samples were all washed with Hoechst buffer and centrifuged at 800g /5 min /Brake 3. Whilst performing this centrifugation step, 20µl/ml of IgG-FITC (stock concentration 50µg/ml) was added to

the control sample. The samples were protected from the light, placed on ice and taken for flow cytometric analysis.

Firstly, the live cellular population (R1) was determined by excluding those cells to the left of a forward scatter (cell size, x) against side scatter (cell granularity, y) plot. For each of the PE-Cy5 concentrations, a plot of the FL-1 channel (FITC channel) against the FL-3 channel (PE-Cy5 filter) was created using the IgG-FITC control. This control identified the population R2 and thereby determined the control region without CD133 fluorescence. In turn, the CD133⁺ R2 was determined for each of the concentrations of PE-Cy5 (2.5µL, 5µL and 7.5µL). The filter on the FL-3 channel was then changed and the analysis repeated for the PE-Cy7 fluorescence.

2.11 Determination of the Functional and Phenotypic

Characteristics of the Prostate Epithelial Cell Subpopulations

2.11.1 Primary Monolayer Cell Culture and Colony-Forming Ability

Forty-eight hours prior to FACS, STO cells were irradiated with a single fraction of 50Gy and seeded in Falcon T-25 culture flasks or 24-well plates at a density of 10^6 cells /flask and 10^5 cells/ well. Following FACS sorting, cells were pelleted and resuspended in growth media prior to being placed on the established irradiated fibroblast feeder layer at known cell densities. The co-cultures were then incubated in 5% CO₂ in air at 37°C. Twice weekly media changes were performed in an MSC. The cell populations were examined prior to each media change to

determine the colony forming efficiency of the population. Colonies were deemed significant if greater than 32 cells in size. Colony-forming efficiency was calculated by dividing the number of colonies formed by the number of cells seeded. Cultures were examined for colonies until confluence was reached, at which point the number of cells in each flask or well was counted, split (one in three) and passaged in a fresh flask or well without a feeder layer. This was repeated until proliferation ceased, at which point 'duration in culture' and 'number of serial passages' were recorded.

2.11.2 Microscopy - Entire Flask Image Capture

Multiple fields of view from the same flask were captured and a montage of these images was then created to evaluate the number, morphology and size of the colonies within an entire flask. The Zeiss Axiovert 200M microscope (Welwyn Garden City, Hertfordshire, UK) was used to examine the cultures. The system was fitted with a motorised three-axis ASI MS200 stage (Applied Scientific Instrumentation, Eugene, Oregon, USA) and a Solent Scientific (Sengensworth, UK) environmental chamber for temperature (37°C) and gas (5% CO₂/air) regulation. A white light emitting diode (LED) was used for transmitted light illumination (Thorlabs Ltd, Ely, Cambridgeshire, UK). A Zeiss A-Plan 10x/0.25NA Ph1 objective lens was used and images were captured with a Roper Coolsnap HQ camera (Photometrics, Tucson, AZ). Utilising the imaging software Metamorph (Molecular Devices, Downington, Pennsylvania, USA), field of view images were captured in a grid-like

fashion with autofocusing after every fifth field of view via a macro which monitored the sample focus (written by Dr Steve Bagley, University of Manchester Paterson Institute for Cancer Research, Manchester, UK). The separate images were then spliced together with a 10% overlap to form a montage of the entire flask using Metamorph. Images were then optimised using Adobe Photoshop CS3 (Adobe Systems Incorporated, San Jose, California, USA).

2.11.3 Protocol for Repeat Flow Cytometric Analysis of Cultured Cells

Once the monolayer was confluent, the media was removed and the monolayer was washed twice with 10ml of PBS. One millilitre of Trypsin was added to the monolayer and placed in the incubator at 37°C/ 5% CO₂ for two minutes or until the cells had lifted off the bottom of the flask. At this point the cells were resuspended in 5ml of growth media with 2%FCS and added to a Falcon tube for differential centrifugation (360g / 1 min / brake 0). The supernatant (fibroblast feeder layer) was discarded and the epithelial cell pellet was resuspended in a further 1ml growth media with 2% FCS. A cell count was performed with a haemocytometer. A further spin (800g/ 5 min/ brake 3) was performed and the pellet resuspended in 3ml of growth media with 2%FCS. After adequate mixing to ensure a single cell suspension, one third (1ml) of the epithelial suspension was added to a fresh collagen coated 25cm² flask for continuation of the monolayer culture.

The remaining two thirds were again centrifuged (800g/ 5 min/ brake 3). This time the supernatant was discarded and the pellet resuspended in 5ml Hoechst buffer and subsequently passed through a 100µm filter before further centrifugation at 800g/ 5 min/ brake 3. The pellet was then resuspended in 100µl Hoechst buffer. Ten microlitres of cell suspension were removed and added to a pop-top tube labelled "Hoechst + Verapamil + IgG FITC". The volume was then made up with 490µl (or an appropriate volume such that cellular concentration remained less than 1×10^6 cells/ml) Hoechst buffer and placed on ice. This served as the first control.

A further 10µl of cell suspension was removed and added to a pop-top tube labelled "Hoechst + Verapamil + IgG FITC + Pyronin Y" containing 490µl (or an appropriate volume such that cellular concentration remained less than 1×10^6 cells/ml) Hoechst buffer and placed on ice. This served as the second control.

A further 10µl of cell suspension was added to a pop-top tube labelled "Hoechst + CD45" containing 490µl (or an appropriate volume such that cellular concentration remained less than 1×10^6 cells/ml) Hoechst buffer and placed on ice. This served as control number three.

The remaining cell volume was added to a pop-top tube (labelled "Hoechst + CD45 + CD133 + Pyronin Y") and 20µl of Hoechst Buffer and 10µl of CD133/2-Biotin (stock concentration 50µg/ml) were also added. This tube was incubated in the fridge at 4°C in the dark. After 30 minutes, the cells were washed with Hoechst buffer and spun in the

centrifuge at 800g / 5 mins / Brake 3. The pellet was resuspended in 195µl Hoechst buffer and 5µl Strep-PE-Cy7 was added. The tube was incubated in the fridge for a further 30 minutes at 4°C in the dark. The cells were then washed again with Hoechst buffer and spun in the centrifuge at 800g / 5 mins / Brake 3 before being resuspended tube in appropriate volumes of Hoechst Buffer for Hoechst 33342 staining (i.e. < 1 x 10⁶ cells per ml). Verapamil (stock concentration 50mM) was added to the appropriate controls (4µl/ml) before the remaining antibodies and Hoechst 33342 dye were added in the dark (Table 2.5). The assorted tubes were then wrapped in foil and incubated on a shaking platform at 37°C in the dark for 90 minutes. After 75 minutes, 0.4µL/ml Pyronin Y (stock concentration 0.5mg/ml) was added to the two tubes labelled "Pyronin Y". After thorough mixing the tubes were returned to 37°C. After a total of 90 minutes, ice cold Hoechst buffer was added to each tube (3-3.5ml) to stop the reaction. The suspensions were then spun in the centrifuge at 800g/ 5 min/ brake 3 and the resultant pellets resuspended in 500µl (control tubes) or 1ml ("Hoechst + CD45 + CD133 + Pyronin Y") of ice cold Hoechst buffer and placed on ice.

The samples were processed in order with the controls before the main test "Hoechst + CD45 + CD133 + Pyronin Y" sample. The Hoechst 33342 dye efflux assay adapted for subfractionation of the SP (section 2.9) was used but the "Hoechst + CD45 + CD133 + Pyronin Y" sample was used as both the CD133 control and the sort sample with the CD45⁺ cells being identified by altering the precise combination of gates (ie CD133 control: Live/CD45^{-ve}/CD133⁺ and Sort: Live/CD45^{-ve} only).

	Stock Concentration	Hoechst + Verapamil + IgG-FITC	Hoechst + Verapamil + IgG-FITC + Pyronin Y	Hoechst + CD45	Hoechst + CD45 + CD133 + Pyronin Y
Verapamil	50mM	4µl/ml	4µl/ml		
IgG-FITC	50µg/ml	10µl/ml	10µl/ml		
CD45-FITC	n/a			10µl/ml	10µl/ml
CD133/2	50µg/ml				100µl/ml
Strep-PE-Cy7	n/a				25µl/ml
Hoechst 33342	1mM	5µl/ml	5µl/ml	5µl/ml	5µl/ml
Pyronin Y	0.5mg/ml		0.4µl/ml		0.4µl/ml

Table 2.5: Table showing the samples used to enable modification of the Hoechst 33342 dye efflux assay for further flow cytometric analysis of prostate epithelial cells following culture.

2.11.4 Immunocytochemistry

2.11.4.1 Citric Acid Buffer Manufacture

Citric acid monohydrate (2.1g) was added to 500ml of double-distilled water and mixed thoroughly. Sufficient 2M Sodium Hydroxide was added to raise the pH to 6.0. Using double-distilled water, the volume of buffer solution was made up to one litre to make a working concentration of 1mM citric acid.

2.11.4.2 Slide Preparation, Cell Fixation, Permeabilisation and Antigen Retrieval

Twelve-well slides were thoroughly cleaned with ethanol, labelled and placed in humidified chambers. A positive charge was applied to the wells by the addition of 10 μ l of 0.1% w/v Poly-L-Lysine per well for 30 minutes. The excess Poly-L-Lysine was removed and the slides dried on Whatmann blotting paper.

The isolated cell populations to be studied were resuspended in PBS such that ideally, depending on available cell numbers, there were 10³ cells in 20 μ l of PBS. Often cell numbers were considerably lower in the region of 100 cells/well. Twenty microlitres of cell suspension were added to each of the wells on the slide and left for 30 minutes to allow the cells to "sit down". The cells were then fixed in 4% Formalin/PBS.

A pilot study was performed to determine the optimal staining conditions for each of the primary antibodies from the panel and thereby determine

for each whether permeabilisation and antigen retrieval after formalin fixation was required (section 2.11.4.4). The antibodies were grouped to different slides depending on the processing required.

After 20 minutes of formalin fixation, those slides that were to be stained with antibodies that required permeabilisation were placed in a bath of methanol for four minutes then acetone for two minutes. Both baths had been pre-cooled to -20°C. After the process of permeabilisation, those slides that required antigen retrieval were placed in a large microwave-safe container and the citric acid buffer was added. The citric acid buffer bath containing the slides was heated in the microwave for 25 minutes at 850 watts then allowed to cool for 15 minutes. The citric acid buffer was exchanged for water.

2.11.4.3 Antibody Staining

The principal of blocking is to reduce non-specific binding. The serum from the host animal of the secondary antibody is used to block the potential non-specific binding sites. For example, if using a mouse anti-human primary antibody and a rabbit anti-mouse secondary antibody, then the blocking agent should be manufactured from rabbit serum.

Rabbit and goat blocking agents (10%) were manufactured by adding 1ml of the appropriate serum to 9ml of 1% Bovine Serum Albumin (BSA) in PBS. The primary antibodies were diluted with 1% BSA/PBS according to the ratios in Table 2.1.

After encircling each well with a wax pen, 20µl of blocking agent was added to each well. After 30 minutes, the blocking agent was aspirated from the well and each well washed twice with PBS. Twenty microlitres of each primary antibody was added to the appropriate well and left at room temperature for an hour or placed at 4°C for 12 hours. Each antibody was then aspirated from the well which was subsequently washed twice with PBS. Three washes of each slide were performed with PBS/ 0.5% Tween 20 (Sigma-Aldrich, Poole, UK) before two further PBS washes.

To maximise the utilisation of cell numbers, dual staining was occasionally used. This was achieved by the addition of two primary antibodies that shared the need for the same blocking agent but were from different species and attracted two different secondary antibodies with different wavelengths (488nm and 555nm). A control well was reserved for each of the three animal species and each of the varied combinations of primary and secondary antibody used (normal mouse IgG1 and 488nm, normal mouse IgG1 and 555nm, normal mouse IgG2a and 488nm, normal rabbit IgG and 488nm and normal goat IgG and 488nm). Twenty microlitres of the appropriate secondary Alexa fluorochrome antibody (2mg/ml) was added to each well and left in the dark. After one hour, the contents of each well were carefully aspirated and each well was washed twice with PBS and subsequently three times with PBS/ 0.5% Tween 20. The washing process was completed with two further PBS washes. All slides were placed in formalin for 20 minutes to aid fixation of the cells to the slide. The coverslips were

mounted using Prolong Gold with DAPI. Following the expulsion of any air bubbles, the slides were left for 12 hours to dry in the dark at room temperature before they were ready to be examined.

2.11.4.4 Staining Optimisation Pilot

The standard processing of cells and manufacture of slides was followed (section 2.11.4.1 – section 2.11.4.3). The same panel of primary antibodies were applied to cells on eight identical slide replicates. All slides were formalin fixed. Four of the eight slide replicates were permeabilised. Half of both the permeabilised and non-permeabilised slides were sent for antigen retrieval. Finally, as there were duplicates of each slide processed in a particular fashion, half of the slides were stained with the standard secondary antibody concentration and for the other half the concentration was doubled (Table 2.6).

2.11.4.5 Microscopy - Immunocytochemical Image Capture

Microscopic evaluation of the immunocytochemical phenotype of cells used the Olympus BX51 upright microscope (Olympus UK Ltd, Watford, Hertfordshire, UK). A UPLSAPO x100 XO oil immersion lens was used and images were captured with the colourview 12 soft imaging system and the analySIS software (both Olympus). Illumination was via a Lambda LS 300W Xenon light source (Sutter, Novato, California, USA) and Chroma (Rockingham, Vermont, USA) UV filters were utilised (ET-DAPI, ET-GFP, and ET-DSRed).

Primary Antibody Panel Number	Permeabilisation	Antigen Retrieval	Standard Secondary Antibody Concentration	Double Secondary Antibody Concentration
1	Y	Y	Y	N
2	Y	N	Y	N
3	Y	Y	N	Y
4	Y	N	N	Y
5	N	Y	Y	N
6	N	N	Y	N
7	N	Y	N	Y
8	N	N	N	Y

Table 2.6: Table demonstrating the varied combinations of slide preparation and secondary antibody concentration applied to each of the eight primary antibody panel replicates.

2.12 Epistem Ltd Small Cell Number Affymetrix® Microarray Study

2.12.1 Epistem Ltd Protocol for Sample Processing, RNA Isolation,

cDNA Manufacture, Labelling and Affymetrix® Microarray

Hybridisation

Thirty four samples from patients with histologically confirmed BPH underwent FACS isolation. A CD133⁺^{ve}/CD45⁻^{ve} Hoechst 33342 SP and a CD133⁺^{ve}/CD45⁻^{ve} Hoechst 33342 NSP for each sample were collected. Epistem Ltd (Manchester, UK) was commissioned to extract the RNA, create and amplify the complementary cDNA, before ultimately labelling it and performing chip hybridisation using their patented small cell number chemistries for microarray (Figure 2.4). FACS isolated cells were processed and transferred immediately to the EpiAmp™/EpiLabel™ lysis buffer. Finer details of the methods used by Epistem Ltd in their small cell number chemistries have not been disclosed but are based on published methods^{560, 561}.

However, in brief, the total RNA was processed using the Epistem Ltd proprietary PolyA Polymerase-Chain Reaction (PCR) system called EpiAmp™ for amplification and EpiLabel™ for labelling. Eight paired samples (SP and NSP from the four patients) with RNA of sufficient quantity and quality were hybridised to the Affymetrix® HG-U133_Plus 2 arrays.

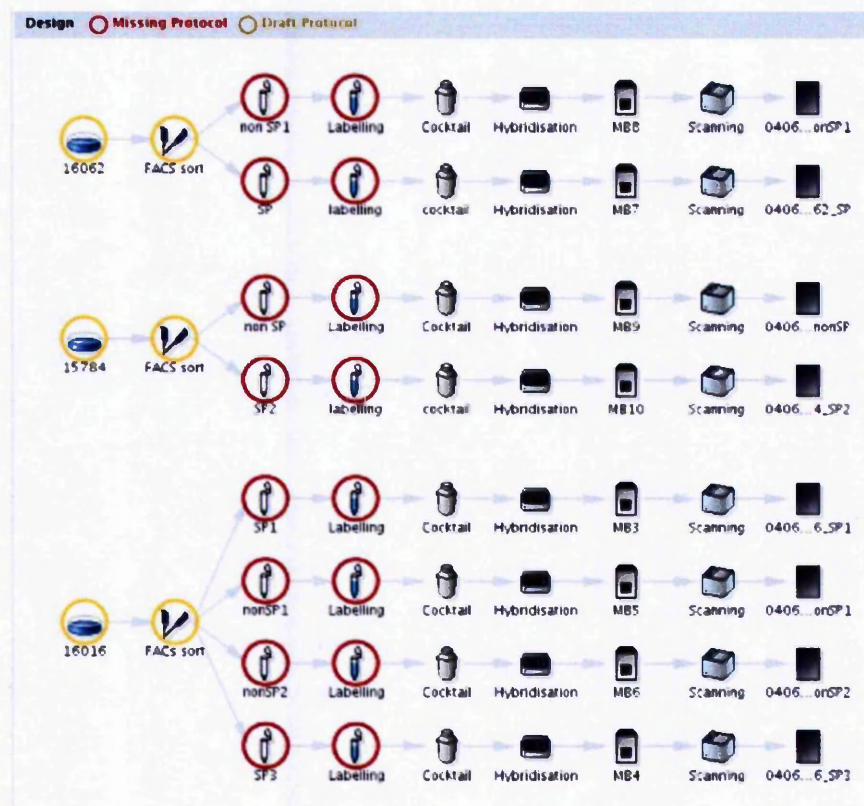


Figure 2.4: Miame Vice schematic illustrating the small cell number microarray protocol for the four paired samples analysed. SP and NSP populations were identified and collected by FACS. Individual SP and NSP samples were labelled and cDNA cocktails prepared before their hybridisation to the Affymetrix® HG-U133_Plus 2 array ready for scanning.

2.12.2 Affymetrix® GeneChip® Microarray Data Analysis

All data were analysed using R (www.r-project.org) and BioConductor (www.bioconductor.org)^{562, 563}. All expression levels were processed using the MAS5 algorithms for expression summary and detection calling^{533, 564}, as implemented in BioConductor.

An initial gene list was generated by filtering to remove probesets not flagged “Present” in three or more members of at least one of the two groups, and then selecting those with a log2 fold change of greater than two. However, data were too variable to apply a statistical filtering based on adjusted p-score. An alternative, less stringent filtering method was therefore applied and excluded only those probesets that were ‘Absent’ in all eight arrays.

The mean average of all the log2 expression values for the four SP and four NSP samples were calculated. The log2 fold change (Fc) between SP and NSP was then calculated by subtracting the log2 NSP Fc from the log2 SP Fc. In turn, this could then be converted to an absolute Fc value by the formula $2^{(\log_2 \text{ Fc value})}$.

2.12.3 Identification of Probesets for Validation by Real-Time PCR

Differentially expressed probesets were to be identified for comparison with results from a subsequent real-time reverse-transcription polymerase chain reaction (qRT-PCR) assay of the same probesets to ensure that the observed differential expression was accurate and that the microarray data could be validated.

Taking each pairwise comparison in turn, the list of SP/NSP Fc's was sorted from the most positive to the most negative. Those probesets with a log2 Fc lying between, but not including, +4 and -4 were then excluded. The next step in the filter was to only include those probesets with log2 Fc's that were all in the same direction (whether that be a positive or negative Fc) in all three of the remaining pairwise comparisons for that particular probeset. Furthermore, all log2 Fc's for the four paired comparisons for each probeset had to be of the magnitude of $>+1$ or <-1 .

The probesets filtered thus far were checked to ensure that at least one of the raw expression values from each of the paired comparisons (SP if a positive Fc or NSP if a negative Fc) had a log2 value in the region of six (absolute expression value 64).

2.13 Revised Small Cell Number Affymetrix® Microarray Protocol

2.13.1 RNA Extraction Protocol

The Qiagen® RNeasy® Mini kit (Crawley, UK Cat #: 74104) was used for RNA extraction and latterly the process was initiated immediately after FACS was completed rather than by storing isolated samples in RNAlater®.

Apart from centrifugation, all steps were undertaken in an MSC laminar flow hood at room temperature. RNase-free pipette tips and tubes were used. The centrifuge temperature was maintained at 23°C. Firstly, the DNase-1 stock solution was prepared. The Qiagen® lyophilised DNase-1

(1500 Kunitz units) was dissolved in 550µL of RNase-free water by injecting the correct volume of water into the vial using an RNase-free needle and syringe. The solution was mixed gently. The stock solution was then divided into aliquots for storage at -20 °C for up to 9 months. Thawed aliquots were stored at 4 °C.

The cell number of each sample was determined and a pellet created by centrifugation at 800g/5 minutes/Brake 3. Disruption of cells was performed by the addition of 350µL (providing cell count less than 3×10^6) of Qiagen® Buffer RLT. The tube containing the sample was then vortexed for one minute to homogenise the cells. Seventy percent ethanol (350µL) was added to the lysate and the resultant 700µL of sample was then transferred to a Qiagen® RNeasy® spin column that had been placed in a 2ml collection tube. After closing the lid, the tube and spin column were centrifuged at $\geq 13,200$ rpm for 15 seconds. The resultant flow-through was then discarded and the spin column carefully re-inserted to the collection tube, ensuring that at all times the column did not make contact with the flow-through.

Residual DNA contamination was removed from the remaining samples by on-column DNase treatment using the RNase-free DNase set (Qiagen® cat #: 79254). Instead of proceeding directly with the first wash step of the standard protocol, 350µL of Qiagen® Buffer RW1 was added to the spin column still placed in the collection tube. Again, after closing the lid, the tube and spin column were centrifuged at $\geq 13,200$ rpm for 15 seconds to wash the spin column membrane. The resultant flow-through

was then discarded and the spin column was carefully re-inserted to the collection tube ensuring that at all times the column did not make contact with the flow-through. DNase-1 stock solution (10 μ L) was then added to 70 μ L of Qiagen[®] Buffer RDD and the two were gently mixed by inverting the tube and briefly centrifuged ($\geq 13,200$ rpm for 60 seconds) to ensure capture of the entire volume. The volume (80 μ L) was then added accurately to the spin column membrane and left in the tissue culture cabinet for 15 minutes at room temperature. Finally, 350 μ L of Qiagen[®] Buffer RW1 was added to the spin column and the lid closed for a further centrifuge at $\geq 13,200$ rpm for 15 seconds.

The resultant flow-through was discarded and again a wash step was performed by the addition of Qiagen[®] Buffer RPE (500 μ L) to the spin column and centrifugation at $\geq 13,200$ rpm for 15 seconds. After discarding the flow-through, the same step was repeated but with a prolonged centrifugation at $\geq 13,200$ rpm for 2 minutes to dry the spin column membrane therefore ensuring no ethanol is carried forward into the RNA elution step. The Qiagen[®] RNeasy[®] spin column was then placed in a fresh collection tube and a further spin at $\geq 13,200$ rpm for 1 minute was performed.

The Qiagen[®] RNeasy[®] spin column was then placed in a 1.5ml RNase-free collection tube. Initial experiments used two 50 μ L volumes of RNase-free water for elution of the RNA. These were added directly to the spin column membrane before the lid was closed and the column spun at $\geq 13,200$ rpm for one minute. Later protocols used a single elution

volume of 30µL. The eluted RNA in RNase-free water was then immediately stored at -80°C until required for further processing.

The Agilent RNA 6000 Pico LabChip® Kit was used to evaluate the RNA from up to 11 samples simultaneously and this was analysed by the Agilent 2100 bioanalyzer.

2.13.2 Assessment of RNA Purity

If sufficient RNA was available, the Nanodrop ND-1000 spectrophotometer (Nanodrop technologies, Thermo Fisher Scientific, Wilmington, USA) was used to determine purity of the sample. The optical density of nucleic acid is 260nm whereas that of protein is 280nm. The 260nm/280nm ratio therefore determines the purity of an RNA preparation. Clean samples have ratio values between 1.9 and 2.1. Organic compounds such as those used in the RNA extraction process have an optical density of 230nm. The 260nm/230nm ratio again depicts sample purity and accepted values lie between 1.5 and 2.

2.13.2.1 Assessment of RNA Degradation

The Agilent Bioanalyzer 2100 (Santa Clara, CA, USA) uses the RNA 6000 Pico LabChip® Kit to generate a simulated gel image as well as electrophoretic data. There are several indicators of RNA degradation:

2.13.2.2 Ribosomal Band 28S/18S Ratio

The assumption is made that all RNA will degrade in a uniform manner. The 28S and 18S ribosomal RNA (rRNA) can therefore act as a

surrogate for mRNA degradation. The 28S rRNA is unstable compared to the 18S rRNA and so is more prone to degradation. The more degraded a sample the lower the ratio. A value of two denotes a perfect 28S/18S ratio.

2.13.2.3 RNA Integrity Number

The RNA Integrity Number (RIN) value takes into consideration the entire electrophoretic trace from a eukaryotic RNA sample rather than simply the ratio between the ribosomal bands. This therefore takes the presence or absence of degradation products into consideration. Overall it allows objective assessment of electrophoretic traces and the comparison of RNA from different samples. Perfect quality RNA has a RIN of 10⁵⁶⁵.

2.13.2.4 Additional Peaks in the Analysis or an Increase in Baseline Fluorescence

The detection of further peaks earlier in the analysis and a rise in the baseline fluorescence both suggest that shorter lengths of nucleotide are being detected and this is indicative of degradation.

2.13.2.5 The 260/280nm Ratio

As already mentioned, the ratio of RNA to total protein is a measure of purity however it will also decrease with degradation as the optical density of the RNA falls.

2.13.3 Revised Protocol for cDNA Manufacture, Labelling and Affymetrix® Microarray Hybridisation

Following RNA extraction (section 2.13.1), the RNA was amplified using the NuGEN WT-Ovation Pico RNA amplification system version-1.0 (San Carlos, California, USA). The cDNA hybridisation cocktail was prepared (fragmented and labelled) using the NuGEN FL-Ovation cDNA Biotin module version-2. The labelled fragmented cDNA was then hybridised to the HG-U133_Plus 2 Affymetrix® microarray.

2.13.4 Affymetrix® GeneChip® Microarray Data Analysis

All data were analysed using R (www.r-project.org) and BioConductor (www.bioconductor.org)^{562, 563}. Normalisation of data used MAS5 algorithms for expression summary and detection calling. However, more detailed interrogation of the differential expression of probesets was provided by Limma software^{566, 567}. The Limma software required Robust Multiarray Averaging (RMA) normalisation. Analysis of variance was used to determine differential expression. The false discovery rate (FDR) of the lists of differentially expressed genes was 1%. The FDR is defined as the expected percentage of the results that are infact false positives⁵⁶⁸⁻⁵⁷⁰. For example, if a list contained 1000 differentially expressed genes with a maximum FDR of 0.01 or 1% then a maximum of 10 genes would be expected to have been falsely called as present. Probe sets were considered to be differentially expressed if they had an adjusted p-Value of 0.01 and a (log2) fold change of 1.

2.13.5 Identification of Probesets for Validation by Real-Time PCR

Again differentially expressed probesets suitable for validation of the microarray data by qRT-PCR were sought. Ideally a probeset would come from each of the nine potential comparisons (DSP vs. PSP, DSP vs. NSP and PSP vs. NSP for normal, BPH and CaP). As some of the comparisons yielded no differentially expressed genes, attention was focused on probesets at the top of the lists of differentially expressed genes (ie those with the most significant adjusted p-value). In addition to a large fold change, a large mean expression value is recommended for qRT-PCR validation. Probe sets with low mean expression values were rejected. Below a log2 expression value of six, the observed mean expression may be close to background signal. It should also be noted that these mean expression values are the average across all arrays.

The qRT-PCR validation of the array data will be the subject of future work but suitable probesets have been identified.

2.14 Statistical Analysis

In addition to the statistics used in the analysis of the Affymetrix[®] microarray data, general descriptive statistics have been given statistical significance with the use of paired (or unpaired) two-tailed student *t*-tests. A significance value of $p < 0.05$ has been applied throughout.

Chapter 3: Analysis of the CD133^{+ve}/CD45^{-ve} Hoechst 33342 SP and CD133^{+ve}/CD45^{-ve} Hoechst 33342 NSP Affymetrix® Microarray Data

3.1 Sample Identification

Thirty-four paired SP and NSP samples from patients with histologically confirmed BPH underwent FACS isolation. A CD133^{+ve}/CD45^{-ve} Hoechst 33342 SP and a CD133^{+ve}/CD45^{-ve} Hoechst 33342 NSP for each patient sample was collected. Epistem Ltd (Manchester, UK) was commissioned to extract the RNA, create and amplify the complementary cDNA, before ultimately labelling it and performing chip hybridisation using their patented small cell number chemistries for microarray. Agarose gels were used to determine RNA and cDNA quality. These gels indicated that only 16 (47.1%) of the samples had sufficient post amplification cDNA quality to proceed to HG-U133_Plus 2 array hybridisation (Figure 3.1). Only four SP and four NSP samples from these 16 (23.5%) formed complementary pairs (16062 SP and 16062 NSP1, 15784 SP2 and 15784 NSP, 16016 SP1 and 16016 NSP1, 16016 SP3 and 16016 NSP2) and were therefore suitable for pairwise comparison of their expression profiles.

3.2 Analysis of Extracted RNA to Determine Quantity and Quality

The mean cell number was 968.63 cells (SD ± 219.58 , range 449-1300 cells). The amount of RNA extracted and put forward for the cDNA amplification step of the Epistem Ltd protocol was low (mean 5.66ng, SD ± 1.05 ng, range 4.48-7.96ng) (Table 3.1). The amount of RNA extracted

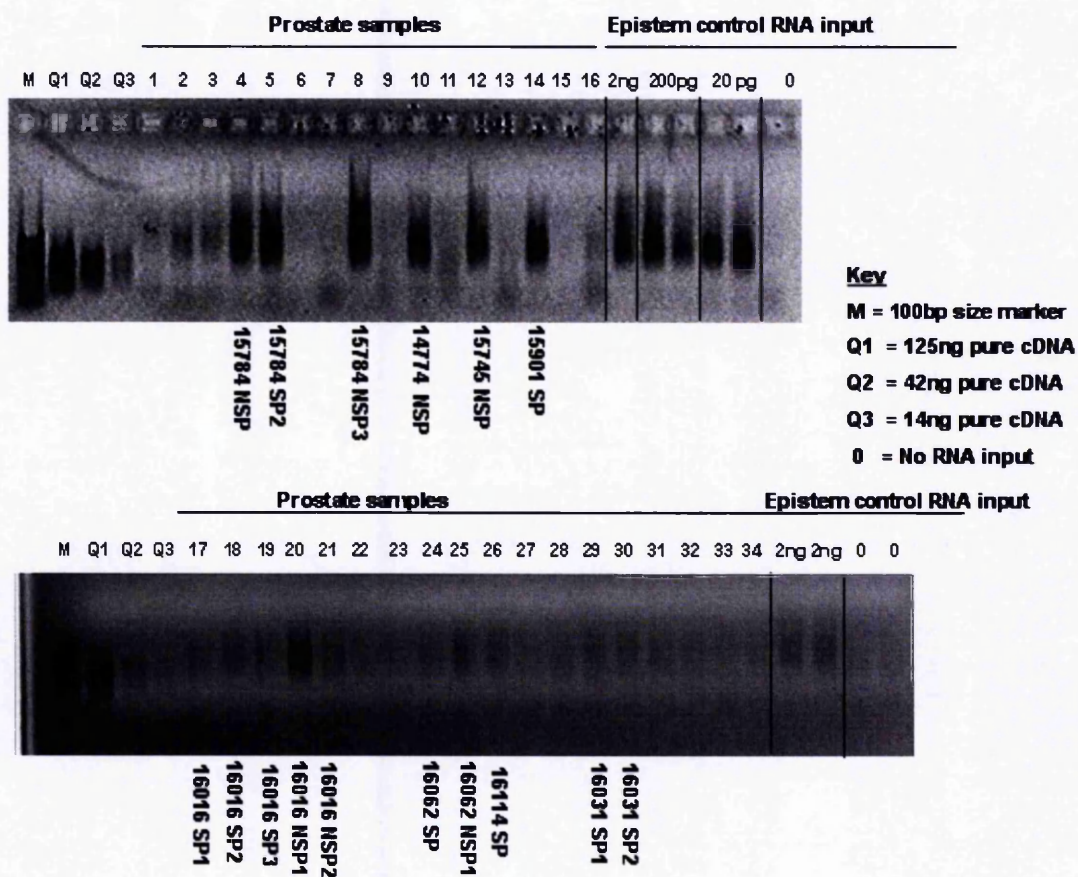


Figure 3.1: Agarose gel (1%) analysis of post amplification cDNA quality. Two separate gels were used to analyse each of the 34 samples from which RNA was extracted. Reference cDNA and RNA bands are shown.

Comparison	Sample ID Number	Cell Number	RNA Concentration (ng/uL)	RNA input to EpiAmp Amplification Step (ng)	RNA isolated per cell (ng)
1	16062 SP	449	2.59	5.18	0.0115
	16062 NSP1	1000	3.13	6.26	0.0063
2	15784 SP2	1000	3.12	6.24	0.0062
	15784 NSP	1000	2.71	5.42	0.0054
3	16016 SP1	1300	2.39	4.78	0.0037
	16016 NSP1	1000	2.49	4.98	0.0050
4	16016 SP3	1000	3.98	7.96	0.0080
	16016 NSP2	1000	2.24	4.48	0.0045
Mean		968.63	2.83	5.66	0.0063
SD		219.58	0.53	1.05	0.0023
Range		449-1300	2.24-3.98	4.48-7.96	0.0037-0.0115

Table 3.1: Table showing the cell number isolated by FACS and the amount of RNA extracted (ng) from each of the samples comprising the four SP vs. NSP comparisons chosen for further analysis. The amount of RNA extracted per cell is also shown (ng).

per cell allowed comparison of populations with different cell numbers and was used as a determinant of an individual cell population's level of transcription activity. Surprisingly, given the relative quiescence of the SP compared to the NSP that has been previously reported, the amount of RNA extracted from each cell in the SP was, on average, greater than that extracted from the NSP. The mean amount of RNA extracted from the SP was 0.0074ng (SD ± 0.0029 ng) compared with 0.0053ng (SD ± 0.0007 ng) from the NSP. However, no statistical difference in RNA yield was seen between the two groups (student paired *t*-test $p=0.2489$) (Table 3.2).

3.3 Affymetrix Genechip Quality Control Data

The chosen eight samples were each hybridised to a separate Affymetrix HG-U133_Plus 2 array. All arrays had a scale factor within three fold of each other which fulfilled criteria set by Affymetrix® for array-comparability (Figure 3.2). The array background fluorescence was high (mean 113.2 SD ± 24.28). Overall the percentage of genes that were called 'Present' by the Affymetrix software were very low (mean 13.15%, SD $\pm 4.84\%$). It was evident that, although still considered low, one sample (16016 NSP1) had a higher gene call at 25.9% but that the remainder, and the majority, were in the range of 10-12.5% (Table 3.3).

Glyceraldehyde 3-phosphate dehydrogenase (GAPDH) and Beta Actin (β -actin) are used by the Affymetrix arrays as housekeeper sequences and provide internal controls to measure the sequence integrity of the

Sample	Amount of RNA Extracted Per Cell (ng)	
	SP	NSP
16062	0.0115	0.0063
15784	0.0062	0.0054
16016	0.0037	0.0050
16016	0.0080	0.0045
Mean	0.0074	0.0053
SD	0.0029	0.0007
Range	0.0037-0.0115	0.0045-0.0063
Paired T-test	0.2489	

Table 3.2: Table showing the amount of RNA extracted per cell from each of the populations (SP and NSP) for each of the four samples. A student paired *t*-test was used to analyse the two groups for statistically significant differences.

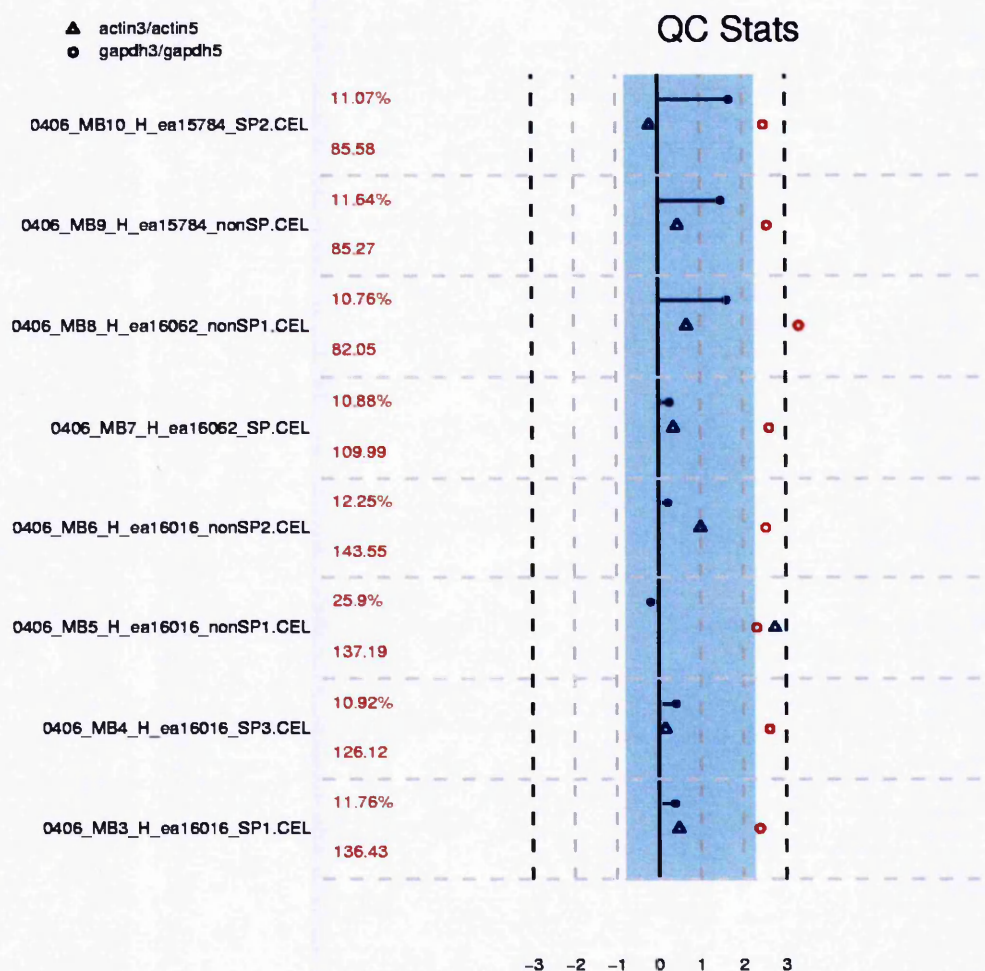


Figure 3.2: Chart summarising the Qc statistics generated by MAS5.0. Each array is represented on one horizontal line. The central black vertical line corresponds to zero fold change (Fc) and the black dotted vertical lines on either side are at $\log_2(3)$ Fc up or down. The blue vertical bar represents the region in which all arrays have a scale factor within 3 fold of each other which fulfils criteria set by Affymetrix® for array-comparability. A line is plotted horizontally out from the central bar to the point denoting the scale factor for each array. The red text on the left denotes the percentage of probesets called 'Present' and the average background signal. Triangles and dots are β -actin and GAPDH 3'/5' ratios respectively and these refer to sequence integrity. Anything blue is within an acceptable Qc range whereas red is not.

Comparison	Sample ID Number	Scale	Background	Gene Call "Present" (%)	GAPDH 3'/5'	GAPDH 3'/M	B-Actin 3'/5'	B-Actin 3'/M
1	16062 SP	1.20	109.88	10.68	6.12	0.49	1.28	0.27
	16062 NSP1	3.05	81.99	10.76	9.98	0.95	1.59	0.28
2	15784 SP2	3.19	85.55	11.07	5.62	0.45	0.87	0.19
	15784 NSP	2.79	85.24	11.64	5.92	0.55	1.38	0.27
3	16016 SP1	1.30	136.32	11.76	5.20	0.72	1.38	0.35
	16016 NSP1	0.87	137.16	25.90	4.98	1.31	6.65	1.47
4	16016 SP3	1.32	125.99	10.92	6.11	0.61	1.11	0.20
	16016 NSP2	1.17	143.43	12.25	5.77	0.97	1.98	0.47
Mean		1.86	113.20	13.15	6.21	0.76	2.03	0.44
SD		0.90	24.28	4.84	1.47	0.28	1.77	0.40
Range		0.87-3.19	81.99-143.43	10.76-25.90	4.98-9.98	0.45-1.31	0.87-6.65	0.19-1.47

Table 3.3: Table showing the quality control statistics for the four paired comparisons including scale, background fluorescence, the percentage of probesets called "present" by the MAS 5.0 software and the degree of degradation using the 3'/5' and 3'/M ratios for the housekeeping genes GAPDH and Beta-Actin. mRNA transcripts degrade in the 5' to 3' direction. Ratios of the transcripts present in such control sequences at the three and five prime (3'/5') ends and the three prime and the middle (3'/M), assess the degree of degradation. The higher the number, the greater the observed degradation.

cDNA transcripts hybridised to the array. mRNA transcripts degrade in the 5' to 3' direction. Ratios of the transcripts present in such control sequences at the three and five prime (3'/5') ends and the three prime and the middle (3'/M), assess the degree of degradation. GAPDH was quite degraded (mean ratio 6.21) and this was indicative of poor RNA quality. Degradation was also evident using the second housekeeper sequence β -actin (mean ratio 2.03) though this was not as severe as GAPDH which was ultimately deemed unacceptable by MAS 5.0 (Table 3.3). This is illustrated by its shift to the right (Figure 3.2).

3.4 Array Normalisation

The data spread was analysed before and after the process of MAS5.0 normalisation. The process of normalisation was indeed effective and no one sample was deemed to be an outlier. The data reported no technical or biological reason why any chip should be excluded (Figure 3.3).

3.5 Biological Comparability of Array Data

An initial gene list was generated by filtering to remove probesets not flagged 'Present' in three or more members of at least one of the two groups (SP or NSP), and then selecting those with a log2 fold-change greater than two (Figure 3.4). The data was too variable to apply a statistical filtering based on a p-value from a *t*-test. Scatter graphs of the SP expression summary (x-axis) for a given patient plotted against its paired NSP expression summary (y-axis) illustrated the low gene call and 'noisy' data with a predominance of probesets being called "Absent"

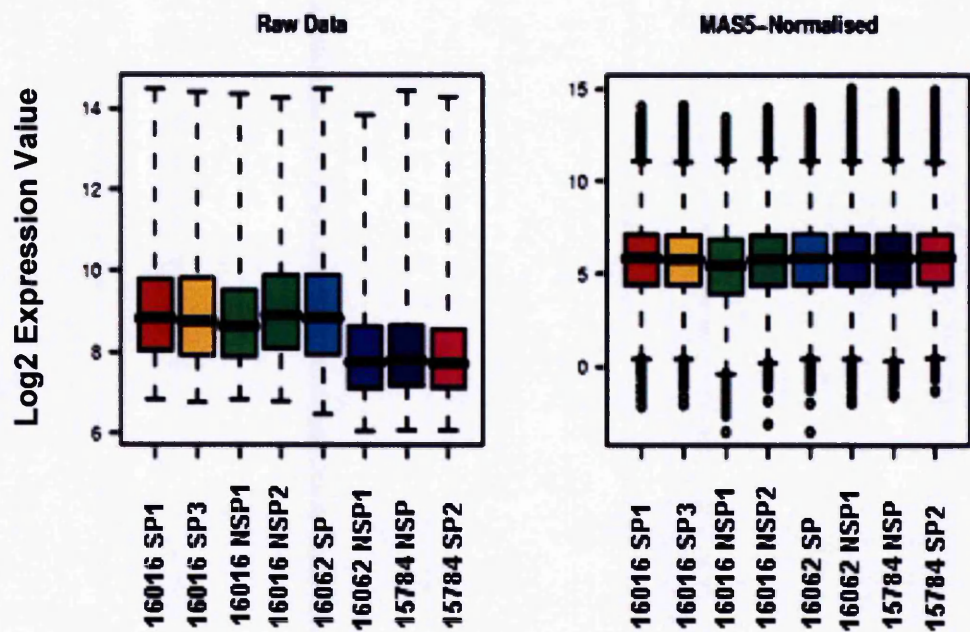


Figure 3.3: Boxplots demonstrating the spread of data before and after MAS5.0 normalisation. Each box shows the median and interquartile range (IQR). Whiskers extend to 1.5x IQR with points beyond the whiskers being outliers.

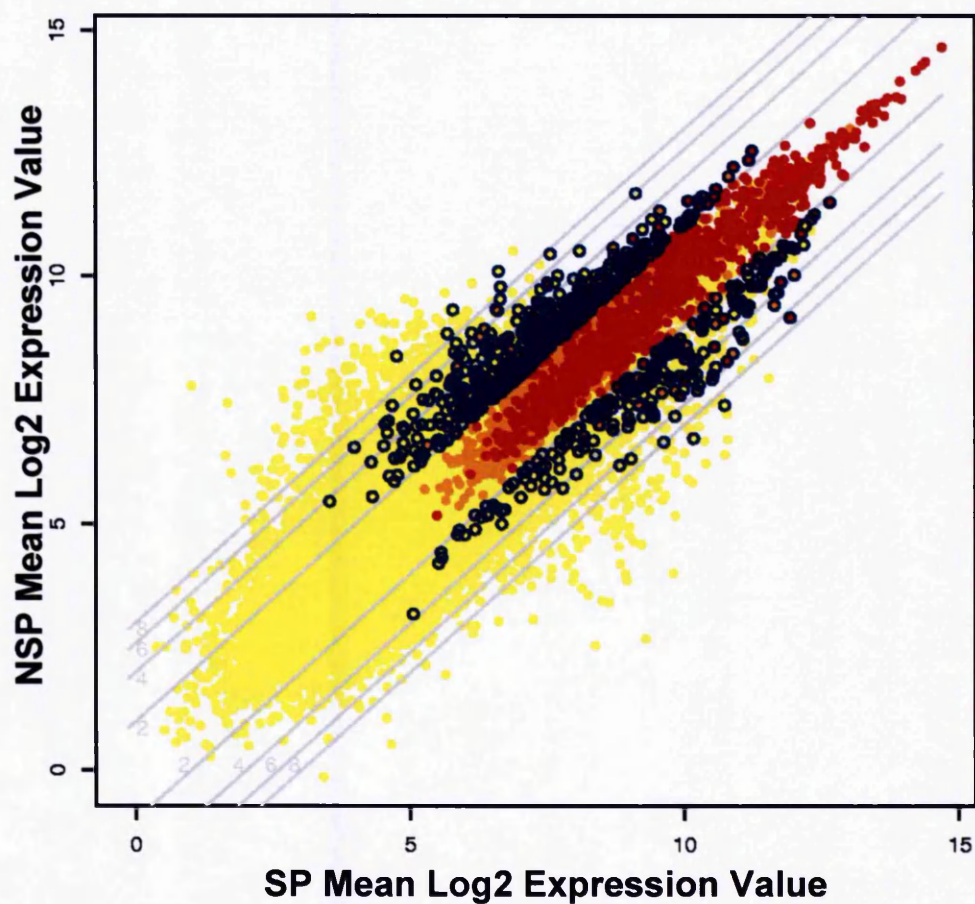


Figure 3.4: Mean log2 expression SP (x-axis) vs. NSP (y-axis) Red: probesets flagged 'Present' in all samples. Yellow: probesets not flagged 'Present' in three or more members of at least one of the two groups (SP or NSP). Orange: probesets flagged 'Present' in all members of at least one of the two groups. Blue circles: probesets selected by filtering.

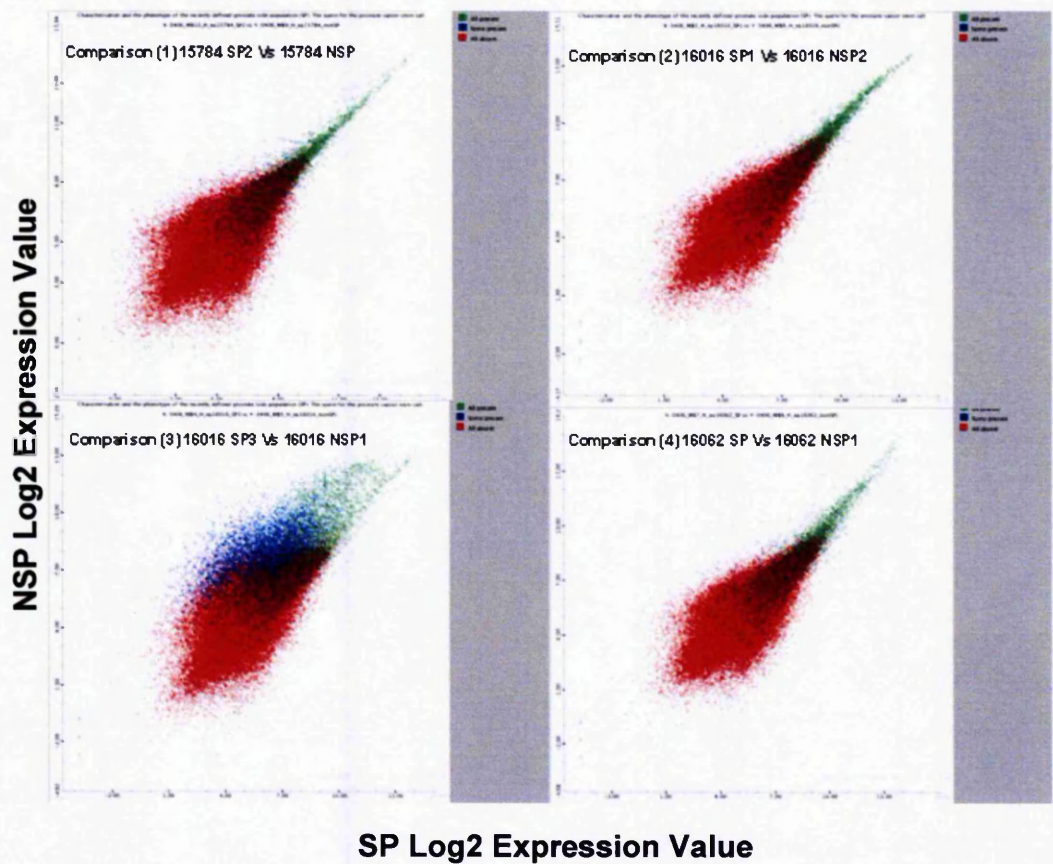


Figure 3.5: Scatter plots showing the differential gene expression of the SP (x-axis) and NSP (y-axis) for each of the four array comparisons. Green dots correspond to those probesets called "Present" by the MAS 5.0 software. Blue dots correspond to "Marginal" calls and red dots "Absent" calls.

(red dots) (Figure 3.5). Overall correlation between the probeset data obtained from different samples was poor. The calculated Pearson correlation scores (R^2) were all low ($R^2=0.48-0.74$) showing that, between patients and between populations (SP and NSP), there was a high degree of variability (Table 3.4).

The observed clustering pattern (Figure 3.6) appears heterogenous in that some samples appear to be most similar to the opposing sample type (SP or NSP) isolated from the same patient (15784 SP2 vs. 15784 NSP and 16016 SP1 vs. 16016 NSP2) and others appear to cluster with samples isolated from different patients but with a similar FACS profile (16016 SP3 vs. 16062 SP).

3.6 Identification of Appropriate Affymetrix® Probesets for Subsequent qRT-PCR Validation of the Microarray Data

In an attempt to maximise the ability of qRT-PCR to detect a fold change and thereby validate the microarray data, probesets with large Fc's were targeted for further study. Following the filtering method described previously (sections 2.12.2 and 2.12.3), only 31 probesets had a log₂ Fc amplitude of greater than four in at least one of the pairwise comparisons as well as a log₂ Fc of greater than one up or down across the other three pairwise comparisons (Table 3.5). This list was reduced to 11 probesets when those probesets without log₂ raw expression values of greater than or equal to log₂(6) in at least one of the samples in a pairwise comparison were removed (highlighted in yellow in Table

		SP				NSP			
		16016 SP1	16016 SP3	16062 SP	15784 SP2	16016 NSP1	16016 NSP2	16062 NSP1	15784 NSP
SP	16016 SP1	1	0.72	0.73	0.64	0.55	0.74	0.66	0.65
	16016 SP3	0.72	1	0.74	0.62	0.51	0.73	0.65	0.63
	16062 SP	0.73	0.74	1	0.63	0.49	0.72	0.66	0.64
	15784 SP2	0.64	0.62	0.63	1	0.48	0.63	0.59	0.61
NSP	16016 NSP1	0.55	0.51	0.49	0.48	1	0.58	0.50	0.51
	16016 NSP2	0.74	0.73	0.72	0.63	0.58	1	0.65	0.65
	16062 NSP1	0.66	0.65	0.65	0.59	0.50	0.65	1	0.60
	15784 NSP	0.65	0.63	0.64	0.61	0.51	0.65	0.60	1

Table 3.4: The degree of biological correlation between each of the eight arrays is denoted by the Pearson Correlation score (R^2) to 2 decimal places.

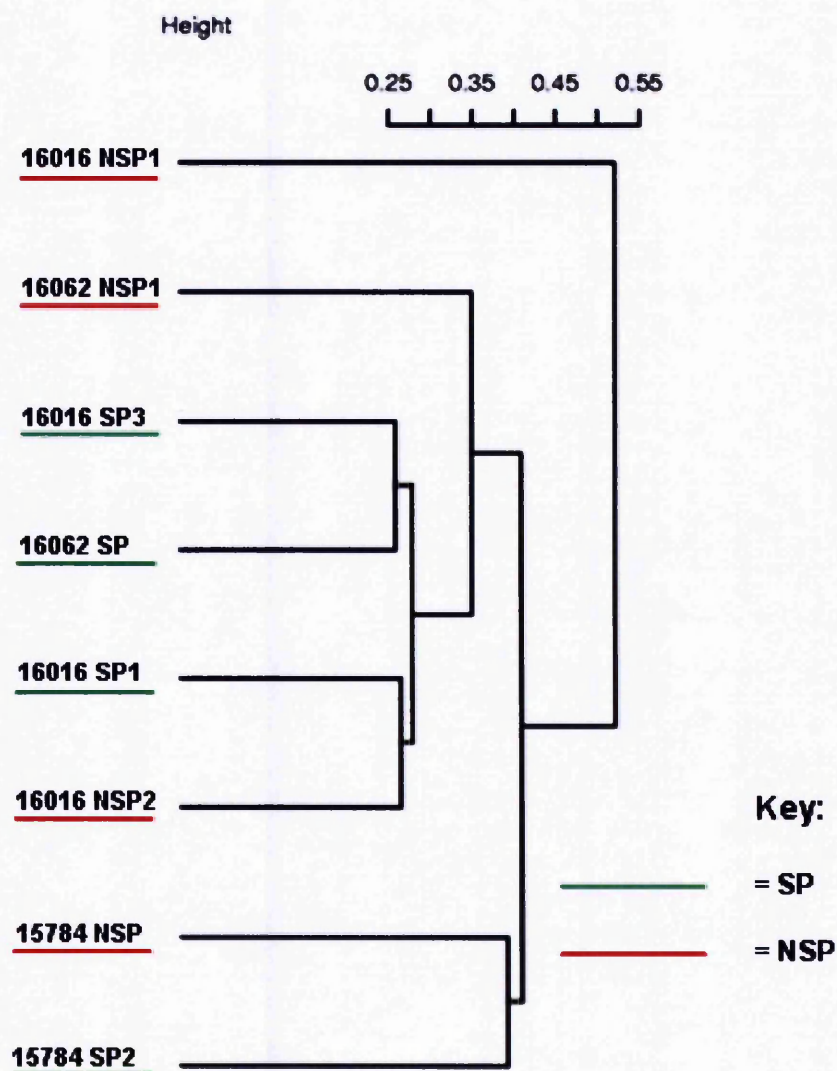


Figure 3.6: Cluster dendrogram illustrating the hierarchical clustering of data from the eight arrays. The degree of clustering is determined by the formula $1 - \text{Pearson Correlation Score } (R^2)$ and this is depicted on the y-axis by the scale.

Probesets	log2 raw expression values								Pairwise Comparison Fc				Mean Fc
	MB5 16016 NSP1	MB6 16016 NSP2	MB8 16062 NSP1	MB9 15784 NSP	MB3 16016 SP1	MB4 16016 SP3	MB7 16062 SP	MB10 15784 SP2	10 vs 9 log2	3 vs 5 log2	4 vs 6 log2	7 vs 8 log2	log2(Fc) SP-NSP
MB10 vs MB9													
214519_s_at	3.98	2.96	2.09	1.08	6.03	4.37	5.34	6.15	5.07	2.05	1.41	3.25	2.95
239090_at	2.93	3.38	4.44	0.07	4.39	5.03	5.48	5.09	5.02	1.45	1.65	1.04	2.29
240828_at	3.62	1.32	1.34	1.79	5.00	3.94	4.54	6.64	4.85	1.38	2.61	3.20	3.01
238948_u_at	1.17	0.81	1.28	1.75	4.77	1.82	4.84	5.76	4.01	3.60	1.01	3.57	3.05
1557883_a_at	-1.49	1.18	-0.35	-0.15	4.84	3.65	1.25	3.86	4.01	6.34	2.47	1.60	3.60
221923_s_at	7.93	5.23	3.67	6.62	4.53	4.12	1.93	2.07	-4.55	-3.40	-1.12	-1.74	-2.70
234522_at	5.46	4.95	4.95	5.73	3.89	2.55	3.75	1.08	-4.65	-1.57	-2.40	-1.20	-2.46
228245_s_at	11.06	8.60	6.06	7.99	6.50	5.84	2.12	2.44	-5.54	-4.56	-2.76	-3.94	-4.20
MB3 vs MB5													
1557883_a_at	-1.49	1.18	-0.35	-0.15	4.84	3.65	1.25	3.86	4.01	6.34	2.47	1.60	3.60
240026_u_at	-1.16	-0.14	1.60	1.70	3.43	2.40	3.93	4.78	3.07	4.59	2.54	2.33	3.14
1553835_a_at	1.51	2.94	1.49	2.79	6.04	4.49	5.28	6.11	3.31	4.53	1.55	3.79	3.30
225942_at	2.10	3.68	4.48	3.74	6.12	5.99	6.10	5.20	1.46	4.02	2.31	1.62	2.35
1558977_at	1.69	3.13	2.68	1.70	5.70	5.14	4.84	5.66	3.97	4.01	2.01	2.16	3.04
228809_at	8.85	7.95	5.40	6.33	4.67	6.81	6.66	4.97	-1.36	-4.19	-1.14	1.26	-1.36
212984_at	4.42	5.02	5.93	4.64	0.22	1.66	3.39	3.63	-1.01	-4.21	-3.36	-2.55	-2.78
214151_s_at	6.53	5.28	6.57	6.89	2.26	1.97	2.74	3.39	-3.50	-4.27	-3.31	-3.82	-3.72
228245_s_at	11.06	8.60	6.06	7.99	6.50	5.84	2.12	2.44	-5.54	-4.56	-2.76	-3.94	-4.20
200823_u_at	10.64	8.26	7.54	8.08	5.89	7.14	5.63	5.51	-2.57	-4.74	-1.12	-1.91	-2.58
1569618_a_at	7.94	6.32	6.70	6.63	2.95	5.20	4.70	5.59	-1.05	-4.99	-1.12	-2.01	-2.29
221920_s_at	10.24	7.79	6.18	7.49	5.15	6.29	2.32	3.76	-3.73	-5.09	-1.80	-3.86	-3.85
207442_at	10.48	7.56	10.06	8.38	4.96	6.26	4.67	4.42	-3.96	-5.52	-1.30	-5.39	-4.04
200965_s_at	8.86	5.13	6.66	8.14	3.17	3.27	4.95	4.74	-3.39	-5.68	-1.86	-1.71	-3.16
219138_at	11.81	8.83	8.59	8.97	5.76	7.38	4.97	5.73	-3.24	-6.05	-1.46	-3.62	-3.59
MB4 vs MB6													
1552582_at	3.48	2.33	4.13	3.80	4.80	6.62	5.45	6.46	2.66	1.32	4.29	1.31	2.40
1561612_at	1.96	2.15	4.30	2.90	3.59	6.35	5.56	6.20	3.31	1.63	4.20	1.26	2.60
236469_at	2.53	1.40	3.62	3.35	3.65	5.53	4.64	5.50	2.15	1.12	4.13	1.02	2.10
209719_u_at	11.53	9.25	8.52	9.00	8.29	5.08	6.69	7.58	-1.42	-3.25	-4.17	-1.83	-2.67
221899_at	9.85	7.60	6.82	8.26	7.58	3.21	5.64	6.84	-1.42	-1.26	-4.39	-1.18	-2.06
235094_at	10.37	7.54	8.53	11.37	7.78	2.82	6.31	10.02	-1.35	-2.59	-4.72	-2.22	-2.72
MB7 vs MB8													
222806_s_at	8.15	6.18	7.63	5.24	3.95	3.59	3.38	3.14	-2.10	-4.20	-2.59	-4.26	-3.29
207442_at	10.48	7.56	10.06	8.38	4.96	6.26	4.67	4.42	-3.96	-5.52	-1.30	-5.39	-4.04

Table 3.5: The final stages of identifying probesets that were suitable for use in an experiment to validate the fold changes seen on the array by qRT-PCR . The filtering method was applied to each of the four paired SP vs. NSP comparisons. The individual log2 expression summaries for each of the probesets from each of the individual arrays are listed on the left half of the table. The observed fold change (Fc) for each of the probesets and the different paired comparisons are featured on the right side of the table. Those probesets with log2 raw expression values of greater than or equal to a log2 fold change of 6 in at least one of the samples in a pairwise comparison are highlighted in yellow. The terminology MB10 vs. MB9, MB3 vs. MB5, MB4 vs. MB6 and MB7 vs. MB8 equate to 15784 SP2 vs. 15784 NSP, 16016 SP1 vs. 16016 NSP1, 16016 SP3 vs. 16016 NSP2 and 16062 SP vs. 16062 NSP1 respectively.

3.5). After initial filtering, the gene list was further reduced to only 10 probesets as probset 228245_s_at was repeated.

Despite high log2 raw expression values, the MAS5.0 software called the majority of such transcripts as 'Absent'. When only those probesets with high raw expression values that were reinforced by a 'Present' gene call in at least one sample of the paired comparison were included, the list was further shortened to only two probesets (Table 3.6).

3.7 Correlation Between MAS5.0 Generated Detection Calls and Raw Expression Values

Analysis was undertaken to determine why a significant proportion of the probesets were called 'Absent' despite being associated with high raw expression values that had already been corrected by the mismatch probe intensities.

One of the arrays (16016 NSP1) was compared with an example of a sound dataset obtained from the MCF7 cell line. The overall signal intensities for each probeset were ranked from lowest (left) to highest (right) on the x-axis. The resultant plots (Figure 3.7) demonstrate that the range of signal intensities for each of the 11 probes within a probeset is wide in the 16016 NSP1 array dataset compared with that of the MCF7 cell line. This is indicative of noisy data. The probesets called 'Present' have been coloured in red. On the MCF7 plot very few probesets have a high overall signal intensity and are still called 'Absent' whereas, in the

Probesets	log2 raw expression values							
	MB5	MB6	MB8	MB9	MB3	MB4	MB7	MB10
	16016 NSP1	16016 NSP2	16062 NSP1	15784 NSP	16016 SP1	16016 SP3	16062 SP	15784 SP2
228245_s_at	A	A	A	A	P	P	P	A
228245_s_at	A	A	A	A	P	P	P	A
200823_x_at	A	A	A	A	M	P	M	A
1568618_a_at	A	A	A	A	P	P	P	P
221920_s_at	A	A	A	A	P	P	P	A
207442_at	A	A	A	A	A	P	A	P
219138_at	A	A	A	A	A	P	P	A
209719_x_at	A	M	A	A	P	P	P	A
221899_at	A	M	A	A	P	P	P	A
235094_at	P	A	A	A	P	P	P	P
207442_at	A	A	A	A	A	P	A	P

Table 3.6: Table depicting the gene calls generated by MAS5.0 for the 10 probesets that were previously identified as being suitable for the qRT-PCR validation experiments on the basis of their log2 raw expression values.

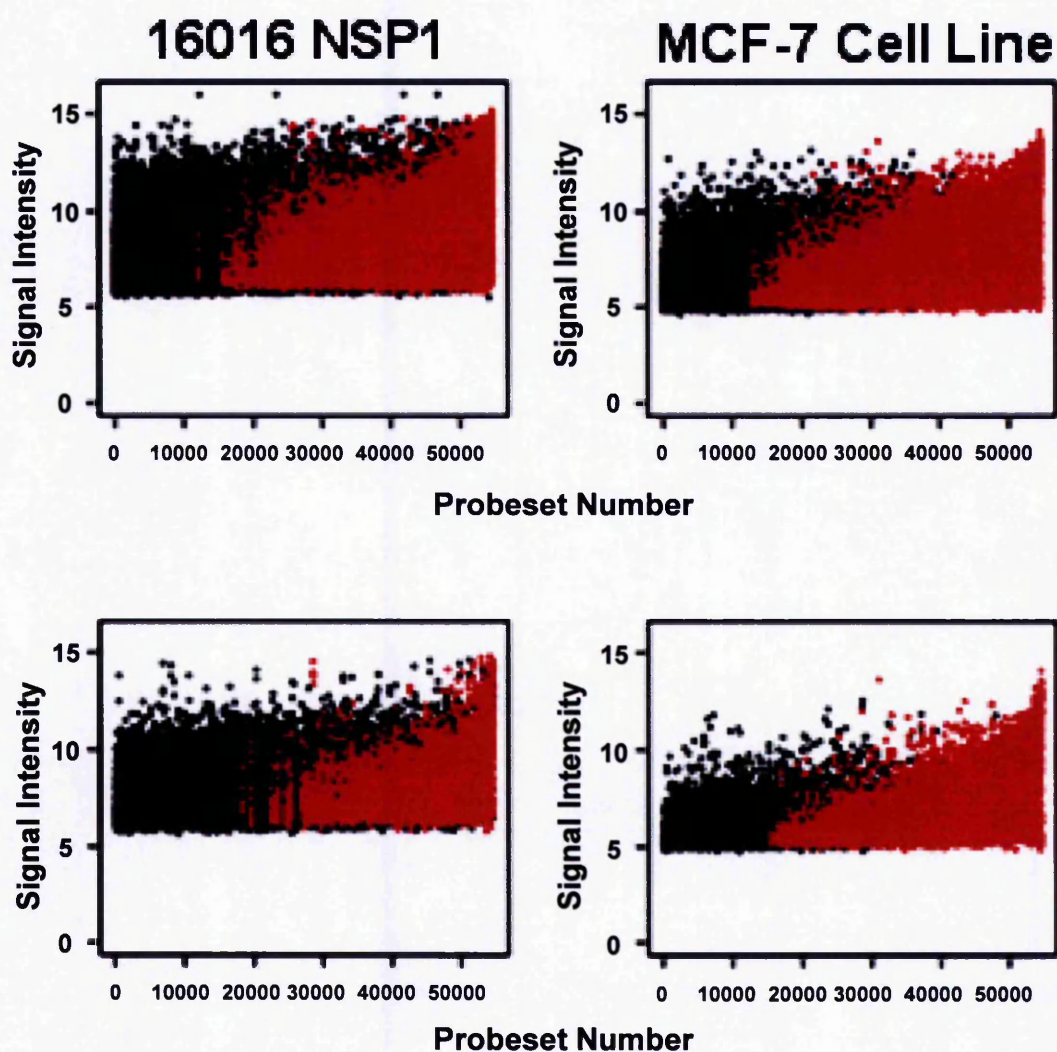


Figure 3.7: Array 16016 NSP1 (left column) was compared with an example of a sound dataset obtained from the MCF7 cell line (right column). The top row shows data for all probesets and the bottom row shows data for every tenth probeset so as to illustrate the distribution pattern more clearly. The overall signal intensities (y-axis) from each probeset were ranked and placed from left (lowest) to right (highest) along the x-axis. Each of the 11 perfect match probes within each probeset was then plotted along the y-axis. The probesets called 'Present' have been coloured in red. The plots serve to show the correlation between the signal intensity and the MAS5.0-generated gene call.

example array used (16016 NSP1), many probesets are still called 'Absent' even with high signal. Further information can be gleaned when the pattern of colour is examined. Those probesets with a narrower range of signals for the 11 individual probes within a probeset are more likely to be called 'Present'. Those probesets with a high overall signal but also a high range still tend to be called 'Absent'. This indicates that even though the median overall signal (i.e. the expression intensity for the probeset) is high, the inconsistency amongst the constituent probes means the detection algorithm is unable to be certain that the probe set is reliably 'Present'.

3.8 Summary of Chapter Results

A small number of cells could be isolated and collected by the CD133⁺/CD45⁻ selected Hoechst 33342 dye efflux protocol. The yield of RNA subsequently extracted from such cells was low and the quality of cDNA isolated poor, such that only 16 out of 34 samples (47.1%) were suitable for hybridisation to the arrays and, of these, only eight out of 34 samples (23.5%) were paired samples.

Quality control data revealed a high background signal, a low percentage of genes called 'Present', a wide variation of probe intensities within a probeset and poor correlation between expression values and MAS5 generated detection calls.

The MAS5 normalisation techniques were effective. However, there was insufficient correlation between arrays to draw any useful or reliable conclusions about the biological significance of the differential gene expression profiles observed. The combination of these factors, in particular the poor correlation between the MAS5-generated gene calls and the raw expression summaries, lead to difficulty in determining suitable probesets for qRT-PCR validation. The Cancer Research UK Molecular Biology Core Facility was consulted for a specialist opinion and the consensus reached was that the Microarray database was not suitable for further datamining for biological significance.

Chapter 4: Results of Introducing RNase-Free Adjuncts to the Hoechst 33342 Dye Efflux Assay Protocol

In chapter three it was shown that the Hoechst 33342 dye efflux assay yielded low quantities of poor quality RNA, therefore a number of modifications were made in an attempt to reduce the effect of RNases and thereby improve the quality of RNA extracted (sections 2.13 and 2.8).

4.1 Initial Pilot Experiment

The first attempt at RNA extraction used five epithelial samples from patients with histologically-confirmed BPH (GU2, GU3, GU18, GU29 and 16341). BPH samples were chosen because they were the most plentiful disease type available in frozen storage. The standard FACS protocol with only a live CD45^{-ve} SP and live CD45^{-ve} NSP gate selection was used to maximise cell yield. The precise cellular phenotype was not deemed important in this pilot experiment providing both an SP and NSP were isolated, so that a comparison could be drawn between them and between the standard and RNase-free protocols.

Good ribosomal peaks were seen in eight of the 10 SP and NSP samples processed using the adapted RNase-free FACS protocols. The two samples that did not demonstrate good peaks were both SP samples (GU29 SP and 16341 SP). Fewer of the samples isolated by standard techniques demonstrated good RNA quality with only five of the 10 samples having good ribosomal peaks (GU2 NSP, GU3 NSP, GU18

NSP, GU29 NSP and 16341 NSP). All five samples were from NSP samples (Figure 4.1).

4.1.1 DNase Treatment

Qiagen® claim that DNase digestion is not required as the silica membrane combines RNA extraction techniques with effective technology to remove genomic DNA. On column DNase treatment was therefore not used in the initial round of experiments. However, marked DNA contamination was demonstrated (Figure 4.1 and 4.2) and this skewed interpretation as well as making assignment of a RIN difficult. Using GU18 as an example from the collection of five samples, the substantial ribosomal peaks demonstrate good RNA quality in samples GU18 NSP but not GU18 SP, both of which were processed by standard protocols. Both GU18 SP RNAF and GU18 NSP RNAF were processed by RNase-free protocols (RNAF) and ribosomal peaks appeared improved. There is evidence of marked contamination by genomic DNA between the peaks when compared with the control sample. The lack of a reliable RIN meant there was no way of objectively differentiating between the standard and RNase-free FACS protocols and determining which of the two protocols was optimal (Table 4.1). Despite reasonable ribosomal peaks being seen in these samples, the RIN fails to confirm good quality compared with those of the control sample. This was believed to be related to the DNA contamination of the ribosomal peaks and in some circumstances (GU3 NSP RNAF, 16341 NSP and 16341

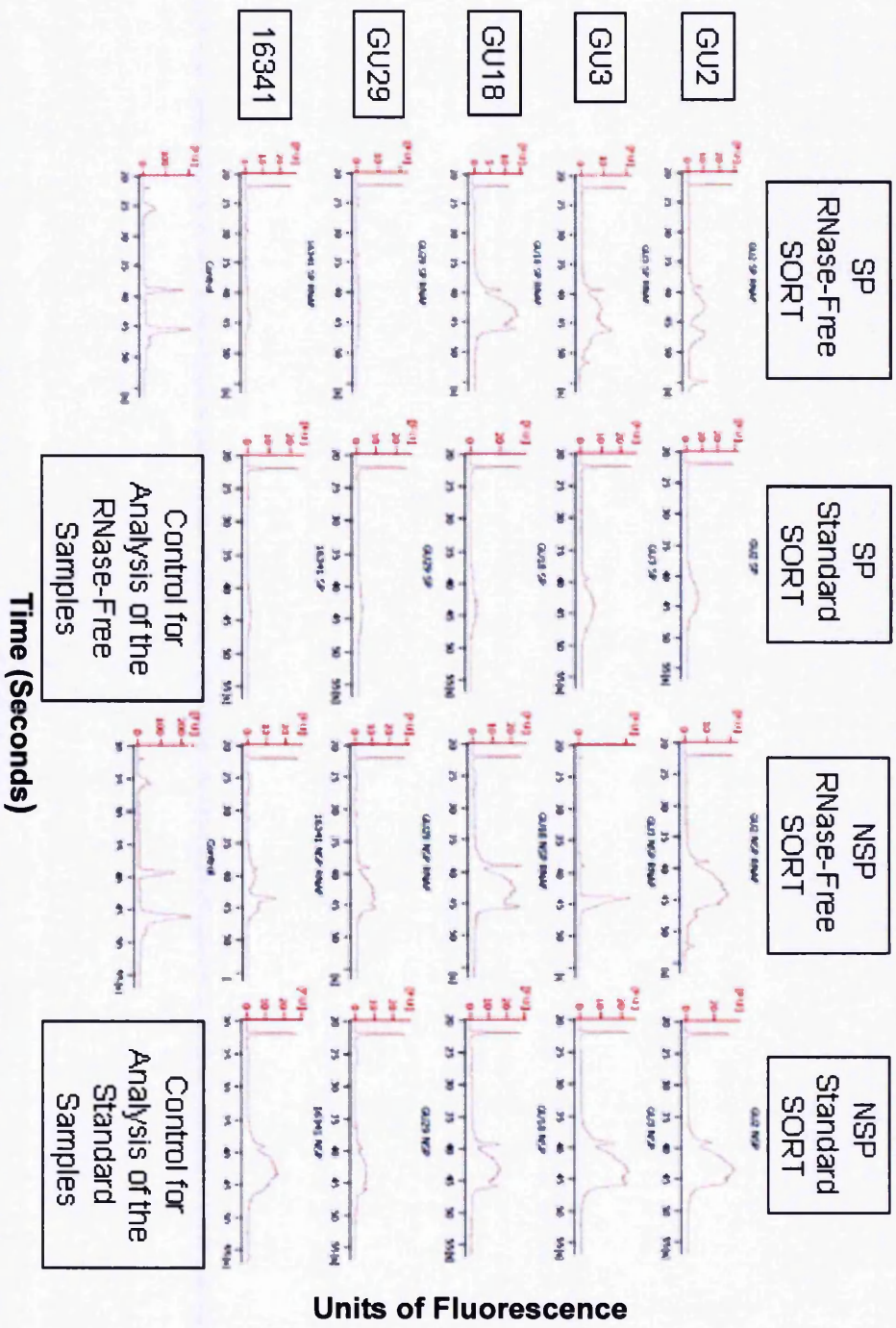


Figure 4.1: Electrophoretic output for the first set of five live CD45^{ve} epithelial SP and NSP patient samples analysed. The RNase-free samples were processed on one Agilent chip and the standard samples on another. The control RNA output for each of these two sample runs is included. The integrity of ribosomal RNA was used as a surrogate for the RNA quality overall. The two peaks of fluorescence correspond with 16S (left-hand peak) and 18S (right-hand peak) ribosomal RNA and appear at characteristic time points on the x-axis (39 and 46 seconds respectively).

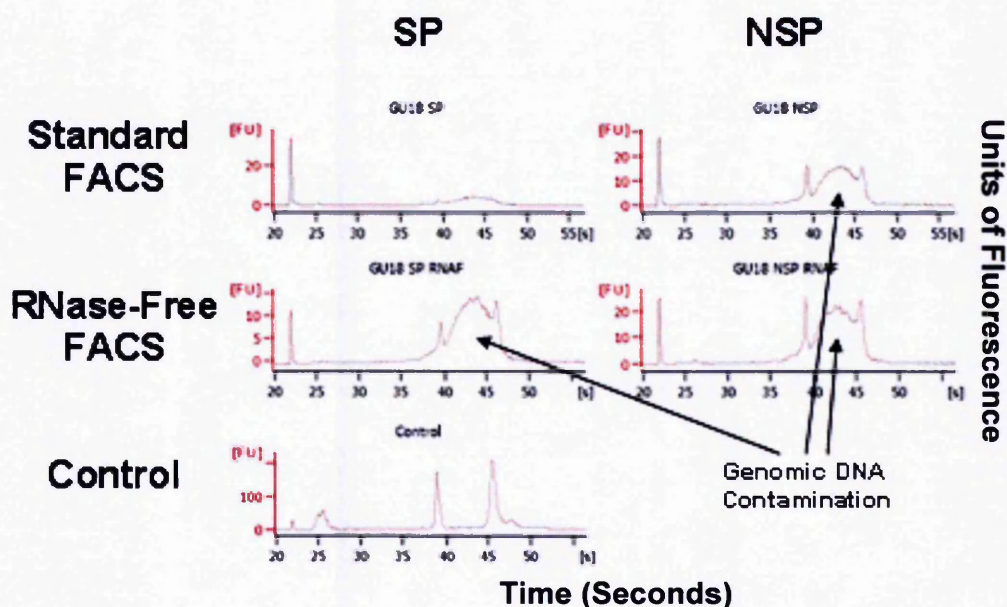


Figure 4.2: An example of the initial electrophoretic output using patient GU18. Half the cell population was processed by the standard FACS protocol and are shown on the top row. The bottom row shows the output for the RNase-free (RNAF) protocol. The SP samples are shown on the left and the NSP on the right. The electrophoretic output of the control RNA for that particular run of samples is shown. The heaped signal between the two fluorescent peaks is consistent with contamination by genomic DNA that has not been removed by DNase. An uncontaminated control sample is shown for comparison.

Sample	RNase-free Protocol	Standard Protocol
GU18 SP	3.3	2.7
GU18 NSP	6	5.1
GU29 SP	1	1.1
GU29 NSP	4.1	2.3
GU2 SP	2.8	2.4
GU2 NSP	3.3	3.9
GU3 SP	5.8	4.3
GU3 NSP	N/A	5.7
16341 SP	1.9	1.2
16341 NSP	N/A	N/A
CONTROL	9.6	9.9

Table 4.1: Table showing the RNA Integrity Number (RIN) for each of the samples isolated by both RNase-free (RNAF) (left) and standard (right) FACS protocols.

NSP RNAF) this was so substantial that an RIN could not be assigned by the software.

The DNA contamination of these samples was treated by subjecting the same samples to on-column DNase treatment. The eluted RNA was subsequently re-analysed. All subsequent samples that were processed were treated with DNase as standard.

4.1.2 Volumes of RNase-free Water for Elution

As suggested by Qiagen, the second analysis examined RNA that had been eluted in two separate 30µl volumes of RNase-free water to maximise the total RNA yield. Ribosomal peaks were less substantial on this occasion and demonstrated poorer RNA quality, although the NSP samples had better ribosomal peaks than the corresponding SP samples (Figure 4.3). Although the DNA had disappeared, the combination of degradation secondary to further work being done on the RNA and relatively low RNA concentration secondary to the high elution volume, meant that little could be seen, particularly in the SP samples.

Acceptable ribosomal peaks were only seen in two of the 10 SP samples processed by both the standard and RNase-free protocols. Values for the RIN reflected the decrease in RNA quality seen on the graphs (Table 4.2). Only one sample (GU18 NSP) had a reasonable RIN score of 5.2. The remainder of the samples processed by RNase-free techniques had unacceptable RIN scores (<3.6) and 60% of these had the poorest RIN score of one. The standard FACS protocol yielded marginally better RIN scores, with three being acceptable (GU18 NSP (7), GU2 NSP (6.5) and

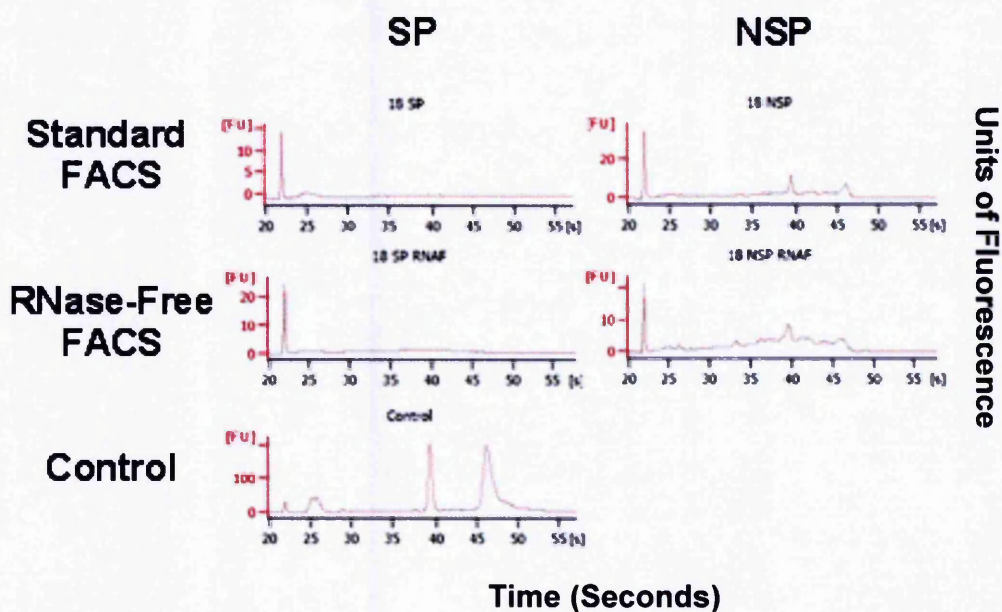


Figure 4.3: An example of the electrophoretic output using patient GU18 following on-column DNase treatment. Half the cell population was processed by the standard FACS protocol and are shown on the top row. The bottom row shows the output for the RNase-free protocol. The SP samples are shown on the left and NSP on the right. The electrophoretic output of the control RNA for that particular run of samples is shown.

Sample	RNase-free Protocol	Standard Protocol
GU18 SP	1	N/A
GU18 NSP	5.2	7
GU29 SP	1	1
GU29 NSP	3.6	4.9
GU2 SP	1	1
GU2 NSP	1.9	6.5
GU3 SP	1	4
GU3 NSP	1	6.3
16341 SP	1.1	1
16341 NSP	1	3.6
CONTROL	9.9	9.9

Table 4.2: Table showing the RNA Integrity Number (RIN) following DNase treatment for each of the samples isolated by both RNase-free (RNAF) (left) and standard (right) FACS protocols.

GU3 NSP(6.3)) and only 30% being assigned a RIN score of one. All samples with acceptable scores were from NSP samples. Again, in some circumstances (GU18 SP) an RIN could not be assigned by the software.

4.1.3 Concentration of Elution Volumes

The initial two attempts at analysis used large volumes (two elution volumes of 30µl each) to maximise RNA yield. However, it became apparent that, with the low total RNA quantity, the resultant RNA concentration was too low for the subsequent analysis steps to be accurate. The third attempt at analysis therefore merely used a single elution volume of 30µl. However, it was not possible to determine whether the continued observation of low RNA quality was related to degradation of the sample or due to a persistently high elution volume and therefore low RNA concentration. On processing the same 10 DNase-treated samples for a third time, the elution volume was reduced by a vacuum concentrator (Eppendorf Vacufuge®, Krackeler Scientific Inc., Albany, NY, USA) at 35°C until approximately 10µl was left (range 8µl to 15µl). The ribosomal peaks were marginally improved when compared with those from the second analysis of the same samples which had been DNase treated but still eluted in a high volume of RNase-free water (Figure 4.4). A RIN could not be calculated by the software for four samples (GU18 SP, GU29 SP, GU29 NSP and 16341 NSP) processed by the standard protocol. Whilst the RIN remained low

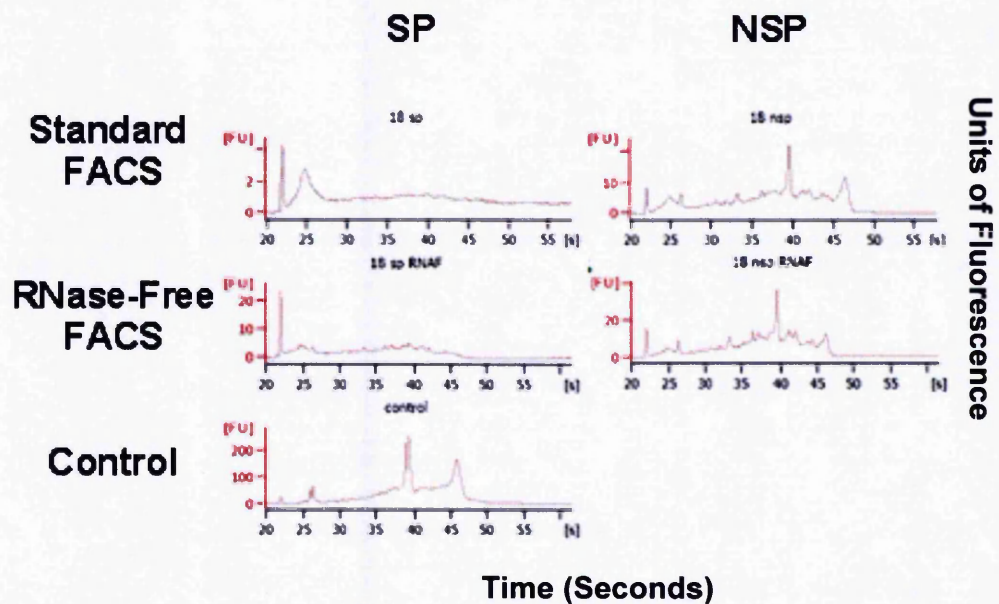


Figure 4.4: Example electrophoretic output for patient GU18 after DNase treatment and vacuum concentration. Half the cell population was processed by the standard FACS protocol and are shown on the top row. The bottom row shows the output for the RNase-free protocol. The SP samples are shown on the left and NSP on the right. The electrophoretic output of the control RNA for that particular run of samples is shown.

Sample	RNase Free Protocol	Standard Protocol
GU18 SP	2.6	N/A
GU18 NSP	5.2	5.5
GU29 SP	1.6	N/A
GU29 NSP	5	N/A
GU2 SP	2	2.4
GU2 NSP	2.7	5.1
GU3 SP	3.5	7
GU3 NSP	4	4.3
16341 SP	2.1	2.5
16341 NSP	2.5	N/A
CONTROL	6.7	8.5

Table 4.3: Table showing the RNA Integrity Number (RIN) following DNase treatment and vacuum concentration for each of the samples isolated by both RNase-free (RNAF) (left) and standard (right) FACS protocols.

Sample	Cell Numbers isolated by FACS	RNA (pg) / Cell (1st Round)	RNA (pg) / Cell (2nd Round)
GU18 SP	10,470	2.13	0.10
GU29 SP	1,500	15.13	7.73
GU2 SP	10,229	6.08	1.51
GU3 SP	21,063	2.06	0.96
16341 SP	6,404	1.56	0.92
Average	9,933	3.23	1.09
GU18 NSP	86,086	1.03	0.69
GU29 NSP	65,281	0.51	0.21
GU2 NSP	121,590	1.61	0.37
GU3 NSP	219,042	0.63	0.30
16341 NSP	56,972	1.73	0.33
Average	109,794	1.01	0.37
GU18 SP RNAF	10,500	8.30	3.00
GU29 SP RNAF	1,800	5.28	6.22
GU2 SP RNAF	9,492	10.44	2.02
GU3 SP RNAF	15,475	5.31	2.14
16341 SP RNAF	1,333	13.35	9.00
Average	7,720	7.66	2.77
GU18 NSP RNAF	85,239	1.76	1.12
GU29 NSP RNAF	63,500	1.14	0.43
GU2 NSP RNAF	91,720	1.39	0.19
GU3 NSP RNAF	166,376	4.66	0.90
16341 NSP RNAF	24,887	1.66	0.64
Average	86,344	2.70	0.71

Table 4.4: Table showing the amount of RNA (pg) extracted per cell (total RNA/cell number) after both the initial (1st round) and DNase-treated (2nd round) stages of analysis for each of the SP and NSP samples processed by the standard and RNase-free (RNAF) protocols.

in the samples processed by RNase-free techniques, all samples could be assigned a value (Table 4.3).

When the total amount of RNA extracted per cell was examined it was noticeable that the amounts of extracted RNA reduced as the number of attempts at analysis increased. In all but one sample (GU29 SP RNAF) the amount of RNA isolated per cell fell between the first and second analysis of the same samples (mean 3.23pg/cell vs. 1.09pg/cell for the standard SP, 1.01pg/cell vs. 0.37pg/cell for the standard NSP, 7.66pg/cell vs. 2.77pg/cell for the RNase-free SP and 2.7pg/cell vs. 0.71pg/cell for the RNase-free NSP). This would suggest that RNA degradation was playing a role in determining the reduced quality observed (Table 4.4).

4.1.4 RNAlater®

The initial attempt at RNA extraction for microarray gene expression analysis had involved cell suspensions being isolated by FACS and collected into pop-top tubes. After centrifugation, the cells were resuspended and stored in RNAlater®. On a number of occasions during the processing of this first set of samples, problems with ice crystal formation had been observed and the decision was taken to discontinue using RNAlater® and instead, for the next attempt, RNA extraction was performed immediately following FACS and the isolated RNA stored in RNase-free water at -80 °C until required.

4.2 Definitive Attempt at Determination of the Effect of RNase-free Adjuncts on RNA Quality

The decision was taken to analyse five further BPH samples (GU37, GU40, GU42, GU50 and 16339). Taking into consideration the results from the initial five samples, on column DNase treatment and reduction of elution volume to 10µl by vacuum concentration were performed *de novo* as integral steps of the revised RNA extraction technique. On this occasion samples were isolated by FACS and collected into PBS (or DEPC-treated PBS if an RNase-free sort) rather than RNAlater®. Also, the larger cell numbers isolated from the NSP samples were reduced so the same numbers of SP and NSP cells went forward to RNA extraction. This allowed a more reliable comparison to be drawn between the total RNA extracted from each of the populations.

The combination of performing both on-column DNase treatment and vacuum concentration appeared to improve the quality of the RNA isolated greatly compared with the analysis of the previous set of five patient samples. This is determined by the improved ribosomal peaks seen on the simulated gel (Figure 4.5). The ribosomal peaks show some improvement with the use of RNase-free techniques though this observation is not uniform as some standard sort samples have better peaks than the corresponding RNase-free sort. Three of the five (60%) SP samples and five out of the five (100%) NSP samples isolated via the RNase-free FACS protocol had acceptable ribosomal peaks. This was

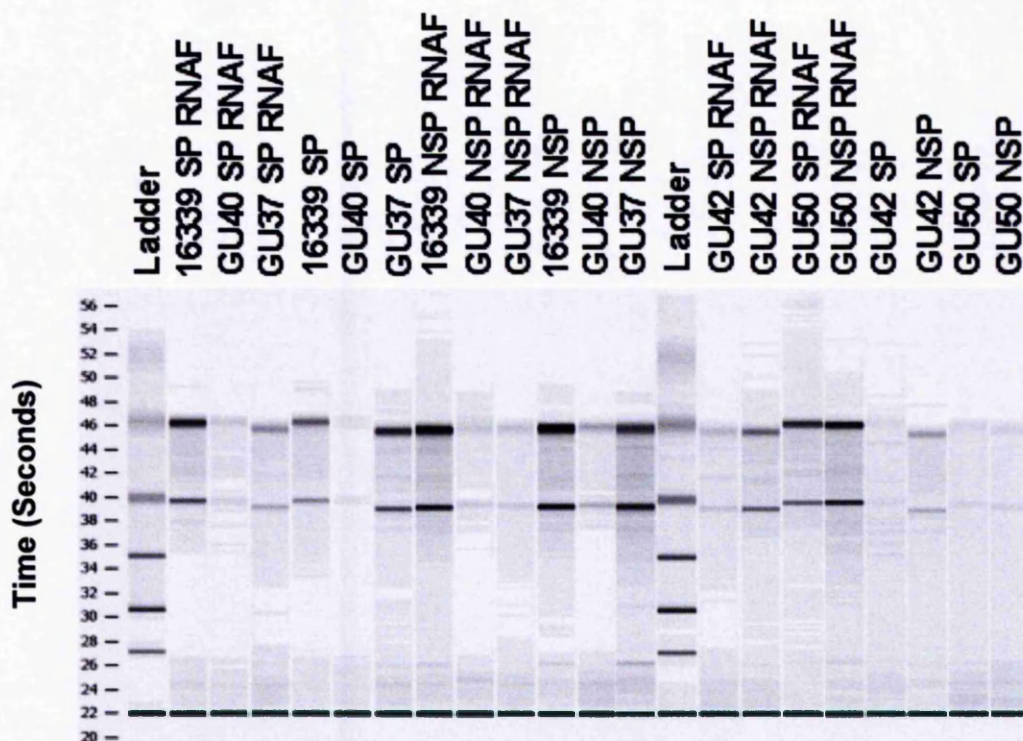


Figure 4.5: A simulation of the traditional electrophoretic gels demonstrating the bands of ribosomal RNA (rRNA) detected for each of the samples from the standard and RNase-free (RNAF) FACS protocols. The y-axis is the time in seconds at which such bands were detected. These are comparable with the ladder gel which depicts the times at which nucleotides of a known size are seen. Gel A encompasses samples 16339, GU40 and GU37 and gel B details GU42 and GU50.

reduced to two (40%) and four (80%) respectively for the samples sorted by the standard protocol (Figure 4.6).

The general trend was for improved RNA quality when RNase-free FACS protocols were used though statistical significance was not reached. The mean RIN was improved for both the SP and NSP when the RNase-free protocol was employed (7.54 vs. 4.44 for SP, $p=0.0998$ and 7.58 vs. 7.18 for the NSP, $p=0.5446$). The respective mean 28S/18S rRNA ratios mirrored these findings (1.88 vs. 0.98 for the SP, $p=0.0856$ and 1.64 vs. 1.4 for the NSP, $p=0.1360$). The RIN and 28S/18S rRNA ratio values were only unacceptably low when the standard FACS protocol was employed. The use of RNase-free sorting for these particular samples (namely GU40 SP and GU42 SP) appeared to salvage good quality RNA (Table 4.5).

Amounts of RNA extracted from the cells were low overall but was felt this was likely to be a function of the small cell numbers rather than the efficiency of the extraction techniques. A calculation to determine the amounts of RNA potentially extractable if the isolated SP and NSP populations had 3,000 cells in them was performed. This indicates whether sufficient RNA would be harvested from sample sizes that were commonly seen with CD45⁺ FACS. A total of 0.5ng of starting RNA is required for entry into the NuGEN RNA amplification step as a prelude to Affymetrix[®] microarray and these results demonstrate that 80% (8 out of 10) of the RNase-free SP and NSP samples had sufficient RNA based on a sample size of 3000 cells (Table 4.6).

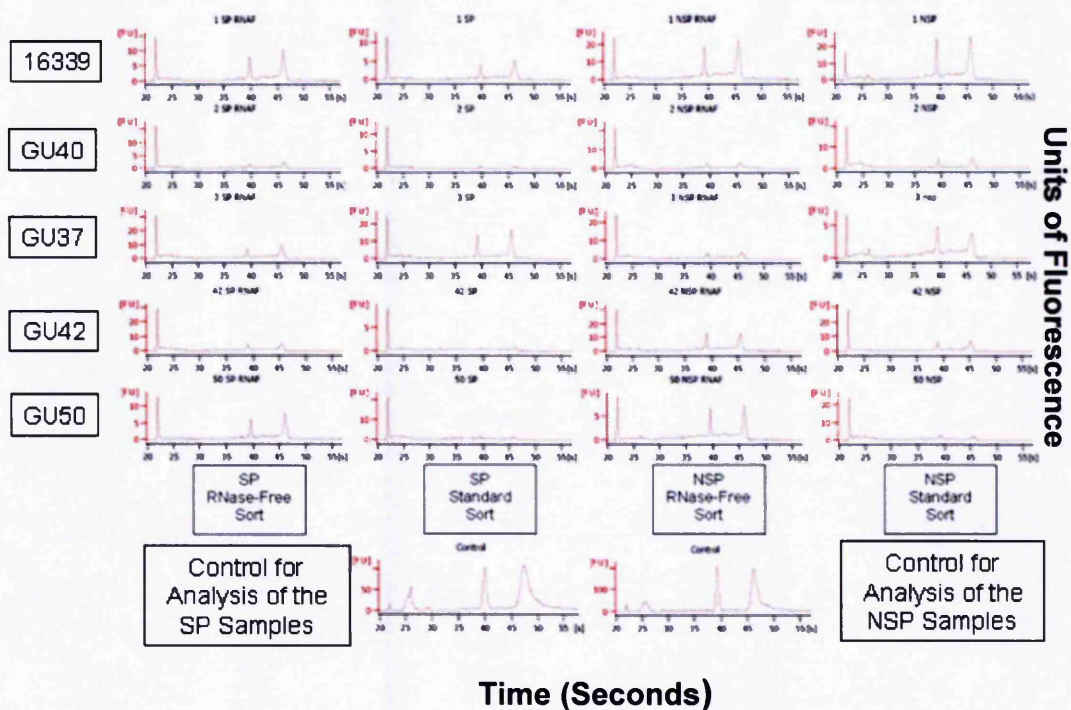


Figure 4.6: Electrophoretic output for the second set of five BPH patient samples analysed after DNase treatment and volume concentration. SP samples are shown in the two left hand columns and NSP samples in the two right hand columns. The output results for the two control RNA samples used during processing of the 20 samples are shown at the bottom left of the figure.

Sample	RNA Integrity Number (RIN)				rRNA Ratio (28S/18S)			
	SP		NSP		SP		NSP	
	Rnase Free	Standard	Rnase Free	Standard	Rnase Free	Standard	Rnase Free	Standard
GU42	7	1	8.2	7.4	1.7	0	1.4	1.5
GU50	8.2	3.5	7.2	4.7	2	1.5	1.5	1.3
16339	8.3	8.2	8.2	8.3	1.9	1.8	1.8	1.6
GU40	6.6	1	8.1	8.2	2	0	1.7	1.5
GU37	7.6	8.5	6.2	7.3	1.8	1.6	1.8	1.1
Average	7.54	4.44	7.58	7.18	1.88	0.98	1.64	1.4
2-Tailed Paired T-test	0.0998		0.5446		0.0856		0.1360	

Table 4.5: Table documenting two objective measures of RNA quality, the RNA Integrity Number (RIN) and the 28S/18S rRNA ratio for each of the five samples processed by both RNase-free (left) and standard (right) protocols.

Sample	Population and Protocol	Cell Numbers Isolated by FACS	RNA (pg) / Cell	Total RNA (pg) if 3,000 Cells
16339	Standard SP	19000	0.047	141
GU40		1750	0.171	513
GU37		15500	0.218	654
GU42		11000	0.115	345
GU50		8000	0.362	1086
Average		11050	0.183	549
16339	Standard NSP	19000	0.302	906
GU40		1750	1.114	3342
GU37		15500	0.229	687
GU42		11000	0.362	1086
GU50		8000	0.488	1464
Average		11050	0.499	1497
16339	RNAF SP	17000	0.122	366
GU40		1700	0.453	1359
GU37		9000	0.320	960
GU42		10758	0.305	915
GU50		15000	0.148	444
Average		10692	0.270	810
16339	RNAF NSP	17000	0.291	873
GU40		1700	0.812	2436
GU37		9000	0.200	600
GU42		10758	0.559	1677
GU50		15000	0.179	537
Average		10692	0.408	1224

Table 4.6: Table showing the cell numbers isolated by FACS and the amount of RNA isolated per cell. The amount of RNA for a cell sample size of 3000 cells was calculated as this was a typical size seen in the CD45^{-ve}-selected SP.

	Cell Population and Protocol Type							
	Standard SP	Standard NSP	RNAF SP	RNAF NSP	Standard SP	RNAF SP	Standard NSP	RNAF NSP
RNA Quantity (pg) / Cell	0.047	0.302	0.122	0.291	0.047	0.122	0.302	0.291
	0.171	1.114	0.453	0.812	0.171	0.453	1.114	0.812
	0.218	0.229	0.320	0.200	0.218	0.320	0.229	0.200
	0.115	0.362	0.305	0.559	0.115	0.305	0.362	0.559
	0.362	0.488	0.148	0.179	0.362	0.148	0.488	0.179
Paired t-test (p value)	0.124		0.174		0.357		0.399	

Table 4.7: Table comparing the RNA yield (pg) per cell for each of the populations (SP and NSP) processed by either standard or RNase-free protocols. A paired *t*-test was used to examine the yields from the five samples for statistical significance in each of four comparisons.

Overall the amount of RNA extracted from the SP compared with the NSP was lower. The average RNA yield from the SP processed by the standard protocol was 0.183pg /cell compared to 0.499pg /cell for the NSP ($p=0.124$). Furthermore, the SP processed by the RNase-free protocol also had lower RNA yields compared with the NSP (mean 0.270pg / cell vs. 0.408pg / cell $p=0.174$) (Table 4.7). Though no statistical significance was observed, the average amounts of RNA extracted from the standard SP population (0.183pg / cell) was improved by RNase-free sorting (0.270pg / cell) ($p=0.357$) but there was a slight decrease in RNA yield when RNase-free protocols were utilised with NSP samples (0.499pg / cell vs. 0.408pg / cell) ($p=0.399$) (Table 4.7).

4.3 Summary of Chapter Results

The RNA extraction protocol was optimised to improve both the quality and size of RNA yields. Thus, the RNase-free protocol was beneficial in ensuring more reliable extraction and in particular, in minimising the risk of RNase degradation of low cell number quiescent samples from the SP. The number of samples deemed suitable for the next step of conversion to cDNA, amplification, labelling and chip hybridisation could therefore be maximised.

Chapter 5: Characterisation of the Hoechst 33342 Dye Efflux Assay

5.1 Analysis of CD133⁺/CD45⁻ Hoechst 33342 Profiles

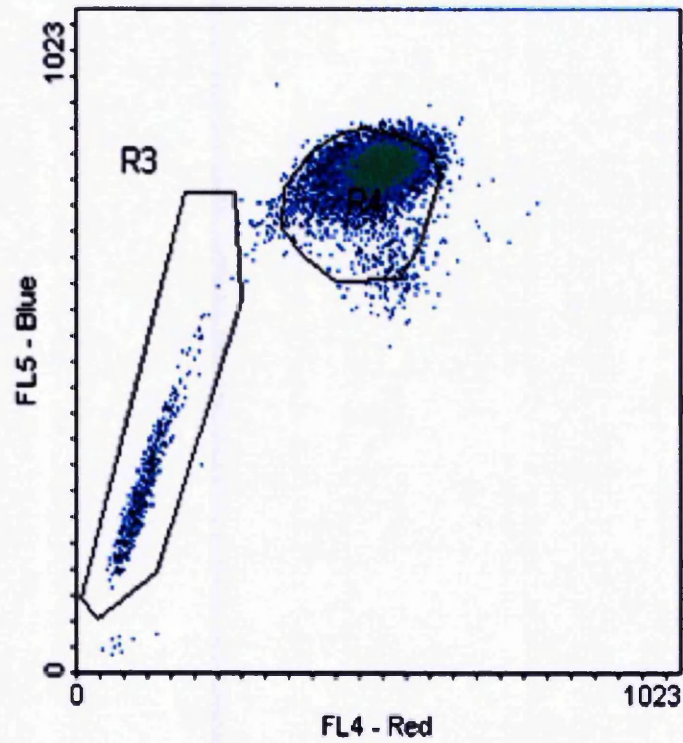
Fifteen BPH and 11 CaP samples underwent FACS in the first year of study. Ten of the BPH and 11 of the CaP samples were sorted for a CD133⁺/CD45⁻ phenotype as described in section 2.6. Resultant populations were to be collected for use in functional assays such as colony-forming and proliferative capacity assays as well as for RNA extraction and microarray gene expression analysis.

It soon became clear that such further study was limited by the extremely low cell numbers, particularly from the SP (BPH SP mean 703, SD ± 635 , range 30-2188 cells vs. BPH NSP mean 3716, SD ± 4036 , range 640-14700 cells ($p=0.028$); CaP SP mean 145, SD ± 173 , range 7-582 cells vs. CaP NSP mean 1383, SD ± 1535 , range 102-5177 cells ($p=0.027$)) that were successfully isolated after the addition of CD133⁺ selection to the protocol. In particular, such low cell numbers were unsuitable for RNA extraction and use in microarray studies. The number of cells isolated from CaP SP samples was significantly lower than those isolated from the BPH SP (BPH SP mean 703 cells vs. CaP SP mean 145 cells ($p=0.0153$)). The number of cells isolated from the CaP NSP appeared lower than from the BPH NSP, though this did not reach statistical significance (BPH NSP mean 3716 cells vs. CaP NSP mean 1383 cells $p=0.1067$) (Table 5.1).

Analysis of the CD133⁺/CD45⁻ profiles revealed that the CD133⁺ phenotype was by no means exclusive to the SP (Figure 5.1) and indeed a significantly larger proportion of CD133⁺ cells were seen to reside in the NSP than the SP when the total (BPH mean total SP 0.11% vs. NSP 0.92%, $p < 0.0005$; CaP mean total SP 0.05% vs. NSP 0.83%, $p = 0.0039$) and gated (BPH mean CD133⁺/CD45⁻ gated SP 5.71% vs. NSP 53.03%, $p < 0.0001$; CaP mean CD133⁺/CD45⁻ gated SP 3.27% vs. NSP 46.71%, $p < 0.0001$) cell populations were examined (Table 5.1). The CD133⁺/CD45⁻ SP comprised a mean of 0.107% (BPH) and 0.049% (CaP) of the total cell population. CD133 appeared to be predominantly in the NSP in both disease types but this was to a greater degree in the CaP samples (mean total BPH SP:NSP ratio 0.11 and mean total CaP SP:NSP ratio 0.08). The proportion of CD133⁺ cells in the SP of BPH was greater than that in the SP of CaP for both total (BPH mean total SP 0.11% vs. CaP mean total SP 0.05%, $p = 0.0629$) and gated (BPH mean CD133⁺/CD45⁻ gated SP 5.71% vs. CaP mean CD133⁺/CD45⁻ gated SP 3.27%, $p = 0.1248$) cell populations. Statistical significance was not reached. The same trend of a greater proportion of CD133⁺ cells being evident in the BPH NSP than the CaP NSP was also seen, although again this did not reach statistical significance (Table 5.2).

BPH	Sample ID	Total SP (%)	Total NSP (%)	Total SP/NSP Ratio	Gated SP (%)	Gated NSP (%)	Gated SP/NSP Ratio	Actual SP Numbers Collected	Actual NSP Numbers Collected
	16045	0.09	0.67	0.04	2.11	48.82	0.04	30	1000
	16068	0.12	0.86	0.18	7.83	44.07	0.18	360	960
	16162	0.09	0.91	0.10	5.15	51.92	0.10	730	3000
	16163	0.19	2.22	0.09	4.88	56.15	0.09	660	4000
	16316	0.26	1.14	0.23	11.71	46.96	0.26	1118	3600
	16087	0.01	0.46	0.02	1.94	61.92	0.03	49	1480
	16334	0.01	0.51	0.02	0.51	48.94	0.01	45	640
	16328	0.16	1.37	0.12	8.50	72.32	0.12	2188	14700
	GU5	0.11	0.63	0.17	7.00	41.46	0.17	704	1483
	GU19	0.09	0.67	0.13	7.46	57.70	0.13	1188	6392
Mean		0.11	0.92	0.11	5.71	53.03	0.11	703	3716
Median		0.10	0.67	0.11	6.08	50.43	0.11	677	2242
SD		0.08	0.51	0.07	3.29	8.77	0.07	635	4036
Paired t-test		0.0004855		0.0000001		0.0281		0.0273	
Cap	Sample ID	Total SP (%)	Total NSP (%)	Total SP/NSP Ratio	Gated SP (%)	Gated NSP (%)	Gated SP/NSP Ratio	Actual SP Numbers Collected	Actual NSP Numbers Collected
	14937	0.04	1.36	0.03	1.49	49.95	0.03	33	1171
	15979	0.01	1.18	0.01	0.29	36.27	0.01	7	311
	14989	0.08	2.54	0.03	1.34	40.36	0.03	36	778
	16322	0.04	1.00	0.04	1.95	55.82	0.03	83	3676
	16366	0.14	0.59	0.24	13.06	56.02	0.23	582	869
	GU6	0.03	0.74	0.04	2.39	64.97	0.04	375	1450
	GU12	0.01	0.39	0.03	1.75	50.00	0.04	33	380
	GU15	0.01	0.08	0.13	4.06	57.46	0.07	110	1356
	GU4	0.16	0.81	0.19	4.70	24.58	0.19	74	142
	GU16	0.02	0.20	0.10	3.03	27.50	0.11	30	102
	GU21	0.01	0.21	0.05	1.93	50.92	0.04	231	6177
Mean		0.05	0.83	0.08	3.27	46.71	0.07	145	1383
Median		0.03	0.74	0.04	1.95	50.80	0.04	74	778
SD		0.05	0.67	0.07	3.32	12.31	0.07	173	1535
Paired t-test		0.0033987		0.0000005		0.0273		0.0273	

Table 5.1: Ten BPH and 11 Cap samples were sorted for a CD133⁺ve/CD45⁻ve phenotype. The percentage of SP and NSP cells in the total live prostate epithelial cell population and the live CD133⁺ve/CD45⁻ve gated population are shown. The ratio of SP to NSP cells is shown as well as the number of cells isolated from the respective populations. The values for the mean, median and standard deviation are reported.



CD133⁺_{ve}/CD45⁻_{ve} selection

Figure 5.1: Density plot of the Hoechst 33342 Red/Blue Profile demonstrating the typical distribution of CD133⁺_{ve}/CD45⁻_{ve} cells observed between the SP and NSP.

BPH	CaP	BPH	CaP	BPH	CaP	BPH	CaP
Total SP (%)	Total SP (%)	Total NSP (%)	Total NSP (%)	Gated SP (%)	Gated SP (%)	Gated NSP (%)	Gated NSP (%)
0.03	0.04	0.67	1.36	2.11	1.49	48.82	49.95
0.12	0.01	0.65	1.18	7.83	0.29	44.07	36.27
0.09	0.08	0.91	2.54	5.15	1.34	51.92	40.36
0.19	0.04	2.22	1.00	4.88	1.95	56.15	55.82
0.26	0.14	1.14	0.59	11.71	13.06	46.96	56.02
0.01	0.03	0.46	0.74	1.94	2.39	61.92	64.97
0.01	0.01	0.51	0.39	0.51	1.75	48.94	50.00
0.16	0.01	1.37	0.08	8.50	4.06	72.32	57.46
0.11	0.15	0.63	0.81	7.00	4.70	41.46	24.58
0.09	0.02	0.67	0.20	7.46	3.03	57.70	27.50
T-Test		T-Test		T-Test		T-Test	
0.0467		0.9070		0.0331		0.1046	

Table 5.2: Table showing the percentage of CD133⁺/CD45⁻ cells that occupied the total live prostate epithelial cell SP and NSP as well as the percentage of CD133⁺/CD45⁻ cells in the SP and NSP regions after application of a CD133⁺/CD45⁻ gate. Both disease groups (BPH and CaP) are represented. Comparisons were drawn between the proportion of CD133⁺ cells in: the BPH and CaP total live prostate epithelial cell SP; the BPH and CaP total live prostate epithelial cell NSP; the percentage of cells gated for CD133⁺/CD45⁻ in the BPH and CaP SP and the percentage of cells gated for CD133⁺/CD45⁻ in the BPH and CaP NSP.

5.2 Relative CD133 Staining of BPH Epithelial Cells with PE-Cy5 and PE-Cy7 Conjugates

This pilot study was performed to ensure that the observed pattern of staining with CD133, namely the low percentage of CD133⁺ cells in the total population was not an artefact of the staining process. This served to ensure that the optimal amount of conjugate antibody was checked.

The methods are described in section 2.10.

A single BPH sample (NC1GU7S1BaE) was used. After defining the live epithelial cell population (R1), a plot of the FL-1 channel (FITC channel, x-axis) against the FL-3 channel (PE-Cy5 or PE-Cy7 channel, y-axis) was created using the IgG-FITC control. This control identified the population R2 and thereby determined the control region without CD133 fluorescence (Figure 5.2). When using the IgG-FITC sample, without CD133 antibody, small numbers of FL-3 fluorescent cells were observed for both PE-Cy5 (0.63% of the live epithelial cell population) and PE-Cy7 (0.96% of the live epithelial cell population) above the baseline defined by the IgG-FITC control (Table 5.3). In turn, the CD133⁺ R2 was determined for each of the test samples with various concentrations of PE-Cy5 (2.5µL, 5µL and 7.5µL). The filter on the FL-3 channel was then changed and the analysis repeated for the PE-Cy7 fluorescence. The percentage of CD133⁺ cells rose with the increase in concentration of both PE-Cy5 and PE-Cy7 used. Whilst it appeared that the 7.5µL concentration provided the best fluorescence, a significant shift of the background fluorescence to the left was also noted and this is likely to

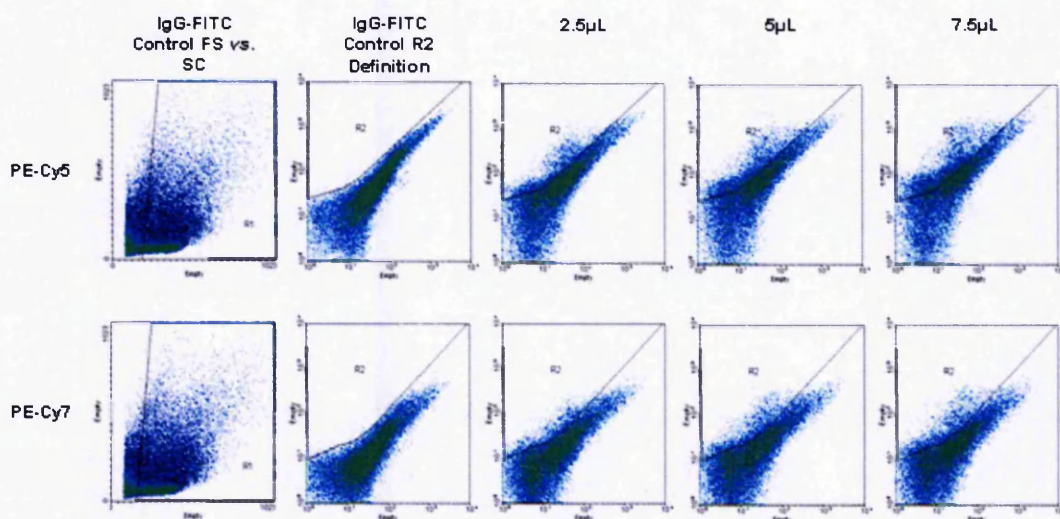


Figure 5.2: Relative fluorescence of secondary antibodies (PE-Cy5 and PE-Cy7) to CD133. Firstly, the IgG-FITC control was used to define the live cellular population (R1) by excluding the dead cells and debris to the left of a forward scatter (cell size, x) against side scatter (cell granularity, y) plot. For each of the PE-Cy5 concentrations, a plot of the FL-1 channel (FITC channel, x) against the FL-3 channel (PE-Cy5 filter, y) was created, again using the IgG-FITC control. This control identified the population R2 and thereby determined the control region without CD133 fluorescence. Prostate epithelial cells were then stained with CD133 and different amounts of conjugate antibody (PE-Cy5). In turn, the CD133⁺ve R2 was determined for each of the concentrations of PE-Cy5 (2.5µL, 5µL and 7.5µL). The filter on the FL-3 channel was then changed and the analysis repeated for the PE-Cy7 fluorescence.

Sample		CD133+ve R2 (%)
IgG-FITC Control		0.63
Strep-PE-Cy5	2.5µL	11.76
	5µL	16.33
	7.5µL	21.58
IgG-FITC Control		0.96
Strep-PE-Cy7	2.5µL	7.73
	5µL	10.76
	7.5µL	12.15

Table 5.3: Table showing the percentage of live epithelial cells residing in region R2 when the IgG-FITC control and three increasing amounts of the fluorochromes PE-Cy5 and PE-Cy7 conjugated to the CD133 secondary antibody were analysed.

have skewed the percentage of cells that were truly positive.

Furthermore, the percentage of CD133⁺ve cells was greater at all three concentrations when PE-Cy5 was used. However, again the degree of background appeared greater with significant contamination of the R2 gate with background fluorescence leaching into the bottom left of the gate (Figure 5.3).

Ultimately, CD133 staining appeared consistent and satisfactory.

Despite the improved percentage of fluorescence cells with increasing concentrations, it was not felt to be beneficial to change to either higher concentrations of PE-Cy7 or PE-Cy5. Instead it was decided that the original concentration of 5µL (a 1 in 40 dilution) PE-Cy7 should be maintained so as to maximise staining without inducing inaccuracies from significant background. It appears that the low levels of CD133 seen in the previous samples were accurate and that the distribution of CD133⁺ve cells between the SP and NSP should be the focus of investigation.

5.3 Identification of a CD133⁻ve/CD45⁻ve Hoechst^{lo} Subfraction of the SP

In the process of analysing the CD133⁺ve/CD45⁻ve FACS plots it became apparent that there was a subpopulation of cells that were present on the CD45⁻ve but not on the CD133⁺ve/CD45⁻ve Hoechst 33342 Red/Blue profiles. These were the cells with the lowest Hoechst 33342 concentration at the very distal tip of the SP tail (bottom left). These

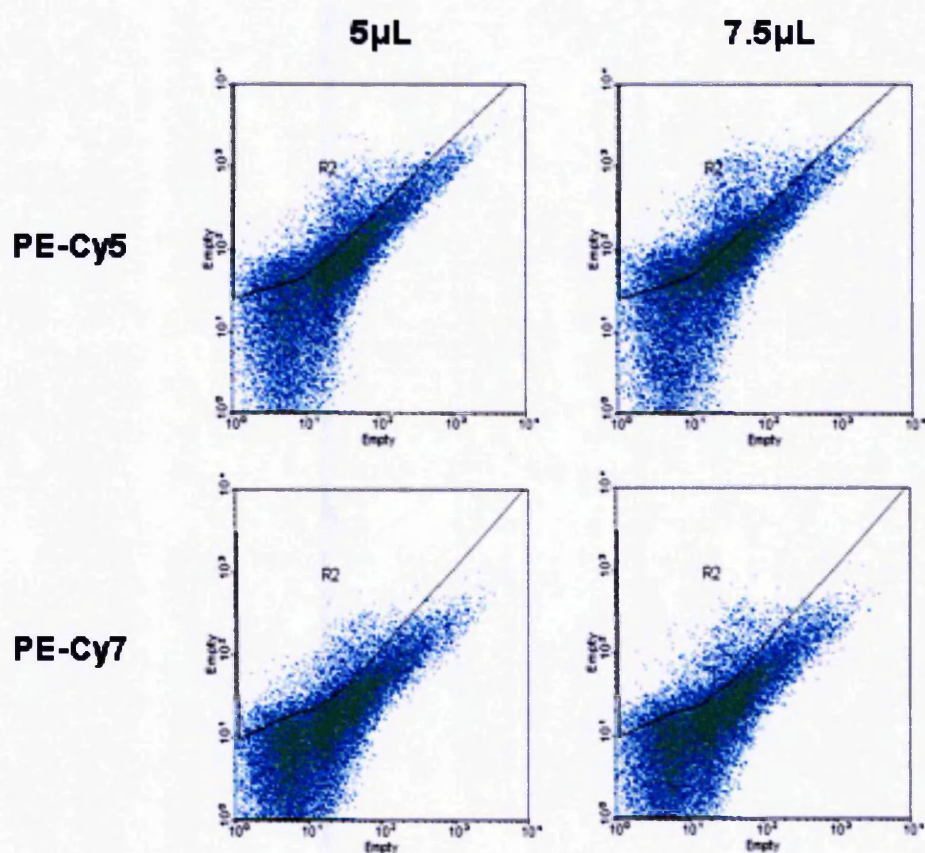


Figure 5.3: Density plots, already gated for live cells only (R1), of FL-1 (x-axis) vs. FL-3 (y-axis) for the 5μL and 7.5μL amounts of both PE-Cy5 and PE-Cy7. In these samples, region R2 gates those cells that have FL-3 (PE-Cy5 or PE-Cy7) fluorescence above the baseline defined by the IgG-FITC control shown in Figure 5.2.

could be isolated by the use of a CD133⁺ve/CD45⁻ve control (Figure 5.4) (Section 2.9).

Twenty two BPH and ten CaP samples were examined to determine the presence of a Hoechst 33342^{lo} CD133⁻ve/CD45⁻ve DSP. Two of the 22 BPH (9.1%) and six of the ten CaP (60%) could not be accurately analysed as the numbers of cells in the CD133⁺ve control was too low to allow accurate delineation of the DSP and PSP. From hereon, only the analysis of the 20 BPH and four CaP samples with an adequate CD133 control to delineate the DSP and PSP will be discussed.

The Winmidi analysis programme was limited by its ability to give percentages to only two decimal places. As a consequence, two of the 20 BPH (10%) and one of the four CaP (25%) samples that were suitable for examination, had a percentage for the DSP (R6) of less than 0.00%. The mean percentage of cells in the BPH DSP was 0.1155% SD± 0.18% (range 0 – 0.74%). The CaP DSP percentage was lower at 0.025% SD± 0.02% (range 0 – 0.06%) but this difference did not reach statistical significance (Student's unpaired *t*-test *p*=0.3549) (Table 5.4).

5.4 Enhanced Cell Number Yield Using the Hoechst 33342^{lo} DSP

Despite the DSP being a smaller region than the standard SP tail that had previously been used for functional analysis, a consistent observation was that the number of cells isolated when CD45⁻ve only selection was utilised was superior to the harvested numbers from the entire SP tail using CD133 selection (BPH CD133⁺ve SP mean 703.20,

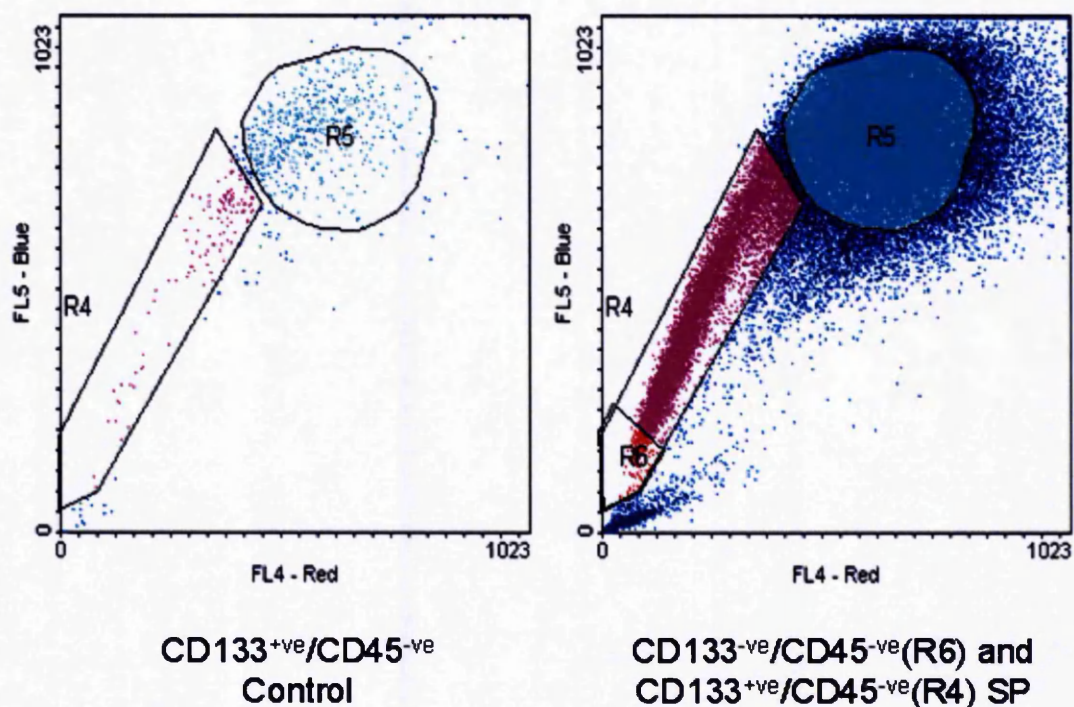


Figure 5.4: Dot plots of Hoechst 33342 Red/Blue prostate epithelial cell profiles with CD133⁺ve/CD45⁻ve (left) and CD45⁻ve only (right) selection, demonstrating the presence of a CD133⁻ve/CD45⁻ve subpopulation of the SP (R6). A CD133⁺ve/CD45⁻ve control (left) is used to define the lower left extent of the CD133⁺ve/CD45⁻ve SP tail and define the R6 gate which is subsequently used to sort cells purely on the basis of CD45⁻ve selection (right).

BPH		CaP	
Sample	R6 % Total	Sample	R6 % Total
15953	0.13	14937	0
16045	0.02	16322	0.03
16058	0.01	16366	0.01
16062	0.13	NC1GU15S1TaE	0.06
16087	0.01	AVERAGE	0.025
16132	0.4	SD	0.02
16144	0.74	Range	0 - 0.06
16162	0.01	Unpaired Student's <i>t</i>-test p=0.3549	
16163	0.01		
16273	0.13		
16295	0.04		
16316	0		
16328	0		
NC1GU5S1BaE	0.09		
NC1GU9S1BaE	0.02		
NC1GU19S1BaE	0.02		
NC1GU22S1BaE	0.4		
NC1GU23S1BaE	0.06		
NC1GU25S1BaE	0.05		
NC1GU56S1BaE	0.04		
AVERAGE	0.1155		
SD	0.18		
Range	0 - 0.74		

Table 5.4: Prostate epithelial cells were sorted by FACS into the live (R1), CD133⁺ve (R2) and CD45⁻ve (R3) Hoechst 33342 SP (R4) and NSP (R5). The CD133⁺ve cell furthest to the bottom left of the SP and consequently with the lowest Hoechst 33342 concentration was used to define gate R6 which subdivided the CD133⁻ve/low distal SP (DSP) from the remainder of the verapamil-sensitive SP, the proximal SP (PSP). The table is showing the percentage of cells in the DSP (R6) from both BPH and CaP patient samples. The Winmidi analysis software was only able to report values to two decimal places.

SD ± 635.25 cells Vs. BPH DSP mean 5540.91, SD ± 3949.84 cells ($p=0.0017$) and BPH PSP mean 27157.91, SD ± 31510.04 cells ($p=0.0206$) and CaP CD133⁺ SP mean 144.91, SD ± 173.37 cells Vs. CaP DSP mean 7029.55, SD ± 10107.29 cells ($p=0.0437$) and CaP PSP mean 22746.18, SD ± 28368.08 cells ($p=0.0204$)) (Table 5.5).

This improvement in the number of cells yielded was important as the required lower limit for entry to the cDNA conversion and amplification step of the NuGEN WT-Ovation Pico RNA amplification kit was 0.5ng of RNA (section 2.13.3). Chapter four details how the RNA quality had been enhanced. In an attempt to maximise the cell numbers yielded and therefore increase the quantity of RNA available for further analysis, it was decided to use CD45^{-ve} selection only and collect the DSP, PSP and NSP.

5.4.1.1 Primary Monolayer Cell Culture and Colony-Forming Ability

This initial attempt at monolayer cell culture investigated the functionality of the DSP and PSP. BPH samples were used as they were the most abundant in frozen storage. The number of sorted PSP cells was reduced so that they were equal to those from the DSP. Twenty-four well plates were used and cells were seeded at between 100 - 500 cells per well depending on the size of the sorted samples.

Ten samples were used for colony-forming assays and five samples were used for immunocytochemical validation of the CD133 status of the DSP and PSP. Cells were placed on microscope slides and stained for

Isolation Type	CD133+ve/CD45-ve Hoechst 33342 Dye Efflux Assay (SP/NSP)				CD45-ve Subfractionation Hoechst 33342 Dye Efflux Assay (DSP/PSP/NSP)					
Population	BPH SP	BPH NSP	CaP SP	CaP NSP	BPH DSP	BPH PSP	BPH NSP	CaP DSP	CaP PSP	CaP NSP
Cell Number Yielded	30	1000	33	1171	4000	24000	32000	29000	75000	97000
	350	960	7	311	6500	20650	3200	25000	72000	82000
	730	3000	36	778	793	700	1786	296	5052	3122
	650	4000	83	3676	3504	1000	18355	423	1370	7235
	1118	3500	582	669	577	6068	10000	7176	30233	31972
	49	1480	375	1450	10283	17713	86815	2212	6279	10000
	45	640	33	380	10033	61606	33873	146	430	1071
	2188	14700	110	1356	1978	4000	6224	63	198	1000
	704	1483	74	142	12390	110000	25000	12000	52000	90000
	1168	6392	30	102	2735	13000	4909	830	7000	22000
			231	5177	8157	40000	56941	179	646	2548
Mean Cell Number	703.20	3715.50	144.91	1382.91	5540.91	27157.91	23554.82	7029.55	22746.18	31631.64
SD	635.25	4035.71	173.37	1534.88	3949.84	31510.04	21133.67	10107.79	28368.08	36808.81
Range	30-2188	640-14700	7-582	102-5177	577-12390	700-11000	1786-66815	63-29000	198-75000	1000-97000
Student's t-test	BPH CD133+ve SP Vs. BPH DSP			p=0.0017	CaP CD133+ve SP Vs. CaP DSP			p=0.0437		
	BPH CD133+ve SP Vs. BPH PSP			p=0.0205	CaP CD133+ve SP Vs. CaP PSP			p=0.0204		
	BPH CD133+ve NSP Vs. BPH NSP			p=0.0120	CaP CD133+ve NSP Vs. CaP NSP			p=0.0173		

Table 5.5: Prostate epithelial cells were initially isolated by the Hoechst 33342 Dye Efflux Assay with additional CD133 selection into a side population (SP) and a non-SP (NSP). (A) The cell numbers yielded by FACS are shown for samples from patients with BPH and CaP. The mean, standard deviation (SD) and range are shown for each of the populations. (B) An alternative technique of subfractionating the SP into a CD133-^{ve/low} distal SP (DSP) and a proximal verapamil-sensitive SP (PSP) was then used and the cell numbers yielded by FACS are shown for comparison. An unpaired student's *t*-test was used to look for statistical significance between the various populations for each of the disease groups.

CD133 in a similar manner to that for the full panel of immunocytochemical markers (materials and methods section 2.11.4.1-2.11.4.3). The DSP expressed significantly lower amounts of CD133 (mean 16.76%, SD $\pm 4.86\%$, range 9.68 – 22.58% of cells) than the PSP (mean 77.17%, SD $\pm 8.42\%$, range 63.79 – 87.07% of cells) ($p=0.000023$) (Table 5.6).

Samples have been compared in two ways; firstly the proportion of wells that developed at least one colony and; secondly the total number of colonies that were formed by each population from a particular sample. The total number of wells seeded and the cell densities were matched for the DSP and PSP from each sample (Table 5.7). The percentage of wells that formed at least one colony was greater in the PSP than the DSP (mean PSP 26.44%, SD $\pm 32.14\%$ vs. mean DSP 11.33%, SD $\pm 18.95\%$ $p=0.24$). The total colony-forming efficiency (total number of colonies / total number of cells seeded) was also greater in the PSP though not to statistical significance (mean DSP 0.0011, SD ± 0.0021 vs. mean PSP 0.0068, SD ± 0.0123 $p=0.1886$) (Table 5.7). Four of the ten DSP samples and six of the ten PSP samples formed colonies. Apart from the sample GU56, all PSP samples yielded more colonies than their respective DSP. Excluding sample GU56 and including only those samples that formed colonies, the DSP colonies appeared at a mean of 11.33 days (SD ± 1.89 days) and reached the peak number of colonies by a mean of 18.33 days (SD ± 6.02 days) (Figure 5.5A). The PSP colonies appeared marginally earlier after 11.2 days (SD ± 3.43 days) and reached a peak

Sample	DSP			PSP		
	Total Cells	CD133+ve Cells	%	Total Cells	CD133+ve Cells	%
14990	96	20	20.83	62	42	67.74
15567	54	10	18.52	51	41	80.39
15630	62	6	9.68	58	37	63.79
15953	55	10	18.18	94	76	80.85
15958	65	7	10.77	116	101	87.07
15984	62	14	22.58	101	84	83.17
Mean Average	65.67	11.17	16.76	80.33	63.50	77.17
SD	14.13	4.71	4.86	24.43	24.68	8.42
Paired t-test	0.000023					

Table 5.6: Prostate epithelial cells from six BPH samples were sorted by FACS into the CD133^{-ve/low} Hoechst 33342^{low} CD45^{-ve} DSP and CD133^{+ve/hi} CD45^{-ve} PSP. The cells were collected and placed on poly-L-lysine coated slides before being formalin fixed and stained with CD133 primary and streptavidin 488nm Alexafluor secondary antibodies according to protocol. CD133^{+ve} cells from each of the populations were counted so as to validate the CD133 status of the DSP and PSP.

Sample	Cell Number Seeded per Well	DSP						PSP					
		Wells Seeded	Total Cell Number Seeded	Total Colony Number	Number of Wells with Colonies	Percentage of Wells with Colonies	Overall Colony-Forming Efficiency	Wells Seeded	Total Cell Number Seeded	Total Colony Number	Number of Wells with Colonies	Percentage of Wells with Colonies	Overall Colony-Forming Efficiency
15520	500	10	5000	0	0	0.00	0.0000	10	5000	0	0	0.00	0.0000
15953	100	10	1000	2	2	20.00	0.0020	10	1000	7	4	40.00	0.0070
15978	250	9	2250	0	0	0.00	0.0000	9	2250	90	8	88.89	0.0400
16062	200	8	1600	0	0	0.00	0.0000	8	1600	0	0	0.00	0.0000
16132	500	18	9000	1	1	5.56	0.0001	18	9000	4	3	16.67	0.0004
16144	500	11	5500	0	0	0.00	0.0000	11	5500	0	0	0.00	0.0000
16273	300	15	4500	10	4	26.67	0.0022	15	4500	80	12	80.00	0.0178
16295	200	15	3000	0	0	0.00	0.0000	15	3000	8	5	33.33	0.0027
G156	500	18	9000	62	11	61.11	0.0069	18	9000	1	1	5.56	0.0001
G158	500	19	9500	0	0	0.00	0.0000	19	9500	0	0	0.00	0.0000
Mean					1.80	11.33	0.0011			3.30	26.44	0.0068	
SD					3.31	18.95	0.0021			3.87	32.14	0.0123	
Student's <i>t</i> test Colony-Forming Efficiency DSP Vs. PSP <i>p</i> =0.1886													

Table 5.7: Table showing the colony forming ability of the DSP and PSP populations from ten BPH samples. The proportion of wells that developed at least one colony, the overall total number of colonies and the total colony forming efficiency (total number of colonies / total cell number seeded) are reported.

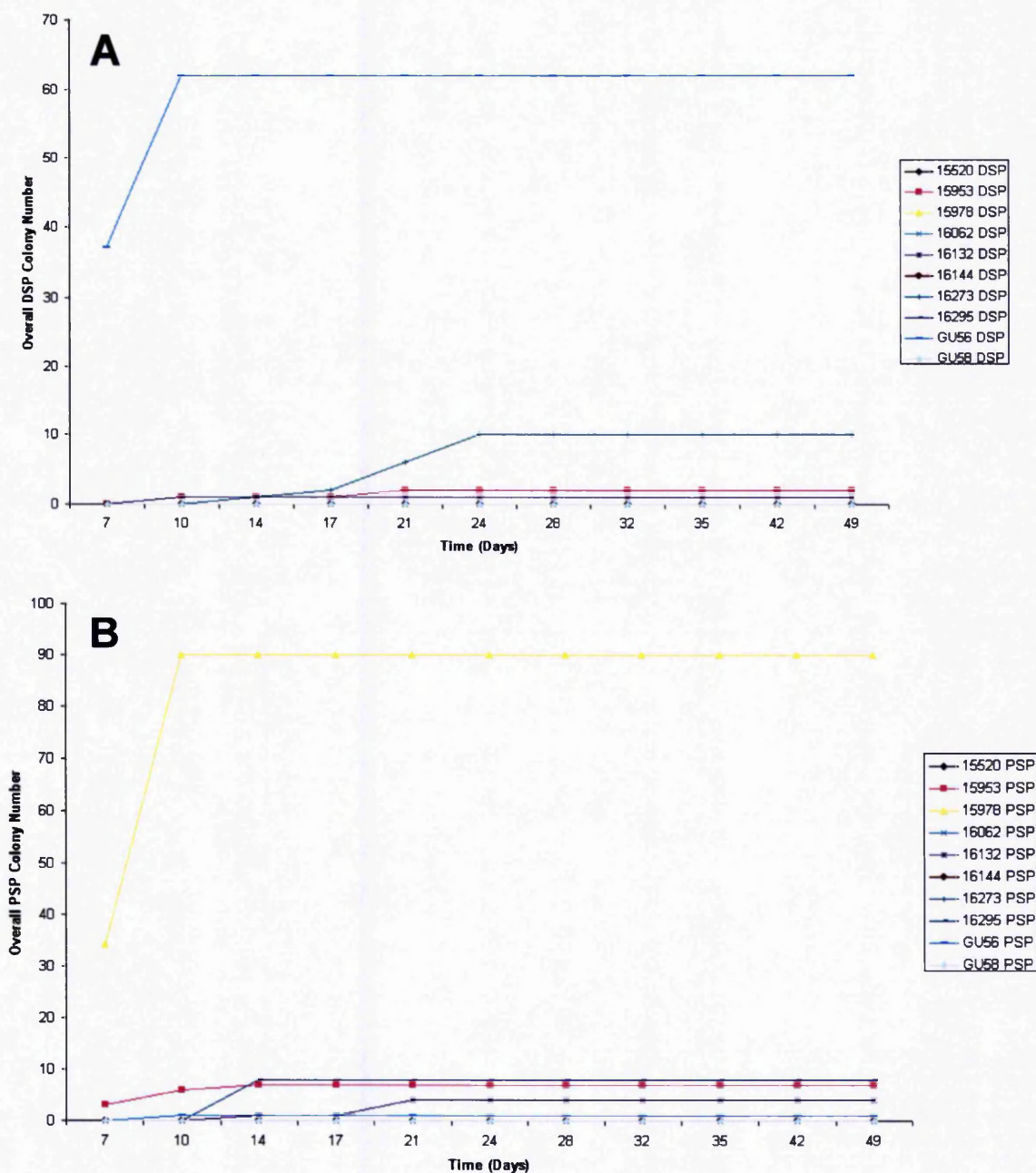


Figure 5.5: Graphs showing the number of colonies counted (y-axis) from both (Figure 5.5A) the DSP and (Figure 5.5B) the PSP at different time points (x-axis). The rate of colony formation is seen from the gradient of the lines. Once the line reaches a plateau the culture had either become confluent or failed to produce any further colonies. overall number of colonies for the DSP samples. Cultures were examined twice weekly for colonies.

number of colonies by a mean of 18.6 days (SD ± 5.64 days), despite developing a larger number of colonies (Figure 5.5B).

Seventeen PSP and eight DSP wells had sufficient cells for passaging and determination of proliferative capacity. However, only eight of the PSP and two of the DSP samples were successfully passaged. The time at which cells reached confluence and were passaged was sooner in the DSP (DSP mean 17 days, SD ± 3.0 days, range 14-20 days vs. PSP mean 22.5 days, SD ± 11.5 days, range 14-43 days). The degree of proliferation was calculated by dividing the number of cells counted after passage by the number of cells seeded. The degree of proliferation was nearly ten times greater in the PSP than the DSP (DSP 2.88 vs. PSP 20.44, $p=0.1365$) (Table 5.8). Fifty percent of the DSP and 37.5% of the PSP cultures died. None of the remaining cultures proliferated sufficiently to be passaged for a second time despite regular observation for two months.

A second attempt at determining colony-forming ability was made. In order that populations were more easily comparable and to maximise the chances of developing colonies, all the sorted cells from five BPH samples (GU59, GU61, GU62, GU72 and GU74) were placed in T₂₅ flasks again on a feeder layer (10^6 irradiated STO cells / flask) at equal cell densities for each DSP and PSP pair. In addition, the growth media was supplemented with 2% FCS.

The flasks from two of the samples succumbed to infection (GU62 and GU74). These two samples had yielded the lowest cell numbers at

Sample	Population	Seeded Cell Number	Day of Passage	Cell Count	Degree of Proliferation
GU56	DSP	230,000	14	550,000	2.39
15953	DSP	30,000	20	200,000	6.67
Average	DSP	130,000	17	375,000	2.88
SD			3		
16273	PSP	30,000	43	110,000	3.67
15978	PSP	50,000	14	800,000	16.00
15978	PSP	30,000	14	400,000	13.33
15978	PSP	20,000	14	750,000	37.50
15978	PSP	20,000	14	700,000	35.00
15978	PSP	20,000	38	150,000	7.50
15978	PSP	20,000	14	650,000	32.50
15978	PSP	10,000	29	180,000	18.00
Average	PSP	25,000	22.5	467,500	20.44
SD			11.5		
Student's t-test	Degree of Proliferation DSP Vs. PSP				p=0.1365

Table 5.8: Table showing the observed proliferation of the two DSP and eight PSP sample wells that successfully reached passage. The number of cells seeded originally, the number of days taken for confluence to be reached and the number of cells counted after passage are reported. The degree of proliferation was calculated by dividing the number of cells counted after passage by the number of cells originally seeded. The degree of proliferation observed was compared between the DSP and PSP populations.

FACS and were consequently seeded at the lowest densities. The colony formation in the remaining flasks was excellent and far improved on the previous attempt (Table 5.9). On this occasion the DSP formed significantly more colonies than the PSP (DSP mean 41.67 SD ± 22.29 colonies vs. PSP mean 21.33 SD ± 17.61 colonies, $p=0.026$). This equated to a mean DSP / PSP fold change of 2.612. In the first round of colony-forming ability experiments there were more colonies in the PSP and therefore a DSP / PSP fold change of 0.165 was observed. The colony-forming efficiency (total colonies / cells seeded) and number of cells per colony (cells seeded / total colonies) revealed enrichment for colony forming cells in the DSP (mean colony-forming efficiency DSP 0.014, SD ± 0.012 Vs. PSP 0.003, SD ± 0.001 ($p=0.2910$) and mean number of cells per colony DSP 132.0, SD ± 74.4 Vs. PSP 388.3, SD ± 138.7 ($p=0.1034$)(Table 5.10) (Figure 5.6).

All the flasks from GU59, GU61 and GU72 developed a confluent monolayer. The total number of colonies for each sample was the last number of colonies recorded before confluence was reached. It was therefore apparent that a smaller number of colonies were required to form a monolayer in the PSP than the DSP. Images of the entire flask taken at the same duration of culture (day 18) show that larger colonies appear to be evident in the PSP flasks and that the PSP colonies can actually be seen on these photomicrographs (Figures 5.7 and 5.8) whereas the colonies forming in the DSP flasks are more numerous but smaller and not clearly visible when the flask is viewed in its entirety (Figures 5.9 and 5.10). Enlarged images of the proliferating cells reveal

Sample	Population	Cell Number Seeded	Colony Number			
			DAY 7	DAY 12	DAY 16	DAY 19
GU59	CD133-ve DSP	15,500	0	38	64	73
GU59	CD133+ve PSP	15,500	0	27	45	46
GU61	CD133-ve DSP	3,467	0	7	15	23
GU61	CD133+ve PSP	3,467	0	4	6	6
GU62	CD133-ve DSP	954	0	Infected		
GU62	CD133+ve PSP	954	0	Infected		
GU72	CD133-ve DSP	3,000	0	12	25	29
GU72	CD133+ve PSP	3,000	0	7	12	12
GU74	CD133-ve DSP	500	0	0	0	Infected
GU74	CD133+ve PSP	500	0	0	0	Infected

Table 5.9: The CD133^{-ve/low} DSP and CD133^{+ve/hi} PSP for five BPH samples were isolated and collected by FACS. A second attempt at placing these cells into culture to determine their colony-forming ability was undertaken. The table shows the number of cells from each population seeded to T-25 flasks with an irradiated STO feeder layer and growth media supplemented with 2%FCS. The number of colonies observed was recorded for each of the flasks at day 7, 12, 16 and 19. The flasks were all confluent by day 19.

Sample	DSP	PSP	Fold Change DSP/PSP	Colony Forming Efficiency DSP	Colony Forming Efficiency PSP	Cells seeded/Colony DSP	Cells seeded/Colony PSP
GU59	73	46	1.587	0.005	0.003	212.3	337.0
GU61	23	6	3.833	0.007	0.002	160.7	577.8
GU72	29	12	2.417	0.030	0.004	32.9	250.0
Mean Average	41.67	21.33	2.612	0.074	0.003	132.0	388.3
SD	22.29	17.61	0.927	0.072	0.007	74.4	138.7
Student's t-test Number of Colonies DSP Vs PSP	p=0.026			Student's t-test Colony Forming Efficiency DSP Vs PSP	p=0.2910	Student's t-test Cells Seeded/Colony DSP Vs PSP	p=0.1034

Table 5.10: Table showing the number of colonies formed from the DSP and PSP of the three BPH samples that were not infected. The DSP/PSP fold change, the colony-forming efficiency (total colonies / cells seeded) and number of cells per colony (cells seeded / total colonies) for both the DSP and PSP are shown.

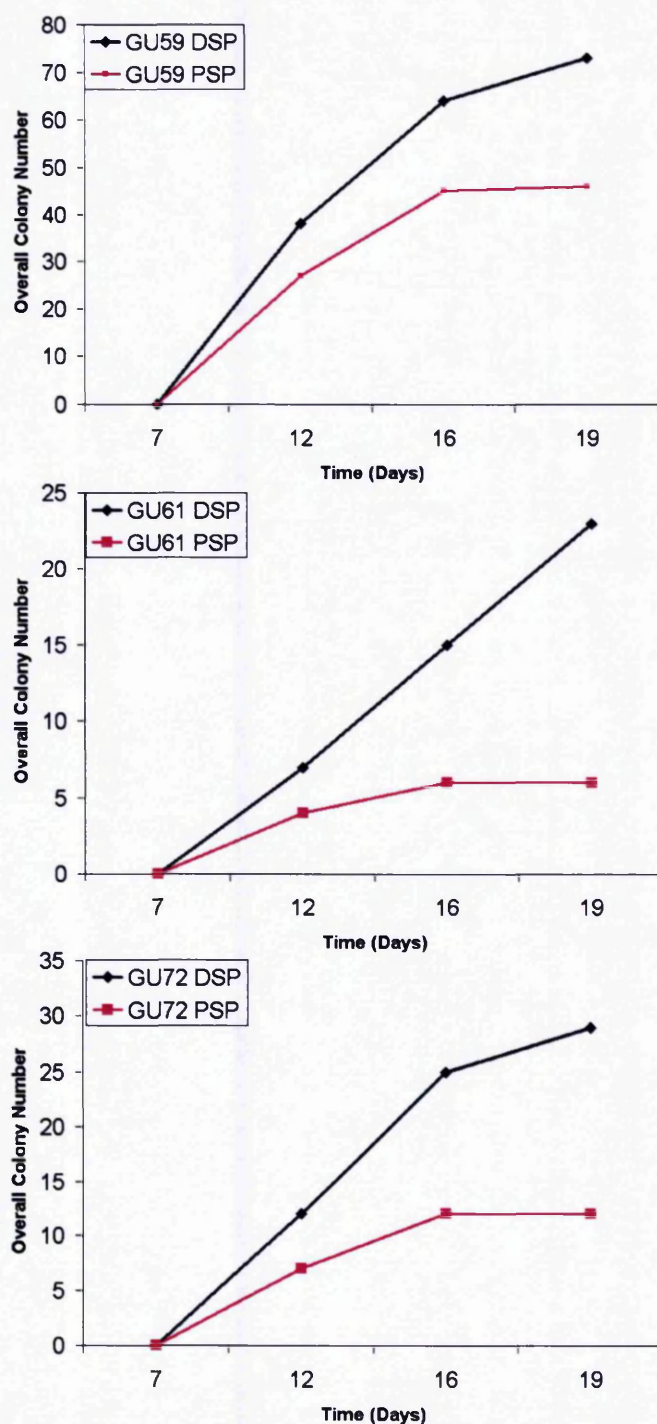


Figure 5.6: Graphs showing the number of colonies counted (y-axis) from both the DSP and the PSP at different time points (x-axis) during a second attempt at colony-forming assays using five different BPH samples. Two samples became infected and could not be analysed. The rate of colony formation is seen from the gradient of the lines. The final number of colonies depicted was equal to the number that had been required to reach confluence or replicative sterility. Cultures were examined twice weekly for colonies.

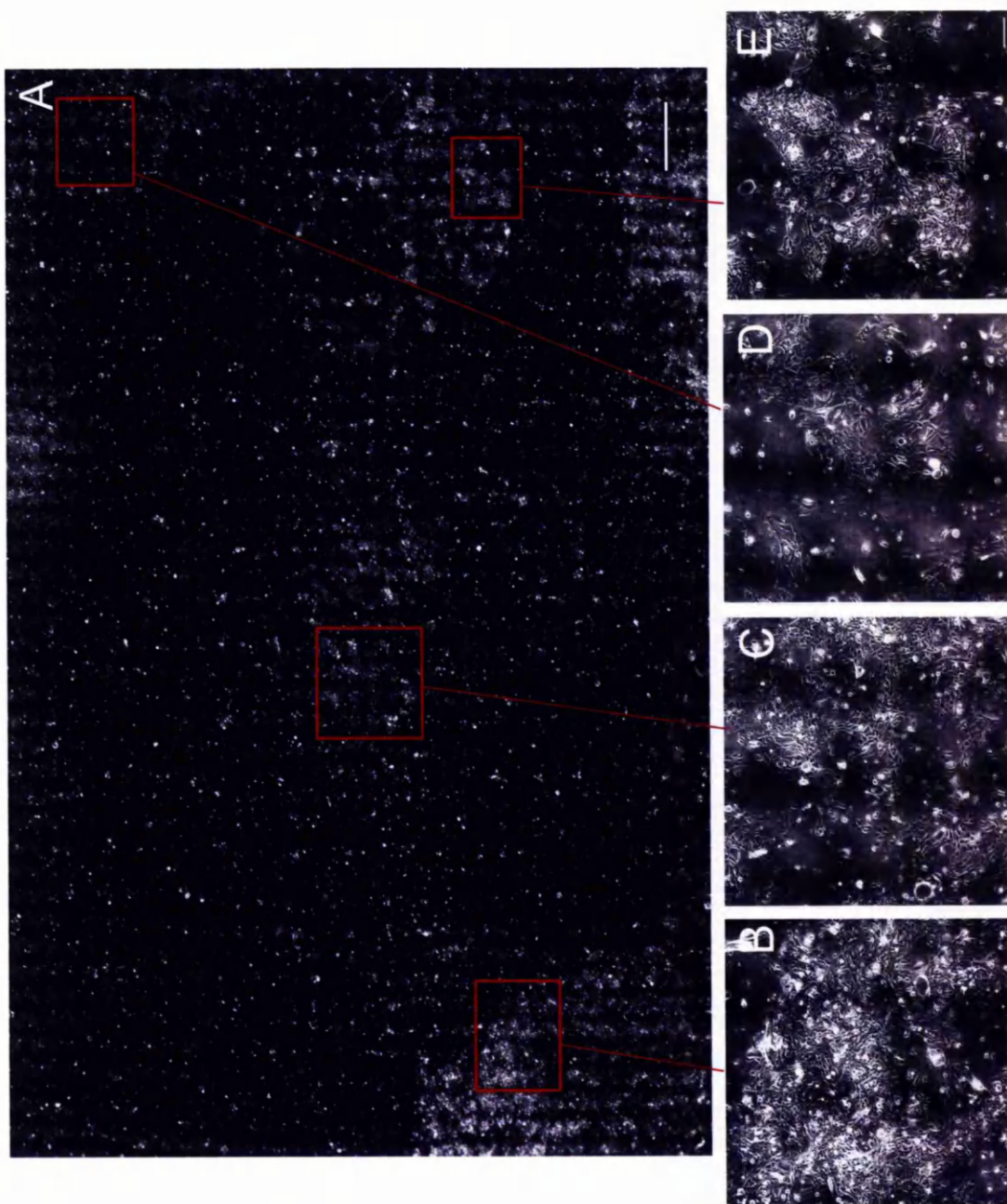


Figure 5.7: Photomicrograph of the entire T-25 flask containing the cultures for GU59 PSP (A). Representative areas have been enlarged to demonstrate improved detail (B-E). Due to slight inaccuracies in stage movement during the scanning process, areas of the flask that have not been photographed have been filled with a neutral colour. Total magnification $\times 100$. The scale bar in the bottom right corner of the whole flask image is $1500\mu\text{m}$ in length and those in the enlarged images are $150\mu\text{m}$ in length.

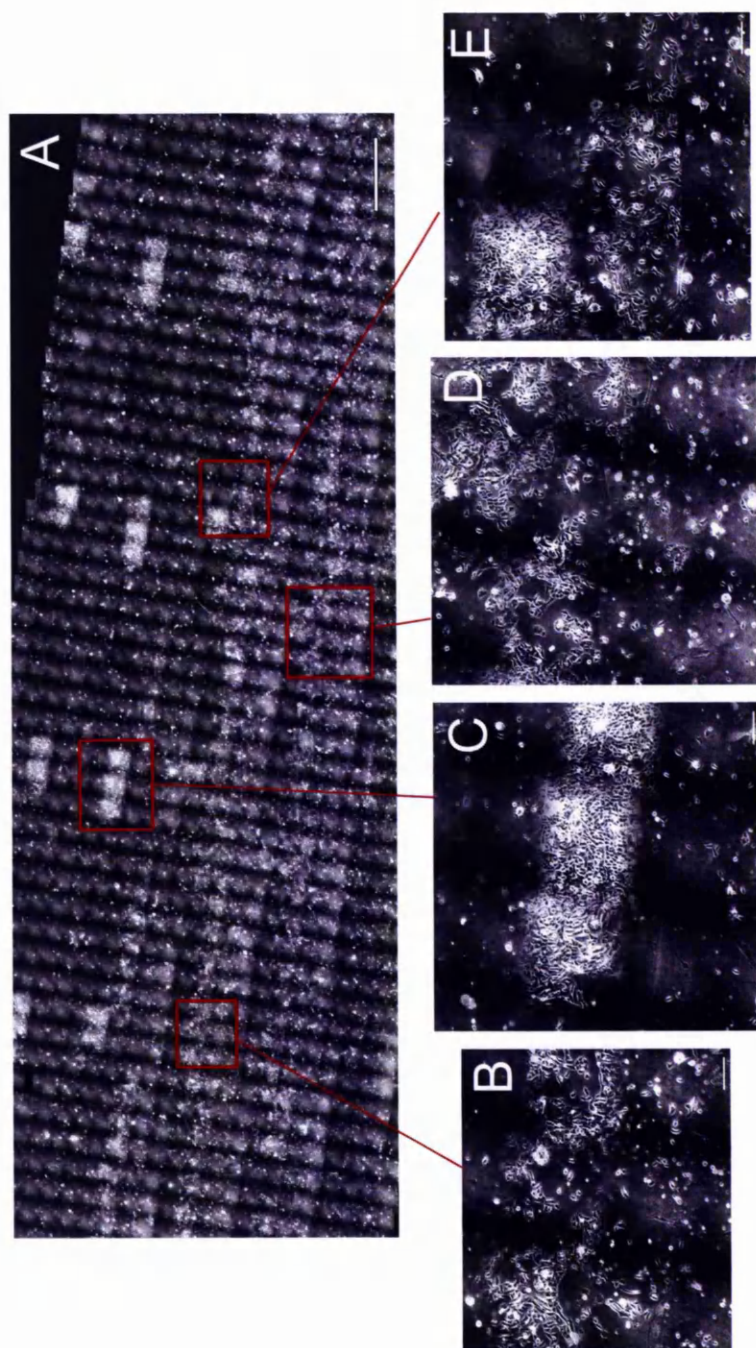


Figure 5.8: Photomicrograph of the entire T-25 flask containing the cultures for GU61 PSP (A). Representative areas have been enlarged to demonstrate improved detail (B-E). Due to slight inaccuracies in stage movement during the scanning process, areas of the flask that have not been photographed have been filled with a neutral colour. Total magnification x100. The scale bar in the bottom right corner of the whole flask image is 1500 μ m in length and those in the enlarged images are 150 μ m in length.

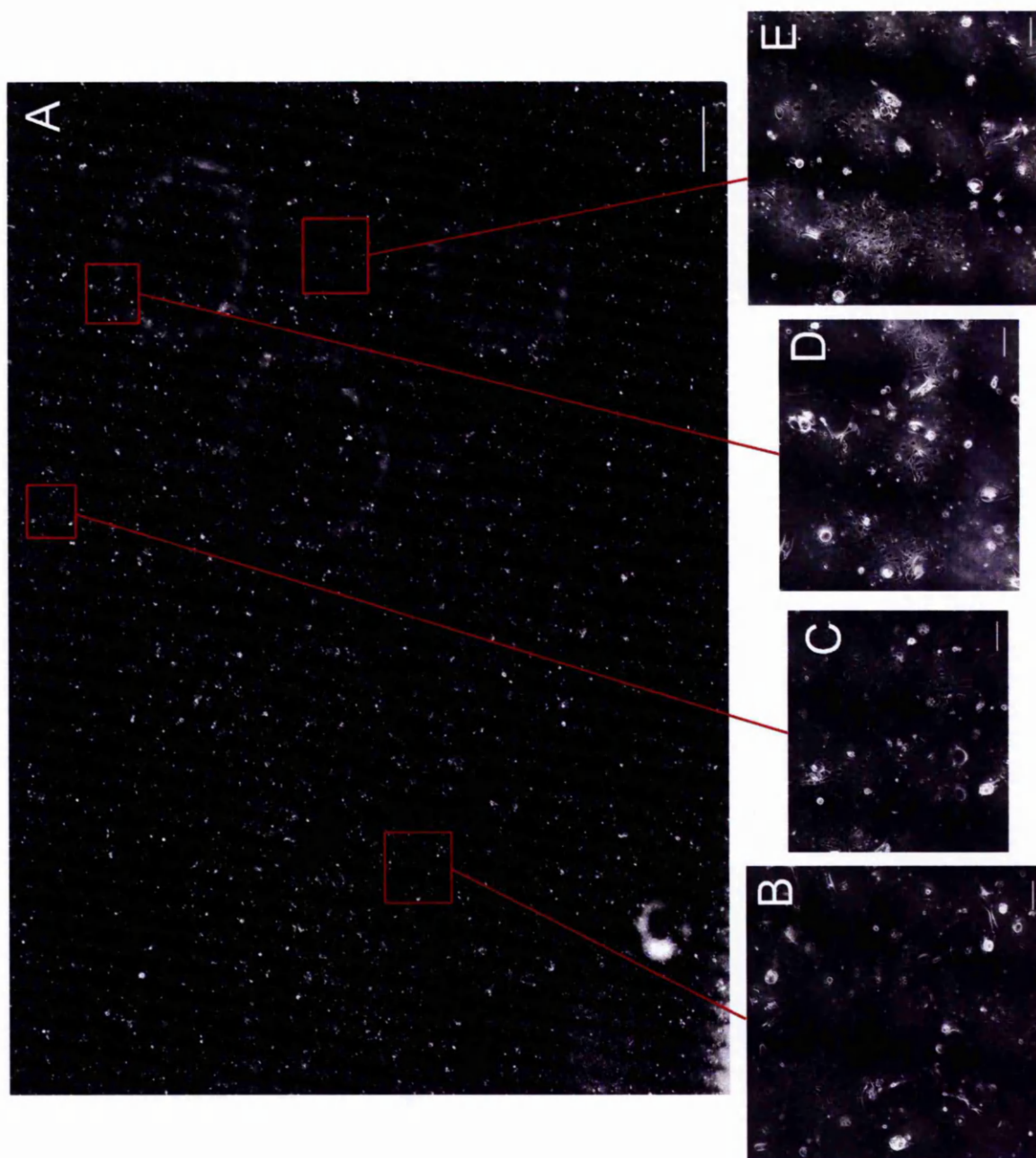


Figure 5.9: Photomicrograph of the entire T-25 flask containing the cultures for GU59 DSP (A). Representative areas have been enlarged to demonstrate improved detail (B-E). Due to slight inaccuracies in stage movement during the scanning process, areas of the flask that have not been photographed have been filled with a neutral colour. Total magnification x100. The scale bar in the bottom right corner of the whole flask image is 1500 μ m in length and those in the enlarged images are 150 μ m in length.

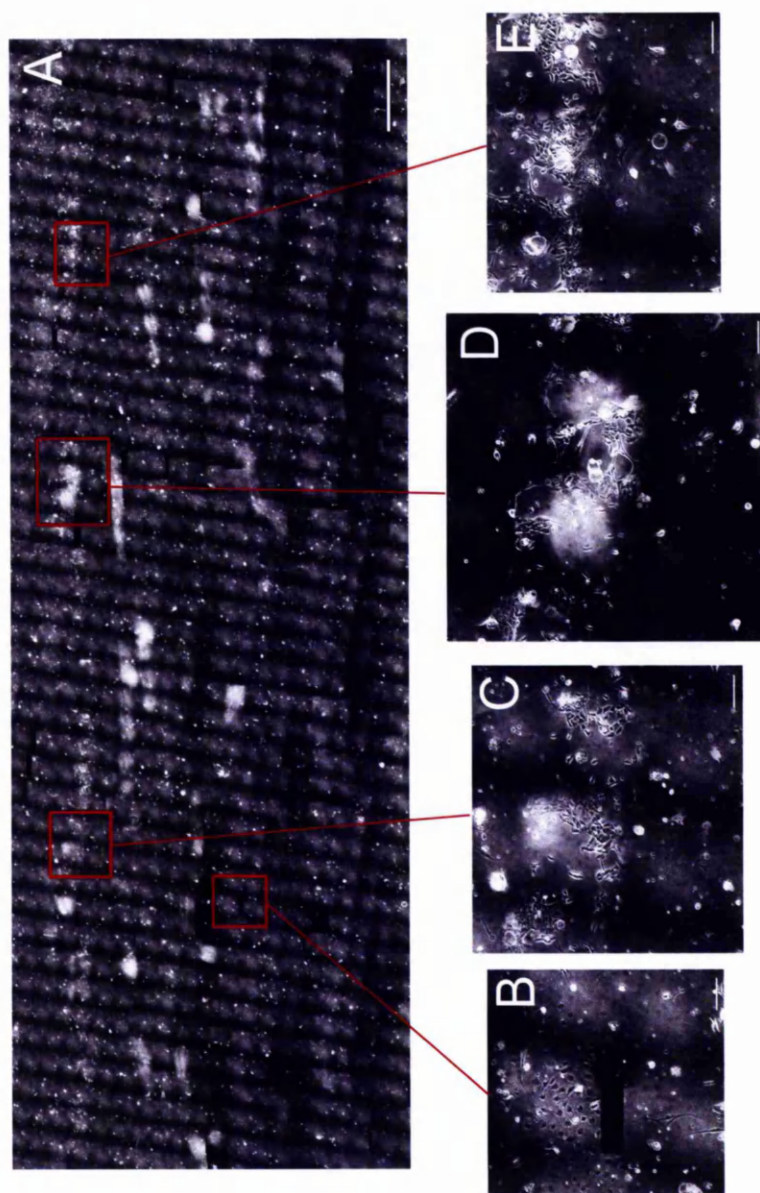


Figure 5.10: Photomicrograph of the entire T-25 flask containing the cultures for GU61 DSP (A). Representative areas have been enlarged to demonstrate improved detail (B-E). Due to slight inaccuracies in stage movement during the scanning process, areas of the flask that have not been photographed have been filled with a neutral colour. Total magnification $\times 100$. The scale bar in the bottom right corner of the whole flask image is $1500\mu\text{m}$ in length and those in the enlarged images are $150\mu\text{m}$ in length.

that the DSP colonies do appear smaller with a cluster of individual colonies appearing to coalesce to eventually form a monolayer. Examples of this are demonstrated on the enlarged images (Figure 5.9 B & C and Figure 5.10 C & E) with two or three small colonies visible within the same image. Enlarged images of the PSP colonies reveal larger colonies that appear to expand from their edges rather than being the product of a number of colonies coalescing (Figure 5.7 B and Figure 5.8 C).

All healthy cultures (GU59 DSP & PSP, GU61 DSP & PSP and GU72 DSP & PSP) were split one in three. Two thirds of the cells were re-analysed by flow cytometry (section 5.4.1.2). The remaining thirds were passaged into a fresh collagen-coated T₂₅ flask. Both the passaged DSP and PSP cells from sample GU72 failed to grow any further colonies. The remaining PSP samples seemed to proliferate quicker after being re-seeded and developed 500,000 (GU59) and 600,000 (GU61) cells by day 10. GU61 DSP failed to grow but GU59 DSP took longer and formed a monolayer of 400,000 cells by day 21. The three successful monolayers were again split one in three and one third of the cells were re-seeded to fresh collagen-coated T₂₅ flasks. None of the cells grew beyond one passage.

5.4.1.2 Repeat Flow Cytometric Analysis of Cultured Cells

On reaching a confluent monolayer for the first time, four of the samples (GU59 DSP, GU59 PSP, GU61 DSP and GU61 PSP) were analysed by flow cytometry according to the method described in section 2.11.3. The

aim was to determine the phenotype of the cells following culture in relation to their Hoechst 33342 red/blue profile and CD133 status. The name ascribed to these passaged samples relates to their original phenotypic profile after primary flow cytometry (ie CD133^{-ve/low} CD45^{-ve} DSP or CD133^{+ve/hi} CD45^{-ve} PSP).

By definition, the DSP populations were CD133^{-ve/low}. At primary FACS both GU59 and GU61 had 0.00% CD133^{+ve} cells in the DSP/ region R6. After passage, both cultures had evidence of CD133^{+ve} cells with 1.86% (GU59) and 0.35% (GU61) of the live epithelial cell populations being CD133^{+ve}. Re-analysis of the profiles after culture revealed the distribution of such cells to be predominantly in the PSP and NSP (Figure 5.11, Column F).

Following culture, a further attempt was made at DSP definition. A small fraction (0.02%) of live CD133^{+ve} cells was evident after the DSP had been defined in the GU61 PSP sample. This equated to one cell and is likely to be a consequence of the difficulty in defining gates with the small cell number observed. The remainder of the samples (GU59 DSP, GU59 PSP and GU61 DSP) were confirmed to have no CD133^{+ve} cells in their DSPs. By definition, this suggests the correct positioning of the DSP relative to the CD133^{+ve} PSP. The Verapamil control was shown to be effective in defining the Verapamil-sensitive SP tail with only low percentages of cells being detectable in the DSP and PSP regions (GU59 DSP 0.124%, GU59 PSP 0.02%, GU61 DSP 0.08% and GU61 PSP 0.05%).

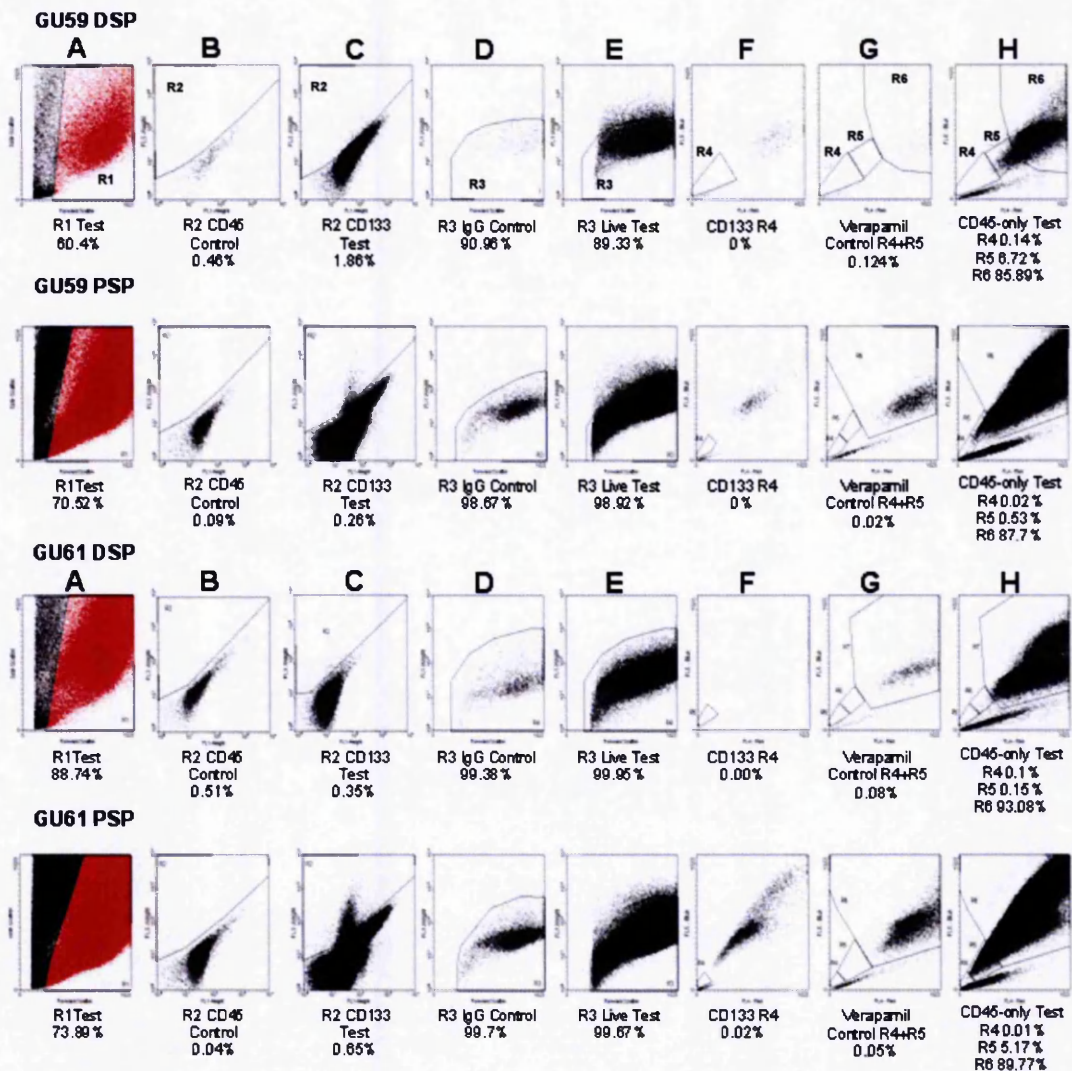


Figure 5.11: Flow cytometric analysis of passaged cells. The original phenotype of the population prior to culture is stated (GU59 DSP, GU59 PSP, GU61 DSP or GU61 PSP). Column A shows the plot of forward scatter versus side scatter and population R1 defines the live population of the test sample. Column B shows the plot of FL-1 (FITC) versus FL-3 (PE). Using a CD45 control sample, population R2 defines the control region for the CD133⁺ live population evident in column C when the test sample (incubated with CD133) is analysed. R3 defines the CD45⁻ population by using the IgG-FITC control sample (column D) and the test sample (column E) on a plot of forward scatter versus FL-1. Definition of the DSP required the use of the test sample (incubated with CD133) and plots of FL-4 (Hoechst red) versus FL-5 (Hoechst blue). The region R4 is defined as the SP tail inferior and to the left of the cell with the lowest Hoechst 33342 concentration (column F). The PSP (R5) equates to the remainder of the verapamil-sensitive tail (column G and H). The remainder of the sample is defined as the NSP (R6). The percentages for each of the populations gated on live cells are given.

When the DSP test samples were examined using selection for CD45^{-ve} cells only, a conserved CD133^{-ve/low} /CD45^{-ve} DSP equivalent to 0.14% (GU59 DSP) and 0.1% (GU61 DSP) of the total live CD45^{-ve} passaged epithelial cell populations was observed. The two DSP samples were shown to have a seven (GU59 DSP 0.14% Vs. GU59 PSP 0.02%) to ten-fold (GU61 DSP 0.1% Vs. GU61 PSP 0.01%) increase in the proportion of cells in the CD133^{-ve/low} DSP compared to either of the passaged PSP samples. Furthermore, this persistent DSP after passage is similar in size to that isolated at primary FACS (primary GU59 DSP 0.22% of live CD45^{-ve} population Vs. passaged GU59 DSP 0.14% and primary GU61 DSP 0.18% Vs. passaged GU61 DSP 0.1%).

The PSP samples had been placed into culture without cells from the DSP. Following passage, the PSP phenotype has been re-confirmed and notably, no significant numbers of cells occupying the DSP have subsequently been detected. The proportion of cells in the PSP of the test sample gated for CD45^{-ve} cells only was higher in GU59 DSP (6.72%) when compared with its corresponding GU59 PSP sample (0.53%) though this was not the case for sample GU61 (PSP in passaged GU61 DSP 0.15% Vs. passaged GU61 PSP 5.17%. Though none of the populations isolated by primary FACS and placed into culture had cells from the DSP, the main populations in all four samples after culture were the DSP (GU59 DSP 85.89%, GU59 PSP 87.7%, GU61 DSP 93.08% and GU61 PSP 89.77%).

5.5 Determination of the Immunocytochemical Phenotype of the DSP and PSP

Four BPH samples (GU9, GU22, GU23 and GU25) were used to determine the immunocytochemical profile of the DSP and PSP. All cells were formalin fixed without antigen retrieval and permeabilised (Table 5.11). The quality of observed staining was poor and it was felt this may have been related to cross-linking secondary to the process of formalin fixation. Furthermore, not all markers needed permeabilisation and as a consequence staining for membranous antibodies may have been compromised. It was decided to repeat the experiment with an unfractionated BPH sample (16062) to determine what preparation technique provided the optimal staining for each antibody (section 2.11.4.4). The optimal staining protocol for each antibody is described in table 5.12.

After optimisation of the technique, the DSP and PSP were isolated by FACS from a further four BPH samples (GU27, GU38, GU54 and GU57). Significantly lower levels of CD133 expression in the DSP compared to the PSP were again confirmed (mean DSP 4.02%, SD $\pm 2.63\%$ vs. PSP 28.87%, SD $\pm 5.91\%$, $p=0.00208$) (Figure 5.12).

The percentage of fluorescent cells for each of the antibodies was recorded (Table 5.13). Compared with the PSP, the DSP was significantly enriched for Beta Catenin (mean DSP 64.3%, SD $\pm 3.58\%$ vs. PSP 48%, SD $\pm 4.49\%$ $p=0.024$), p27 (mean DSP 60.19%, SD $\pm 17.57\%$ vs. PSP 30.31%, SD $\pm 3.63\%$, $p=0.04$) and Notch 1 (mean DSP

Samples	Cell Number Isolated	Cells Seeded Per Well
GU23 DSP	7979	400
GU23 PSP	57974	2900
GU25 DSP	4557	225
GU25 PSP	38354	1900
GU9 DSP	1056	50
GU9 PSP	18156	900
GU22 DSP	3142	155
GU22 PSP	4277	210

Table 5.11: Cell numbers isolated and seeded from the DSP and PSP of four samples (GU23, GU25, GU9 and GU22) for the initial attempt at the immunocytochemical assessment.

Antibody	Antigen-Retrieval Required?	Permeabilisation Required?
Beta Catenin	Y	Y
Cleaved Notch	Y	Y/N
Musashi-1	Y	Y
Notch-1	Y	N
SHH	Y	Y
p21	Y	Y
p27	Y	Y
p63	Y	Y
CK5	Y	Y/N
CK8	Y	Y/N
PSA	Y	Y
AR	Y	Y/N
CD133	Y/N	N
c-myc	Y	Y

Table 5.12: Results of the staining optimisation pilot study determined whether antigen retrieval and permeabilisation of the cells was required for each of the antibodies in the immunocytochemical panel. The staining with some antibodies was equivocal with or without performing a specific technique (denoted by Y/N).

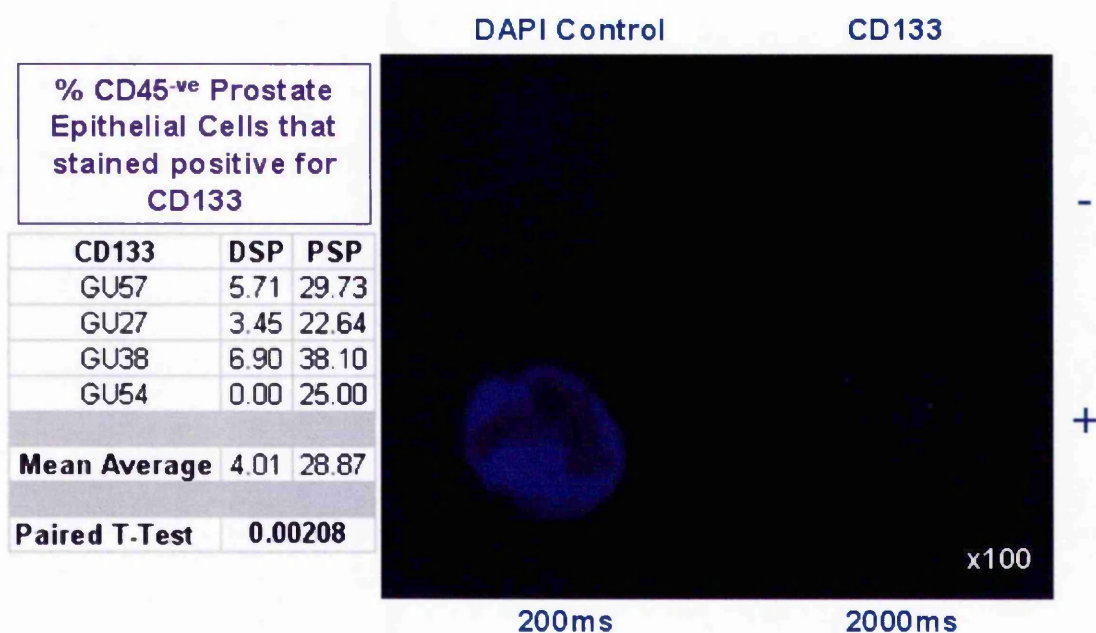


Figure 5.12: Representative images depicting differential CD133 expression. A DAPI control image is shown at 200ms exposure. Examples of both CD133^{ve} and CD133^{-ve} cells are shown at 2000ms exposure. The proportion of cells that were CD133^{ve} in each the two CD45^{ve} prostate epithelial cell populations (DSP and PSP) are shown in tabular format. All images are at x100 magnification.

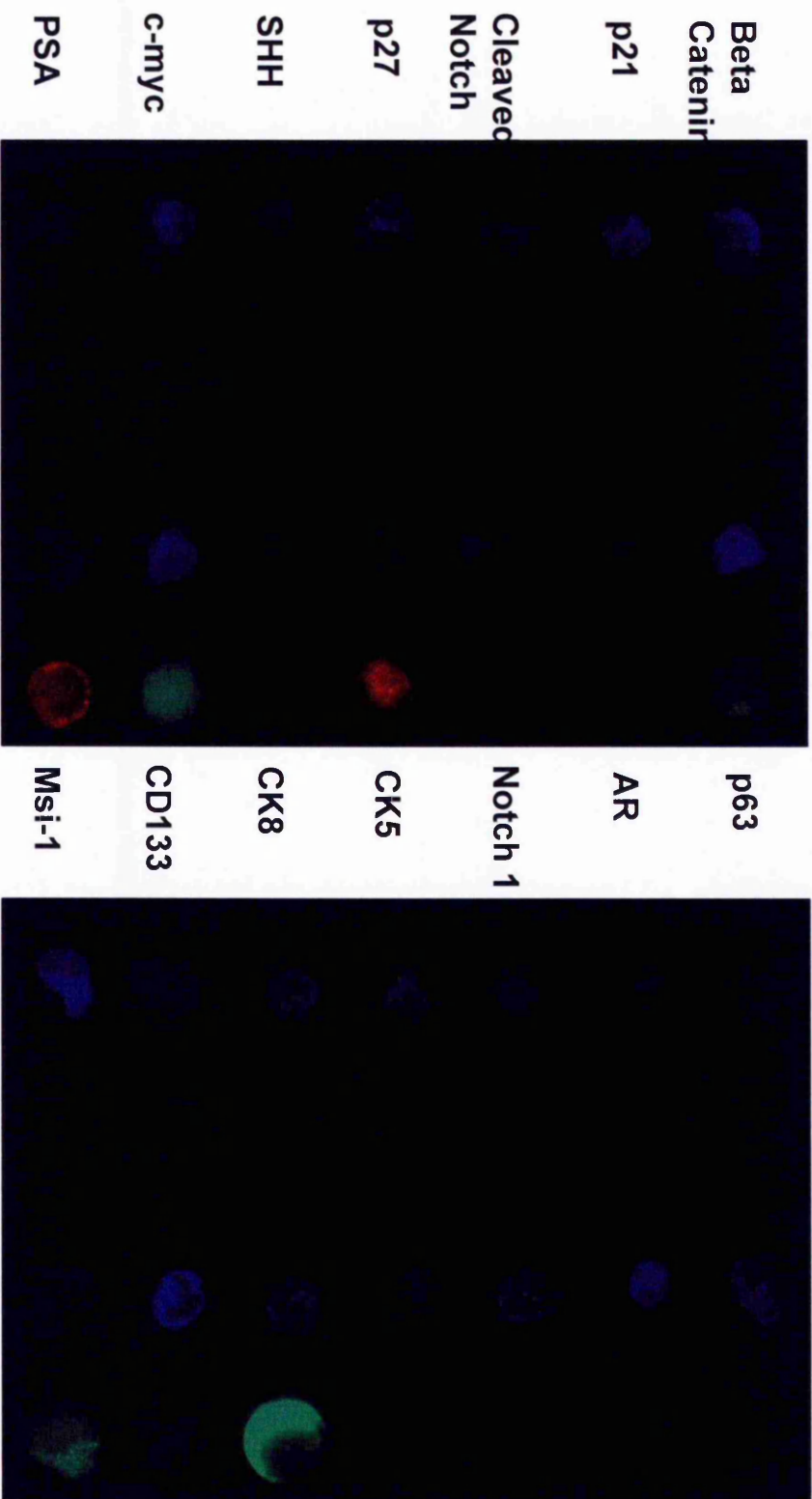


Figure 5.13: Images representative of the observed staining for the lineage-specific and putative stem cell immunocytochemical markers. For each primary antibody, a cell deemed to be negative for expression of the marker is shown as a control, having been taken at the same exposure time as the cell deemed to be positive for expression. DAPI controls for each image are shown. All images are taken at x100 magnification.

10.54%, SD \pm 2.75% vs. PSP 3.46%, SD \pm 0.94, $p=0.042$). In addition to CD133, several markers exhibited significantly lower levels of expression in the DSP compared with the PSP. These were PSA (mean DSP 16.76%, SD \pm 6.49% vs. PSP 30.67%, SD \pm 10.87%, $p=0.042$), p63 (mean DSP 0.81%, SD \pm 1.4% vs. PSP 18.53%, SD \pm 3.15%, $p=0.001$) and CK8 (mean DSP 11.64%, SD \pm 9.65% vs. PSP 39.77%, SD \pm 9.21%, $p=0.005$). There was a trend towards DSP enrichment of p21 (mean DSP 15.07%, SD \pm 7.82% vs. PSP 6.92%, SD \pm 2.58%, $p=0.149$) and cleaved notch (mean DSP 50.78%, SD \pm 15.62% vs. PSP 35.64%, SD \pm 7.28%, $p=0.077$) though these did not reach statistical significance. SHH also appeared to be expressed to a higher extent in the DSP of three out of four samples but the expression in GU54 PSP was considerably higher (mean DSP 10.46%, SD \pm 4.59% vs. PSP 20.74%, SD \pm 26.56%, $p=0.536$). No specific pattern was seen to the levels of expression of Musashi-1, CK5 and c-myc. The staining for androgen receptor was unclear (Figure 5.13).

5.6 Summary of Chapter Results

Additional CD133 selection during the Hoechst dye efflux assay has been shown to reduce the number of cells yielded, particularly from CaP samples. The distribution of CD133⁺ cells between the SP and NSP shows that the marker is by no means exclusive to the SP and indeed significantly more CD133⁺ cells are seen in the NSP compared to the SP in both BPH and CaP samples.

Antibody	DSP	PSP	t-Test	Antibody	DSP	PSP	t-Test
Beta Catenin	62.50	44.44	0.024	p63	0.00	19.05	0.001
	69.70	43.18			3.23	21.74	
	65.00	54.39			0.00	13.33	
	60.00	50.00			0.00	20.00	
Mean Average	64.30	48.00		Mean Average	0.81	18.53	
SD	3.58	4.49		SD	1.40	3.15	
p21	25.00	5.56	0.149	AR	0.00	0.00	0.391
	20.00	11.36			0.00	0.00	
	5.26	5.77			4.26	7.14	
	10.00	5.00			0.00	0.00	
Mean Average	15.07	6.92		Mean Average	1.07	1.79	
SD	7.82	2.58		SD	1.84	3.09	
Cleaved Notch	43.75	35.00	0.077	Notch 1	11.76	3.03	0.042
	77.42	45.45			14.29	2.17	
	44.44	37.10			9.09	4.65	
	37.50	25.00			7.00	4.00	
Mean Average	50.78	35.64		Mean Average	10.54	3.46	
SD	15.62	7.28		SD	2.75	0.94	
p27	30.00	25.00	0.040	CK5	17.86	20.97	0.271
	71.88	32.81			28.13	30.95	
	72.22	29.03			20.59	18.92	
	66.67	34.38			18.18	33.33	
Mean Average	60.19	30.31		Mean Average	21.19	26.04	
SD	17.57	3.63		SD	4.14	6.20	
SHH	5.88	5.26	0.536	CK8	11.54	39.02	0.005
	6.45	3.33			26.67	48.00	
	17.02	7.69			0.00	25.00	
	12.50	66.67			8.33	47.06	
Mean Average	10.46	20.74		Mean Average	11.64	39.77	
SD	4.59	26.56		SD	9.65	9.21	
c-myc	4.35	5.88	0.697	CD133	5.71	29.73	0.002
	7.89	5.26			3.45	22.64	
	2.08	2.27			6.90	38.10	
	11.11	10.53			0.00	25.00	
Mean Average	6.36	5.99		Mean Average	4.02	28.87	
SD	3.44	2.96		SD	2.63	5.91	
PSA	18.18	34.78	0.042	Musashi-1	3.03	4.35	0.642
	26.67	40.91			0.00	3.03	
	9.68	12.36			3.23	2.22	
	12.50	34.62			12.50	3.85	
Mean Average	16.76	30.67		Mean Average	4.69	3.36	
SD	6.49	10.87		SD	4.69	0.81	

Table 5.13: Differential expression of a panel of lineage-specific and putative stem cell markers between the DSP and PSP isolated from four CD45^{ve} BPH samples. For each antibody the percentage of cells staining positive for that marker are shown for each of the four samples. The mean is then reported with the standard deviation (SD) and statistical significance is determined by a paired t-test ($p < 0.05$).

A CD133^{low} subfraction of the SP tail (DSP) with the lowest Hoechst 33342 concentration has been demonstrated to comprise 0.1155% of the total live BPH population and 0.025% of the total live CaP population. Once a CD133 control sample had been used to define this CD133^{low} DSP, the remainder of the Verapamil-sensitive SP (PSP) and the main body of the sample (NSP), CD45^{-ve} only selection was used to isolate cells from each of the regions. This enhanced the cell numbers yielded and therefore addressed the previous problems of low cell number and maximised the RNA available for further processing of samples for microarray analysis.

The DSP was shown to possess significant enhancement for colony-forming ability compared to the PSP when growth media supplemented with 2% FCS was used. Though not to significance, the reverse was true when standard growth media was used in that the colony forming ability of the PSP was superior to the DSP. PSP colonies grown in supplemented growth media appeared to grow quicker and produce a greater number of cells than the DSP. Particularly when growth media was used without supplementary serum, the number of colonies that formed was relatively low and many wells failed to grow any colonies at all.

FACS analysis of disaggregated monolayers cultured from primary DSP cells suggested the persistence of a CD133^{low} DSP. Repeat FACS analysis of the cultured DSP showed that the phenotype of cells with respect to their Hoechst 33342 dye efflux ability had changed after

culture, with cells that were originally confined to the DSP producing progeny that subsequently appeared in either the PSP or NSP on flow cytometry plots. Furthermore, the DSP had previously been selected on the basis of its CD133^{-ve/low} phenotype but following culture increased levels of CD133^{+ve} cells were evident.

The DSP was demonstrated to be significantly enriched for cells expressing the putative SC markers Beta Catenin and Notch 1 and the lineage-specific marker p27 whilst also expressing significantly lower levels of the phenotypic markers CD133, PSA, p63 and CK8.

Chapter 6: Analysis of the Affymetrix® Microarray Data for the CD45^{-ve} DSP, PSP and NSP Isolated from Normal, Benign Prostatic Hyperplasia and Carcinoma of the Prostate Samples

6.1 Sample Identification

Following the methods described in section 2.5, the epithelial cell fractions of ten normal, 11 BPH and 11 CaP samples were isolated. It was preferable that the samples were processed immediately after receiving them from the operating theatre though some were used after being in liquid nitrogen storage. In light of the results detailed in chapter five and in particular the demonstration of a CD133^{low}/CD45^{-ve}/Hoechst 33342^{low} DSP, it was decided to collect three populations for each patient sample (the DSP, PSP and NSP) (section 2.9) rather than the CD133^{+ve}/CD45^{-ve} Hoechst 33342 SP and a CD133^{+ve}/CD45^{-ve} Hoechst 33342 NSP that had been studied during the initial round of arrays reported in chapter three.

RNA was extracted (section 2.13.1) and again the Agilent Bioanalyzer 2100 used the RNA 6000 Pico LabChip® Kit to provide data on the quantity and quality of RNA extracted (section 2.13.2) (Table 6.1, 6.2 and 6.3). Ideally a total of 0.5ng RNA was required for entry into the cDNA amplification step and initially five normal (GU39, GU33, 15992, 16668, 14812), two BPH (GU87, GU84) and four CaP (GU32, 16355, 16189, 15457) samples were deemed to have provided a sufficient amount of quality RNA to proceed (Table 6.4). The cDNA yields for these samples were excellent and it was felt that the samples with a

Patient	Sample type	Cell Number	Agilent (After concentration to 5uL)		
			RNA Concentration (pg/uL)	rRNA Ratio (28S/18S)	RIN
14865	DSP	4000	60	0	1
	PSP	24000	525	1.5	8.4
	NSP	32000	1475	1.4	7
15991	DSP	6500	112	1.4	6.8
	PSP	20650	715	1.4	8.1
	NSP	3200	1932	1.1	7.6
GU63	DSP	793	185	1	6.4
	PSP	700	58	0	1
	NSP	1786	78	0	1
GU64	DSP	3504	69	0	1
	PSP	10000	474	2.2	7.5
	NSP	18355	633	2.1	6.7
GU65	DSP	577	69	0	1
	PSP	6088	115	1.5	6.5
	NSP	10000	456	1.1	6.5
GU68	DSP	10283	628	1.5	8.4
	PSP	17713	80	0	1
	NSP	66815	5254	1.4	8.9
GU72	DSP	10033	50	0	1
	PSP	61,606	480	1.5	7
	NSP	33,873	49	0	1
GU74	DSP	1978	33	0	1
	PSP	4000	165	0	1
	NSP	6224	261	0	2.3
GU84	DSP	12390	779	1.6	9.1
	PSP	110000	46561	0.9	8.2
	NSP	25000	978	2.2	9.3
GU85	DSP	2735	391	1.6	9.1
	PSP	13000	811	1.2	6.7
	NSP	4909	70	1.6	8.5
GU87	DSP	8157	187.5	1.5	8.8
	PSP	40000	3550	1.6	8.8
	NSP	56941	2975	1.4	8.4

*

*

*

*

*

*

Table 6.2: m RNA recovery details for the 11 BPH samples isolated by FACS into a DSP, PSP and NSP. For each population the cell number, RNA concentration (pg/ μ L), RIN and 28S/18S ratio are reported. Those samples ultimately deemed suitable for further analysis are marked with an asterix.

Patient	Sample type	Cell Number	Agilent (After concentration to 5uL)			
			RNA Concentration (pg/uL)	rRNA Ratio (28S/18S)	RIN	
GU32	DSP	29000	1775	1.5	6.6	*
Manipulated	PSP1	75000	11693	0.7	6.7	
T3bN1M1B	PSP2	75000	600	1.1	7.3	
4+4 50% PSA 79	NSP1	97000	4011	1.2	6.3	
	NSP2	97000	3241	1	6.1	
16355	DSP	25000	1179	1.1	7.2	*
Testosterone Failure	PSP	72000	2954	1.1	7.3	
T3aNxM1	NSP	82000	2540	1.4	7.3	
4+5 70% PSA 72						
GU28	DSP	296	39	0	1	*
HRPC	PSP	5052	39	0	1.1	
T1cNxM0	NSP	3122	234	1.1	7.5	
5+4 40% PSA 69						
15035	DSP	423	44	0	1	
Primary	PSP	1370	17	0	1	
T3NxMx	NSP	7235	413	1.7	8.2	
5+4 90% PSA 115						
15457	DSP	7176	135	2	8.6	
Primary	PSP	30233	594	1.2	8.6	*
T3NxM1	NSP	31972	1438	1.6	8.1	
4+4 60% PSA 19						
16143	DSP	2212	16	0	1	*
Primary	PSP	6279	255	1.5	8.5	
T2cNxM0	NSP	10000	166	1.8	8.4	
4+4 50% PSA 14						
15371	DSP	146	33	0	1	
Primary	PSP	430	56	0	1	
T1cNxM0	NSP	1071	31	0	1	
4+3 70% PSA 23						
14836	DSP	63	13	0	1	
0.8	PSP	198	15	0	1	
	NSP	1000	32	0	1	
16189	DSP	12000	148	1.8	7.7	
Primary	PSP	52000	487	1	7.8	*
T2cNxM0	NSP	90000	1272	0.9	7	
3+4+5 40% PSA 40						
15937	DSP	830	24	0	1	
Primary	PSP	7000	152	1	7	
T1bNxMx	NSP	22000	413	1.4	7.4	
PSA 400						
GU30	DSP	179	45	0	1	
HRPC	PSP	646	129	0	N/A	
T4NDM1B	NSP	2548	90	0	5.9	
4+3 15% PSA 62						

Table 6.3: mRNA recovery details for the 11 CaP samples isolated by FACS into a DSP, PSP and NSP. For each population the cell number, RNA concentration (pg/ μ L), RIN and 28S/18S ratio are reported. Those samples ultimately deemed suitable for further analysis are marked with an asterix. Brief clinical details are detailed including stage, treatment received, Gleason score, serum PSA (μ g/l) and the percentage of tissue involved with malignancy scored by an independent pathologist.

Normal																		
Sample	DSP						PSP						NSP					
	PICR name	Conc. ng/ul	yield ng	RIN	cDNA yield ug	% present	PICR name	Conc. ng/ul	yield ng	RIN	cDNA yield ug	% present	PICR name	Conc. ng/ul	yield ng	RIN	cDNA yield ug	% present
GU39	MB(2)19	0.169	0.68	8.6	7.6	51	MB(2)31	3.836	15.3	8.7	7.4	51.8	MB(2)37	2.036	8.1	8.2	8	56.9
GU33	MB(2)65	0.0325	0.13	N/A	8.1	46.7	MB(2)68	0.135	0.54	8.1	9.7	58.3	MB(2)69	0.598	2.39	7.9	8.6	56.9
GU14	MB(2)73	0.0275	0.11	1	6.4	32.1	MB(2)74	0.13	0.52	7.3	8.7	48.2	MB(2)75	0.1175	0.47	7.6	9.1	54.1
GU13	MB(2)61	0.051	0.21	1	4.1	23.7	MB(2)62	0.115	0.46	7.7	7.2	46.6	MB(2)63	0.09	0.36	7.9	7.5	50.8
GU11	MB(2)58	0.065	0.26	1	6.2	36.9	MB(2)59	0.065	0.22	7.8	8.5	43.6	MB(2)60	0.55	42.2	7.8	9.9	51.9
15992	MB(2)20	3.07	12.3	8.7	47.4	47.4	MB(2)32	8.779	35.1	8	7.4	52.7	MB(2)38	17.229	88.9	7.1	7.6	54.9
15668	MB(2)21	8.77	35.1	8.6	5.5	52.7	MB(2)33	4.514	18.1	8.6	8.6	57.8	MB(2)39	0.815	3.26	7.6	7.3	54.9
14812	MB(2)22	0.96	3.84	8.7	5.8	48.2	MB(2)34	3.309	13.24	8.7	6.8	49.5	MB(2)40	0.751	3	7.2	6.9	54.1
Benign samples																		
Sample	DSP						PSP						NSP					
	PICR name	Conc. ng/ul	yield ng	RIN	cDNA yield ug	% present	PICR name	Conc. ng/ul	yield ng	RIN	cDNA yield ug	% present	PICR name	Conc. ng/ul	yield ng	RIN	cDNA yield ug	% present
GU87	MB(2)55	0.1875	0.75	8.8	7.8	45.5	MB(2)56	3.55	14.2	8.8	7.8	50.8	MB(2)57	2.975	11.9	8.4	7.7	50.3
GU85	MB(2)45	0.391	1.56	9.1	7.2	48.9	MB(2)48	0.811	3.24	6.7	7.2	50.1	MB(2)61	0.07	0.28	8.5	7.9	52.6
GU84	MB(2)44	0.779	3.12	9.1	8.6	53.3	MB(2)47	46.561	186	8.2	7.7	51.9	MB(2)60	0.978	3.9	9.3	8.8	58
GU64	MB(2)64	0.0775	0.31	1	5.4	38	MB(2)66	1.05	4.2	7.5	7.6	45.5	MB(2)67	1.4	5.6	6.7	8.2	50.8
15991	MB(2)43	0.112	0.45	6.8	7.8	48.5	MB(2)46	0.715	2.86	8.1	9.2	57.3	MB(2)49	1.932	7.7	7.6	7.6	52.3
14865	MB(2)52	0.06	0.24	1	6.4	51.7	MB(2)53	0.525	2.01	8.4	8.5	57.4	MB(2)54	1.475	5.9	7	7.2	55.3
Cancer																		
Sample	DSP						PSP						NSP					
	PICR name	Conc. ng/ul	yield ng	RIN	cDNA yield ug	% present	PICR name	Conc. ng/ul	yield ng	RIN	cDNA yield ug	% present	PICR name	Conc. ng/ul	yield ng	RIN	cDNA yield ug	% present
GU32	MB(2)23	1.775	7.1	6.6	7.3	50.3	MB(2)35	0.6	2.4	7.3	7.7	55.6	MB(2)41	4.011	16	6.3	7.2	52.6
GU28	MB(2)70	0.04	0.16	1	6.9	39.7	MB(2)71	0.04	0.16	1.1	7.8	41.6	MB(2)72	0.235	0.94	7.5	8	43.2
16355	MB(2)24	1.179	4.7	7.2	6.7	48.9	MB(2)36	2.954	11.8	7.3	8.3	56.4	MB(2)42	2.54	10.2	7.3	8.7	57.5
16189	MB(2)25	0.148	0.59	7.7	7.5	50.5	MB(2)27	0.487	1.95	7.8	8.3	57.4	MB(2)29	1.272	5.09	7	7.4	56.5
16143	MB(2)76	0.015	0.06	1	7.6	42.1	MB(2)77	0.285	1.02	8.5	8.3	55.2	MB(2)78	0.165	0.66	8.4	8.1	54.6
15457	MB(2)26	0.135	0.54	8.6	4.1	37.7	MB(2)28	0.594	2.38	8.6	7.8	57.4	MB(2)30	1.438	5.75	8.1	6.8	54.3

Table 6.4: Table showing the array name (PICR name), RNA yield (ng), RIN, cDNA yield following amplification (ug) and percentage of genes called present by the array software for the DSP, PSP and NSP for each of the normal, BPH and CaP samples previously deemed to have yielded RNA of sufficient quantity and quality for array hybridisation.

lower RIN or less than 0.5ng total RNA should also be utilised with the quality control data taken into consideration when microarray results were interpreted. This provided a further three normal (GU14, GU13, GU11), four BPH (GU85, GU64, 15991, 14865) and two CaP (GU28, 16143) samples. Five microgrammes of cDNA was suggested as being required for effective hybridisation to the microarray chips. Only one normal (GU13 DSP) and one CaP (15457 DSP) sample had less than the suggested cDNA quantity but the decision was taken to continue with array hybridisation and again take this into consideration when analysing the final expression data (Table 6.4).

6.2 Analysis of Extracted RNA to Determine Quantity and Quality

Only the results for those samples used for array hybridisation in the PICR Molecular Biology Core Facility (MBCF) will be the subject of any subsequent discussion. The average cell number was improved compared to the data series from the previous attempt at microarray performed by Epistem Ltd (section 3.2) (Table 6.5). No significant differences in RNA yield per cell were demonstrated between the three populations within each of the three histological subtypes (Table 6.6). However, the mean amount of RNA extracted per cell was significantly lower when compared to the 7.4pg mRNA per SP cell and 5.3pg mRNA per NSP cell extracted from BPH samples by Epistem Ltd (MBCF DSP Vs. Epistem Ltd SP $p=0.0006$ and MBCF NSP Vs. Epistem Ltd NSP $p=0.001$). The mean amount of RNA per cell for this set of BPH

Cell Number											
Normal			BPH			CaP					
Sample	DSP	PSP	NSP	Sample	DSP	PSP	NSP	Sample	DSP	PSP	NSP
GU11	3630	12260	56767	14865	4000	24000	32000	GU32	29000	150000	194000
GU39	6613	33367	42436	15991	6600	20650	3200	16355	25000	72000	82000
GU13	784	6747	10000	GU64	3604	10000	18365	GU28	296	5052	3122
GU14	1194	7721	12400	GU84	12390	110000	25000	15457	7176	30233	31972
GU33	4101	20367	23660	GU85	2735	13000	4909	16143	2212	6279	10000
15992	28973	92000	178271	GU87	8157	40000	56941	16189	12000	5200	90000
15668	36420	106860	150000								
14812	8896	28755	50000								
Mean	11326.38	38507.13	65304.25		6214.33	36275	23400.83		12614	44794	68515.67
Range	784-36420	6747-106860	12400-178271		2735-12390	10000-110000	3200-56941		296-29000	5052-150000	3122-194000
SD	12720.37	36449.16	59564.04		3325.39	34341.83	18151.80		10891.87	52679.86	65096.82

Table 6.5: Table showing the mean cell numbers, range and standard deviation (SD) yielded for the DSP, PSP and NSP from normal, BPH and CaP patient samples.

RNA Yield (pg) / Cell											
	Normal				BPH				CaP		
Sample	DSP	PSP	NSP	Sample	DSP	PSP	NSP	Sample	DSP	PSP	NSP
GU11	0.041	0.169	0.947	14865	0.075	0.109	0.230	GU32	0.306	0.820	0.374
GU39	0.128	0.575	0.240	15991	0.086	0.173	0.019	16355	0.236	0.206	0.155
GU13	0.332	0.085	0.046	GU64	0.098	0.237	0.172	GU28	0.659	0.039	0.375
GU14	0.117	0.084	0.048	GU84	0.314	2.116	0.196	15457	0.094	0.098	0.225
GU33	0.039	0.033	0.127	GU85	0.715	0.312	0.071	16143	0.036	0.203	0.083
15992	0.530	0.477	0.483	GU87	0.115	0.444	0.261	16189	0.062	0.047	0.071
15668	1.204	0.211	0.027								
14812	0.540	0.575	0.075								
Average	0.366	0.276	0.249	Average	0.234	0.565	0.658	Average	0.232	0.235	0.214
SD	0.369	0.214	0.300	SD	0.230	0.702	1.057	SD	0.214	0.270	0.124
t-test				t-test				t-test			
DSP vs. PSP		0.558		DSP vs. PSP		0.334		DSP vs. PSP		0.984	
DSP vs. NSP		0.590		DSP vs. NSP		0.449		DSP vs. NSP		0.773	
PSP vs. NSP		0.845		PSP vs. NSP		0.888		PSP vs. NSP		0.848	

Table 6.6: Table showing the yield of RNA per cell for the DSP, PSP and NSP from normal, BPH and CaP patient samples. Statistics (paired t-test) are shown for comparisons between the DSP and PSP, DSP and NSP and PSP and NSP within each histological subtype.

samples was 0.234pg (DSP), 0.565pg (PSP) and 0.658pg (NSP) (Table 6.6).

The techniques used by Epistem Ltd to determine RNA quality were different from the MBCF and therefore cannot be directly compared. However, the RNA quality was good (minimum RIN 6.3) except in four normal samples (GU33 DSP (RIN n/a), GU14 DSP (RIN 1), GU13 DSP (RIN 1) and GU11 DSP (RIN 1)), two BPH samples (GU64 DSP (RIN 1) and 14865 DSP (RIN 1)) and three CaP samples (GU28 DSP (RIN 1), GU28 PSP (RIN 1.1) and 16143 DSP (RIN 1)).

6.3 Clinical Data for the Patient Samples Utilised

Samples were processed, hybridised to arrays and analysed based on the histological diagnosis made from the representative chips taken for histological confirmation of the research specimen. Later, a thorough review of the clinical notes was performed and the clinical details and histology reports for the main operative specimens were correlated with the representative sample taken from the research tissue itself. This confirmed that the majority of the prostates termed "normal" were composed of normal or inflamed tissue. However, on more detailed examination of the main operative specimen, two of the samples (14812 and 15668) were noted to have small foci (<1% and <5% respectively) of Gleason 3+3 CaP. Sample GU33 was also shown to have a single focus of high grade PIN. All lesions were completely excised and did not encroach on the area of the prostate from which the research sample was taken (Table 6.7). Whilst the arrays from these two

Disease Type	Sample Number	Hospital	Date of Birth	Operation Date	Age (Years)	Pre-Operative PSA (ng/L)	TRUS Biopsy	Diagnosis
Normal	GU39	CHFT	29/08/1940	Aug-07	66	8.2	XI - Negative	TCC Bladder
	GU33	CHFT	25/11/1942	Jun-07	64	n/a	n/a	TCC Bladder
	GU14	SRFT	15/12/1934	Jan-07	72	0.87	n/a	SCC Bladder
	GU13	SRFT	07/09/1941	Dec-06	65	n/a	n/a	TCC Bladder
	GU11	CHFT	29/02/1968	Dec-06	38	n/a	n/a	TCC Bladder + CIS
	15992	CHFT	25/08/1936	Oct-05	69	n/a	n/a	TCC Bladder
Normal	15668	CHFT	24/10/1968	Jan-05	36	n/a	n/a	TCC Bladder
	14812	CHFT	10/10/1955	Oct-03	48	n/a	n/a	Multifocal Recurrent TCC Bladder
Disease Type	Sample Number	Pre-Operative Treatment		Operation	Clinical Stage	Tumour Grade		
Normal	GU39	Neoadjuvant Gemcitabine / Cisplatin		Radical Cystoprostatectomy	T3aN0M0	Grade 3		
	GU33	n/a		Radical Cystoprostatectomy	T3bN2M0	Grade 3		
	GU14	n/a		Radical Cystoprostatectomy	T3aN0M0	Moderate		
	GU13	n/a		Radical Cystoprostatectomy	T3bN1M0	Grade 3		
	GU11	Neoadjuvant Gemcitabine / Cisplatin		Radical Cystoprostatectomy	T2N2M0	Grade 3		
	15992	Neoadjuvant Gemcitabine / Cisplatin		Radical Cystoprostatectomy	T3bN1M0	Grade 3		
Normal	15668	n/a		Radical Cystoprostatectomy	T1N0M0	Grade 3		
	14812	n/a		Radical Cystoprostatectomy	TaNDM0	Grade 2		
Disease Type	Sample Number	Histology				Outcome		
Normal	GU39	No TCC invasion to the prostate. No prostatic malignancy or significant BPH				Alive		
	GU33	No TCC invasion into the prostate. Prostate showed chronic prostatitis and single focus of high grade PIN. No invasive prostatic malignancy				Died metastatic disease		
	GU14	SCC showed no invasion of the prostate or seminal vesicles. The urethral margin was free. No prostatic malignancy				Alive		
	GU13	No TCC invasion of the prostate. Active prostatitis but no evidence of neoplasia				Alive		
	GU11	Mild focal prostatic inflammation at apex but otherwise prostate normal				Alive		
	15992	Extensive prostatitis				Died Coronary Event		
Normal	15668	Small (<5%) focus of Gleason 3+3 CaP at right apex				Alive. Last PSA <0.1 Sept 2007		
	14812	Pre-op trans-urethral prostate biopsies showed involvement with TCC. Incidental Gleason 3+3 in <1% of prostate. This was fully excised and unlikely to be part of the research sample				Alive		

Table 6.7: Table showing the available clinical details for the normal patient samples.

samples were included in the quality control analysis, they were excluded from the differential gene expression analysis (section 6.8). Seven patients in the normal group had undergone radical cystoprostatectomy for transitional cell carcinoma (TCC) of the bladder and one for Squamous Cell Carcinoma (SCC). Three patients had received neoadjuvant chemotherapy (GU39, GU11 and 15992). The mean age was 57.25 years.

The majority of BPH samples demonstrated no other significant pathology after review of the chips that had been sent to the Pathology Department at the originating NHS trust. Sample GU85 was noted to have active chronic inflammatory disease present. The mean age of the BPH group was 69.17 years. Only one patient had not had a serum PSA test pre-operatively. The remainder had all undergone at least one negative prostate biopsy if their PSA was above that of the age-specific reference range (Table 6.8). Two patients (GU84 and GU64) had been established on a 5 α -reductase inhibitor for greater than six months prior to TURP.

The mean age of the patients in the CaP group was higher than the other two groups at 74.67 years. More detailed assessment of the tumour phenotype was possible for the CaP samples with more accurate determination of histological details such as stage, Gleason score and volume of tissue involved with tumour. The samples used in this series were deliberately selected for high grade (Gleason score ≥ 7), high volume (>40%) disease so as to minimise the inevitable

Disease Type	Sample Number	Hospital	Date of Birth	Operation Date	Age (Years)	Pre-Operative PSA (ng/L)	TRUS Biopsy	Diagnosis
BPH	GU87	SRFT	11/06/1934	May-08	73	0.58	n/a	BOO
	GU85	SRFT	18/12/1933	Jun-08	74	1.4	n/a	Chronic Retention and BOO on UDS
	GU84	SRFT	11/12/1943	Jun-08	64	9.3	X1 Negative	BOO
	GU64	SRFT	11/06/1944	Jan-08	63	n/a	n/a	BOO
	15591	SRFT	21/07/1934	Dec-04	70	9.7	X2 Negative	AUR and Failed TWOC
	14885	SRFT	29/07/1932	Oct-03	71	7.1	X1 Negative	BOO

Disease Type	Sample Number	Pre-Operative Treatment		Operation	Clinical Stage	Histology		
BPH	GU87	α -Blocker		TURP	40g BPH	BPH and No evidence of neoplasia		
	GU85	α -Blocker		TURP	30g BPH	BPH and active chronic inflammation. No evidence of malignancy		
	GU84	α -Blocker / 5- α -Reductase Inhibitor / Anticholinergic		TURP	40g BPH	BPH. No evidence of malignancy		
	GU64	α -Blocker / 5- α -Reductase Inhibitor / Previous TURP		TURP	40g BPH	BPH. No evidence of malignancy		
	15591	α -Blocker		TURP	50g BPH	BPH. No evidence of malignancy		
	14885	α -Blocker		TURP	50g BPH	BPH. No evidence of malignancy		

Table 6.8: Table showing the available clinical details for the BPH patient samples.

contamination with associated normal and BPH tissue. Clinical information such as pre-operative serum PSA, additional pre-operative treatment and specifically whether the individual had been hormone manipulated were all noted (Table 6.9). Three of the patients were either diagnosed with CaP as a consequence of TURP or underwent concurrent bilateral subcapsular orchidectomy (BSCO) at the same operation. All three samples (15457, 16143 and 16189) were therefore from primary unmanipulated CaP. Two samples were collected from patients who were effectively castrate. GU32 had commenced an LHRH analogue three months prior to surgery and 16355 was confirmed as having primary testosterone failure with a testosterone level of $<1\text{nmol/L}$ ($7\text{-}30\text{nmol/L}$). Finally, sample GU28 was taken from a patient with HRPC. This patient had undergone radical radiotherapy 11 years prior to his surgery and required BSCO two years later. At the time of his TURP he had been on third-line hormone manipulation (1mg Stilboestrol daily) for 12 months.

6.4 Affymetrix Genechip Quality Control Data

The 60 samples (a DSP, PSP and NSP from each of the twenty samples) chosen were each hybridised to a separate Affymetrix HG-U133_Plus 2 array. All but one of the arrays (GU13 DSP) had a scale factor within three fold of each other which fulfilled criteria set by Affymetrix® for array-comparability. The array background fluorescence was improved over threefold (mean 33.34, range 27.15-70.56)

Disease Type	Sample Number	Hospital	Date of Birth	Operation Date	Age (Years)	Pre-Operative PSA (ng/L)	Diagnosis
CaP	GU32	SRFT	31/07/1929	Jan-03	78	79	Hormone Manipulated CaP
	GU28	SRFT	06/03/1926	Apr-07	81	63	Hormone Escaped CaP
	16355	SRFT	27/09/1930	Aug-06	75	72	Hormone Manipulated CaP (Testosterone Failure)
	16189	SRFT	08/09/1942	Apr-06	63	40	Primary Unmanipulated CaP
	16143	UHSMT	19/03/1929	Mar-06	77	14	Primary Unmanipulated CaP
	15457	UHSMT	12/02/1930	Aug-04	74	19	Primary Unmanipulated CaP

Disease Type	Sample Number	Pre-Operative Treatment	Operation
CaP	GU32	Started LHRH Analogue 3 months before TURP	Channel TURP
	GU28	Radical DXT 1996, BSCO 1998, Failed 2nd -line hormone manipulation. On 3rd -line (Stilboestrol) for 12 months before TURP	Channel TURP
	16355	No hormonal manipulation as already in testosterone failure (Testosterone level <1)	Channel TURP
	16189	n/a	Channel TURP
	16143	n/a	Channel TURP + BSCO
	15457	n/a	Channel TURP + BSCO

Disease Type	Sample Number	Clinical Stage	Histology (Gleason Score and Core Volume)	Outcome
CaP	GU32	T3bN1M1B	4+4 / 50%	Died
	GU28	T1cNxMx	5+4 / 40%	Last seen Feb 2008 PSA 155
	16355	T3aNxM1	4+5 / 70%	Died Dec 2007
	16189	T2cNxM0	3+4 + Tertiary Pattern 5 / 40%	Nepadl hormones % DXT 2006, Last PSA 0.22 Mar 2008
	16143	T2cNxM0	4+4 / 50%	Last seen Oct 2007 and PSA <0.04
	15457	T3NxM1	4+4 / 60%	Last seen Sept 2007 PSA <1

Table 6.9: Table showing the available clinical details for the CaP patient samples.

compared with the previous series of arrays (mean 113.2, range 81.99-143.43). Indeed there was no overlap in the ranges (Table 6.10).

As discussed in section 3.3, mRNA transcripts degrade in the 5' to 3' direction. Ratios of the transcripts present in such control sequences at the three and five prime (3'/5') ends and the three prime and the middle (3'/M), assess the degree of degradation. The higher the number, the greater the observed degradation. The 3'/5' ratio for the housekeeper sequence β -actin suggested that the overall RNA transcript integrity was slightly poorer compared with the data from Epistem Ltd (3.12, range 1.71-6.43 vs. 2.03, range 0.87-6.65). However, there was a considerable improvement in the previously unacceptable GAPDH ratios (0.62, range -0.15-1.73 vs. 6.21, range 4.98-9.98) (Table 6.11). The individual array statistics are shown for each of the normal (Table 6.12, Figure 6.1), BPH (Table 6.13, Figure 6.2) and CaP (Table 6.14, Figure 6.3) tissue types.

There was a vast improvement in the overall percentage of genes that were called 'Present' by the Affymetrix software such that the majority of samples reached standards equivalent to arrays derived from cell lines (generally considered to be between 45% and 55%). In the Epistem Ltd arrays, one sample (16016 NSP1) had a markedly higher gene call of 25.9% whereas the majority were considerably lower (10-12.5%) (section 3.3). This second series of arrays from the MBCF had a mean percentage present gene call of 50.19% (SD \pm 6.83%, range 23.69-58.53%). Excluding sample 16016 NSP1 with its higher gene call

Array	Scale	Average Background	Gene Call "Present" (%)	GAPDH 3'/5'	GAPDH 3'/M	B-actin 3'/5'	B-actin 3'/M
Overall Mean	0.61	33.34	50.19	0.62	1.69	3.12	1.82
SD	0.23	6.19	6.83	0.44	0.67	1.15	0.89
Range	0.39-1.96	27.15-70.56	23.69-58.53	0.15-1.73	0.68-3.82	1.71-6.43	0.83-4.5
DSP Mean	0.67	35.05	44.69	0.81	1.96	3.33	2.02
PSP Mean	0.56	32.36	52.25	0.56	1.51	2.97	1.70
NSP Mean	0.59	32.62	53.62	0.48	1.61	3.06	1.75

Table 6.10: Table showing the overall quality control statistics for the 60 arrays including scale, background fluorescence, the percentage of probesets called "present" by the MAS 5.0 software and the degree of degradation using the 3'/5' and 3'/M ratios for the housekeeping genes GAPDH and Beta-Actin. mRNA transcripts degrade in the 5' to 3' direction. Ratios of the transcripts present in such control sequences at the three and five prime (3'/5') ends and the three prime and the middle (3'/M), assess the degree of degradation. The higher the number, the greater the observed degradation.

Experimental Series	Statistic	Scale	Average Background	Gene Call "Present" (%)	GAPDH 3'/5'	GAPDH 3'/M	B-actin 3'/5'	B-actin 3'/M
Epistem Ltd	Overall Mean	1.86	113.20	13.15	6.21	0.76	2.03	0.44
	Range	0.87-3.19	81.99-143.43	10.76-25.90	4.98-9.98	0.45-1.31	0.87-6.65	0.15-1.47
MBCF	Overall Mean	0.61	33.34	50.19	0.62	1.69	3.12	1.82
	Range	0.39-1.96	27.15-70.56	23.69-58.53	-0.15-1.73	0.68-3.82	1.71-6.43	0.83-4.5

Table 6.11: Table compares the overall quality control statistics for the eight arrays processed and analysed by Epistem Ltd with the 60 arrays processed and analysed by the MBCF. Statistics shown are scale, background fluorescence, the percentage of probesets called "present" by the MAS 5.0 software and the degree of degradation using ratios of housekeeping genes GAPDH and Beta-Actin.

Normal							
Array	Scale	Average Background	Gene Call "Present" (%)	GAPDH 3'/5'	GAPDH 3'/M	B-actin 3'/5'	B-actin 3'/M
GU39 DSP	0.41	31.40	51.04	1.04	1.98	2.60	1.44
GU39 PSP	0.44	31.64	51.60	0.01	0.82	2.07	0.97
GU39 NSP	0.46	30.62	56.92	0.44	1.28	2.81	1.39
GU33 DSP	0.57	32.64	46.71	1.08	2.13	2.83	1.43
GU33 PSP	0.44	32.68	58.33	1.37	1.88	3.07	1.91
GU33 NSP	0.50	32.24	56.93	0.12	1.42	2.43	1.30
GU14 DSP	0.66	31.46	32.15	1.24	2.49	4.72	3.11
GU14 PSP	0.69	31.85	48.18	0.46	2.91	5.49	3.06
GU14 NSP	0.71	32.04	54.07	1.19	2.40	4.46	2.81
GU13 DSP	1.96	30.13	23.69	0.64	3.63	6.43	4.09
GU13 PSP	0.73	30.18	46.69	0.65	1.84	3.86	2.25
GU13 NSP	0.77	31.56	50.78	0.77	2.82	3.08	1.82
GU11 DSP	1.12	30.72	36.93	1.04	3.82	4.46	2.98
GU11 PSP	0.65	31.60	49.55	0.28	1.25	4.52	3.25
GU11 NSP	0.50	29.64	51.94	0.95	2.89	5.07	3.44
15592 DSP	0.46	58.88	47.35	-0.05	0.99	1.71	0.93
15592 PSP	0.45	33.12	52.70	0.46	1.26	1.99	1.01
15592 NSP	0.53	31.98	54.90	0.06	1.13	2.50	1.32
15668 DSP	0.49	30.28	52.72	0.34	1.04	2.10	1.12
15668 PSP	0.45	36.10	57.76	-0.02	1.27	2.26	1.16
15668 NSP	0.82	32.90	54.88	0.44	1.30	2.46	1.32
14812 DSP	0.44	33.19	48.18	1.37	1.00	1.93	1.06
14812 PSP	0.55	30.51	49.49	0.55	0.95	2.38	1.08
14812 NSP	0.66	32.02	54.06	0.10	0.94	2.54	1.49
Overall Normal Sample Mean	0.64	32.89	49.23	0.61	1.81	3.24	1.91
SD	0.32	5.58	8.10	0.45	0.87	1.28	0.93
Range	0.41-1.96	29.64-58.8	23.69-58.33	-0.05-1.37	0.82-3.82	1.71-6.43	0.93-4.09
DSP Mean	0.79	34.84	42.35	0.84	2.14	3.33	2.02
PSP Mean	0.54	32.21	51.05	0.47	1.52	3.20	1.84
NSP Mean	0.59	31.62	54.31	0.51	1.77	3.17	1.86

Table 6.12: Table showing the overall quality control statistics for the 24 normal tissue arrays. Statistics shown are scale, background fluorescence, the percentage of probesets called "present" by the MAS 5.0 software and the degree of degradation using ratios of housekeeping genes GAPDH and Beta-Actin.

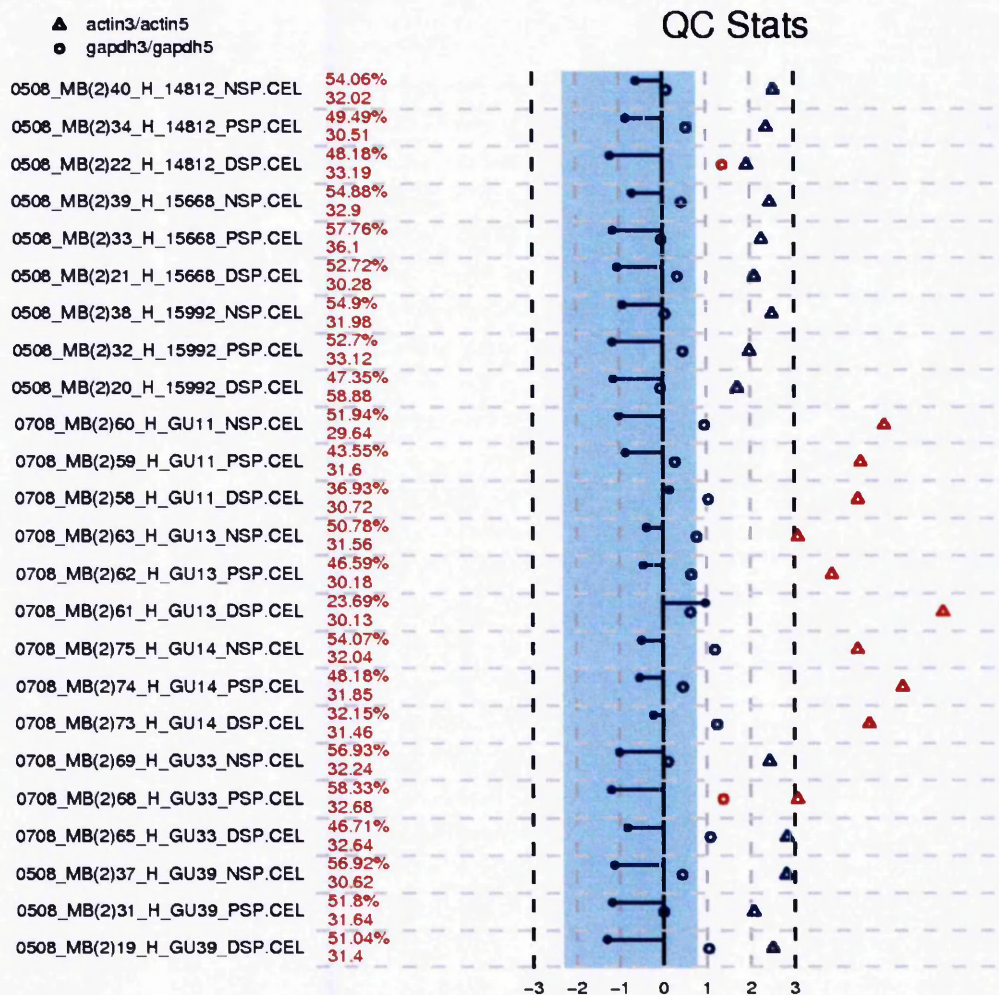


Figure 6.1: Chart summarising the Qc statistics generated by MAS5.0. Each DSP, PSP and NSP array from the normal samples is represented on a separate horizontal line. The full array name assigned by the software is shown and the sample and population type are evident within it. The central black vertical line corresponds to zero Fc and the black dotted vertical lines on either side are at $\log_2(3)$ Fc up or down. The blue vertical bar represents the region in which all arrays have a scale factor within 3 fold of each other which fulfils criteria set by Affymetrix® for array-comparability. A line is plotted horizontally out from the central bar to the point denoting the scale factor for each array. The red text on the left denotes the percentage of probesets called 'Present' and the average background signal. Triangles and dots are β -actin and GAPDH 3'/5' ratios respectively and these refer to sequence integrity. Anything blue is within an acceptable Qc range whereas red is not.

BPH	Array	Scale	Average Background	Gene Call "Present" (%)	GAPDH 3'/5'	GAPDH 3'/M	B-actin 3'/5'	B-actin 3'/M
	GU87 DSP	0.54	31.57	46.46	0.18	1.61	3.96	2.21
	GU87 PSP	0.48	30.59	50.82	0.18	0.68	1.86	0.97
	GU87 NSP	0.66	31.69	50.33	-0.15	1.00	2.16	0.96
	GU85 DSP	0.59	33.31	48.92	1.09	1.66	1.79	0.94
	GU85 PSP	0.51	33.96	50.11	0.55	1.48	2.26	0.98
	GU85 NSP	0.48	34.88	52.80	0.96	2.12	1.86	0.89
	GU84 DSP	0.46	33.65	53.29	0.40	1.47	2.17	1.06
	GU84 PSP	0.39	35.71	51.87	0.08	1.33	1.80	0.83
	GU84 NSP	0.46	36.21	58.02	0.38	1.57	2.49	1.24
	GU64 DSP	0.74	28.56	37.96	0.28	1.16	1.89	1.10
	GU64 PSP	0.57	34.14	45.52	0.23	1.49	2.81	1.44
	GU64 NSP	0.55	33.30	50.84	0.00	0.97	2.73	1.68
	15991 DSP	0.50	32.71	48.46	1.73	2.42	3.01	1.29
	15991 PSP	0.54	32.96	57.30	0.70	1.77	2.51	1.53
	15991 NSP	0.62	33.36	52.27	0.39	1.50	2.45	1.29
	14865 DSP	0.57	30.94	51.89	1.28	1.29	1.89	0.93
	14865 PSP	0.45	32.00	57.41	0.44	1.08	2.35	1.08
	14865 NSP	0.49	33.91	55.27	0.23	1.25	2.49	1.18
	Overall BPH Sample Mean	0.53	32.97	51.01	0.50	1.44	2.36	1.20
	SD	0.08	1.82	4.73	0.47	0.40	0.53	0.33
	Range	0.39-0.74	28.56-36.21	37.96-58.02	0.15-1.73	0.68-2.42	1.79-3.96	0.83-2.21
	DSP Mean	0.57	31.79	47.63	0.83	1.60	2.45	1.25
	PSP Mean	0.49	33.22	52.17	0.36	1.31	2.27	1.14
	NSP Mean	0.54	33.89	53.22	0.30	1.40	2.36	1.21

Table 6.13: Table showing the overall quality control statistics for the 18 BPH arrays. Statistics shown are scale, background fluorescence, the percentage of probesets called "present" by the MAS 5.0 software and the degree of degradation using ratios of housekeeping genes GAPDH and Beta-Actin.

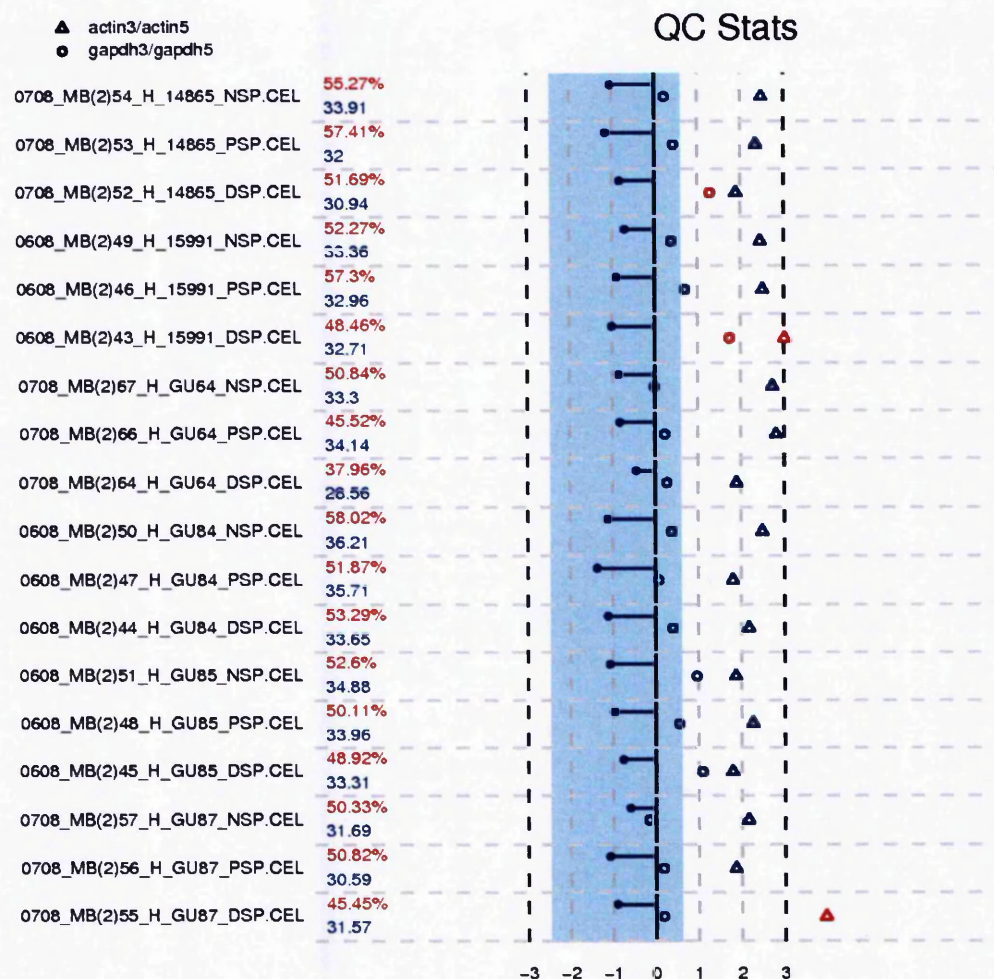


Figure 6.2: Chart summarising the Qc statistics generated by MAS5.0. Each DSP, PSP and NSP array from the BPH samples is represented on a separate horizontal line. The full array name assigned by the software is shown and the sample and population type are evident within it. The central black vertical line corresponds to zero Fc and the black dotted vertical lines on either side are at $\log_2(3)$ Fc up or down. The blue vertical bar represents the region in which all arrays have a scale factor within 3 fold of each other which fulfils criteria set by Affymetrix® for array-comparability. A line is plotted horizontally out from the central bar to the point denoting the scale factor for each array. The red text on the left denotes the percentage of probesets called 'Present' and the average background signal. Triangles and dots are β -actin and GAPDH 3'/5' ratios respectively and these refer to sequence integrity. Anything blue is within an acceptable Qc range whereas red is not.

Cap	Scale	Average Background	Gene Call "Present" (%)	GAPDH 3'/5'	GAPDH 3'/M	B-actin 3'/5'	B-actin 3'/M
Array							
GU32 DSP	0.67	30.70	50.31	0.32	1.54	3.20	1.79
GU32 PSP	0.57	33.35	55.63	0.35	1.23	2.78	1.56
GU32 NSP	0.63	34.39	52.56	0.13	1.40	2.98	1.70
GU28 DSP	0.80	33.33	39.74	0.76	2.84	5.73	3.93
GU28 PSP	0.92	32.95	41.65	1.13	1.74	4.17	3.01
GU28 NSP	0.60	32.66	43.25	0.69	1.48	5.84	3.25
16355 DSP	0.49	70.56	48.89	0.77	1.44	2.37	1.41
16355 PSP	0.59	31.11	56.41	0.89	1.51	2.84	1.48
16355 NSP	0.46	33.69	57.47	0.41	1.49	3.13	1.76
16189 DSP	0.62	31.59	50.50	1.45	2.78	4.06	2.54
16189 PSP	0.97	27.15	57.38	0.95	1.88	3.95	2.44
16189 NSP	1.00	27.22	56.53	0.79	1.35	3.72	2.38
16143 DSP	0.43	34.48	42.09	0.36	1.94	4.96	2.54
16143 PSP	0.46	33.24	55.18	1.35	2.52	3.67	2.32
16143 NSP	0.47	34.81	54.59	1.16	2.43	3.39	2.13
15457 DSP	0.74	30.83	37.71	0.88	1.89	4.80	4.50
15457 PSP	0.50	32.29	57.38	0.50	1.34	2.78	1.62
15457 NSP	0.60	33.22	54.26	0.62	1.54	2.67	1.56
Overall Cap Sample Mean	0.64	34.31	50.64	0.75	1.80	3.73	2.33
SD	0.17	9.04	6.59	0.36	0.50	1.01	0.85
Range	0.43-1.00	27.15-70.56	37.71-57.47	0.13-1.45	1.23-2.84	2.37-5.84	1.41-4.5
DSP Mean	0.62	38.58	44.87	0.75	2.07	4.19	2.78
PSP Mean	0.67	31.68	53.94	0.86	1.71	3.37	2.07
NSP Mean	0.63	32.67	53.11	0.63	1.61	3.62	2.13

Table 6.14: Table showing the overall quality control statistics for the 18 Cap arrays. Statistics shown are scale, background fluorescence, the percentage of probesets called "present" by the MAS 5.0 software and the degree of degradation using ratios of housekeeping genes GAPDH and Beta-Actin.

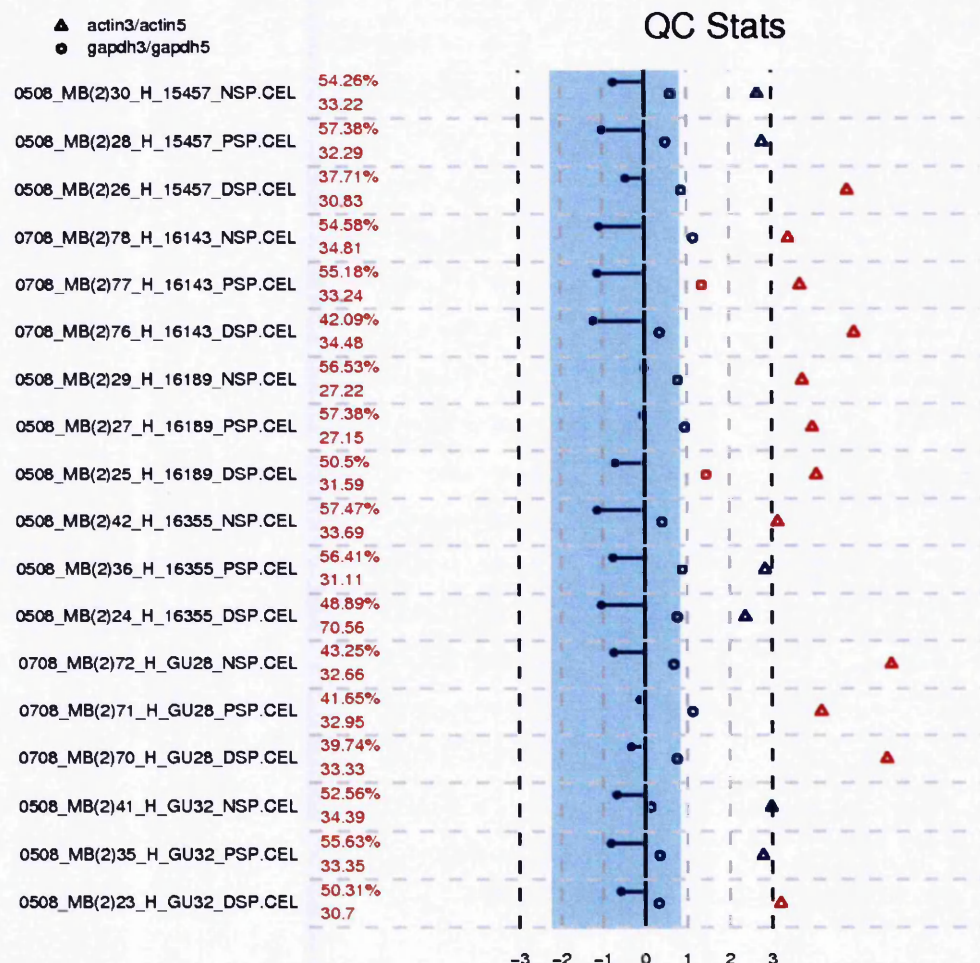


Figure 6.3: Chart summarising the Qc statistics generated by MAS5.0. Each DSP, PSP and NSP array from the CaP samples is represented on a separate horizontal line. The full array name assigned by the software is shown and the sample and population type are evident within it. The central black vertical line corresponds to zero Fc and the black dotted vertical lines on either side are at $\log_2(3)$ Fc up or down. The blue vertical bar represents the region in which all arrays have a scale factor within 3 fold of each other which fulfils criteria set by Affymetrix® for array-comparability. A line is plotted horizontally out from the central bar to the point denoting the scale factor for each array. The red text on the left denotes the percentage of probesets called 'Present' and the average background signal. Triangles and dots are β -actin and GAPDH 3'/5' ratios respectively and these refer to sequence integrity. Anything blue is within an acceptable Qc range whereas red is not.

of 25.9%, the range of genes called “present” for the MBCF series was separated from the first (Table 6.11). These statistics appeared to be conserved across each of the populations (DSP, PSP and NSP) and each of the tissue types (normal, BPH and CaP). Overall, the improvement in percentage present gene call is indicative of this data series being much improved on that from Epistem Ltd and ultimately suitable for biological datamining (Figure 6.4).

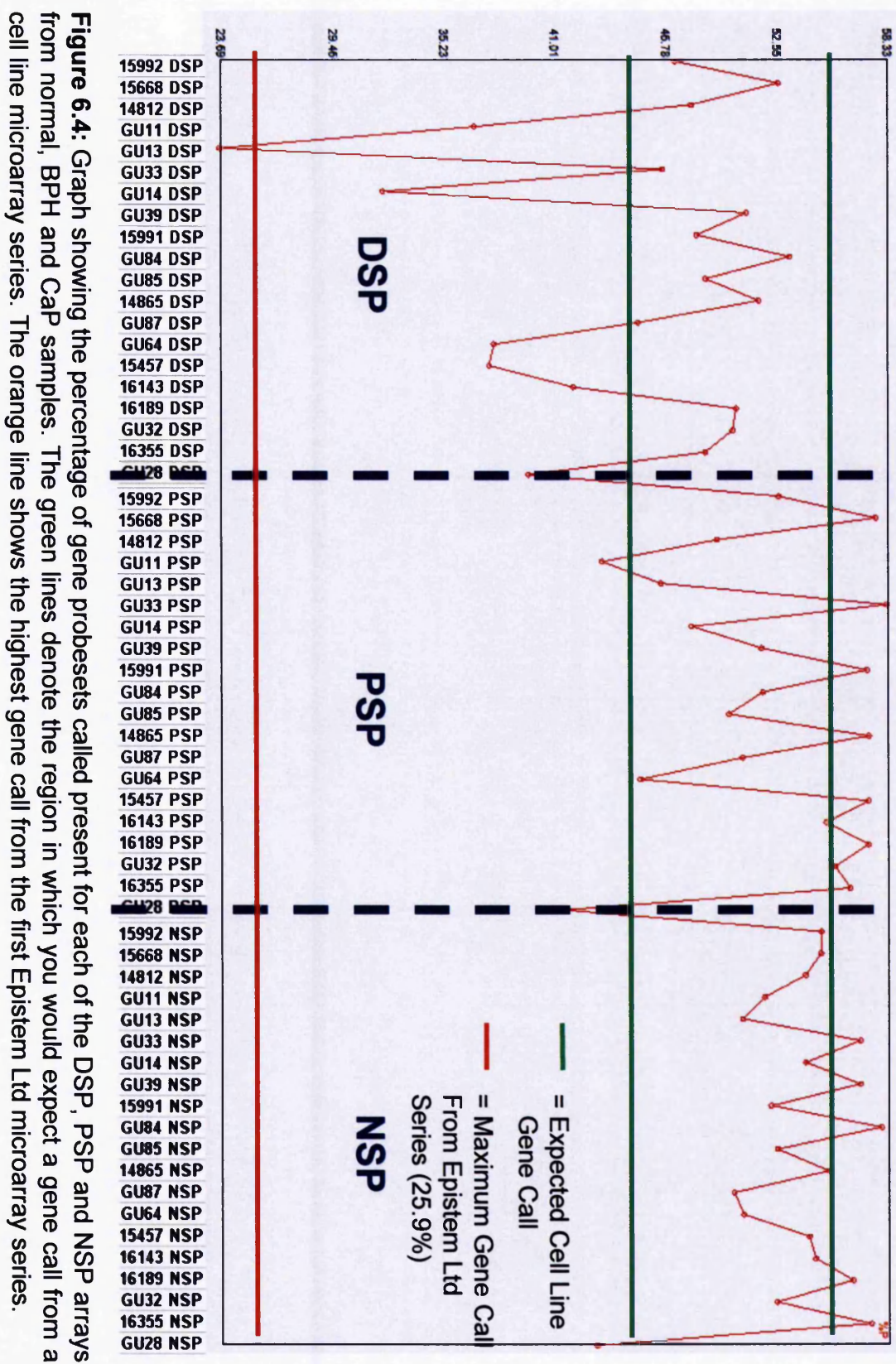
6.5 Array Normalisation

The data spread was analysed before and after the process of both MAS5.0 and RMA normalisation. MAS5.0 software was used for normalisation of the data to allow determination of the “present”, “marginal” and “absent” gene calls. However, normalisation with RMA software was performed prior to expression analysis as this fitted better with the Limma analysis package.

The process of normalisation was effective and no one sample was deemed to be an outlier. The data reported no technical or biological reason why any chip should be excluded (Figure 6.5, 6.6 and 6.7).

6.6 Biological Comparability of Arrays

Scatter graphs showing paired expression summaries for the three cellular populations for each of the three tissue types illustrated the improved gene call and quality of data (Figure 6.8, 6.9 and 6.10). Each scatter plot compares the expression summary value for each probeset from each of the populations being compared. Gene probesets with the



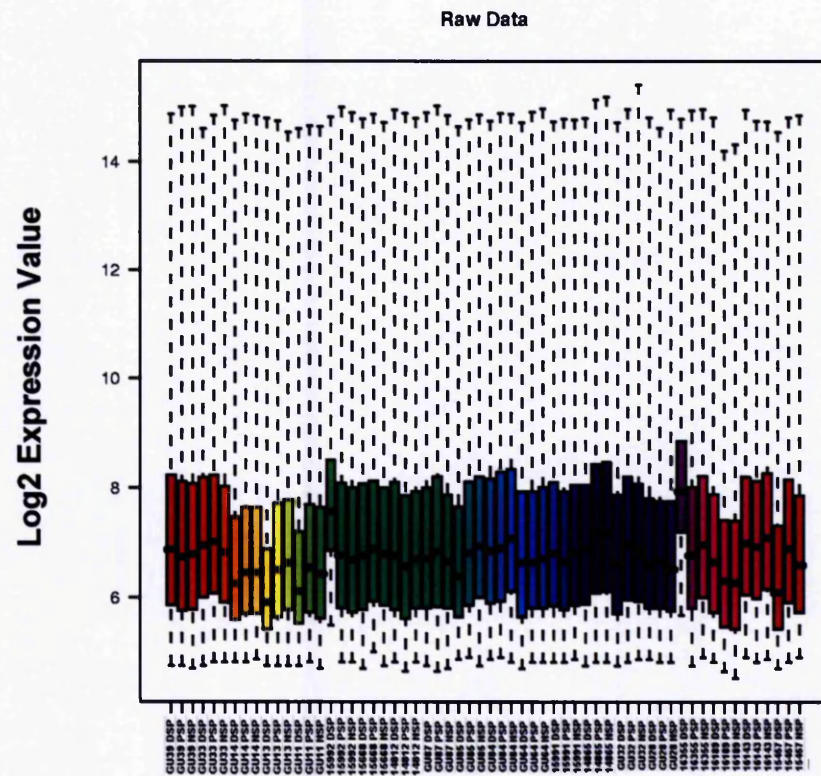


Figure 6.5: Boxplot demonstrating the spread of raw data for all microarrays before normalisation. Each box shows the median and interquartile range (IQR). Whiskers extend to 1.5x IQR with points beyond the whiskers being outliers.

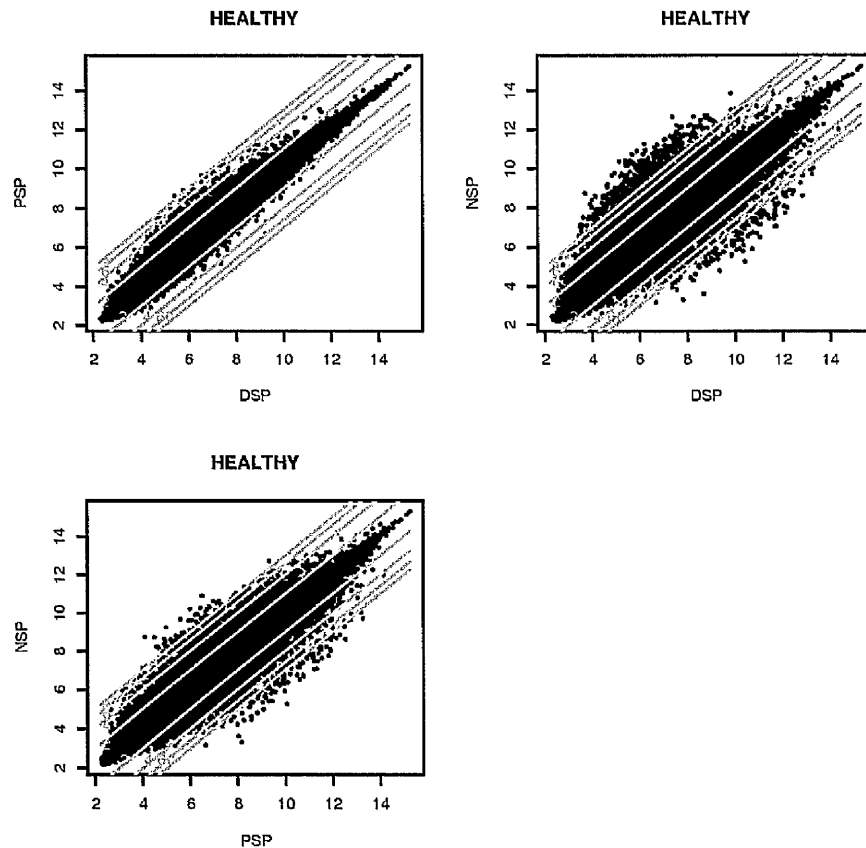


Figure 6.8: Scatter plots showing the differential mean log₂ expression of probesets from all normal samples between the DSP and PSP, DSP and NSP and the PSP and NSP arrays. Each scatter plot compares the expression summary value for each probeset from each of the populations being compared. Gene probesets with the same expression summaries lie on a straight diagonal line between the two axes ($x=y$). Genes up-regulated in a population are then shown lying towards that population's axis. The degree of up- or down-regulation is determined by the fold change and quantified by diagonal lines parallel with the line $x=y$.

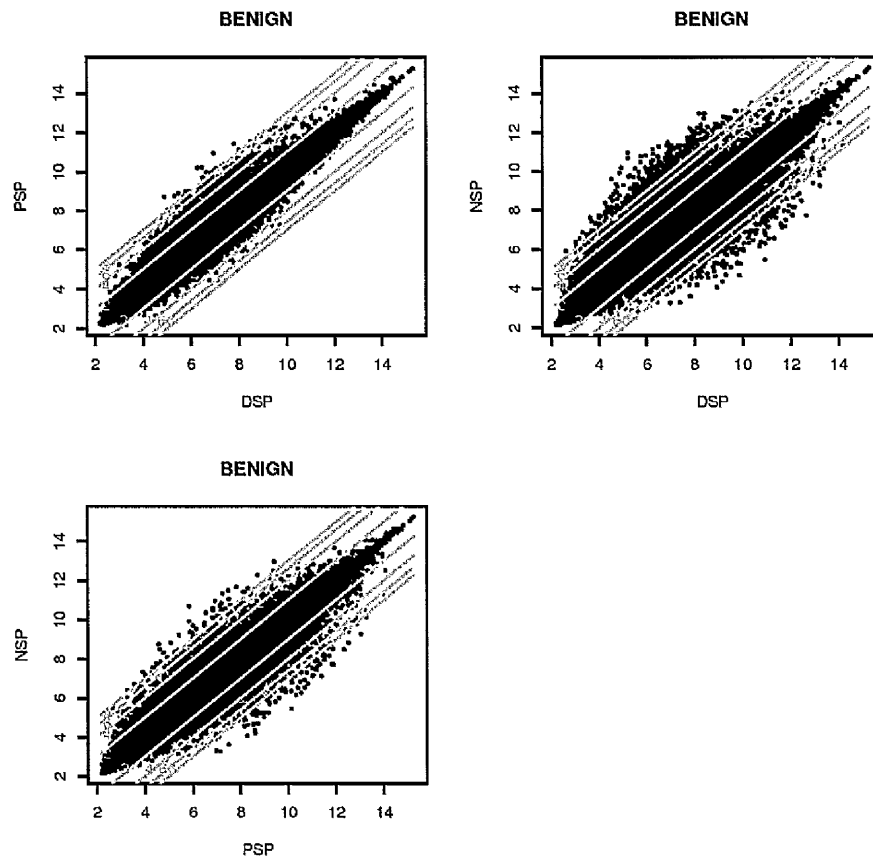


Figure 6.9: Scatter plots showing the mean log₂ expression of probesets between the DSP and PSP, DSP and NSP and the PSP and NSP of BPH arrays. Each scatter plot compares the expression summary value for each probeset from each of the populations being compared. Gene probesets with the same expression summaries lie on a straight diagonal line between the two axes ($x=y$). Genes up-regulated in a population are then shown lying towards that population's axis. The degree of up- or down-regulation is determined by the fold change and quantified by diagonal lines parallel with the line $x=y$.

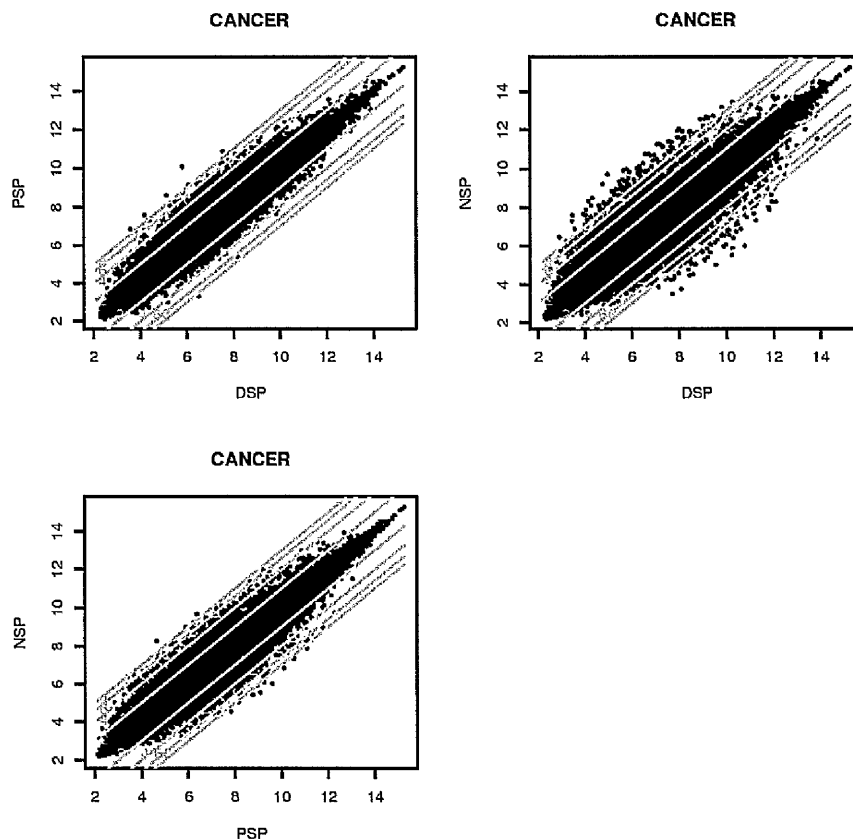


Figure 6.10: Scatter plots showing the mean log₂ expression of probesets between the DSP and PSP, DSP and NSP and the PSP and NSP of CaP arrays. Each scatter plot compares the expression summary value for each probeset from each of the populations being compared. Gene probesets with the same expression summaries lie on a straight diagonal line between the two axes ($x=y$). Genes up-regulated in a population are then shown lying towards that population's axis. The degree of up- or down-regulation is determined by the fold change and quantified by diagonal lines parallel with the line $x=y$.

same expression summaries lie on a straight diagonal line between the two axes ($x=y$). Genes up-regulated in a population are then shown lying towards that population's axis. The degree of up- or down-regulation is determined by the fold change and quantified by diagonal lines parallel with the line $x=y$. The greatest degree of differential expression appeared to be between the DSP and NSP in each of the tissue types.

Overall, correlation between the probeset data obtained from different samples was good. The calculated Pearson correlation scores for the MBCF arrays ($R^2=0.762-1.00$) were all much improved on the previous attempt at microarray by Epistem Ltd ($R^2=0.47-0.74$). The heatmap allows a visual interpretation of array comparability. The heatmap comparing all 60 arrays (Figure 6.11) has been filtered to remove those samples that had low or unrecordable RIN values but had been included on the basis of them producing good cDNA yields (Figure 6.12). Filtering these samples out improved the minimum R^2 value from 0.762 to 0.799.

Examination of all the arrays together reveals evidence of clustering within each of the cell populations across all three tissue types. The observed clustering amongst the DSPs was probably less tight for the BPH and CaP samples with correlation being a little more heterogeneous. BPH and CaP array correlation appeared more homogeneous at the PSP level instead. For all tissue types there was a definite trend that the NSP samples were different to the combined DSP

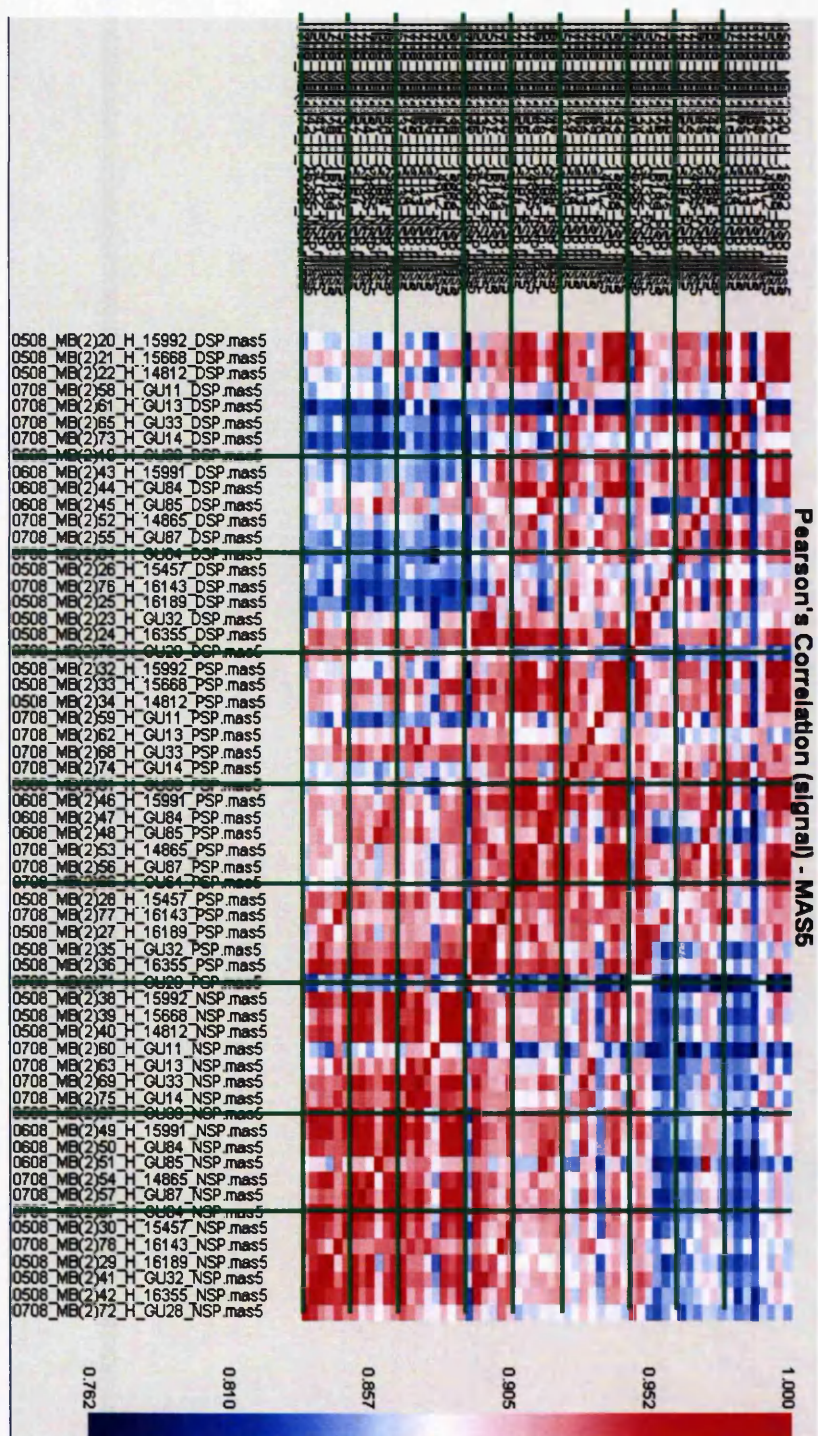
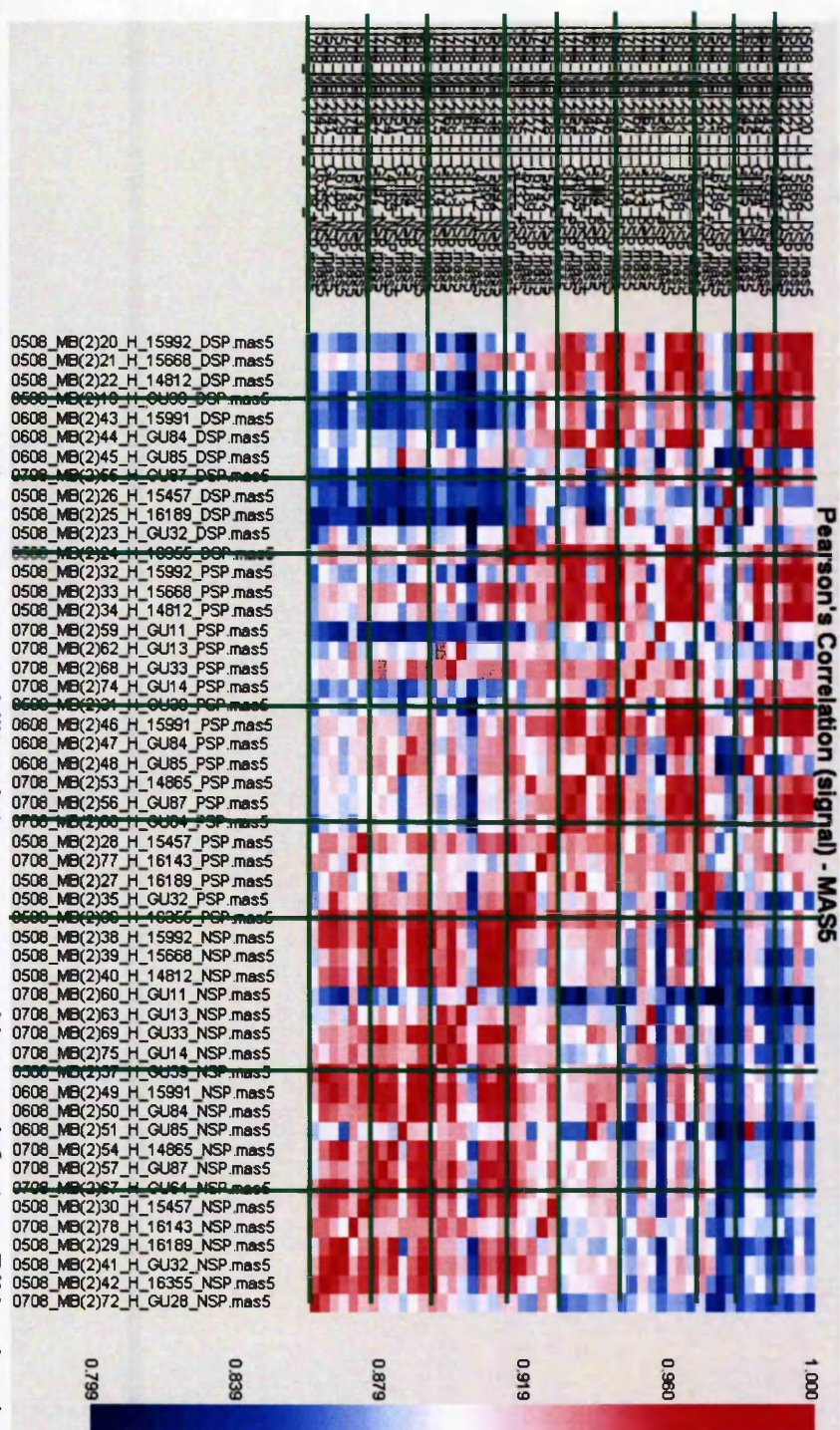


Figure 6.12: Heatmap demonstrating the comparability of those arrays with a satisfactory RIN value (≥ 6.3). Those samples with an unrecordable RIN or a RIN of 1 have been excluded. The full array name assigned by the software is shown and the sample and population type are evident within it. Green lines separate the three populations and three tissue types. The sequence of arrays reads normal DSP (4), BPH DSP (4), Cap DSP (4), normal PSP (8), BPH PSP (6), Cap PSP (5), normal NSP (8), BPH NSP (6) and Cap NSP (6) from left to right (x-axis) and top to bottom (y-axis). The degree of correlation is determined from the key scale on the right (Pearson Correlation Coefficient R^2).



and PSP arrays reinforcing the observation made from the scatter graphs.

Reviewing the heatmap detailing all 60 arrays, some arrays appeared to be somewhat different to those within the same population and disease subtype (eg the HRPC sample GU28). GU85 DSP and GU85 PSP appeared to show an inverse relationship to that of the arrays from the same subgroup and appeared to have a profile akin to that expected of a BPH NSP. The converse was true for GU85 NSP. Array 15457 did not appear to correlate particularly strongly with other arrays and certainly not to the same extent as adjacent arrays from the same subgroups. The arrays for samples GU11 DSP, GU11 PSP and GU11 NSP were quite different from the other arrays within their respective subgroups. The normal arrays GU13 DSP and GU14 DSP also initially appeared quite different but were filtered out by the heatmap featuring only those arrays with satisfactory RINs.

Due to the heterogeneity of the six CaP samples a separate heatmap was constructed to specifically focus on them (Figure 6.13). The primary unmanipulated arrays appeared to correlate with each other satisfactorily at the DSP level. The arrays for the DSPs isolated from the hormone manipulated arrays also correlated well with each other. The relationship within each of the two groups and between themselves was more homogeneous at the PSP level. All the NSP arrays correlated well with each other. The array from the patient with HRPC (GU28) was quite different, particularly at the DSP but to some extent also at the

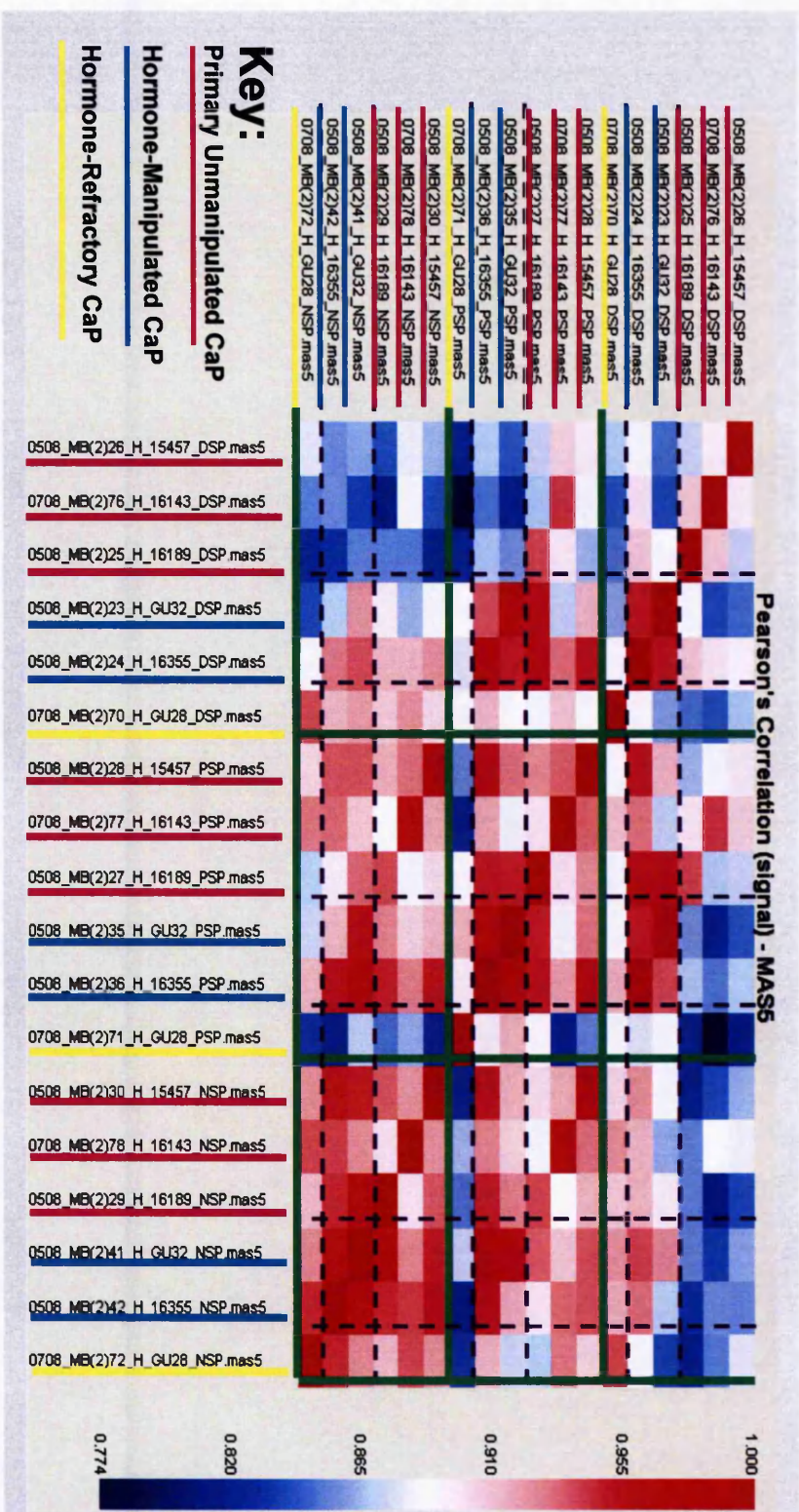


Figure 6.13: Heatmap demonstrating the comparability of all 18 CaP arrays. The full array name assigned by the software is shown and the sample and population type are evident within it. Green lines separate the three populations and dashed lines separate the arrays into primary unmanipulated CaP (samples 15457, 16143 and 16189-underlined in pink), hormone manipulated CaP (samples GU32 and 16355-underlined in turquoise) and hormone-escaped CaP (sample GU28-underlined in yellow). The sequence of arrays reads DSP (6), PSP (6) and NSP (6) from left to right (x-axis) and top to bottom (y-axis). The degree of correlation is determined from the key scale on the right (Pearson Correlation Coefficient R2).

PSP array level. The GU28 DSP array appeared to correlate best with the arrays taken from the NSP of other cancers. The primary unmanipulated DSPs were similar to their corresponding PSP arrays but markedly different to the PSP arrays from other tumour phenotypes and all the NSPs. The DSP arrays from the hormone manipulated samples correlated well with each other but again quite different to arrays from other cancer subtypes.

Using a cluster dendrogram based on 1-Pearson correlation score ($1-R^2$), the clustering pattern (Figure 6.14) appears less heterogeneous than after the first attempt at microarray by Epistem Ltd. Again, there appears to be a greater degree of differential expression between the DSP, PSP and NSP than between the histological subtypes (normal, BPH and CaP). There appear to be two clusters with the DSP and PSP correlating with each other and being different from the NSPs, which clustered together.

A principle component analysis (PCA) was performed using the expression data from all the three Hoechst 33342 subpopulations of all three tissue types. The PCA software finds the probeset with the largest difference between all the arrays and plots all the samples based on this across the x-axis. Subsequently, it takes the next largest degree of separation and plots this on the y-axis. The third largest degree of separation is then plotted on the z-axis. This plot is particularly useful for ensuring that changes in the data are due to the sample biology. Ellipsoids can be drawn to link data points and again

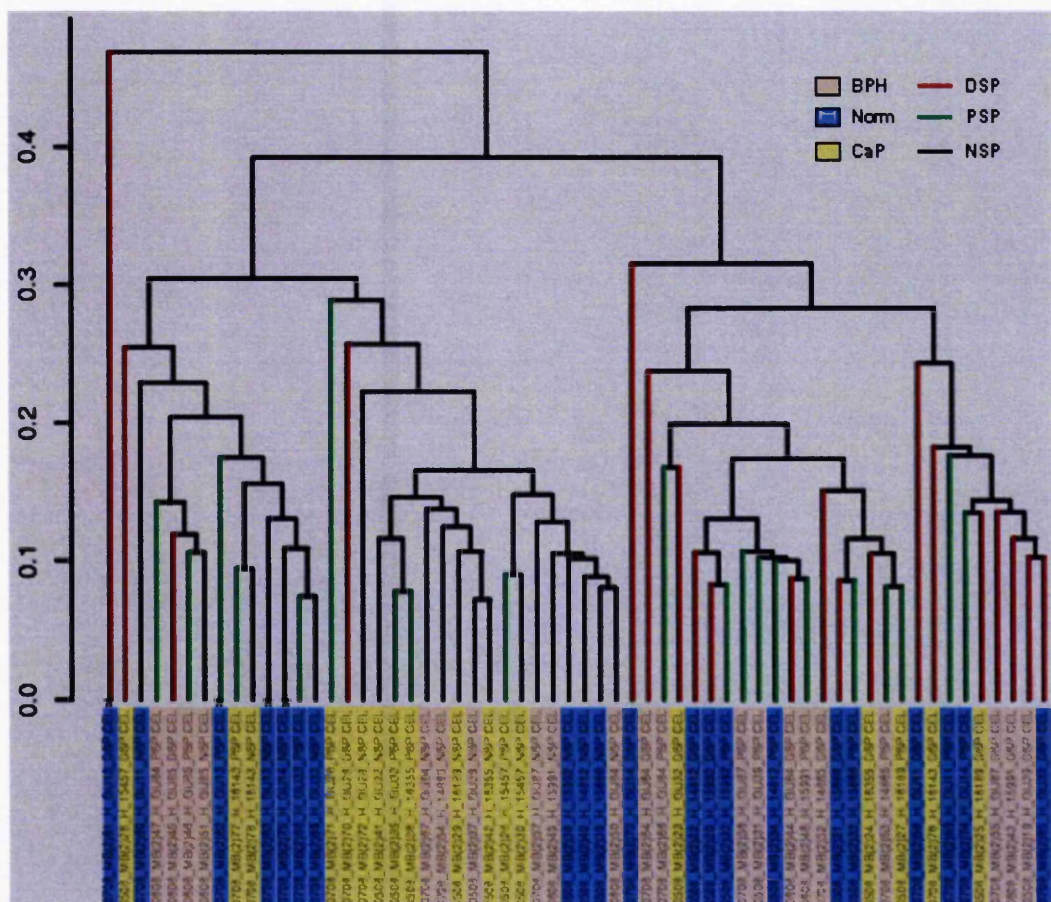


Figure 6.14: Cluster dendrogram indicating the clustering pattern for all 60 arrays. The tissue type and cellular populations are colour coded.

the DSP and PSP appear the most similar. The apparent clustering patterns seen in the dendrogram were confirmed but in addition there is separation of the DSP and PSP into defined populations (Figure 6.15).

6.7 Correlation between MAS5.0 Generated Detection Calls and Raw Expression Values

In the previous Epistem Ltd microarray series, many probesets were called "Absent" despite high expression intensity. For example, even on the array with the highest "Present" gene call (25.9%) from 16016 NSP1, one probeset was called "Absent" despite a log₂ expression summary of over ten, 496 probesets were called "Absent" even though their log₂ signal was greater than eight and 18,513 probesets despite log₂ signal intensities of greater than six. The array with the worst present gene call (10.76%) had 51 probe sets called "Absent" even with a log₂ signal above ten. In the new project, the worst array MB(2)61 from GU13 DSP (23.7%), showed vast improvement with only two probesets being called "Absent" with a log₂ signal above ten, 38 with a log₂ signal above eight and 1,063 with a log₂ signal above six. Most of the arrays had less, for example MB(2)19 from GU39 DSP had one "Absent" probeset with a log₂ expression summary above ten, two above eight and 64 above six.

When the distribution of the absent probesets for the worst array from the second series undertaken in the MBCF (MB(2)61 from GU13 DSP) and three other randomly chosen arrays (Figure 6.16A) were plotted and compared to four arrays including the best array from the first series performed by Epistem Ltd (16016 NSP1) (Figure 6.16B), clearly fewer

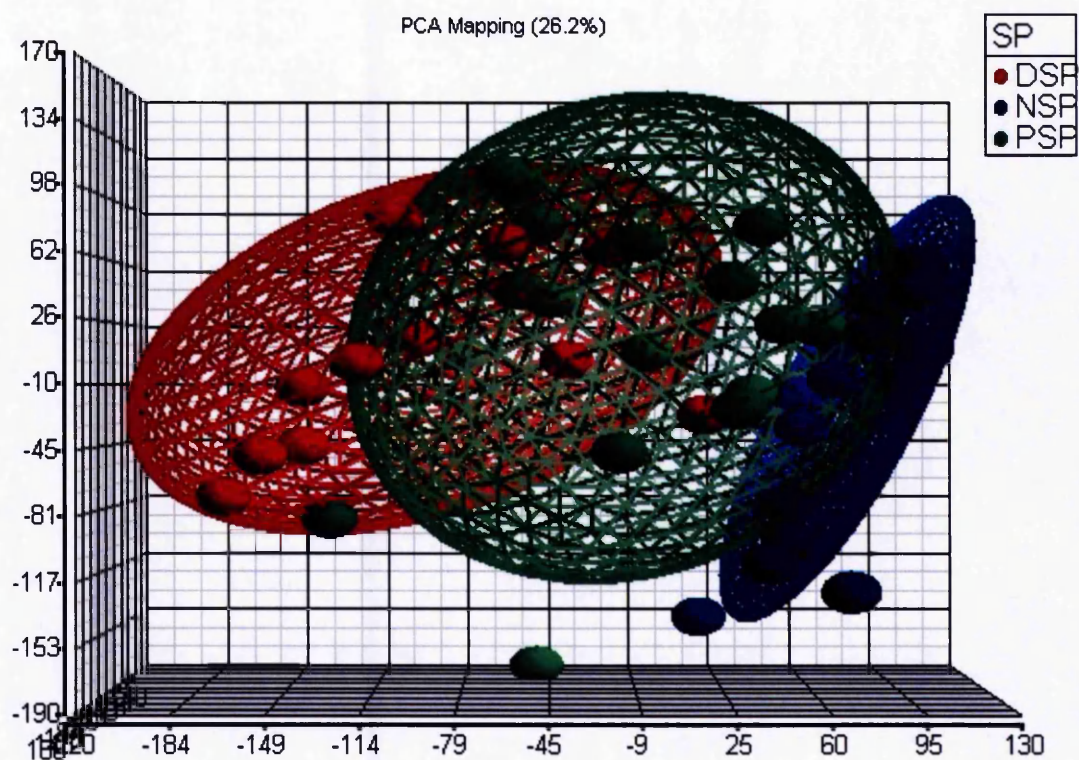


Figure 6.15: Principal component analysis (PCA) mapping showing the three largest degrees of separation between the DSP, PSP and NSP arrays for each of the patient samples. Ellipsoids group similar data points.

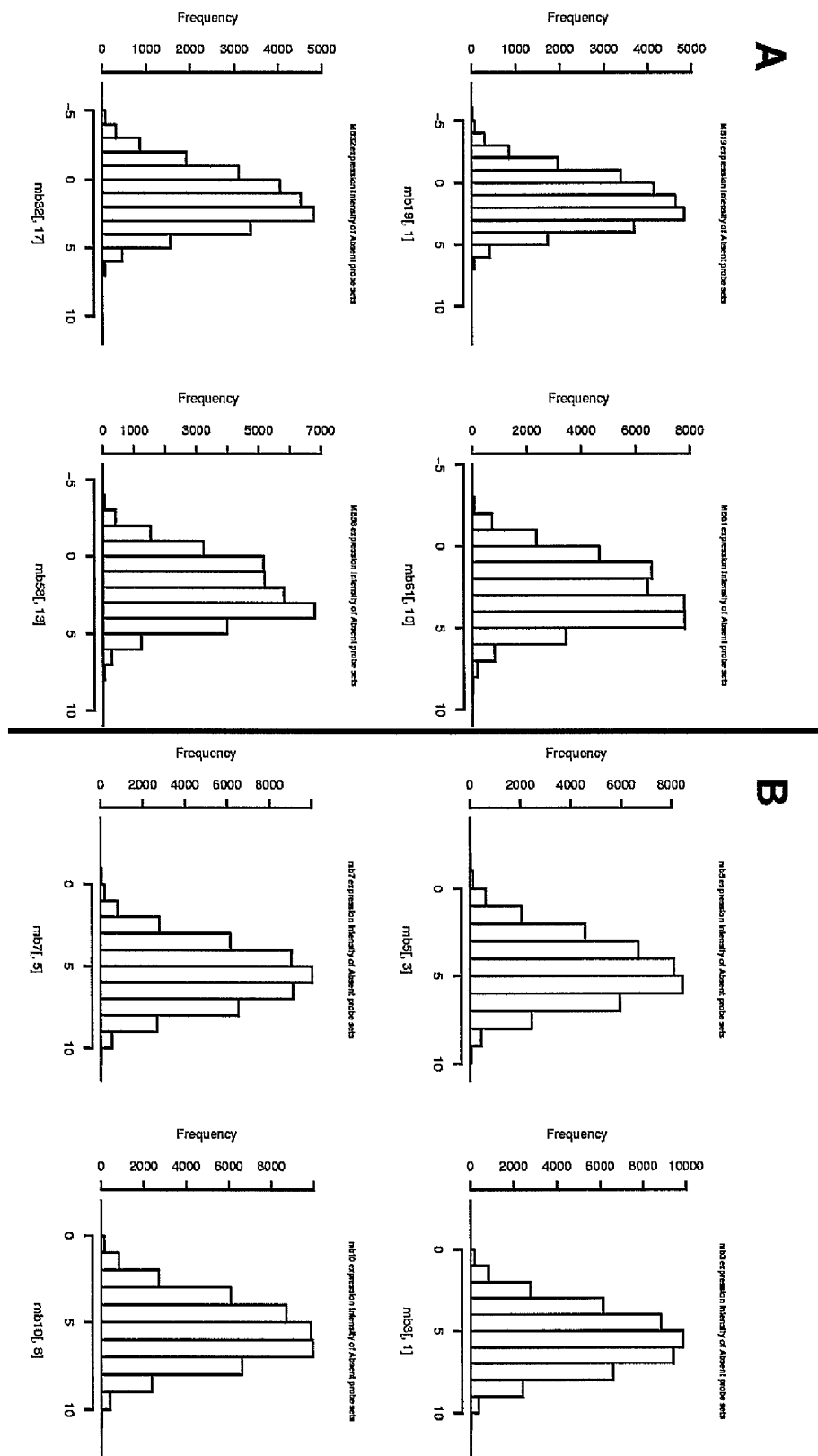


Figure 6.16: Plots from both the second (MBCF) (A) and first (Epistem Ltd) rounds (B) of microarrays showing the frequency of probesets called "Absent" by the MAS5.0 software (y-axis) and their corresponding \log_2 expression summaries (x-axis).

probesets are now called "Absent" despite a high expression signal. Figure 6.17A shows clear separation between the distribution of perfect match (black line) and mismatch (red line) expression summaries for three representative arrays from the second series of microarrays and this pattern is similar to that seen in cell lines MCF 7 and MCF 10a (Figure 6.17B) and is a huge improvement on the first data series (Figure 6.17C).

6.8 Determination of the Differentially Expressed Affymetrix

Probesets

As previously suggested by the scatter plots and PCA plots with ellipsoids, the differential expression of probesets appears greater in the comparisons between the three cell populations from the same histological tissue subtypes rather than between similar cell populations from the three different histological tissue subtypes. Indeed, in the latter comparisons (Table 6.15A, Figure 6.18) only one probeset has a log₂ fold change of -1 or more and this was evident in the comparison between BPH NSP and CaP NSP. A further probeset has a log₂ fold change of +1 or more between the CaP DSP and Normal DSP and the remaining 13 log₂ fold changes of +1 or greater are evident between the BPH NSP and Normal NSP (7), CaP NSP and Normal NSP (3) and BPH NSP and CaP NSP (3). Also in support of the previous data, the greatest differential expression is seen between the DSP and NSP, then the PSP and NSP and finally the DSP and PSP for each of the normal, BPH and CaP tissue types (Table 6.15B, Figure 6.18).

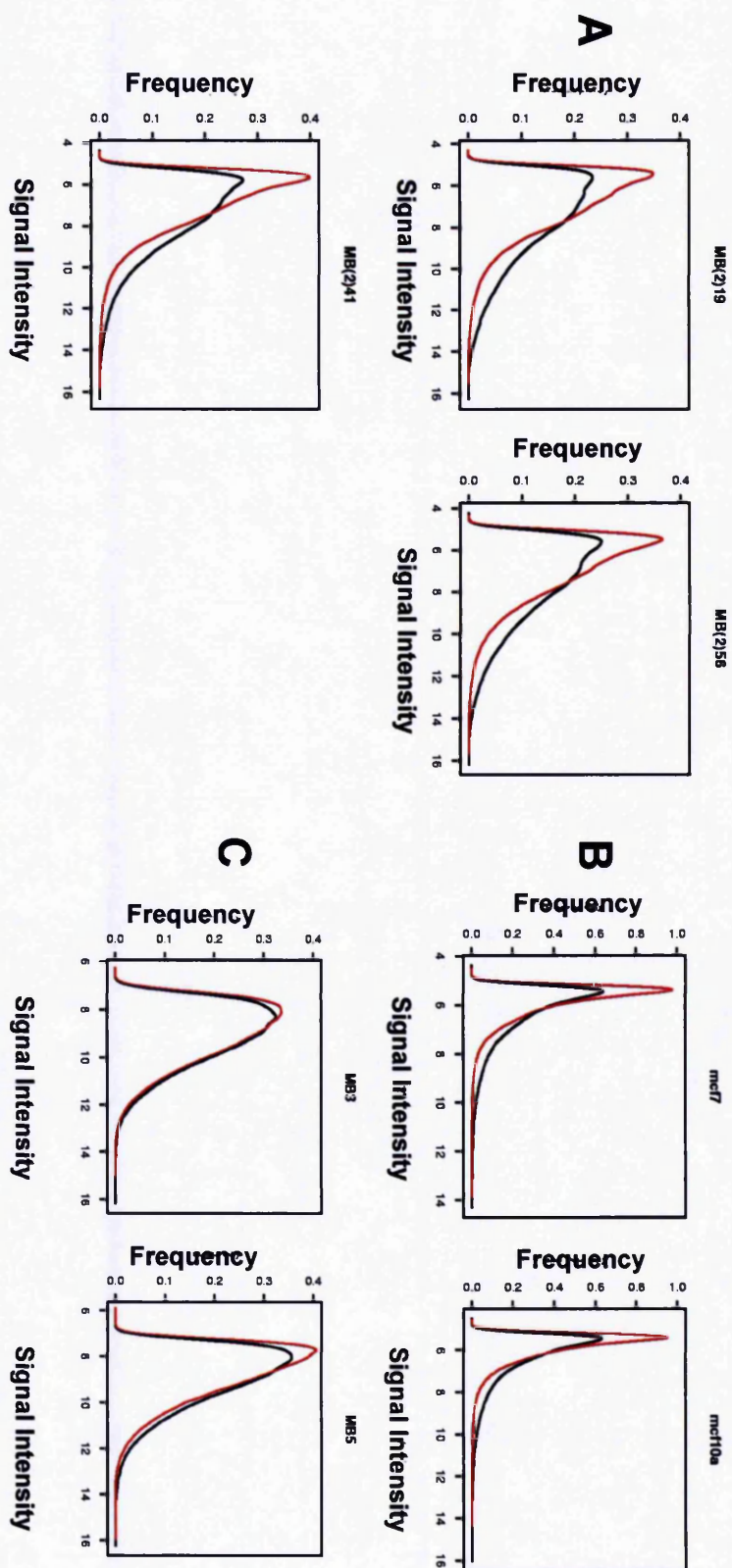


Figure 6.17: The frequency (y-axis) of both perfect match and mismatch probes at different signal intensities (x-axis). (A) Three arrays representative of the MBCF microarray data (a normal DSP MB(2)19, a BPH PSP MB(2)56 and a CaP NSP MB(2)41) are shown. The perfect match (black line) and mismatch (red line) expression data has been placed on the same plot and can be compared to (B) that of the cell lines MCF7 and MCF10a and (C) the first set of data from Epistem Ltd.

Number of Differentially Expressed Probes	Log2 Fold Change	DSP			PSP			NSP		
		BPH DSP vs. Normal DSP	Cap DSP vs. Normal DSP	BPH DSP vs. Cap DSP	BPH PSP vs. Normal PSP	Cap PSP vs. Normal PSP	BPH PSP vs. Cap PSP	BPH NSP vs. Normal NSP	Cap NSP vs. Normal NSP	BPH NSP vs. Cap NSP
		0	0	0	0	0	0	0	0	1
0	0	54675	54674	54675	54675	54675	54675	54668	54672	54671
1	1	0	1	0	0	0	0	7	3	3

Number of Differentially Expressed Probes	Log2 Fold Change	Normal			BPH			Cap		
		Normal DSP vs. Normal PSP	Normal DSP vs. Normal NSP	Normal DSP vs. Normal PSP	BPH DSP vs. BPH PSP	BPH DSP vs. BPH NSP	BPH PSP vs. BPH NSP	Cap DSP vs. Cap PSP	Cap DSP vs. Cap NSP	Cap PSP vs. Cap NSP
		11	2428	324	0	1175	166	3	624	34
0	0	54654	51059	53895	54675	52823	54197	54672	53634	54614
1	1	10	1188	456	0	877	312	0	417	27

Table 6.15: Table showing the number of Affymetrix probesets that were differentially expressed by at least a log2 fold change of +1 of -1 for each of the potential comparisons within (A) each of the three population types (DSP, PSP and NSP) and (B) each of the tissue types (Normal, BPH and Cap).

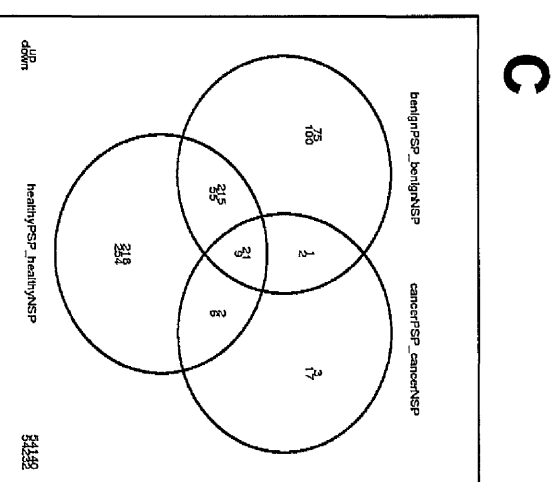
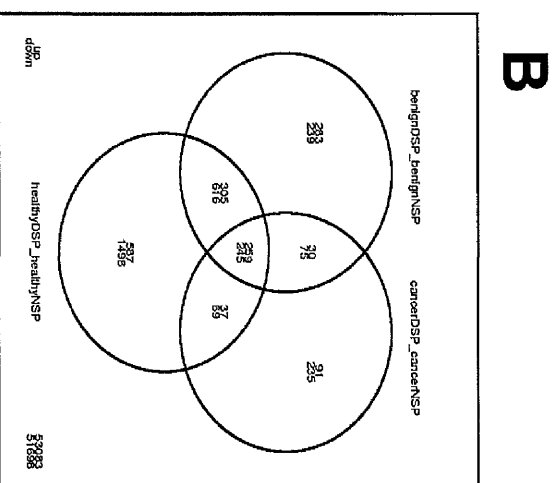
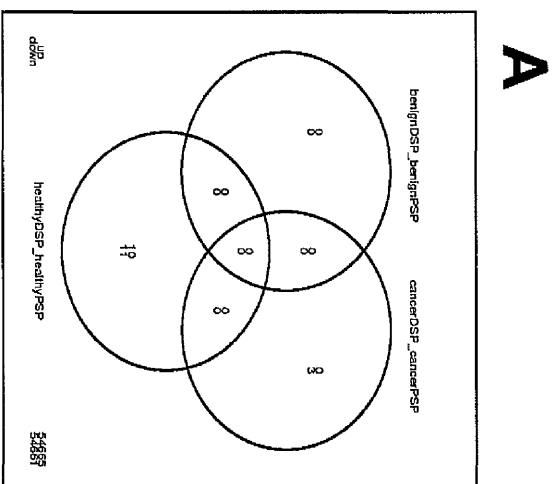


Figure 6.18: Venn diagrams illustrating the number of Affymetrix probesets that were differentially expressed by a log2 fold change of greater than +1 (top number) or by a log2 fold change of more than -1 (bottom figure) for each of the three histological subtypes. The results from comparison of the DSP and PSP (A), DSP and NSP (B) and PSP and NSP (C) cellular populations are shown.

6.9 Correlation Between Array Expression Data and Immunocytochemistry Phenotype

Initial analysis of the MBCF microarray data was conducted to specifically determine the differential expression of the probesets which corresponded to the putative SC and lineage-specific markers used in the immunocytochemical study of the DSP and PSP (section 5.5). Beta Catenin, Cleaved Notch and Androgen Receptor were markers used in the immunocytochemical analysis of the populations but they could not be identified from the array probeset lists. Where multiple probesets for the same marker existed in the microarray data, (p21, p63, PSA, SHH, CK8 and Notch-1), both were compared in turn to the fold changes from the immunocytochemical analysis. This introduced some potential difficulties as the log2 fold change between the DSP and PSP populations for these probesets had different polarities in p21, p63 and SHH. However, at least one of the versions of the duplicate probesets for each of these three markers had the same polarity to the immunocytochemistry fold change.

All the fold changes from both the array and immunocytochemical analyses are reported (Table 6.16) and those markers for which the fold changes are in the same direction are highlighted in yellow. Fold changes from the microarray probesets were validated by the immunocytochemistry fold changes for p21 microarray 0.144 Vs. immunocytochemistry 1.124; p63 -0.740 Vs. -4.506; PSA -0.397 Vs.

Marker	Affymetrix Probeset ID	Affymetrix Probeset Symbol	Description	Array Log2 Fold Change	Adjusted p Value	Immunocyte- chemistry Log2 Fold Change	p Value
p21	1555186_at	CDKN1A	cyclin-dependent kinase inhibitor 1A (p21, Cip1)	0.144	0.818	1.124	0.149
p21	202284_s_at	CDKN1A	cyclin-dependent kinase inhibitor 1A (p21, Cip1)	-0.130	0.815	1.124	0.149
p63	200998_s_at	CKAP4	cytoskeleton-associated protein 4	-0.740	0.642	-4.506	0.001
p63	200999_s_at	CKAP4	cytoskeleton-associated protein 4	0.289	0.754	-4.506	0.001
PSA	201454_s_at	NPEPPS	aminopeptidase puromycin sensitive	-0.367	0.704	-0.873	0.042
PSA	201455_s_at	NPEPPS	aminopeptidase puromycin sensitive	-0.342	0.758	-0.873	0.042
CK5	201820_at	KRT5	keratin 5	-0.623	0.818	-0.297	0.271
c-myc	244089_at	MYC	Similar to ORF 114	0.152	0.831	0.067	0.697
p27	203114_at	SSSCA1	Sjogren syndrome/scleroderma autoantigen 1	0.159	0.913	0.990	0.040
CD133	204304_s_at	PROM1	prominin 1	-1.323	0.731	-2.847	0.002
Msi-1	206333_at	MSI1	musashi homolog 1 (Drosophila)	0.290	0.803	0.481	0.642
SHH	207586_at	SHH	sonic hedgehog homolog (Drosophila)	0.091	0.883	-0.989	0.536
SHH	236263_at	SHH	sonic hedgehog homolog (Drosophila)	-0.534	0.609	-0.989	0.536
CK8	209008_x_at	KRT8	keratin 8	-1.157	0.503	-1.771	0.005
CK8	216821_at	KRT8	keratin 8 /// similar to keratin 8 /// keratin 8 pseudogene 9	-0.057	0.927	-1.771	0.005
Notch 1	218902_at	NOTCH1	Notch homolog 1, translocation-associated (Drosophila)	0.234	0.879	1.607	0.042
Notch 1	223608_at	NOTCH1	Notch homolog 1, translocation-associated (Drosophila)	0.299	0.592	1.607	0.042

Table 6.16: Table showing the log2 fold change between the DSP and PSP for the markers that had previously been utilised in the immunocytochemical determination of the DSP and PSP phenotypes. The log2 fold change between the DSP and PSP is also shown for the immunocytochemical assessment of marker expression. Those markers that had fold changes in the same direction are highlighted in yellow.

-0.873; CK5 -0.623 Vs. -0.297; c-myc 0.152 Vs. 0.087; p27 0.159 Vs. 0.990; CD133 -1.323 Vs. -2.847; Msi-1 0.290 Vs. 0.481; SHH -0.534 Vs. -0.989; CK8 -1.157 Vs. -1.771 and Notch 0.299 Vs. 1.607.

6.10 Identification of Appropriate Affymetrix® Probesets for

Subsequent qRT-PCR Validation of the Microarray Data

A more accurate method of validating the array data is qRT-PCR.

Suitable probesets were identified using the criteria described in section 2.13.5 (Table 6.17).

6.11 Summary of Chapter Results

Overall, data from sixty arrays has been generated and encompasses gene expression data for the DSP, PSP and NSP isolated from normal, BPH and CaP epithelial samples. Generally, quality control data for these arrays is far superior to that from the first attempt performed by Epistem Ltd and the vast improvement in the percentage of genes called "Present" is the best global measure of this. The observed improvement in array data quality appears to be a product of the improved RNA quality rather than quantity.

The favourable comparison of the observed gene and immunocytochemical marker expression fold changes for some of the putative SC and proliferation markers has reinforced the authenticity of the array data but more robust validation of the array is still required by qRT-PCR. Suitable probesets for such validation have been identified.

Probe Set ID	Gene Title	Gene Symbol	Biological Process	Cellular Component Term	Samples with Differential Expression	Log2 Fold Change
222108_at	adhesion molecule with Ig-like domain 2	AMIGO2	Cell adhesion	Nucleus / Membrane	Cap DSP Vs Normal DSP Normal DSP Vs Normal PSP	3.55 -3.35
219134_at	EGF, latrophilin and seven transmembrane domain containing 1	ELTD1	Signal transduction	Membrane	BPH PSP Vs BPH NSP BPH DSP Vs BPH NSP	4.11 3.71
204642_at	sphingosine-1-phosphate receptor 1	SPR1	Angiogenesis / Cell adhesion / Signal transduction / Cell migration	Membrane	Cap DSP Vs Cap NSP Normal DSP Vs Normal NSP	4.35 4.43
230061_at	Transmembrane 4 L six family member 18	TM4 SF18			Cap PSP Vs Cap NSP Normal DSP Vs BPH NSP	3.58 4.91
					Cap DSP Vs Cap NSP BPH DSP Vs BPH NSP	4.75 3.55
210815_s_at	calcitonin receptor-like	CACRL	Signal transduction / Heart development	Membrane	Cap PSP Vs Cap NSP Cap DSP Vs Cap NSP	4.72 4.72
201518_at	podocalyxin-like	PODXL	Negative regulation of cell adhesion	Membrane	Normal PSP Vs Normal NSP	2.84
203934_at	kinase insert domain receptor	KDR	Angiogenesis / Tyrosine Kinase Signaling / Cell differentiation	Membrane	Cap DSP Vs Cap NSP	3.82
212382_at	transcription factor 4	TCF4	Regulation of transcription	Nucleus	Normal DSP Vs Normal NSP	3.26

Table 6.17: Table showing the Affymetrix probe set ID number, the gene title, the biological processes with which it is associated and its site within the cell for eight probesets chosen for qRT-PCR validation of the microarray data series. Genes were chosen from the top of lists of the most differentially expressed genes (ie those with the most significant adjusted p-value). In addition to a large fold change, the chosen probesets had large mean expression values. However, the chosen genes were not differentially expressed between all the population and disease type comparisons therefore the samples between which differential expression was seen are documented. The log2 fold change for each of these particular comparisons is shown.

Chapter 7: Discussion

7.1 Overview

The adult tissue-specific SC is believed to be present in most human tissues and defined by the specific properties of self renewal, clonogenicity and pluripotentiality²⁷⁶⁻²⁷⁸. The SC is thought to play a key role in organogenesis as well as the homeostasis and repair of tissues. Despite their proliferative potential, SCs usually remain quiescent within their niche constituting only a small fraction of the total cellularity of a tissue⁵⁷¹. By the process of asymmetric division these primitive cells produce an identical copy of themselves, thus maintaining their own status, as well as a daughter cell that divides into numerous intermediate cell types termed committed progenitors or the TAP. Whilst having a limited phenotypic potential, the TAP expands the numbers of cells for which the differentiation pathway is now already determined and is responsible for generating the population of terminally differentiated cells of the mature tissue.

The attributes of self renewal and asymmetrical division in combination with their intrinsic growth potential, make SCs relevant to carcinogenesis^{286, 287}. The cancer stem cell theory has gained popularity and it is postulated that the CSC arises from the direct mutation of the normal SC or from de-differentiation of the TAP leading to a cell with stem-like properties^{290, 291}. Both BPH and CaP are diseases characterised by disruption of cell growth regulation within the prostate. There is gathering evidence that this arises because of disordered cellular control in the SC

compartment⁴⁰⁰. SCs are vital for normal prostate function, as illustrated by studies of androgen withdrawal and replacement, whereby the withdrawal precipitates prostate cellular regression to the basal layer of the prostatic acinus and subsequent hormone replacement stimulates regrowth from that same stem-rich compartment^{409, 411}.

Previously, the expression of cell surface markers has been used as the method of SC and CSC identification. Studies have suggested a number of candidate populations as being enriched for the prostatic SC and for progenitor cells. Such populations have been reported to be enriched for cells expressing the cellular markers CD44⁴³³, CD133^{432, 446} and $\alpha 2\beta 1$ ⁴³⁴. However, as yet, no consensus has been reached regarding a single SC or CSC marker in the prostate and the molecular markers that define the SC and CSC populations remain controversial⁵⁷².

This has lead to an alternative approach to identify the SC population based on their physical and physiological properties. One such mechanism for SC isolation is to exploit a cyto-protective mechanism possessed by non-committed SCs. SCs express ABC and MDR efflux pumps and thus are able to remove toxic metabolites and xenobiotics from the interior of the cell. This survival advantage is clearly beneficial to the organ or tissue as it is the SC that would survive and be able to repair and repopulate an injured tissue⁵⁷³. In the case of CSCs, these would potentially have greater resistance to therapy, a feature which could pre-dispose to disease resistance and/or recurrence⁴⁶³. The DNA-binding dye Hoechst 33342 is an example of one such chemical.

Because of this property, cells able to efflux Hoechst 33342 appear to the bottom left corner of a dual parameter FACS analysis as a Hoechst 33342^{lo} SP⁴⁴⁸. Goodell *et al*⁴⁴⁷ developed this technique to identify a population of cells from the mouse haematopoietic system that was able to actively efflux cytotoxic agents (such as the Hoechst 33342 dye): the SP displayed enrichment for characteristics consistent with stem-like behaviour. Subsequent work (reviewed by Challen and Little⁴⁵⁰) has identified an SP in various solid tissues including breast^{371, 372, 574}, skeletal muscle^{454, 455}, intestinal tract⁴⁵², liver⁴⁵³ and brain⁴⁵¹. An SP has also been identified and characterised in the prostate^{431, 458}, the kidney^{456, 575} and bladder⁵⁷⁶.

The GUCR Group at the PICR has adopted and utilised the Hoechst 33342 dye efflux technique of SC enrichment in the prostate and have previously shown the SP from prostate epithelial cells to be enriched for quiescent cells with SC properties^{431, 458}. However, whilst it is believed the SP contains the SC, it has been acknowledged that it remains a heterogeneous population in need of further purification⁵⁷⁷.

Genetic characterisation of the SP and NSP was performed with the hope that new markers specific to the SC-enriched SP would be identified to aid prospective SC isolation. Furthermore, genetic analysis of the SP and NSP would help to determine the molecular pathways specific to SC homeostasis and the changes that confer a genotype consistent with BPH and CaP. Accurate identification and isolation of such SCs/CSCs would afford the opportunity to determine the underlying

mechanisms of disease, with the ultimate aim of developing novel diagnostics, new prognostic markers and targeted treatments.

7.2 The Epistem Ltd Microarray Dataset

CD133 has emerged as a putative SC marker in BPH and CaP^{432, 446}. As part of a previous project, an attempt was made to improve the purity of the heterogeneous SP by additional CD133⁺ selection, thereby combining two proposed mechanisms of SC enrichment. The resultant size of the populations that were isolated meant that the cell number was very low (BPH SP mean 703, SD± 635 and BPH NSP mean 3716, SD± 4036) making further study challenging. At the time, chemistries to support microarray analysis of these populations were not widely available. Epistem Ltd offered a small cell number microarray service and they were therefore commissioned to extract the RNA from the small cell number populations and perform the microarray analysis.

The first microarray series used prostate epithelial samples taken from BPH patients and was performed to determine the genetic signature of the SP and NSP in benign tissue. The first dataset from Epistem Ltd produced poor quality data (Chapter 3). The very low number of genes called "Present" for these eight arrays by the MAS5.0 software (mean 13.15%, SD±4.84%) was felt to be the ultimate measure of this poor quality.

Technical data from Affymetrix indicates that the precise proportion of the probesets that are called "Present" on an array depends upon the

cell or tissue type being studied and the biological and environmental stimuli to which it has been subjected. In addition, a low percentage of genes called "Present" may be secondary to poor quality samples⁵⁷⁸. No specific values indicative of acceptable data are available in press. Furthermore, detailed quality control statistics are rarely reported alongside the differential gene expression data available in the literature. The range for genes called "Present" that is usually accepted as being indicative of good quality data is between 45% and 55% (personal communication with Dr Stuart Pepper at the MBCF). The proportion of genes called "Present" may not in itself be an unacceptable finding in a series from a quiescent SP, as the number of transcripts expected would be low. However, against this and supporting the suggestion that the low gene call was related to poor quality RNA, was the fact that the percentage of genes called present in the NSP was also low. The "noisy" heterogeneous data evident on the scatter plots of the SP versus NSP expression summaries, the poor biological comparability of arrays evidenced by the cluster dendrogram, the low Pearson correlation coefficients (0.48-0.74) and the poor correlation between log2 expression summaries for probesets and their MAS5.0-generated gene detection calls provided further reinforcement of the conclusion that the quality of data was low. Taken together, this information shows that the quality of data from this series was low and was of insufficient quality for meaningful differential gene expression analysis.

Before interrogating the list of differentially expressed genes for biological significance, the fold changes between the SP and NSP

epithelial populations reported by the microarray had to be validated. The accepted method of achieving this is to examine selected probesets by qRT-PCR to ensure that the microarray fold changes between the two populations can be reproduced and therefore that the array data is genuine. To maximise the chances of reproducing such fold changes, probesets with large fold changes were targeted for further study. The filtering method for selecting such probesets (section 2.12.3) was suggested and endorsed by the CRUK MBCF but failed to provide sufficient numbers of suitable probesets to validate the arrays. Such difficulty in identifying suitable probesets provided further support for this being a heterogeneous dataset of poor quality. As a consequence, the data was not deemed suitable for the datamining of genes for biological significance.

The poor quality microarray data from the Epistem Ltd series is likely to be partly attributable to the isolated populations containing small cell numbers (mean 968.63 SD ± 219.58 cells), particularly from the CD133⁺ SP, as well as the low mRNA yield (mean 5.66ng SD ± 1.05 ng). In turn, the low mRNA yield was not only a reflection of the small cell number but was also shown to have degraded during the processing of the epithelial samples. Despite the use of sterile experimental conditions, the long experiment time (typically ten hours from completing epithelial cell isolation to RNA extraction) is likely to have exposed samples to the effect of RNases particularly during FACS.

The quality control statistics for the Epistem Ltd samples revealed a high mean background signal of 113.2 (reference range 20-100⁵⁷⁸) and evidence of transcript degradation based on the high 3'/5' ratios of the housekeeper control sequences β -actin (mean 2.03) and GAPDH (mean 6.21) (reference range ≤ 3 ⁵⁷⁸). Whilst the β -actin ratio was still passed as acceptable by the MAS5.0 software, the GAPDH ratio was deemed unacceptably high. β -actin is a shorter mRNA transcript and therefore is less likely to be affected by degradation. Indeed, lack of sequence integrity and therefore poor mRNA quality was probably the single most important contributory factor to explain the low number of genes that were called "Present" and consequently the poor microarray data.

7.3 Steps Taken to Optimise the Affymetrix Microarray Data

7.3.1 Minimisation of the Effect of RNase Degradation of Transcripts

RNA quality was shown to be poor with evidence within the quality control statistics revealing marked RNA degradation. Ribonuclease (RNase) catalyses the degradation of RNA into smaller fragments. Whilst this has an important role *in vivo*, RNase is an important cause of transcript degradation during mRNA isolation and expression analysis. Degradation of transcripts by RNases was successfully reduced by the introduction of RNase-free adjuncts to the FACS protocols (Chapter 4). The first attempt at examining the effect of RNase-free protocols on RNA quality used five paired CD45^{-ve} SP and NSP epithelial cell fractions and revealed the need for on-column DNase treatment to minimise the

contamination of the electrophoretic output with genomic DNA. Elution of the extracted RNA in 30µl of RNase-free water and subsequent concentration of the volumes to approximately 10µl increased the RNA concentration and therefore improved the detection of ribosomal RNA peaks. Whilst elution volume and concentration of samples will not have affected the RNA quality it was essential to ensure the RNA could be detected and measured. SP and NSP samples from the same patient were split into two with one SP/NSP pair being sorted by an RNase-free protocol and the other by the standard protocol. The RNase-free samples were always processed first as the FACS machine required preparation and priming with the DEPC-treated PBS buffer. The buffer was changed for normal PBS before processing the standard samples. A limitation of this precise ordering of samples for FACS was that the standard samples would have had longer to be exposed to any RNases that were present whilst the RNase-free FACS was undertaken. This was limited to 20-30 minutes and the samples remained on ice in sealed tubes throughout. This delay was felt to be inevitable and ultimately acceptable. Any bias introduced would be countered by the fact that the cell sorter would still initially be low in RNase activity on commencement of the standard FACS. Thus the RNA quality of the samples sorted by standard techniques may be falsely raised with the observed difference in RNA quality between standard and RNase-free sorted samples actually being greater.

The amounts of RNA yielded by the Epistem Ltd RNA extraction protocol was greater for the SP than the NSP (mean SP 7.4pg, SD± 2.9pg per

cell vs. mean NSP 5.3pg, SD \pm 0.7pg per cell) though this did not reach statistical significance. This was a surprising finding given the evidence in the literature from the GUCR group showing the SP-enrichment for quiescent cells in G0^{431, 458}. Quiescent cells should in theory produce lower transcript numbers therefore such a finding may suggest that the SP still has a heterogeneous phenotype. Furthermore, this finding may be an artefact of the observed RNA degradation, with amounts of RNA procured from each population being altered to such an extent that the true relationship between the mRNA yields from the SP and NSP could no longer be identified.

The same finding was not seen when the SP and NSP populations were compared during the experiments to determine the effects of RNase-free (RNAF) adjuncts to the FACS protocols. In line with the expected observations, the average RNA yield was greater from the NSP than SP (mean standard SP 0.183pg/cell vs. mean standard NSP 0.499pg per cell and mean RNAF SP 0.270pg/cell vs. mean standard NSP 0.408pg per cell) though not to a statistically significant degree. The amount of RNA extracted from the SP was improved from 0.183pg/cell to 0.270pg/cell with the addition of RNase-free adjuncts.

The amount of RNA extracted from both the pilot experiment to determine the use of RNase-free adjuncts and the MBCF microarray series was considerably lower than the amounts put forward to the EpiAmpTM step of the Epistem Ltd protocol. However, the improvement in RNA quantity extracted from the same populations with the addition of

RNase-free adjuncts was matched by the improved quality. Again, no statistical significance was reached but a trend towards an improved RIN score was seen when RNase-free cell sorting was undertaken (RNAF SP 7.54 vs. standard SP 4.44 and RNAF NSP 7.58 vs. standard NSP 7.18). More importantly, all of the SP samples provided good quality RIN scores and only the samples sorted by standard protocols were lost to RNA degradation as evidenced by a RNA Integrity Number (RIN) score of one. In conclusion the role of RNase-free sorting appears to be to offer some improvement in RNA quality and quantity but more importantly it appears necessary in preventing the serious consequence of losing an entire sample to RNase activity during the analytical process.

7.3.2 Subfractionation of the SP Tail into the Distal (DSP) and Proximal (PSP) Subpopulations

The minimum amount of cDNA currently required for hybridisation to the HG-U133_Plus 2 array is 5µg. To ensure that adequate numbers of cells (and therefore mRNA) were isolated, CD133 selection of the entire epithelial population was no longer used. Instead CD133 was used to define the DSP and PSP and the functionality of the Hoechst 33342 dye efflux assay with CD45^{-ve} selection to exclude the lymphocytes was relied upon entirely. Rather than extract RNA from the entire SP, attempts were made to enrich the population further by subfractionating the SP tail into two subpopulations (DSP and PSP). This was seen as a logical methodological step to enrich the SP as the Hoechst 33342^{lo} SP

in the haematopoietic system had shown enrichment for SC properties compared with the subfraction of the SP tail with higher Hoechst 33342 concentration.

Previously, investigators have subfractionated the SP tail into subpopulations based on their differential ability to efflux dyes. It has been shown that the distal tip of the SP tail has the highest ability to efflux Hoechst 33342 dye and this correlates with enrichment for progenitor activity^{579, 580}. As the expression of the dye efflux pump ABCG2 may be a direct measure of cellular differentiation with the expression falling as the cellular population matures²⁹⁰, it has been suggested that isolation of cells with the highest dye efflux capabilities will provide further enrichment for primitive cells⁵⁷². Furthermore there had been consistent evidence of a DSP based on differential CD133 expression throughout the early study of the CD133⁺^{ve} Hoechst dye efflux FACS analysis (discussed further in section 7.5.2).

7.3.3 Cellular Amplification Versus Amplification of the Transcriptome

The EpiAmp™ system for RNA amplification employed by Epistem Ltd uses the Oligo dT method of transcript amplification. A sequence of adenine bases at the 3' prime end of a transcript encodes for the amplification of that transcript by an amplification primer with complementary thymine bases. Although probesets are clustered towards the 3' prime end of a transcript, fragmentation of transcripts has greater significance when the Oligo dT method is employed as only the

sequence in continuity with the adenine start sequence will ultimately be amplified. As already mentioned, transcript degradation was evident in the Epistem Ltd series and therefore the resultant effect this had on Oligo dT priming may have been to contribute to the low gene call in the Epistem Ltd series. Technical data for the EpiAmp™ system is not available.

Since acquisition of the first microarray dataset from Epistem Ltd, new RNA amplification chemistries have become available commercially, allowing gene expression analysis of small cell number samples. The NuGEN WT-Ovation Pico RNA amplification system v1.0 is utilised in the MBCF protocol for small cell number microarray and provides a sensitive, reproducible and reliable method for amplification of the entire transcriptome. Amounts of total RNA as low as 5-50ng have been amplified to microgram quantities of cDNA across a broad range of transcript abundance without a 3' bias. The manufacturers recommend that as little as 0.5ng can be reliably and reproducibly amplified. Differential gene expression has also been shown to be conserved⁵⁸¹. Improved amplification is achieved as it employs random primers, which generate amplified transcripts from both intact and fragmented mRNA transcript, as well as Oligo dT priming. This is likely to be an extremely important reason why the gene call was improved⁵⁸¹.

The primary tissue samples acquired at TURP or radical cystoprostatectomy were often relatively small and yielded low cell numbers. In addition, the SC is a rare and quiescent cell and so not only

are the putative SC population samples harvested low in cell number (Benign 0.93-1.0%^{431, 432} and CaP 0.1-0.57%^{431, 446}) they are also likely to have low numbers of mRNA transcripts. Extraction of sufficient mRNA from such SC-enriched samples is therefore challenging. Primary tissue was preferred to immortalised cell lines so as to ensure the SC population had not been manipulated and that it was totally representative of the pathological process in humans.

Due to the low cell numbers isolated by the Hoechst 33342 dye efflux assay with additional CD133 selection and the resultant effect on the quantity of RNA extracted, it was desirable to increase the amount of RNA available for subsequent array hybridisation. In order to increase the constituent cell numbers and consequently the RNA yields, some groups have favoured amplification of small SC-enriched populations by cell number expansion in culture^{546, 547}. The concerns about cell culture expansion after initial selection for a particular phenotype is that the culture may induce genetic drift such that the population studied after culture is not the same as that originally selected. Groups that have employed this approach of amplifying the cell numbers by culture argue that the SC population occupies a given proportion of the overall cell population and that, by using a specialised serum-free culture medium and feeder layers, the proportion of cells does not change but merely the entire cell number is increased^{546, 547}.

Collins *et al* reported that although some degree of cellular differentiation was observed under serum-free culture conditions, increased expression

of standard differentiation markers like prostatic acid phosphatase (PAP) and AR were only seen once serum was added to the media. The proportion of CD133^{+ve} cells within those samples placed in culture prior to analysis remained relatively constant and was not significantly different from the proportion seen in primary samples isolated and studied directly from fresh tissue ⁴⁴⁶. The same group reviewed the evidence surrounding the use of expansion of cell numbers in culture ⁵⁴⁶. Firstly, they claimed to confirm the CaP phenotype by the use of several established CaP markers including alpha-methylacyl-CoA racemase and matrix metalloproteinase 9 (MMP9) and thereby commented that expansion of the CaP epithelial cell populations did not introduce overgrowth of any contaminating benign epithelial populations. It has been noted that *ex vivo* and *in vitro* transcriptional profiles did differ by 2.1% (human dermal lymphatic endothelial cells) and 4% (blood endothelial cells) in a study by Wick *et al* but it was suggested that this may have been partly related to methodological differences between the labelling of the *ex vivo* and *in vitro* populations ⁵⁸². A study using hepatic stellate cells initially reported showing substantial differences in the transcriptional profiles of primary and cultured cells but that this effect was nullified when the cells to be cultured were grown with a Kupffer cell feeder layer ⁵⁸³.

As part of their study into CD133-based gene expression profiling, Shepherd *et al* had needed to expand their CaP samples as a consequence of low cell number. They aimed to quantify the effect cell culture expansion had on the transcriptome. The group confirmed a

progressive drift of the molecular profile of CD133⁺ selected cells cultured beyond one passage and therefore limited their study to single passage cells⁵⁴⁷. To validate their results they had expanded a representative portion of four primary BPH samples and compared the resultant gene expression profile to that of the uncultured cells from the same patient. Hierarchical clustering revealed that the cultured cells did not cluster away from the uncultured cells and that all CD133⁺ cells clustered away from the CD133⁻ population. However, the cultured and non-cultured cells shared only 46% of the top 50 differentially-expressed genes and principle component analysis did eventually separate the profiles derived from cultured and uncultured cells.

Our study opted for RNA amplification as the method for gaining a sufficiently large transcriptome for array hybridisation. This afforded the opportunity to study the transcriptome specific to a particular population at a specific time point. Isolation of sufficient RNA for high-throughput genomic methodologies such as the Affymetrix HG-U133_Plus 2 microarray may not be a significant problem for whole organ or regional tissue series but study of the transcriptome from small or single cell populations (population cells analysis) is often not possible using standard procedures⁵⁸⁴. Amplification of large numbers of differentially expressed genes by enzymatic manipulation of RNA or cDNA can still distort the *in vivo* genetic relationships of cell populations. Generation of high quality amplified RNA that is representative of the original mRNA isolated from a given cell population is vital.

The MBCF microarray series used the NuGEN amplification protocol. The manufacturers validate its use for 0.5ng of starting RNA and above though lower amounts were, on occasion, used in this study. The NuGEN protocol uses both random primers as well as oligo dT priming, generating labelled single stranded cDNA which is then hybridised to the array. Hybridisation of DNA to DNA microarrays gives lower background signals and consequently a cleaner result than when cRNA is hybridised. The percentage of genes called "Present" is in the region of 5% higher when using the Affymetrix HG-U133_Plus 2 arrays ⁵⁸⁵.

Shepherd *et al* amplified up to 2ng of total RNA using the Arcturus HS RiboAmp kit (Arcturus, CA, USA). RNA was converted to cDNA and then back to cRNA before a second round of amplification was performed and cRNA was hybridised to a smaller array manufactured by CRUK comprising only 28 thousand probesets compared to the 47 thousand on the HG-U133_Plus 2 array ⁵⁴⁷. Birnie *et al* used the HG-U133_Plus 2 array and the Affymetrix amplification protocol which employs the same RNA to cDNA to cRNA workflow with cRNA hybridisation to the array ⁵⁴⁶. Both studies used oligo dT priming only. Whilst the isolated RNA in the MBCF microarray series had been amplified, these CD133-based series had expanded their cell numbers in culture and amplified the resultant transcriptome, thereby increasing the potential for associated biases.

Whilst amplification of the mRNA is still required to gain sufficient genetic material for array hybridisation, the commercially available linear amplification chemistries have been subjected to robust quality control

measures such that errors induced by the chemistries can be accommodated and corrected for in the final data series. Although it did not directly study the NuGEN RNA amplification system used in our repeat microarray study performed in the MBCF, a study of two cell lines showed that the microarray fold changes are highly consistent between samples processed by either standard labelling protocols or following an amplification protocol and that systematic biases introduced by amplification can be accounted for providing the correct data analysis techniques are employed⁵⁸⁶.

7.4 The Molecular Biology Core Facility Microarray Dataset

7.4.1 Improvement in Data Quality

The Hoechst 33342 dye efflux assay was adapted to improve the quality of mRNA for microarray analysis. However, comparison of the two samples directly has been hampered by the fact that the two quality control systems used were different. This stemmed from the change in protocol in the time period between the first and second microarray series. Furthermore, the precise subpopulations of prostate epithelial cells being studied had changed. No RNA quality control data was produced for the Epistem Ltd series; instead the available data details the quality of amplified cDNA by agarose gels. The quality control measures used for the second set of microarray experiments performed in the MBCF used the Agilent Bioanalyzer 2100 and the RNA 6000 Pico Labchip. This system provided a more objective determinant of RNA quality through its use of the RIN score. Whilst the quality control data

from the Epistem Ltd and MBCF series cannot be directly compared, the quality of the cDNA hybridised to arrays in the MBCF did appear superior to that inferred by the cDNA quality in the Epistem Ltd series. Of those samples put forward for cDNA amplification, the mean RIN was 6.3 denoting good quality RNA. There were four normal DSP, two BPH DSP, two CaP DSP and one CaP PSP samples that were also put forward to cDNA amplification despite RIN scores of ≤ 1 . Regardless of this reduction in quality, all the samples apart from one (GU13 DSP) could be satisfactorily amplified to produce the required amount of cDNA for array hybridisation ($>5\mu\text{g}$) and produce improved "Present" gene calls (32.1%-51.7%) compared to the Epistem Ltd series. Even GU13 DSP yielded $4.1\mu\text{g}$ of cDNA and resulted in a gene call of 23.7%, which was only marginally lower than the best array from the Epistem Ltd series (16016 NSP1 25.9%) which in turn was considerably better than the remaining seven. Satisfactory gene calls were achieved but the decrease in RNA quality for these nine samples will need to be taken into consideration when interpreting the gene expression data for biological significance. The samples, particularly GU13 DSP, may need to be excluded and replaced with additional replicates. The scale factor required to normalise the GU13 DSP array data was the only one which was not within 3-fold of the other 59 and therefore further supports its exclusion before gene expression analysis.

Improved RNA quality is likely to have resulted in the superior microarray data in the MBCF series. Compared to the Epistem Ltd series, the MAS5.0 quality control statistics revealed that background fluorescence

(mean 33.34, range 27.15-70.56) was improved over three-fold and was now within the limits generally accepted by Affymetrix® (reference range 20-100). The 3'/5' ratio for GAPDH was now acceptable with a mean value of 0.62 (reference range ≤ 3). However, the 3'/5' ratio of β -actin showed slightly more degradation with a mean value of 3.12 (reference range ≤ 3). This suggestion that the transcripts were more degraded did not fit with the perceived improvement in RNA quality. When the individual expression summaries and signal intensities for the β -actin and GAPDH housekeepers were analysed it was apparent that the β -actin was probably not degraded after all as the expression summaries remained high. The high 3'/5' ratio was actually a product of exceptionally high signal intensity values at the 3' end of the transcript rather than reduced signal because of degradation at the 5' end. Rather than transcripts degrading from the 5' end and therefore raising the 3'/5' ratio, the 5' expression summaries appeared congruous with other series analysed by the MBCF and the GAPDH expression values from this series. Instead the 3' signal intensity was unusually high and caused an artefactual rise in the 3'/5' ratio. The same phenomenon was seen when the raw data from other series was reviewed and ultimately it was decided that the inference of poor quality data from the high 3'/5' ratio for β -actin could be ignored⁵⁸⁷.

The consequence of improved RNA quality was that the microarray data was much improved with the proportion of genes called "Present" being excellent (mean 50.19%, $SD \pm 6.83\%$) and in the region expected of microarray series acquired from cell lines (45-55%). The data was less

heterogeneous than the Epistem Ltd series with improved Pearson correlation coefficients (0.762-1.00) and the heatmaps, PCA plots and cluster dendrograms all providing evidence of arrays from each of the three populations studied (DSP, PSP and NSP) clustering with arrays from the same subpopulation. There was greater concordance between the raw expression values and the assignment of the "Present" "Marginal" and "Absent" gene detection calls by MAS5.0.

qRT-PCR validation of the arrays is still required. Unfortunately, this could not be achieved within the timescale of this project. However, there were no problems in identifying suitable probesets and a list of eight suitable probes for validation has been generated. Preliminary validation of the fold changes has been achieved by drawing comparisons with the markers used in the determination of the immunocytochemical phenotype of the DSP and PSP, with all the immunocytochemical markers represented on the microarray showing differential expression and fold changes in the same direction as the immunocytochemical markers. The biological significance of this will be discussed in more detail in section 7.5.4.

The degree of differential probeset expression inferred by the scatterplots (Figures 6.8-6.10) appears superior to that reported by Table 6.15 and the Venn diagrams in Figure 6.18. It should be noted that the scatterplots report the mean log₂ expression of all probesets between two populations isolated from each of the three disease groups. Table 6.15 and the Venn diagrams reported only the number of

probesets that were differentially expressed (log2 fold change ± 1) to statistical significance (adjusted p-value of <0.01) between particular sample subtypes.

Whilst accepting that the data still requires validation, the microarray series created and analysed in the MBCF suggests differential expression between the DSP, PSP and NSP within each of the sample types (normal, BPH and CaP). The degree of differential expression is greatest between the DSP and NSP, followed by the PSP and NSP and finally the DSP and PSP. Log2 fold changes of greater than plus or minus one showed that apart from one gene being up-regulated in the CaP DSP compared to the normal DSP, differential expression of genes from the same population between different tissue types was only seen when the NSP was compared. As the NSP phenotype is consistent with the differentiated prostate epithelial cell phenotype⁴³¹, this differential expression is likely to be representative of the altered luminal phenotype seen in BPH and CaP. The probeset that was differentially expressed between the CaP DSP and normal DSP (222108_at, adhesion molecule with Ig-like domain 2, AMIGO2) is linked with cell adhesion and negatively regulates programmed cell death. Providing qRT-PCR validation of the microarray data is successful, this probeset would provide an exciting start point for biological datamining, as both cell adhesion and manipulation of the apoptotic pathways may potentially be representative characteristic of CSCs.

7.4.2 Limitations of the Dataset

The advantage of the MBCF series is that much more information is gleaned. In addition to the subfractionation of the SP tail into DSP and PSP, the second series was expanded to look at these three populations in normal, BPH and CaP samples whereas only BPH was studied in the Epistem Ltd series. This potentially allows comparison of the various populations' gene signatures and therefore determination of important SC-specific genes and the determination of how such genotypes may alter between normal and diseased tissues. However, the observed differential gene expression patterns showed only one gene to be differentially expressed between the normal and CaP DSP with the remaining difference of expression being between the normal, BPH and CaP NSPs and between each of the three subpopulations within each of the tissue types. Therefore the hierarchical clustering pattern of genes for the DSP, PSP and NSP within each tissue type will need to be interrogated to glean the individual differential gene expression patterns for given tissue and these gene signatures will require correlation globally with the other histological types to determine the presence of any conserved or altered patterns of expression. Detailed datamining of the differentially expressed genes will also have to include examination of those probesets that have more subtle fold changes of less than a \log_2 value of one.

There is debate amongst investigators as to the precise source of the CSC. Some believe that it is a mutated normal SC. Others believe it is a

TAP cell that has de-differentiated and regained some properties of the SC^{287, 588}. As a consequence, in addition to the comparison of the DSP from one tissue type solely with another, comparisons should also be made between all the different populations from each of the three histological subtypes. Functional assessment of the three subpopulations is required so as to ultimately determine which of the populations is likely to contain the SC, or more precisely in the case of cancer, the cancer-initiating cell.

The three histological subgroups of epithelial cells used in the second series of microarray experiments were normal, BPH and CaP. Whilst the gene expression analysis of entire populations from normal, BPH and CaP tissues has been performed, no studies are known to have examined the SC-enriched population across all three histological subgroups with the majority of studies favouring comparative analysis between only two of the three. This highlights this study as unique.

Normal tissue was obtained from prostates removed as part of the cystoprostatectomy specimens of patients undergoing surgery for bladder malignancy. Ensuring the tissue was normal is difficult and the phenotype of the cells actually put forward for *in vitro* experimentation is based on the histological examination of samples representative of the entire research sample. Efforts were made to ensure that tissue removed from cystoprostatectomy specimens appeared macroscopically normal. Histological review of a representative portion of the research sample was undertaken and the formal report of the remaining tissue

was reviewed to ensure there was no other significant pathology. Some of the normal samples were contaminated by inflammatory tissue. Only one of the reports commented on the presence of BPH though this is not to say that BPH was not evident in other samples as the slides themselves were not re-reviewed. Two samples (15668 and 14812) were excluded from analysis of the differential gene expression as low volume Gleason 3+3 CaP was identified in the main operative specimen. Whilst no evidence of CaP was seen in the representative research samples, which in turn did not encroach on the areas of CaP, it is possible that the genotype of the prostate in these "normal" patients had been altered due to a generalised field change. Indeed, subtle nuclear changes have been reported in epithelial cells adjacent to areas of CaP in RPs⁵⁵⁵. Furthermore, sample 14812 was also excluded as pre-operative trans-urethral biopsies of the prostatic urethra revealed involvement with TCC.

It is worthy of note that three patients (GU39, GU11 and 15992) received neo-adjuvant chemotherapy. It is unknown what effect this may have on the phenotype of these patients' tissues but hypothetically it may alter the hierarchical balance between the SP cells that are able to efflux such xenobiotic agents (reviewed by Hadnagy *et al*⁵⁷²) and the NSP cells that are chemosensitive with these tissue comprising a higher proportion of cells that are resistant to treatment. Similarly, two of the BPH patient samples (GU64 and GU84) had been treated with a 5 α -reductase inhibitor prior to TURP.

Coexistent malignancy within the BPH samples was excluded to the greatest extent possible. In addition to the histological examination of representative samples taken from each individual TURP chip and correlation of this with that of the main operative specimen, only those patients who had undergone at least one TRUS and prostate biopsy and had been shown to have no malignancy or those patients who had a PSA within the age-related normal range ¹⁵⁷ were included within the cohort.

TURP chips were the source of all CaP prostate epithelial cells. The patients were undergoing bladder outflow surgery to alleviate the lower urinary tract symptoms associated with their disease. Many patients in this clinical situation are already receiving hormone manipulative therapies which may alter the phenotype of the populations isolated. Despite this, three samples (16189, 16143 and 15457) from the series of six were retrieved from patients with primary unmanipulated CaP. These patients had undergone a bilateral subcapsular orchidectomy (BSCO) during the same operative session as their TURP and provided a rare opportunity to study primary unmanipulated CaP acquired by TURP. A limitation of TURP specimens in the provision of CaP material is that there is usually contamination with normal and BPH tissue. An attempt to minimise the impact of this was made by only analysing those patients whose representative research samples were shown to have a large proportion of the core involved (>40%). Furthermore, in an attempt to maximise the differential expression of genes, high grade tumours were selected (combined Gleason scores of 3+4=7 and above). The gene

expression analysis performed by Birnie et al was only able to achieve a differential gene expression profile for CaP patient samples with a minimum combined Gleason score of seven. Inclusion of samples taken from CaP tissue with combined Gleason score of 3+3 meant that the malignant gene expression profiles could not be segregated from BPH. Notwithstanding this we have deliberately selected for tumours with a combined Gleason score of 3+4 and greater, future work will have to extend the profiling to lower grade tumour though sampling of them may be more challenging.

7.5 Refinement of the Hoechst 33342 Dye Efflux Assay

7.5.1 Overview

The traditional stochastic theory of cancer suggested that any cell within a tumour population had the potential ability to proliferate extensively and induce carcinogenesis (reviewed by Ward and Dirks ⁴⁷²). The life span of differentiated cells is comparatively low and it seems unlikely that such a cell would survive long enough to receive the necessary number of mutations required for carcinogenesis and tumour formation. Many investigators now favour the SC theory of cancer ²⁹⁰. The relative quiescence and prolonged life span of the stem population means the cells are exposed to multiple potential carcinogenic events and are therefore more likely to develop oncogenic mutations which are maintained by asymmetric division and consequently long term self renewal ^{589, 590}. Furthermore, the ability of SCs or CSCs to produce a number of phenotypically distinct lineages offers explanation for the

observed heterogeneity of tumours. Failure to adequately treat the mutated CSC results in a persistent potential for disease recurrence as the CSC has the ability to repopulate the entire tumour.

Over the last decade several specific prostate SC markers have been proposed including $\alpha_2\beta_1$ -integrin and CD44^{+ve} ⁴³⁴. However, it is the haematological marker CD133 that has gained favour. CD133 (Prominin-1) is a five domain transmembrane glycoprotein within the outer cell membrane and it has been shown to be a marker for primitive haemopoietic cells. Enhanced long term re-population potential was demonstrated by cells harvested from primary sheep donors, which were successfully engrafted in secondary recipients ⁵⁰⁷.

Isolating cellular sub-populations using a separation protocol based on expression of CD133, CD44^{+ve} and the $\alpha_2\beta_1$ -integrin in normal / BPH tissue resulted in the isolation of an epithelial sub-population representing 0.75% of the basal cell population. This population was enriched for cells with the SC properties of high colony forming ability, prolonged clonal growth and importantly the capacity to differentiate and form glandular acini *in vivo* ⁴³². This population has also been reported in prostatic malignancy, suggesting that CD133 may be a marker expressed on CSCs and that expression could be used to differentiate between the CSC ($\alpha_2\beta_1$ -integrin^{hi}/CD44^{+ve}/CD133^{+ve}) and the TAP ($\alpha_2\beta_1$ -integrin^{hi}/CD44^{+ve}/CD133^{-ve}). CD133^{+ve} cells were shown to be maintained in culture at a constant level and they could differentiate into

a population with an AR^{+ve} phenotype, highly suggestive of the presence of a stem-like population ⁴⁴⁶.

However, there is uncertainty as to whether the CD133^{+ve} phenotype represents a true stem population. Furthermore, the CD133^{-ve} population also contained clonogenic cells, albeit in a lower proportion. Whilst the CD133^{+ve} cells did not express the TAP marker c-MET ⁵⁹¹ or markers of terminal differentiation (PSA, AR), colony forming efficiency is only relative to the populations being compared and is not exclusive to the SC as the early TAP will also form colonies. Furthermore, the study by Collins *et al* failed to demonstrate true asymmetric division, characterised by retention of the original genome by the SC ⁴⁴⁶. There is therefore a lack of definitive evidence for the proposition that CD133 positivity is synonymous with the SC phenotype. As previously discussed, the proposed SC population in CD133-based studies in the prostate was expanded from the outset, with potential for non-stem population out-growth and also, for “genetic drift”. Not only does this mean a bias may have been introduced to the expression profile obtained from such expanded cellular populations but it also means that the precise phenotype of the cell population may have been altered by expansion and therefore it is difficult to confirm or refute that the original CD133^{+ve} population was enriched for SCs.

The role of CD133 as a CSC marker has also been questioned in other tumours. In a study of CSCs in glioblastoma, four out of the 15 tumours examined were composed of cells with a CD133^{-ve} phenotype: these

cells also displayed SC characteristics⁵¹⁵. Although the CD133^{-ve} cells had a lower proliferative index in comparison with the CD133^{+ve} phenotype, the findings suggest that in neural CSCs, CD133 status is not the determinant of the SC compartment.

The question still remains, is CD133 a SC/CSC marker or a marker of early transient amplification? Wang *et al*⁵¹⁶ suggested that CD133 expression is not required for brain tumour initiation but that it may be involved in its progression. Brain tumour biopsy material expressed little or no CD133 until passaged. During passage, expression of CD133 appeared and increased, coinciding with a shorter survival; a finding more characteristic of an amplifying / differentiating population than a stem one. Subsequent implantation of CD133^{-ve} cells into the brains of six nude rats led to the confirmation of tumourigenesis in three cases. Interestingly, CD133^{+ve} cells were ultimately harvested from these tumour populations. It is therefore arguable that a more likely hierarchy in relation to CD133 is that the CD133^{-ve} population represents either the SC or terminally differentiated populations and that the TAP has a CD133^{+ve} phenotype (Figure 7.1).

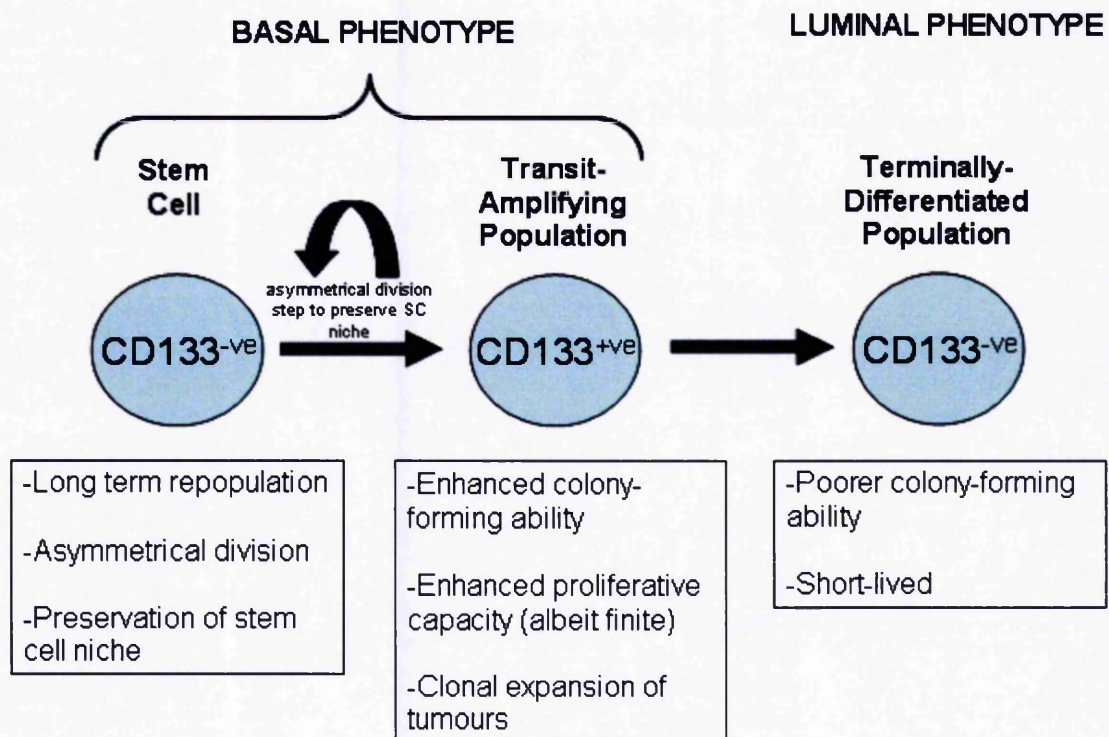


Figure 7.1: A flow diagram illustrating the proposed hierarchy for the CD133 phenotype within the prostate epithelial population.

However, it may be the specific AC133 epitope of CD133 and not the actual CD133/Prominin-1 mRNA expression that is important for the detection of SCs. Florek *et al*⁵¹⁴ found that, although the antigen AC133 decreased, CD133/Prominin-1 expression did not alter during the differentiation of the colonic adenocarcinoma cell line Caco-2. This was also confirmed by the detection of CD133/Prominin-1 in a range of renal cells as well as cells within the lactiferous ducts of the breast⁵¹⁴. To attempt to resolve any uncertainties about CD133 expression, Shmelkov *et al* developed a transgenic mouse model using CD133 endogenous promoters driving the expression *lacZ*⁵⁹². This study demonstrated that both undifferentiated and differentiated colonic epithelial cells expressed CD133. Interestingly, of the tumours formed in this model, it was the CD133^{-ve} cells which were the most aggressive and they expressed the typical cancer-initiating phenotype (CD44^{+ve}CD24^{-ve}), whereas the CD133^{+ve} fraction was composed of CD44^{low}CD24^{+ve} cells⁵⁹².

It therefore remains unclear as to where the CD133^{+ve} phenotype fits in to the prostate cellular hierarchy. Examination of the Hoechst 33342 red/blue FACS profiles with additional CD133^{+ve} selection revealed that significantly more CD133 was present in the NSP than the SP. If the fundamental principles of the Hoechst 33342 dye efflux assay⁴⁴⁷ and the subsequent functional and phenotypic characterisation of the SP are to be believed^{431, 458}, the observed distribution of CD133 between the SP and NSP does not discriminate between the putative SC-enriched population (SP) compared with the bulk of the epithelial sample (NSP).

7.5.2 Demonstration of a Conserved Population of Hoechst 33342^{lo}

Cells Towards the Distal Tip of the Side Population (DSP)

Additional CD133 selection was shown not to be specific to the SP. Whilst performing the analysis of the CD133^{+ve}/CD45^{-ve} FACS plots it became apparent that there was a consistent population of cells in the SP tail which had very low Hoechst 33342 dye concentrations. When only CD45^{-ve} selection was applied to the same FACS plots, the cells appeared to sit below and to the left of the CD133^{+ve} cell with the lowest Hoechst 33342 dye concentration and constitute a small proportion of the overall epithelial cellularity (BPH mean 0.1155%, SD± 0.18% and CaP mean 0.025%, SD± 0.02%). The populations identified were shown to be rare which is a feature characteristic of the SC population.

At this point in the project, it was becoming apparent that the cell number isolated from the CD133^{+ve} SP and NSP was very low and this was having a negative impact on the success of both microarray and, in particular, functionality studies of the respective populations. Ideally, functional and phenotypic analysis of the populations isolated would be performed using the same patient samples as those used in any microarray series. This was not possible with such small samples.

The evidence suggesting that there is enrichment for SC characteristics with increased dye efflux activity towards the tip of the SP tail (reviewed by Hadnagy *et al*⁵⁷²) lead to the hypothesis that subfractionation of the SP tail would further enrich for SCs. CD45^{-ve} only selection would improve the numbers of cells for isolation whilst also allowing full genetic

characterisation of the SP and NSP without the profile being limited by CD133 selection. This hypothesis was supported by the findings of additional work undertaken within the GUCR group in renal tissue. This body of work demonstrated that, although the addition of CD133⁺ SP and NSP cells revealed a greater proliferative capacity than comparable CD133⁻ cells, no other enhancement for SC behaviour or expression of putative SC markers was seen. Again work in renal tissue identified a primitive DSP population of CD133⁻ cells that possessed enhanced stem-like behaviour and marker expression whilst also demonstrating the ability to acquire CD133 expression following passage. This suggested that CD133 is a marker of the TAP in renal cells⁵⁹³. The GUCR group have reported that the SP is a conserved and unified mechanism for isolating SC-enriched cells from urological malignancies⁵⁷⁶ and it is therefore reasonable to propose a hypothesis that the functionality of the DSP in prostatic tissues would mirror the experience in the kidney.

Compared to the CD133⁺ CD45⁻ BPH SP (mean 703.2, SD±635.25 cells) isolated for the Epistem Ltd series, the mean number of cells isolated from the CD45⁻ BPH DSP (5540.91 SD±3949.84 cells) in the second microarray series was much improved. Validation of the functional and phenotypic characteristics of the DSP and PSP compared to the NSP was required so that the acquisition of microarray data as a consequence of the increased cell numbers was not associated with the perception that enrichment for SC characteristics within the studied populations had been reduced.

7.5.3 Functional Characteristics

7.5.3.1 Differential Colony-Forming Ability and Proliferation

Capacity of the DSP and PSP

The problems arising from working with small cell numbers became particularly evident when functional studies such as colony-forming ability and proliferative capacity were investigated. The first attempt at culturing the DSP and PSP isolates was assessed by the number of wells forming at least one colony and the total number of colonies for each of the two populations. A limitation of the study was that the NSP was not isolated for these functional assays. The basis for this was that the entire Verapamil-sensitive SP had already been shown to be enriched for SC characteristics and therefore the focus of attention was now placed on the DSP and PSP ⁴³¹.

The SC-enriched population should have a greater colony-forming efficiency than the TAP though this was not evident in this first series of functional studies with all but one of the PSP samples appearing to form more colonies and having a greater proportion of wells that had at least one colony form within them. This could infer that the SC occupied the PSP. The exception to this was sample GU56 DSP that was markedly more clonogenic than the other DSP samples and its corresponding PSP (GU56 PSP). Serum-free media and feeder layers, like those used in this study, are designed to maintain the population of primitive cells and a possible explanation for the poor colony-forming ability of the DSP relative to the PSP is that culture conditions succeeded in maintaining

the SC population in its quiescent state. Research in the renal SP has shown that the DSP was slower than the PSP to initiate colonies but provided a better duration of culture long term⁵⁹³. Perhaps those wells that were reported as not developing colonies contained a SC-enriched population which was in a lag phase prior to being stimulated to grow. Many wells/flasks succumbed to infection before this and proliferation capacity could be determined definitively though it did appear that the degree of proliferation in the PSP was nearly ten times greater.

Addition of serum to the media is known to allow differentiation⁴³⁰ and this was performed for the second series of growth assays. The idea being to try and stimulate growth thereby eradicating any lag phase and in turn determine the numbers of colony-forming cells more efficiently by stimulating the SCs to divide. It was acknowledged that this may be at the expense of long term proliferative capacity assays with cells reaching senescence earlier. On this occasion the number of colonies formed in the DSP was significantly ($p=0.026$) better than the PSP with a 2.612-fold enhancement for colonies in the DSP. It appeared that the number of cells that were able to initiate a colony was enriched in the DSP.

Subjectively, whole flask photography revealed that resultant cell colonies were larger in the PSP compared to the DSP after the same duration in culture. These results suggest that the DSP may have characteristics akin to a SC population, with the PSP being more consistent with a TAP. This is reinforced by the fact that a confluent monolayer was achieved quicker in the flasks containing the PSP

compared to their corresponding DSP and that after passage the reseeded PSP cells reached population sizes of 500,000 and 600,000 cells after 10 days whereas the single DSP sample that survived only reached a population size of 400,000 by 21 days. The TAP works to rapidly increase the cell number but it is believed that its reproductive potential is limited by its lack of the self renewal properties possessed by the SC ⁵⁷³. Ultimately, neither the DSP nor the PSP survived beyond one passage and therefore neither population possesses unlimited self renewal capacity though it is also likely that the culture conditions, including the addition of 2% FCS will have played a part.

The definition of the growth characteristics of the various populations isolated by the Hoechst 33342 dye efflux assay needs further characterisation and many more replicates of the clonogenic and proliferative capacity assays are required to establish the functionality of the DSP and PSP. Unfortunately this was not possible within the timeframe of this project.

7.5.3.2 FACS Analysis of Cultured Cells Suggests Preservation of the DSP in Cultured DSP Cells and Evidence of Lineage Differentiation

The adult SC is able to reconstitute all the cell lineages within its tissue type by a process termed pluripotentiality (reviewed in ²⁷⁵). Cells from the DSP and PSP were isolated and cultured with 2% FCS. In order to determine the Hoechst 33342 dye phenotype of such cells following

culture, the labelling steps of the Hoechst 33342 dye efflux assay were repeated and cells were re-analysed by FACS.

Similar to the primary FACS profile of each of two DSP samples, the two cell populations cultured from the DSP subpopulations revealed the presence of a persistent CD45^{-ve} cell population that was lower in Hoechst 33342 dye concentration than the CD133 cell with the lowest Hoechst 33342 dye concentration. This conserved DSP encompassed 0.14% and 0.1% of the total cell population after culture. Hoechst 33342^{lo} cells were also seen in gate R4 which defined the DSP when the cell populations cultured from PSP samples were examined. There was a 7 to 10-fold increase in the proportion of cells within this R4 FACS gate in the populations derived from DSP cultures compared to those from PSP cultures. This finding suggests that a small proportion of DSP and to a lesser extent PSP cells placed into culture is capable of asymmetric division and retention of their original phenotype.

Furthermore, despite the tight definition of the DSP and PSP populations at primary FACS, the repeat FACS analysis following culture identified the majority of cells to occupy both the PSP and NSP population, suggesting differentiation in culture and loss of their ability to efflux the Hoechst 33342 dye which is consistent with a differentiated cell phenotype²⁹⁰.

Definition of the DSP and PSP gates was performed using a CD133 control which is often a small cell number sample. The accuracy with which the CD133 status of cells can be used to delineate the DSP and

PSP populations was called into question during primary FACS when 9.1% of BPH and 60% of CaP samples had CD133 control samples that were too low in cell number to allow accurate delineation of the CD133^{ve/low} DSP and CD133^{+ve} PSP. This is a potential criticism of the FACS analysis of the DSP and PSP cellular populations after culture as the CD133 control was even smaller. Interestingly, despite the DSP having low CD133 expression compared to the PSP in both the subsequent immunocytochemical and microarray analysis of the two populations and the fact that no CD133^{+ve} cells were identified within the DSP at primary FACS, evidence of CD133^{+ve} cells was shown after culture of the DSP. Again this may merely be an artefact of the small cell number CD133 control used in defining the DSP and PSP gates at primary FACS but in support of this being a phenotypic change, with some cells acquiring the CD133 phenotype, was the fact that the cells appeared to have also changed their phenotype with respect to their Hoechst 33342 dye efflux status and now appeared higher up the SP tail in the PSP or in the NSP. Comment on the exclusion of CD133 from the DSP after culture is not possible as the DSP gates after culture have been re-defined purely on the basis of a CD133^{ve/low} phenotype. The PSP samples also provide evidence of movement of cells from their original position on the Hoechst 33342 red/blue profile towards the NSP.

The limitation of this part of the phenotyping studies is that only two samples have been examined with three other paired DSP/PSP samples being lost to infection prior to reaching this stage. Drawing firm conclusions from this is therefore difficult but the profiles do suggest a

potentially exciting observation of the SC attributes of asymmetrical division and pluripotentiality. Furthermore, they provide support for the hypothesised hierarchy with respect to CD133 with the DSP having low levels of CD133 expression, the PSP being CD133 positive and the NSP being composed of a mixed population.

7.5.4 Immunocytochemical Phenotype of the DSP and PSP

Significant differences between the immunocytochemical expression of CD133 in the DSP and PSP were seen confirming the gating strategy used during FACS. The DSP was not completely CD133^{-ve} but rather CD133^{low}. Overall, the DSP was enriched for all the putative SC markers used. However, only Beta Catenin, p27 and Notch 1 reached statistical significance.

Beta Catenin is believed to play an integral part in the Wnt signalling pathway which controls cellular self renewal, proliferation and differentiation⁴⁸⁵. Beta Catenin has been proposed as a putative SC marker in keratinocytes and is thought to function through stimulation of the transcription factors Tcf-1 and Lef-1 rather than by effecting cell cycle kinetics or cell to cell adhesion⁴⁸⁸. Although these immunocytochemical studies examined BPH samples only, the Wnt pathway has been linked with carcinogenesis and specifically the development of murine breast tumours³⁶⁷ and colon cancer⁴⁹¹ as well as enhanced tumorigenicity of human CaP^{492, 493}. Beta Catenin also regulates the DNA binding protein c-myc. The differential

immunocytochemical expression of this marker was also examined though no significant trends regarding its expression were identified.

Wang *et al* demonstrated that inhibition of Notch prevented normal organogenesis in the murine prostate ⁴⁸¹. Conversely, upregulation of Notch 1 was evident in the TRAMP mouse model suggesting over expression may precipitate the increased proliferative state seen in tumourigenesis ⁴⁸². The finding presented herein relating to the DSP would support the DSP being enriched for this particular SC marker.

The immunocytochemical analysis of markers also provided some validation of the genes differentially expressed between the DSP and PSP. Of those markers represented on the array, all DSP/PSP fold changes were matched by immunocytochemical fold changes in the same direction. Whilst the polarity of such changes provided qualitative validation, the amplitude of comparable fold changes was not always achieved. Three markers (SHH, p63 and p21) were represented by two probesets on the array. One of the pair showed a positive DSP/PSP fold change whilst the other was negative. Whilst one of the pair was validated by the immunocytochemistry, the results are potentially weakened for these particular markers. qRT-PCR will be required to more accurately determine the quantitative relationship between the DSP and PSP.

7.6 Realisation of Original Aims and Objectives

The existing CD133⁺ SP and NSP Affymetrix microarray data from BPH tissue was analysed and the quality of the microarray data was determined. However, due to the poor quality of this data, the project was revised to enhance the FACS and RNA protocols to maximise the quality of data from small cell number samples.

As a consequence of these adaptations, the BPH and CaP SP and NSP were not isolated or characterised further with additional CD133 selection. Further analysis of the Hoechst 33342 profile identified a distinct CD133^{low} population (DSP). A microarray series was generated using DSP, PSP and NSP isolates from BPH and CaP with the addition of normal samples. Immunocytochemical and functional studies were performed for the DSP and PSP isolated from BPH. A previous study by the GUCR group looked at the differential functionality of the combined DSP and PSP (SP) and the NSP⁴³¹. Unfortunately, due to the time constraints of the project, replicate immunocytochemical and functional studies could not be extended to normal and CaP samples.

Whilst lists of differentially expressed genes have been generated, unfortunately, qRT-PCR validation of the database and detailed biological datamining for genes of interest has not been possible within the timeframe of this project due to the steps taken in the first year of the project to optimise the protocols and thereby reach the ultimate goal of microarray analysis.

Whilst this project has not addressed each of the aims directly, the direction has been appropriately adapted in light of the initial findings. Successful optimisation will allow the remaining aims to be achieved in a reproducible and standardised manner in the months to come.

7.7 Conclusions

Improvements in RNA amplification technologies as well as the optimization of the Hoechst 33342 dye efflux assay to minimise the effect of RNases has improved the quality of Affymetrix microarray data such that it has been possible to isolate a good quality dataset now ready for validation and determination of gene expression profiles.

Most importantly, such improvements in microarray quality are secondary to improvement in the quality of RNA extracted and that of the cDNA hybridized to the HG-U133_Plus 2 arrays. The successful acquisition of good quality gene expression data now affords the opportunity to determine the differential gene expression between very small number primary cell populations that are believed to be enriched for SC characteristics. The unique dataset will now hopefully glean new markers of the SC and CSC compartments and therefore aid the prospective purification of the SP phenotype to reduce the heterogeneity currently present. Gene expression data will be correlated with known SC-regulatory pathways and in turn, this may provide novel diagnostic, prognostic and therapeutic targets to combat the root cause of BPH and CaP.

7.8 Future Direction

A new subpopulation of cells within the prostatic SP termed the DSP, has been identified. Provisional data suggests the presence of functional SC properties of enhanced colony-forming ability, pluripotentiality and asymmetrical division as well as the enrichment for phenotypic markers suggestive of a more primitive SC population. This provides support for the notion that the DSP is enriched for cells with SC characteristics. The project timescale meant that further functional and phenotypic characterisation of the DSP, PSP and NSP subpopulations was not possible. However, this work can now be continued on the secure platform provided by this body of work. The colony-forming and proliferative capacity assays should be repeated in multiple replicates. Cell cycle analysis is required to determine if there is enrichment for quiescent cells as the putative maturity of the subpopulations decreases. The demonstration of asymmetrical division by dye retention studies would add interesting information though the gold standard determinant of the differential stem activity between the three groups must ultimately be confirmed *in vivo*. Such *in vivo* work is likely to be required to allow full acceptance of the microarray data by the SC research community.

If satisfactory qRT-PCR validation of the microarray data is achieved, future work will concentrate on interrogation of the gene lists to allow application of biological significance to the genes that are differentially expressed between the three subpopulations and three disease groups. Gene ontology will provide information and annotation about the

attributes of the genes and gene products. Such information will cover three domains; cellular component, the parts of a cell or its extracellular environment; molecular function, the activities of a gene product at the molecular level and biological process, series of molecular events with a defined beginning and end, pertinent to the functioning of prostatic cells and tissue. Bioinformatic tools such as gene network analysis will then be used to piece this biological information together and thereby determine the important regulatory processes specific to the prostate SC-enriched population and how these pathways may be altered in diseased states. This would be critical in identifying SC-specific diagnostic and prognostic markers as well as potentially identifying novel therapeutic targets to the SC compartment. Such an advance would go a long way to addressing the challenges that clinicians regularly face when managing patients with suspected or confirmed CaP (section 1.5).

Bibliography

1. Sinnatamby, C.S. *Last's anatomy: regional and applied*. 10 ed. 1999, Edinburgh: Churchill Livingstone.
2. Brooks, J.D. *Anatomy of the lower urinary tract and male genitalia*. Eighth ed. Campbell's Urology, ed. Walsh, et al. Vol. 4: Saunders.
3. McNeal, J.E. *Normal histology of the prostate*. Am J Surg Path, 1988. 12: p. 619-633.
4. Clemente, C.D. *Gray's Anatomy*. 30th ed. 1985, Philadelphia: Lea & Febiger.
5. Batson, O.V. *The function of the vertebral veins and their role in the spread of metastases*. Ann Surg, 1940. 112: p. 138-149.
6. Burkitt, H.G., Young, B., Heath, J.W. *Wheater's functional histology*. Third ed, ed. H.G. Burkitt, B. Young, and J.W. Heath. 1993, Edinburgh: Churchill Livingstone.
7. Colville, C.C., Masters, J.R., Parkinson, M.C. *The prostate and cancer: an introduction to normal morphology and histopathology for research scientists*. Prostate cancer: clinical and scientific aspects-bridging the gap., ed. P.D. Abel and E. Lalani. 2003: Imperial College Press. 111-140.
8. Signoretti, S., Loda, M. *Prostate stem cells from development to cancer*. Seminars in cancer biology, 2006. 17(3): p. 219-224.
9. Jost, A. *Organogenesis*, ed. R.L. Ursprung and H. De Haan. 1965, New York: Holt, Rinehart and Winston. 611-628.
10. Sadler, T.W. *Langman's medical embryology*. Seventh ed, ed. T.W. Sadler. 1993, Baltimore: Williams & Wilkins.
11. Cunha, G.R., Donjacour, A.A., Hayward, S.W., Thomson, A.A., Dahiya, R., Marker, P.C., Abate-Shen, C., Shen, M. *Development and differentiation of the prostate gland*. Prostate cancer: clinical and scientific aspects-bridging the gap, ed. P.D. Abel and E. Lalani. 2003: Imperial College Press. 71-91.
12. Guyton, A.C., Hall, J.E. *Textbook of medical physiology*. Ninth ed, ed. A.C. Guyton and J.E. Hall. 1996: Saunders.
13. CancerResearchUK. *Prostate Cancer Statistics*. 2005, Cancer Research UK.
14. *Cancer Registration Statistics 2003*. 2003, Office for National Statistics.
15. Reiter, R.E., deKernion, J.B. *Epidemiology, etiology and prevention of prostate cancer*. Eighth ed. Campbell's Urology, ed. Walsh, et al. Vol. Volume 4. 2002: W.B. Saunders.
16. Post, P.N., Kil, P.J., Coebergh, P.W. *Trends in survival of prostate cancer in southeastern Netherlands, 1971-1989*. Int J Cancer, 1999. 81: p. 551.
17. *Cancer incidence in Sweden 2000*. 2002, The National Board of Health and Wealthfare: Stockholm.
18. Parker, S.L., Tong, T., Bolden, S., Wingo, P.A. *Cancer statistics*. CA Cancer J Clin, 1997. 47(1): p. 5-27.

19. Hankey, B.F., Feuer, E.J., Clegg, L.X., Hayes, R.B., Legler, J.M., Prorok, P.C., Ries, L.A., Merrill, R.M., Kaplan, R.S. *Cancer surveillance series: interpreting trends in prostate cancer-part 1: evidence of the effects of screening in recent prostate cancer incidence, mortality and survival rates.* J Natl Cancer Inst, 1999. 91: p. 1017.
20. Newcomer, L.M., Stanford, J.L., Blumenstein, B.A., Brawer, M.K. *Temporal trends in rates of prostate cancer: Declining incidence of advanced stage disease, 1974 to 1994.* J Urol, 1997. 158: p. 1427.
21. George, N.J. *Natural history of localised prostatic cancer managed by conservative therapy alone.* Lancet, 1988. 1: p. 494-497.
22. Johansson, J.E., Holmberg, L., Johansson, S., Bergström, R., Adami, H.O. *Fifteen-year survival in prostate cancer. A prospective, population-based study in Sweden.* JAMA, 1997. 277: p. 467-71.
23. Stamey, T.A., Donaldson, A.N., Yemoto, C.E., McNeal, J.E., Sözen, S., Gill, H. *Histological and clinical findings in 896 consecutive prostates treated only with radical retropubic prostatectomy: Epidemiologic significance of annual changes.* J Urol, 1998. 160: p. 2412.
24. Merrill, R.M., Stephenson, R.A. *Trends in mortality rates in patients with prostate cancer in the era of prostate specific antigen screening.* J Urol, 2000. 163: p. 503.
25. Tarone, R.E., Chu, K.C., Brawley, O.W. *Implications of stage-specific survival rates in assessing recent declines in prostate cancer mortality rates.* Epidemiology, 2000. 11: p. 167.
26. Boyle, P., Maissonneuve, P., Napalkov, P. *Geographical and temporal patterns of incidence and mortality from prostate cancer.* Urology, 1995. 46(3 Suppl A): p. 47-55.
27. Helgesen, F., Holmberg, L., Johansson, J.E., Bergstrom, R., Adami, H.O. *Trend in prostate cancer survival in Sweden, 1960 through 1988: Evidence of increasing diagnosis of nonlethal tumors.* J Natl Cancer Inst, 1996. 88: p. 1216.
28. Sandblom, G., Dufmats, M., Nordenskjöld, K., Varenhorst, E. *Prostate carcinoma trends in three counties in Sweden 1987-1996: Results from a population-based national cancer register. South-East Region Prostate Cancer Group.* Cancer, 2000. 88: p. 1445.
29. Osegbe, D.N. *Prostate cancer in Nigerians: Facts and nonfacts.* J Urol, 1997. 157: p. 1340.
30. Haenszel, W., Kurihara, M. *Studies of Japanese migrants. I. Mortality from cancer and other diseases among Japanese in the United States.* JNCI, 1968. 40(1): p. 43-68.
31. Haenszel, W. *Cancer mortality among the foreign-born in the United States.* JNCI, 1961. 26: p. 37-132.
32. Zaridze, D.G., Boyle, P., Smans, M. *International trends in prostatic cancer.* Int J Cancer, 1984. 33: p. 223-230.
33. Parkin, D.M. *Cancer incidence in five continents. IARC Scientific Publications.* 1997, World Health Organisation: Lyon.
34. Meyer, F., Bairati, I., Shadmani, R., Fradet, Y., Moore, L. *Dietary fat and prostate cancer survival.* Cancer Causes Control, 1999. 10(4): p. 245-51.

35. Steinberg, G.D., Carter, B.S., Beaty, T.H., Childs, B., Walsh, P.C. *Family history and the risk of prostate cancer*. Prostate, 1990. 17: p. 337.
36. Gronberg, H., Damber, L., Damber, J.E. *Familial prostate cancer in Sweden. A nationwide register cohort study*. Cancer, 1996. 77(138-143).
37. Carter, B.S., Beaty, T.H., G.D., S., Childs, B., Walsh, P.C. *Mendelian inheritance of familial prostate cancer*. Proc Natl Acad Sci U S A, 1992. 89: p. 3367.
38. Carter, B.S., Bova, G.S., Beaty, T.H., al, e. *Hereditary prostate cancer: epidemiologic and clinical features*. J Urol, 1993. 150: p. 797.
39. Bastacky, S.I., Wojno, K.J., Walsh, P.C., Carmichael, M.J., Epstein, J.I. *Pathological features of hereditary prostate cancer*. J Urol, 1995. 153: p. 987.
40. Ross, R.K., Bernstein, L., Lobo, R.A., Shimizu, H., Stanczyk, F.Z., Pike, M.C., Henderson, B.E. *5-Alpha-reductase activity and risk of prostate cancer among Japanese and US white and black males*. Lancet, 1992. 339: p. 887-9.
41. Gann, P.H., Hennekens, C.H., Ma, J., Longcope, C., Stampfer, M.J. *Prospective study of sex hormone levels and risk of prostate cancer*. J Natl Cancer Inst, 1996. 88: p. 1118-1126.
42. Barrett-Connor, E., Garland, C., McPhillips, J.B., Khaw, K.T., Wingard, D.L. *A prospective, population-based study of androstenedione, estrogens, and prostatic cancer*. Cancer Res, 1990. 50: p. 169-73.
43. Guess, H.A., Friedman, G.D., Sadler, M.C., Stanczyk, F.Z., Vogelstein, J.H., Imperato-McGinley, J., Lobo, R.A., Orentreich, N. *5 alpha-reductase activity and prostate cancer: a case-control study using stored sera*. Cancer Epidemiol Biomarkers Prev, 1997. 6: p. 21-24.
44. Shaneyfelt, T., Husein, R., Bubley, G., Mantzoros, C.S. *Hormonal predictors of prostate cancer: a meta-analysis*. J Clin Oncol, 2000. 18: p. 847-853.
45. Makridakis, N., Ross, R.K., Pike, M.C., Chang, L., Stanczyk, F.Z., Kolonel, L.N., Shi, C.Y., Yu, M.C., Henderson, B.E., Reichardt, J.K. *A prevalent missense substitution that modulates activity of prostatic steroid 5alpha-reductase*. Cancer Res, 1997. 57: p. 1020-1022.
46. Makridakis, N.M., Ross, R.K., Pike, M.C., Crocitto, L.E., Kolonel, L.N., Pearce, C.L., Henderson, B.E., Reichardt, J.K. *Association of missense substitution in SRD5A2 gene with prostate cancer in African-American and Hispanic men in Los Angeles, USA*. Lancet, 1999. 354: p. 975-78.
47. Febbo, P.G., Kantoff, P.W., Platz, E.A., Casey, D., Batter, S., Giovannucci, E., Hennekens, C.H., Stampfer, M.J. *The V89L polymorphism in the 5alpha-reductase type 2 gene and risk of prostate cancer*. Cancer Res, 1999. 59: p. 5878-81.
48. Sartor, O., Zheng, Q., Eastham, J.A. *Androgen receptor gene CAG repeat length varies in a race-specific fashion in men without prostate cancer*. Urology, 1999. 53: p. 378-80.
49. Bishop, D.T. *The epidemiology of prostate cancer*. Prostate cancer: clinical and scientific aspects-bridging the gap, ed. P.D. Abel and E. Lalani. 2003: Imperial College Press. 23-34.

50. Peehl, D.M., Skowronski, R.J., Leung, G.K., Wong, S.T., Stamey, T.A., Feldman, D. *Antiproliferative effects of 1,25-dihydroxyvitamin D3 on primary cultures of human prostatic cells*. Cancer Res, 1994. 54: p. 805-10.
51. Getzenberg, R.H., Light, B.W., Lapco, P.E., Konety, B.R., Nangia, A.K., Acierno, J.S., Dhir, R., Shurin, Z., Day, R.S., Trump, D.L., Johnson, C.S. *Vitamin D inhibition of prostate adenocarcinoma growth and metastasis in the Dunning rat prostate model system*. Urology, 1997. 50: p. 999-1006.
52. Lokeshwar, B.L., Schwartz, G.G., Selzer, M.G., Burnstein, K.L., Zhuang, S.H., Block, N.L., Binderup, L. *Inhibition of prostate cancer metastasis in vivo: a comparison of 1,23-dihydroxyvitamin D (calcitriol) and EB1089*. Cancer Epidemiol Biomarkers Prev, 1999. 8: p. 241-48.
53. Hanchette, C.L., Schwartz, G.G. *Geographic patterns of prostate cancer mortality. Evidence for a protective effect of ultraviolet radiation*. Cancer, 1992. 70(12): p. 2861-9.
54. Chan, J.M., Stampfer, M.J., Giovannucci, E., Gann, P.H., Ma, J., Wilkinson, P., Hennekens, C.H., Pollack, M. *Plasma insulin-like growth factor-I and prostate cancer risk: a prospective study*. Science, 1998. 279: p. 563-66.
55. Wang, Y., Corr, J.G., Thaler, H.T., Tao, Y., Fair, W.R., Heston, W.D. *Decreased growth of established human prostate LNCaP tumors in nude mice fed a low-fat diet*. J Natl Cancer Inst, 1995. 87: p. 1456-62.
56. Aronson, W.J., Tymchuk, C.N., Elashoff, R.M., McBride, W.H., McLean, C., Wang, H., Heber, D. *Decreased growth of human prostate LNCaP tumors in SCID mice fed a low-fat, soy protein diet with isoflavones*. Nutr Cancer, 1999. 35: p. 130-36.
57. Clinton, S.K., Palmer, S.S., Spriggs, C.E., Visek, W.J. *Growth of Dunning transplantable prostate adenocarcinomas in rats fed diets with various fat contents*. J Nutr, 1988. 118: p. 908-14.
58. Hill, P., Wynder, E.L., Garbaczewski, L., Garnes, H., Walker, A.R. *Diet and urinary steroids in black and white North American men and black South African men*. Cancer Res, 1979. 39: p. 5101-5.
59. Hamalainen, E., Adlercreutz, H., Puska, P., Pietinen, P. *Diet and serum sex hormones in healthy men*. J Steroid Biochem, 1984. 20: p. 459-64.
60. Rosenthal, M.A., Taneja, S., Bosland, M.C. *Phytoestrogens and prostate cancer: possible preventive role*. Med J Aust, 1998. 168: p. 467.
61. Kolonel, L.N., Nomura, A.M., Cooney, R.V. *Dietary fat and prostate cancer: current status*. J Natl Cancer Inst, 1999. 91: p. 414-28.
62. Ghosh, J., Myers, C.E. *Arachidonic acid stimulates prostate cancer cell growth: critical role of 5-lipoxygenase*. Biochem Biophys Res Commun, 1997. 235: p. 418-23.
63. Ghosh, J., Myers, C.E. *Inhibition of arachidonate 5-lipoxygenase triggers massive apoptosis in human prostate cancer cells*. Proc Natl Acad Sci U S A, 1998. 95: p. 13182-87.
64. Ghosh, J., Myers, C.E. *Central role of arachidonate 5-lipoxygenase in the regulation of cell growth and apoptosis in human prostate cancer cells*. Adv Exp Med Biol, 1999. 469: p. 577-82.

65. Brown, M.D., Hart, C.A., Gazi, E., Bagley, S., Clarke, N.W. *Promotion of prostatic metastatic migration towards human bone marrow stroma by Omega 6 and its inhibition by Omega 3 PUFAs*. Br J Cancer, 2006. 94: p. 842-53.
66. Giovannucci, E., Rimm, E.B., Wolk, A., Ascherio, A., Stampfer, M.J., Colditz, G.A., Willett, W.C. *Calcium and fructose intake in relation to risk of prostate cancer*. Cancer Res, 1998. 58: p. 442-47.
67. Di Mascio, P., Kaiser, S., Sies, H. *Lycopene as the most efficient biological carotenoid singlet oxygen quencher*. Arch Biochem Biophys, 1989. 274: p. 532-8.
68. Giovannucci, E., Ascherio, A., Rimm, E.B., Stampfer, M.J., Colditz, G.A., Willett, W.C. *Intake of carotenoids and retinol in relation to risk of prostate cancer*. J Natl Cancer Inst, 1995. 87: p. 1767-76.
69. Giovannucci, E. *Tomatoes, tomato-based products, lycopene, and cancer: review of the epidemiologic literature*. J Natl Cancer Inst, 1999. 91: p. 317-31.
70. De Marzo, A.M., Marchi, V.L., Epstein, J.I., Nelson, W.G. *Proliferative inflammatory atrophy of the prostate: implications for prostatic carcinogenesis*. Am J Pathol, 1999. 155: p. 1985-92.
71. Karas, M., Amir, H., Fishman, D., Danilenko, M., Segal, S., Nahum, A., Koifmann, A., Giat, Y., Levy, J., Sharoni, Y. *Lycopene interferes with cell cycle progression and insulin-like growth factor I signaling in mammary cancer cells*. Nutr Cancer, 2000. 36: p. 101-11.
72. van den Brandt, P.A., Goldbohm, R.A., van 't Veer, P., Bode, P., Dorant, E., Hermus, R.J., Sturmans, F. *A prospective cohort study on toenail selenium levels and risk of gastrointestinal cancer*. J Natl Cancer Inst, 1993. 85: p. 224-29.
73. Clark, L.C., Combs, G.F., Turnbull, B.W., Slate, E.H., Chalker, D.K., Chow, J., Davis, L.S., Glover, R.A., Graham, G.F., Gross, E.G., Krongrad, A., Leshner, J.L., Park, H.K., Sanders, B.B., Smith, C.L., Taylor, J.R. *Effects of selenium supplementation for cancer prevention in patients with carcinoma of the skin. A randomized controlled trial. Nutritional Prevention of Cancer Study Group*. JAMA, 1996. 276: p. 1957-63.
74. Yoshizawa, K., Willett, W.C., Morris, S.J., Stampfer, M.J., Spiegelman, D., Rimm, E.B., Giovannucci, E. *Study of prediagnostic selenium level in toenails and the risk of advanced prostate cancer*. J Natl Cancer Inst, 1998. 90: p. 1219-24.
75. Sigounas, G., Anagnostou, A., Steiner, M. *dl-alpha-tocopherol induces apoptosis in erythroleukemia, prostate, and breast cancer cells*. Nutr Cancer, 1997. 28: p. 30-35.
76. Heinonen, O.P., Albanes, D., Virtamo, J., Taylor, P.R., Huttunen, J.K., Hartman, A.M., Haapakoski, J., Malila, N., Rautalahti, M., Ripatti, S., Mäenpää, H., Teerenhovi, L., Koss, L., Virolainen, M., Edwards, B.K. *Prostate cancer and supplementation with alpha-tocopherol and beta-carotene: incidence and mortality in a controlled trial*. J Natl Cancer Inst, 1998. 90: p. 440-46.

77. Hartman, T.J., Albanes, D., Pietinen, P., Hartman, A.M., Rautalahti, M., Tangrea, J.A., Taylor, P.R. *The association between baseline vitamin E, selenium, and prostate cancer in the alpha-tocopherol, beta-carotene cancer prevention study.* Cancer Epidemiol Biomarkers Prev, 1998. 7: p. 335-40.
78. Giovannucci, E., Ascherio, A., Rimm, E.B., Colditz, G.A., Stampfer, M.J., Willett, W.C. *A prospective cohort study of vasectomy and prostate cancer in US men.* JAMA, 1993. 269: p. 873-77.
79. Stanford, J.L., Wicklund, K.G., McKnight, B., Daling, J.R., Brawer, M.K. *Vasectomy and risk of prostate cancer.* Cancer Epidemiol Biomarkers Prev, 1999. 8: p. 881-86.
80. Honda, G.D., Bernstein, L., Ross, R.K., Greenland, S., Gerkins, V., Henderson, B.E. *Vasectomy, cigarette smoking, and age at first sexual intercourse as risk factors for prostate cancer in middle-aged men.* Br J Cancer, 1988. 57: p. 326-31.
81. Wideroff, L., Schottenfeld, D., Carey, T.E., Beals, T., Fu, G., Sakr, W., Sarkar, F., Schork, A., Grossman, H.B., Shaw, M.W. *Human papillomavirus DNA in malignant and hyperplastic prostate tissue of black and white males.* Prostate, 1996. 28: p. 117-23.
82. Rotkin, I.D. *Studies in the epidemiology of prostatic cancer: expanded sampling.* Cancer Treat Rep, 1977. 61: p. 173-180.
83. Schuman, L.M., Mandel, J., Blackard, C., Bauer, H., Scarlett, J., McHugh, R. *Epidemiologic study of prostate cancer: preliminary report.* Cancer Treat Rep, 1977. 61: p. 181-186.
84. Hiatt, R.A., Armstrong, M.A., Klatsky, A.L., Sidney, S. *Alcohol consumption, smoking, and other risk factors and prostate cancer in a large health plan cohort in California (United States).* Cancer Causes Control, 1994. 5: p. 66-72.
85. Engeland, A., Andersen, A., Haldorsen, T., Tretli, S. *Smoking habits and risk of cancers other than lung cancer: 28 years' follow-up of 26,000 Norwegian men and women.* Cancer Causes Control, 1996. 7: p. 497-506.
86. Adami, H.O., Bergström, R., Engholm, G., Nyrén, O., Wolk, A., Ekblom, A., Englund, A., Baron, J. *A prospective study of smoking and risk of prostate cancer.* Int J Cancer, 1996. 67: p. 764-68.
87. Breslow, R.A., Wideroff, L., Graubard, B.I., Erwin, D., Reichman, M.E., Ziegler, R.G., Ballard-Barbash, R. *Alcohol and prostate cancer in the NHANES I epidemiologic follow-up study. First National Health and Nutrition Examination Survey of the United States.* Ann Epidemiol, 1999. 9: p. 254-61.
88. Andersson, S.O., Wolk, A., Bergström, R., Adami, H.O., Engholm, G., Englund, A., Nyrén, O. *Body size and prostate cancer: a 20-year follow-up study among 135006 Swedish construction workers.* J Natl Cancer Inst, 1997. 89: p. 385-89.
89. Whittemore, A.S., Paffenbarger, R.S., Anderson, K., Lee, J.E. *Early precursors of site-specific cancers in college men and women.* J Natl Cancer Inst, 1985. 74: p. 43-51.
90. Snowden, D.A., Phillips, R.L., Choi, W. *Diet, obesity and risk of fatal prostate cancer.* Am J Epidemiol, 1984. 120: p. 244-245.

91. Wynder, E.L., Mabuchi, K., Whitmore, W.F. *Epidemiology of cancer of the prostate*. Cancer, 1971. 28: p. 344-360.
92. Graham, S., Haughey, B., Marshall, J., Priore, R., Byers, T., Rzepka, T., Mettlin, C., Pontes, J.E. *Diet in the epidemiology of carcinoma of the prostate gland*. JNCI, 1983. 70: p. 687-692.
93. Boyle, P., Zaridze, D.G. *Risk factors for prostate and testicular cancer*. European Journal of Cancer, 1993. 29A(7): p. 1048-1055.
94. Morrison, H., Savitz, D., Semenciw, R., Hulka, B., Mao, Y., Morison, D., Wigle, D. *Farming and prostate cancer mortality*. Am J Epidemiol, 1993. 137: p. 270-280.
95. Tulinius, H. *Latent malignancies at autopsy: a little used source of information on cancer biology*. IARC Sci Publ, 1991. 112: p. 253-61.
96. Konety, B.R., Bird, V.Y., Deorah, S., Dahmouch, L. *Comparison of the incidence of latent prostate cancer detected at autopsy before and after the prostate specific antigen era*. J Urol, 2005. 174: p. 1785-8.
97. Rich, A. *On the frequency of occurrence of occult carcinoma of the prostate*. J Urol, 1935. 33: p. 215-223.
98. Scott, R.J., Mutchnik, D.L., Laskowski, T.Z., Schmalhorst, W.R. *Carcinoma of the prostate in elderly men: incidence, growth characteristics and clinical significance*. J Urol, 1969. 101: p. 602-607.
99. Underwood, J.C.E. *General and systematic pathology*. Second ed, ed. J.C.E. Underwood. 1996, Edinburgh: Churchill Livingstone.
100. Franks, L. *Latent carcinoma of the prostate*. J Pathol Bacteriol, 1954. 68c: p. 603-616.
101. Epstein, J.I., Paull, G., Eggleston, J.C., Walsh, P.C. *Prognosis of untreated stage A1 prostatic carcinoma: a study of 94 cases with extended followup*. J Urol, 1986. 136(4): p. 837-9.
102. McLaren, D.B., McKenzie, M., Duncan, G., Pickles, T. *Watchful waiting or watchful progression? Prostate specific antigen doubling times and clinical behaviour in patients with early untreated prostate carcinoma*. Cancer, 1998. 82: p. 342-348.
103. Adolfsson, J., Ronstrom, L., Carstensen, J., Lowhagen, T., Hedlund, P.O. *The natural course of low grade, non-metastatic prostatic carcinoma*. Br J Urol, 1990. 65: p. 611-614.
104. Adolfsson, J., Oksanen, H., Salo, J.O., Steineck, G. *Localized prostate cancer and 30 years of follow-up in a population-based setting*. Prostate Cancer Prostatic Dis, 2000. 3(1): p. 37-42.
105. Aus, G., Hugosson, J., Norlen, L. *Long-term survival and mortality in prostate cancer treated with noncurative intent*. J Urol, 1995. 154(2 Pt 1): p. 460-5.
106. Chodak, G.W., Thisted, R.A., Gerber, G.S., Johansson, J.E., Adolfsson, J., Jones, G.W., Chisholm, G.D., Moskovitz, B., Livne, P.M., Warner, J. *Results of conservative management of clinically localized prostate cancer*. N Engl J Med, 1994. 330(4): p. 242-8.
107. Lu-Yao, G.L., Yao, S.L. *Population-based study of long-term survival in patients with clinically localised prostate cancer*. Lancet, 1997. 349(9056): p. 906-10.

108. Etzioni, R., Penson, D.F., Legler, J.M., di Tommaso, D., Boer, R., Gann, P.H., Feuer, E.J. *Overdiagnosis due to prostate-specific antigen screening: lessons from U.S. prostate cancer incidence trends*. J Natl Cancer Inst, 2002. 94(13): p. 981-90.
109. Parker, C., Muston, D., Melia, J., Moss, S., Dearnaley, D. *A model of the natural history of screen-detected prostate cancer, and the effect of radical treatment on overall survival*. British Journal of Cancer, 2006. 94(10): p. 1361-1368.
110. McNeal, J.E., Redwine, E.A., Freiha, F.S., Stamey, T.A. *Zonal distribution of prostatic adenocarcinomas. Correlation with histologic pattern and direction of spread*. Am J Surg Pathol, 1988. 12: p. 897-906.
111. Gaudin, P.B., Sesterhenn, I.A., Wojno, K.J., Mostofi, F.K., Epstein, J.I. *Incidence and clinical significance of high grade prostatic intraepithelial neoplasia in TURP specimens*. Urology, 1997. 49: p. 558-563.
112. Epstein, J.I. *Pathology of prostatic neoplasia*. Eighth ed. Campbell's Urology, ed. Walsh, et al. Vol. 4: Saunders.
113. Byar, D.P., Mostofi, F.K. *Veterans Administrative Cooperative Urologic Research Groups: Carcinoma of the prostate; prognostic evaluation of certain pathologic features in 208 radical prostatectomies*. Cancer, 1972. 30: p. 5-13.
114. Clarke, N.W., Hart, C.A., Brown, M.D. *Molecular mechanisms of metastasis in prostate cancer*. Asian J Androl, 2009. 11: p. 57-67.
115. McNeal, J.E., Bostwick, D.G. *Intraductal dysplasia: a premalignant lesion of the prostate*. Hum Pathol, 1986. 17(1): p. 64-71.
116. Haggman, M.J., Macoska, J.A., Wojno, K.J., Oesterling, J.E. *The relationship between prostatic intraepithelial neoplasia and prostate cancer: Critical issues*. J Urol, 1997. 158: p. 12-22.
117. Bostwick, D.G., Pacelli, A., Lopez-Beltran, A. *Molecular biology of prostatic intraepithelial neoplasia*. Prostate, 1996. 29: p. 117-134.
118. Montironi, R., Mazzucchelli, R., Algaba, F., Lopez-Beltran, A. *Morphological identification of the patterns of prostatic intraepithelial neoplasia and their importance*. J Clin Pathol, 2000. 53: p. 655-665.
119. Davidson, D., Bostwick, D.G., Qian, J., Wollan, P.C., Oesterling, J.E., Rudders, R.A., Siroky, M., Stilmant, M. *Prostatic intraepithelial neoplasia is a risk factor for adenocarcinoma: predictive accuracy in needle biopsies*. J Urol, 1995. 154: p. 1295-1299.
120. O'Dowd, G.J., Miller, M.C., Orozco, R., Veltri, R.W. *Repeat biopsy cancer incidence rates following a negative, high grade prostatic intraepithelial neoplasia or suspicious diagnosis*. J Urol, 1999. 161((Suppl)): p. 73.
121. Kronz, J.D., Allan, C.H., Shaikh, A.A., Epstein, J.I. *Predicting cancer following a diagnosis of high grade prostatic intraepithelial neoplasia on needle biopsy: data on men with more than one follow-up biopsy*. Am J Surg Pathol, 2001. 25: p. 1079-1085.
122. Ronnette, B.M., Carmichael, M.J., Carter, H.B., Epstein, J.I. *Does prostatic intraepithelial neoplasia result in elevated serum prostate specific antigen levels?* J Urol, 1993. 150: p. 386-389.

123. Keetch, D.W., Humphrey, P., Stahl, D., Smith, D.S., Catalona, W.J. *Morphometric analysis and clinical follow-up of isolated prostatic intraepithelial neoplasia in needle biopsy of the prostate.* J Urol, 1995. 154: p. 347-351.
124. Brawer, M.K., Bigler, S.A., Sohlberg, O.E., Nagle, R.B., Lange, P.H. *Significance of prostatic intraepithelial neoplasia on prostate needle biopsy.* Urology, 1991. 38: p. 103-107.
125. Gleason, D.F., Mellinger, G.T. *Veterans Administration Cooperative Urological Research Group: prediction of prognosis for prostatic adenocarcinoma by combined histologic grading and clinical staging.* J Urol, 1974. 111(58-64).
126. McNeal, J.E., Villers, A.A., Redwine, E.A., Freiha, F.S., Stamey, T.A. *Histologic differentiation, cancer volume, and pelvic lymph node metastasis in adenocarcinoma of the prostate.* Cancer, 1990. 66: p. 1225-33.
127. Sogani, P.C., Israel, A., Lieberman, P.H., Lesser, M.L., Whitmore, W.F.J. *Gleason grading of prostate cancer: a predictor of survival.* Urology, 1985. 25: p. 223-227.
128. Bostwick, D.G. *Gleason grading of prostatic needle biopsies. Correlation with grade in 316 matched prostatectomies.* Am J Surg Pathol, 1994. 18: p. 796-803.
129. Spires, S.E., Cibull, M.L., Wood, D.P.J., Miller, S., Spires, S.M., Banks, E.R. *Gleason histologic grading in prostatic carcinoma. Correlation of 18-gauge core biopsy with prostatectomy.* Arch Pathol Lab Med, 1994. 118: p. 705-708.
130. Steinberg, D.M., Sauvageot, J., Piantadosi, S., Epstein, J.I. *Correlation of prostate needle biopsy and radical prostatectomy Gleason grade in academic and community settings.* Am J Surg Pathol, 1997. 21: p. 566-576.
131. Sobin, L.H., Wittekind, C.H. *TNM Classification of Malignant Tumours.* 6th Edition ed. 2002, New York: Wiley-Liss.
132. Etzioni, R., Legler, J.M., Feuer, E.J., Merrill, R.M., Cronin, K.A., Hankey, B.F. *Cancer surveillance series: interpreting trends in prostate cancer--part III: Quantifying the link between population prostate-specific antigen testing and recent declines in prostate cancer mortality.* J Natl Cancer Inst, 1999. 91: p. 1033-39.
133. Bartsch, G., Horninger, W., Klocker, H., Reissigl, A., Oberaigner, W., Schönitzer, D., Severi, G., Robertson, C., Boyle, P., Group., T.P.C.S. *Prostate cancer mortality after introduction of prostate-specific antigen mass screening in the Federal State of Tyrol, Austria.* Urology, 2001. 58: p. 417-24.
134. Roberts, R.O., Bergstralh, E.J., Katusic, S.K., Lieber, M.M., Jacobsen, S.J. *Decline in prostate cancer mortality from 1980 to 1997, and an update on incidence trends in Olmsted County, Minnesota.* J Urol, 1999. 161: p. 529-33.
135. Labrie, F., Candas, B., Dupont, A., Cusan, L., Gomez, J.L., Suburu, R.E., Diamond, P., Lévesque, J., Belanger, A. *Screening decreases prostate cancer death: first analysis of the 1988 Quebec prospective randomized controlled trial.* Prostate, 1999. 38: p. 83-91.

136. van der Crujisen-Koeter, I.W., Vis, A.N., Roobol, M.J., Wildhagen, M.F., de Koning, H.J., van der Kwast, T.H., Schröder, F.H. *Comparison of screen detected and clinically diagnosed prostate cancer in the European randomized study of screening for prostate cancer, section rotterdam.* J Urol, 2005. 174: p. 121-25.
137. Chamberlain, J., Melia, J., Moss, S., Brown, J. *The diagnosis, management, treatment and costs of prostate cancer in England and Wales.* Health Technol Assess, 1997. 1(3): p. 1-53.
138. Albertsen, P.C., Hanley, J.A., Fine, J. *20-year outcomes following conservative management of clinically localized prostate cancer.* JAMA, 2005. 293: p. 2095-2101.
139. Houston, T.P., Elster, A.B., Davis, R.M., Deitchman, S.D. *The U.S. Preventive Services Task Force Guide to Clinical Preventive Services, 2nd ed. AMA Council on Scientific Affairs.* Am J Prev Med, 1998. 14: p. 374.
140. *Prostate-specific antigen (PSA) best practice policy. American Urological Association (AUA).* Oncology (Williston Park), 2000. 14: p. 267-72.
141. Aus, G., Abbou, C.C., Bolla, M., Heidenreich, A., Schmid, H.P., van Poppel, H., Wolff, J., Zattoni, F., Urology, E.A.o. *EAU guidelines on prostate cancer.* Eur Urol, 2005. 48: p. 546-51.
142. Watson, E., Jenkins, L., Bukach, C., Austoker, J. *The PSA test and prostate cancer: information for primary care., in NHS Cancer Screening Programmes.* 2002: Sheffield.
143. Partin, A.W., Yoo, J., Carter, H.B., Pearson, J.D., Chan, D.W., Epstein, J.I., Walsh, P.C. *The use of prostate specific antigen, clinical stage and Gleason score to predict pathological stage in men with localized prostate cancer.* J Urol, 1993. 150(1): p. 110-4.
144. Lilja, H. *A kallikrein-like serine protease in prostatic fluid cleaves the predominant seminal vesicle protein.* J Clin Invest, 1985. 76: p. 1899.
145. Rao, A.R., Motiwala, H.G., Karim, O.M.A. *The discovery of prostate-specific antigen.* BJUI, 2008. 101: p. 5-10.
146. Stephan, C., Jung, K., Brux, B., Lein, M., Sinha, P., Schnorr, D., Loening, S.A. *ACT-PSA and complexed PSA elimination kinetics in serum after radical retropubic prostatectomy: proof of new complex forming of PSA after release into circulation.* Urology, 2000. 55: p. 560.
147. Partin, A.W., Piantadosi, S., Subong, E.N., Kelly, C.A., Hortopan, S., Chan, D.W., Wolfert, R.L., Rittenhouse, H.G., Carter, H.B. *Clearance rate of serum free- and total-PSA following radical prostatectomy.* Prostate, 1996. 7((Suppl)): p. 35.
148. Pizzo, S.V., Mast, A.E., Feldman, S.R., Salvesen, G. *In vivo catabolism of alpha1-antichymotrypsin is mediated by the serpin receptor which binds alpha1-proteinase inhibitor, antithrombin II and heparin cofactor II.* Biochem Biophys Acta, 1988. 967: p. 158.
149. Stamey, T.A., Yang, N., Hay, A.R., McNeal, J.E., Freiha, F.S., Redwine, E. *Prostate-specific antigen as a serum marker for adenocarcinoma of the prostate.* N Engl J Med, 1987. 317: p. 909.
150. Chybowski, F.M., Bergstralh, E.J., Oesterling, J.E. *The effect of digital rectal examination on the serum prostate specific antigen concentration: Results of a randomized study.* J Urol, 1992. 148: p. 83.

151. Crawford, E.D., Schutz, M.J., Clejan, S., al, e. *The effect of digital rectal examination on prostate-specific antigen levels.* JAMA, 1992. 267: p. 2227.
152. Young, C.Y., Montgomery, B.T., Andrews, P.E., Qui, S.D., Bilhartz, D.L., Tindall, D.J. *Hormonal regulation of prostate-specific antigen messenger RNA in human prostatic adenocarcinoma cell line LNCaP.* Cancer Res, 1991. 51: p. 3748.
153. Henttu, P., Liao, S., Vihko, P. *Androgens up-regulate the human prostate-specific antigen messenger ribonucleic acid (mRNA) but down-regulate the prostatic acid phosphatase mRNA in the LNCaP cell line.* Endocrinology, 1992. 130: p. 766.
154. Guess, H.A., Heyse, J.F., Gormley, G.J., Stoner, E., Oesterling, J.E. *Effect of finasteride on serum PSA concentration in men with benign prostatic hyperplasia: results from the North American Phase III Clinical Trial.* Urol Clin North Am, 1993. 20: p. 627.
155. Catalona, W.J., Smith, D.S., Wolfert, R.L., Wang, T.J., Rittenhouse, H.G., Ratliff, T.L., Nadler, R.B. *Evaluation of percentage of free serum prostate-specific antigen to improve specificity of prostate cancer screening.* Jama, 1995. 274(15): p. 1214-20.
156. Schröder, F.H., van der Maas, P., Beemsterboer, P., Kruger, A.B., Hoedemaeker, R., Rietbergen, J., Kranse, R. *Evaluation of the digital rectal examination as a screening test for prostate cancer. Rotterdam section of the European Randomized Study of Screening for Prostate Cancer.* J Natl Cancer Inst, 1998. 90: p. 1817.
157. Oesterling, J.E., Jacobsen, S.J., Chute, C.G., Guess, H.A., Girman, C.J., Panser, L.A., Lieber, M.M. *Serum prostate-specific antigen in a community-based population of healthy men. Establishment of age-specific reference ranges.* JAMA, 1993. 270: p. 860-64.
158. *Referral guidelines for suspected cancer.* 2002, Department of Health.
159. *Meeting of the Prostate Cancer Risk Management Programme Scientific Reference Group.* 2002.
160. Thompson, I.M., Pauler, D.K., Goodman, P.J., Tangen, C.M., Lucia, M.S., Parnes, H.L., Minasian, L.M., Ford, L.G., Lippman, S.M., Crawford, E.D., Crowley, J.J., Coltman, C.A.J. *Prevalence of prostate cancer among men with a prostate-specific antigen level ≤ 4.0 ng per milliliter.* New England Journal of Medicine, 2004. 350(22): p. 2239-46.
161. Stamey, T.A., Freiha, F.S., McNeal, J.E., Redwine, E.A., Whittemore, A.S., Schmid, H.P. *Localized prostate cancer. Relationship of tumor volume to clinical significance for treatment of prostate cancer.* Cancer, 1993. 71(3 Suppl): p. 933-8.
162. Benson, M.C., Whang, I.S., Pantuck, A., Ring, K., Kaplan, S.A., Olsson, C.A., Cooner, W.H. *Prostate specific antigen density: means of distinguishing benign prostatic hypertrophy and prostate cancer.* J Urol, 1992. 147: p. 815.
163. Seaman, E., Whang, M., Olsson, C.A., Am, e.a.U.C.N. *Prostate-specific antigen density (PSAD): Role in patient evaluation and management.* Urol Clin North Am, 1993. 20: p. 653.

164. Rommel, F.M., Agusta, V.E., Breslin, J.A., Huffnagle, H.W., Pohl, C.E., Sieber, P.R., Stahl, C.A. *Use of prostate specific antigen and prostate specific antigen density in diagnosis of prostate cancer in community based urology practice.* J Urol, 1994. 151: p. 88.
165. Bazinet, M., Meshref, A.W., Trudel, C., Aronson, S., Péloquin, F., Nachabe, M., Bégin, L.R., Elhilali, M.M. *Prospective evaluation of prostate-specific antigen density and systematic biopsies for early detection of prostatic carcinoma.* Urology, 1994. 43: p. 44.
166. Carter, H.B., Pearson, J.D., Metter, E.J., Brant, L.J., Chan, D.W., Andres, R., Fozard, J.L., Walsh, P.C. *Longitudinal evaluation of prostate specific antigen levels in men with and without prostate disease.* JAMA, 1992. 267: p. 2215.
167. Smith, D.S., Catalona, W.J. *Rate of change in serum prostate specific antigen levels as a method for prostate cancer detection.* J Urol, 1994. 152: p. 1163.
168. Carter, H.B., Pearson, J.D., Morrell, C.H., al, e. *What is the shortest time interval over which PSA velocity should be measured?* J Urol, 1995. 153: p. 419A.
169. Carter, H.B., Pearson, J.D., Waclawiw, Z., Metter, E.J., Chan, D.W., Guess, H.A., Walsh, P.C. *Prostate-specific antigen variability in men without prostate cancer: the effect of sampling interval and number of repeat measurements on prostate-specific antigen velocity.* Urology, 1995. 45: p. 591.
170. Okihara, K., Cheli, C.D., Partin, A.W., Fritche, H.A., Chan, D.W., Sokoll, L.J., Brawer, M.K., Schwartz, M.K., Vessella, R.L., Loughlin, K.R., Johnston, D.A., Babaian, R.J. *Comparative analysis of complexed prostate specific antigen, free prostate specific antigen and their ratio in detecting prostate cancer.* J Urol, 2002. 167(5): p. 2017-23; discussion 2023-4.
171. Huber, P.R., Schmid, H.P., Mattarelli, G., Strittmatter, B., van Steenbrugge, G.J., Maurer, A. *Serum free prostate specific antigen: isoenzymes in benign hyperplasia and cancer of the prostate.* Prostate, 1995. 27(4): p. 212-9.
172. Elgamal, A.A., Van Poppel, H.P., Van de Voorde, W.M., Van Dorpe, J.A., Oyen, R.H., Baert, L.V. *Impalpable invisible stage T1c prostate cancer: characteristics and clinical relevance in 100 radical prostatectomy specimens--a different view.* J Urol, 1997. 157(1): p. 244-50.
173. Aus, G., Ahlgren, G., Hugosson, J., Pedersen, K.V., Rensfeldt, K., Soderberg, R. *Diagnosis of prostate cancer: optimal number of prostate biopsies related to serum prostate-specific antigen and findings on digital rectal examination.* Scand J Urol Nephrol, 1997. 31(6): p. 541-4.
174. Hodge, K.K., McNeal, J.E., Terris, M.K., Stamey, T.A. *Random systematic versus directed ultrasound guided transrectal core biopsies of the prostate.* J Urol, 1989. 142: p. 71-4.
175. Aus, G., Bergdahl, S., Hugosson, J., Lodding, P., Pihl, C.G., Pileblad, E. *Outcome of laterally directed sextant biopsies of the prostate in screened males aged 50--66 years. Implications for sampling order.* Eur Urol, 2001. 39(6): p. 655-60; discussion 661.

176. Eskew, L.A., Bare, R.L., McCullough, D.L. *Systematic 5 region prostate biopsy is superior to sextant method for diagnosing carcinoma of the prostate.* J Urol, 1997. 157(1): p. 199-202; discussion 202-3.
177. Djavan, B., Ravery, V., Zlotta, A., Dobronski, P., Dobrovits, M., Fakhari, M., Seitz, C., Susani, M., Borkowski, A., Boccon-Gibod, L., Schulman, C.C., Marberger, M. *Prospective evaluation of prostate cancer detected on biopsies 1, 2, 3 and 4: when should we stop?* J Urol, 2001. 166(5): p. 1679-83.
178. Aus, G., Abbou C.C, Bolla M, Heidenreich A, van Poppel H, Schmid H-P, Wolff J.M, Zattoni F. *Chapter 5: Diagnosis, in European Association of Urology Guidelines on Prostate Cancer.* 2005. p. 11-18.
179. Konety, B., Naraghi, R., Googing, W., O'Donnell, W., Bahnson, R. *Evaluation of computerized tomography for staging clinically localised adenocarcinoma of the prostate.* Urol Oncol, 1996. 2: p. 14-19.
180. Rifkin, M.D., Zerhouni, E.A., Gatsonis, C.A., Quint, L.E., Paushter, D.M., Epstein, J.I., Hamper, U., Walsh, P.C., McNeil, B.J. *Comparison of magnetic resonance imaging and ultrasonography in staging early prostate cancer. Results of a multi-institutional cooperative trial.* N Engl J Med, 1990. 323(10): p. 621-6.
181. Albertsen, P.C., Hanley, J.A., Gleason, D.F., Barry, M.J. *Competing risk analysis of men aged 55 to 74 years at diagnosis managed conservatively for clinically localized prostate cancer.* Jama, 1998. 280(11): p. 975-80.
182. Griebeling, T.L., Williams, R.D. *Staging of incidentally detected prostate cancer: role of repeat resection, prostate-specific antigen, needle biopsy, and imaging.* Semin Urol Oncol, 1996. 14(3): p. 156-64.
183. Brasso, K., Friis, S., Juel, K., Jorgensen, T., Iversen, P. *Mortality of patients with clinically localized prostate cancer treated with observation for 10 years or longer: a population based registry study.* J Urol, 1999. 161(2): p. 524-8.
184. Hugosson, J., Aus, G., Bergdahl, C., Bergdahl, S. *Prostate cancer mortality in patients surviving more than 10 years after diagnosis.* J Urol, 1995. 154(6): p. 2115-7.
185. Johansson, J.E., Andren, O., Andersson, S.O., Dickman, P.W., Holmberg, L., Magnuson, A., Adami, H.O. *Natural history of early, localized prostate cancer.* Jama, 2004. 291(22): p. 2713-9.
186. Holmberg, L., Bill-Axelson, A., Helgesen, F., Salo, J.O., Folmerz, P., Haggman, M., Andersson, S.O., Spangberg, A., Busch, C., Nordling, S., Palmgren, J., Adami, H.O., Johansson, J.E., Norlen, B.J. *A randomized trial comparing radical prostatectomy with watchful waiting in early prostate cancer.* N Engl J Med, 2002. 347(11): p. 781-9.
187. Lundgren, R., Nordle, O., Josefsson, K. *Immediate estrogen or estramustine phosphate therapy versus deferred endocrine treatment in nonmetastatic prostate cancer: a randomized multicenter study with 15 years of followup. The South Sweden Prostate Cancer Study Group.* J Urol, 1995. 153(5): p. 1580-6.
188. Adolfsson, J., Steineck, G., Hedlund, P.O. *Deferred treatment of locally advanced nonmetastatic prostate cancer: a long-term followup.* J Urol, 1999. 161(2): p. 505-8.

189. Parker, M.C., Cook, A., Riddle, P.R., Fryatt, I., O'Sullivan, J., Shearer, R.J. *Is delayed treatment justified in carcinoma of the prostate?* Br J Urol, 1985. 57(6): p. 724-8.
190. Rana, A., Chisholm, G.D., Khan, M., Rashwan, H.M., Elton, R.A. *Conservative management with symptomatic treatment and delayed hormonal manipulation is justified in men with locally advanced carcinoma of the prostate.* Br J Urol, 1994. 74(5): p. 637-41.
191. *Immediate versus deferred treatment for advanced prostatic cancer: initial results of the Medical Research Council Trial. The Medical Research Council Prostate Cancer Working Party Investigators Group.* Br J Urol, 1997. 79(2): p. 235-46.
192. Wirth, M.P., See, W.A., McLeod, D.G., Iversen, P., Morris, T., Carroll, K. *Bicalutamide 150 mg in addition to standard care in patients with localized or locally advanced prostate cancer: Results from the second analysis of the early prostate cancer program at median followup of 5.4 years.* Journal of Urology, 2004. 172(5): p. 1865-1870.
193. Aus, G., Abbou C.C, Bolla M, Heidenreich A, van Poppel H, Schmid H-P, Wolff J.M, Zattoni F. *Chapter 7: Treatment: Deferred Treatment (Watchful Waiting; Active Monitoring), in European Association of Urology Guidelines on Prostate Cancer.* 2005. p. 25-30.
194. Memmelaar, J.M., T. *Total prostatovesiculectomy; retropubic approach.* Journal of Urology, 1949. 62: p. 340-348.
195. Young, H. *Radical perineal prostatectomy.* Johns Hopkins Hospital Bulletin, 1905. 16: p. 315-321.
196. Berryhill, R., Jhaveri, J., Yadav, R., Leung, R., Rao, S., El-Hakim, A., Tewari, A. *Robotic Prostatectomy: A Review of Outcomes Compared with Laparoscopic and Open Approaches.* Urology, 2008. 72: p. 15-23.
197. Lowe, B.A., Listrom, M.B. *Incidental carcinoma of the prostate: an analysis of the predictors of progression.* J Urol, 1988. 140(6): p. 1340-4.
198. Van Poppel, H., Ameye, F., Oyen, R., Van de Voorde, W., Baert, L. *Radical prostatectomy for localized prostate cancer.* Eur J Surg Oncol, 1992. 18(5): p. 456-62.
199. Partin, A.W., Mangold, L.A., Lamm, D.M., Walsh, P.C., Epstein, J.I., Pearson, J.D. *Contemporary update of prostate cancer staging nomograms (Partin Tables) for the new millennium.* Urology, 2001. 58(6): p. 843-8.
200. Graverson, P.H., Nielsen, K.T., Gasser, T.C., Corle, D.K., Madsen, P.O. *Radical prostatectomy versus expectant primary treatment in stages I and II prostatic cancer. A fifteen-year follow-up.* Urology, 1990. 36(6): p. 493-8.
201. Ohori, M., Goad, J.R., Wheeler, T.M., Eastham, J.A., Thompson, T.C., Scardino, P.T. *Can radical prostatectomy alter the progression of poorly differentiated prostate cancer?* J Urol, 1994. 152(5 Pt 2): p. 1843-9.
202. Pound, C.R., Partin, A.W., Epstein, J.I., Walsh, P.C. *Prostate-specific antigen after anatomic radical retropubic prostatectomy. Patterns of recurrence and cancer control.* Urol Clin North Am, 1997. 24(2): p. 395-406.

203. Gibbons, R.P. *Total prostatectomy for clinically localized prostate cancer: long-term surgical results and current morbidity*. NCI Monogr, 1988(7): p. 123-6.
204. Hodgson, D., Warde, P., Gospodarowicz, M. *The management of locally advanced prostate cancer*. Urol Oncol, 1998. 4: p. 3-12.
205. Fallon, B., Williams, R.D. *Current options in the management of clinical stage C prostatic carcinoma*. Urol Clin North Am, 1990. 17(4): p. 853-66.
206. van den Ouden, D., Davidson, P.J., Hop, W., Schroder, F.H. *Radical prostatectomy as a monotherapy for locally advanced (stage T3) prostate cancer*. J Urol, 1994. 151(3): p. 646-51.
207. Lerner, S.E., Blute, M.L., Zincke, H. *Extended experience with radical prostatectomy for clinical stage T3 prostate cancer: outcome and contemporary morbidity*. J Urol, 1995. 154(4): p. 1447-52.
208. Di Silverio, F., D'Eramo, G., Buscarini, M., Sciarra, A., Casale, P., Di Nicola, S., Loreto, A., Seccareccia, F., De Vita, R. *DNA ploidy, Gleason score, pathological stage and serum PSA levels as predictors of disease-free survival in C-D1 prostatic cancer patients submitted to radical retropubic prostatectomy*. Eur Urol, 1996. 30(3): p. 316-21.
209. Gerber, G.S., Thisted, R.A., Chodak, G.W., Schroder, F.H., Frohmuller, H.G., Scardino, P.T., Paulson, D.F., Middleton, A.W., Jr., Rukstalis, D.B., Smith, J.A., Jr., Ohori, M., Theiss, M., Schellhammer, P.F. *Results of radical prostatectomy in men with locally advanced prostate cancer: multi-institutional pooled analysis*. Eur Urol, 1997. 32(4): p. 385-90.
210. Theiss, M., Langer, W., Hofmockel, G., Frohmuller, H. *[Radical prostatectomy as primary monotherapy in capsule penetrating prostatic carcinoma. 15 years outcome]*. Urologe A, 1997. 36(4): p. 343-7.
211. van den Ouden, D., Hop, W.C., Schroder, F.H. *Progression in and survival of patients with locally advanced prostate cancer (T3) treated with radical prostatectomy as monotherapy*. J Urol, 1998. 160(4): p. 1392-7.
212. Van Poppel, H., Goethuys, H., Callewaert, P., Vanuytsel, L., Van de Voorde, W., Baert, L. *Radical prostatectomy can provide a cure for well-selected clinical stage T3 prostate cancer*. Eur Urol, 2000. 38(4): p. 372-9.
213. Ghavamian, R., Bergstralh, E.J., Blute, M.L., Slezak, J., Zincke, H. *Radical retropubic prostatectomy plus orchiectomy versus orchiectomy alone for pTxN+ prostate cancer: a matched comparison*. J Urol, 1999. 161(4): p. 1223-7; discussion 1227-8.
214. Messing, E.M., Manola, J., Yao, J., Kiernan, M., Crawford, D., Wilding, G., di'SantAgnese, P.A., Trump, D., 3886, E.C.O.G.s.E. *Immediate versus deferred androgen deprivation treatment in patients with node-positive prostate cancer after radical prostatectomy and pelvic lymphadenectomy*. Lancet Oncol, 2006. 7: p. 472-9.
215. Aus, G., Abbou C.C, Bolla M, Heidenreich A, van Poppel H, Schmid H-P, Wolff J.M, Zattoni F. *Chapter 8: Radical Prostatectomy*, in *European Association of Urology Guidelines on Prostate Cancer*. 2005. p. 30-41.

216. Davidson, P.J., van den Ouden, D., Schroeder, F.H. *Radical prostatectomy: prospective assessment of mortality and morbidity.* Eur Urol, 1996. 29(2): p. 168-73.
217. Murphy, G.P., Mettlin, C., Menck, H., Winchester, D.P., Davidson, A.M. *National patterns of prostate cancer treatment by radical prostatectomy: results of a survey by the American College of Surgeons Commission on Cancer.* J Urol, 1994. 152(5 Pt 2): p. 1817-9.
218. Sokoloff, M.H., Brendler, C.B. *Indications and contraindications for nerve-sparing radical prostatectomy.* Urol Clin North Am, 2001. 28(3): p. 535-43.
219. Noldus, J., Michl, U., Graefen, M., Haese, A., Hammerer, P., Huland, H. *Patient-reported sexual function after nerve-sparing radical retropubic prostatectomy.* Eur Urol, 2002. 42(2): p. 118-24.
220. Huland, H., Hubner, D., Henke, R.P. *Systematic biopsies and digital rectal examination to identify the nerve-sparing side for radical prostatectomy without risk of positive margin in patients with clinical stage T2, N0 prostatic carcinoma.* Urology, 1994. 44(2): p. 211-4.
221. Van der Aa, F., Joniau, S., De Ridder, D., Van Poppel, H. *Potency after unilateral nerved sparing surgery: A report on functional and oncological results of unilateral nerve sparing surgery.* Prostate Cancer and Prostatic Diseases, 2003. 6(1): p. 61-65.
222. Fowler, F.J., Jr., Barry, M.J., Lu-Yao, G., Wasson, J.H., Bin, L. *Outcomes of external-beam radiation therapy for prostate cancer: a study of Medicare beneficiaries in three surveillance, epidemiology, and end results areas.* J Clin Oncol, 1996. 14(8): p. 2258-65.
223. *Consensus statement: The management of clinically localized prostate cancer., in National Institutes of Health Consensus Development Panel.* 1988, NCI Monogr. p. 3-6.
224. Hanks, G.E., Hanlon, A.L., Schultheiss, T.E., Pinover, W.H., Movsas, B., Epstein, B.E., Hunt, M.A. *Dose escalation with 3D conformal treatment: five year outcomes, treatment optimization, and future directions.* Int J Radiat Oncol Biol Phys, 1998. 41(3): p. 501-10.
225. Pollack, A., Zagars, G.K., Smith, L.G., Lee, J.J., von Eschenbach, A.C., Antolak, J.A., Starkschall, G., Rosen, I. *Preliminary results of a randomized radiotherapy dose-escalation study comparing 70 Gy with 78 Gy for prostate cancer.* J Clin Oncol, 2000. 18(23): p. 3904-11.
226. Zietman, A.L., DeSilvio, M., Slater, J.D et al. *A randomized trial comparing conventional dose (70.2GyE) and high dose (79.2 GyE) conformal radiation in early stage adenocarcinoma of the prostate: results of an interim analysis of PROG 95-09.* Int J Radiat Oncol Biol Phys, 2004. 60: p. S131 (Abstract 4).
227. Aus, G., Abbou C.C, Bolla M, Heidenreich A, van Poppel H, Schmid H-P, Wolff J.M, Zattoni F. *Chapter 9 Treatment: Definitive Radiation Therapy, in European Association of Urology Guidelines on Prostate Cancer.* 2005. p. 41-49.
228. D'Amico, A.V., Manola, J., Loffredo, M., Renshaw, A.A., DellaCroce, A., Kantoff, P.W. *6-month androgen suppression plus radiation therapy vs radiation therapy alone for patients with clinically localized prostate cancer - A randomized controlled trial.* Jama-Journal of the American Medical Association, 2004. 292(7): p. 821-827.

229. Asbell, S.O., Krall, J.M., Pilepich, M.V., Baerwald, H., Sause, W.T., Hanks, G.E., Perez, C.A. *Elective pelvic irradiation in stage A2, B carcinoma of the prostate: analysis of RTOG 77-06*. Int J Radiat Oncol Biol Phys, 1988. 15(6): p. 1307-16.
230. Spaas, P.G., Bagshaw, M.A., Cox, R.S. *The value of extended field irradiation in surgically staged carcinoma of the prostate*. Int J Radiat Oncol Biol Phys, 1988. 15: p. 133 (Abstract 36).
231. Zelefsky, M.J., Fuks, Z., Hunt, M., Yamada, Y., Marion, C., Ling, C.C., Amols, H., Venkatraman, E.S., Leibel, S.A. *High-dose intensity modulated radiation therapy for prostate cancer: early toxicity and biochemical outcome in 772 patients*. Int J Radiat Oncol Biol Phys, 2002. 53(5): p. 1111-6.
232. Kupelian, P.A., Reddy, C.A., Carlson, T.P., Altsman, K.A., Willoughby, T.R. *Preliminary observations on biochemical relapse-free survival rates after short-course intensity-modulated radiotherapy (70 Gy at 2.5 Gy/fraction) for localized prostate cancer*. Int J Radiat Oncol Biol Phys, 2002. 53(4): p. 904-12.
233. Bolla, M., Gonzalez, D., Warde, P., Dubois, J.B., Mirimanoff, R.O., Storme, G., Bernier, J., Kuten, A., Sternberg, C., Gil, T., Collette, L., Pierart, M. *Improved survival in patients with locally advanced prostate cancer treated with radiotherapy and goserelin*. N Engl J Med, 1997. 337: p. 295-300.
234. Ash, D., Flynn, A., Battermann, J., de Reijke, T., Lavagnini, P., Blank, L. *ESTRO/EAU/EORTC recommendations on permanent seed implantation for localized prostate cancer*. Radiother Oncol, 2000. 57(3): p. 315-21.
235. Kupelian, P.A., Potters, L., Ciezki, J.P., Reddy, C.A., Reuther, A.M., Klein, E.A. *Radical prostatectomy, external beam radiotherapy <72Gy, external radiotherapy >72Gy, permanent seed implantation or combined seeds / external beam radiotherapy for stage T1-2 prostate cancer*. in 44th annual ASTRO Meeting. 2002. New Orleans: Int J Radiat Oncol Biol Phys.
236. Ataman, F., Zurlo, A., Artignan, X., van Tienhoven, G., Blank, L.E., Warde, P., Dubois, J.B., Jeanneret, W., Keuppens, F., Bernier, J., Kuten, A., Collette, L., Pierart, M., Bolla, M. *Late toxicity following conventional radiotherapy for prostate cancer: analysis of the EORTC trial 22863*. Eur J Cancer, 2004. 40(11): p. 1674-81.
237. Robinson, J.W., Moritz, S., Fung, T. *Meta-analysis of rates of erectile function after treatment of localized prostate carcinoma*. Int J Radiat Oncol Biol Phys, 2002. 54(4): p. 1063-8.
238. Bolla, M., Van Poppel, H., Van Cangh, P. *Does postoperative radiotherapy after radical prostatectomy improve progression-free survival in pT3N0 prostate cancer? in American Society of Clinical Oncology*. 2004: J Clin Oncol.
239. Bolla, M., Van Poppel, H., Van Cangh, P.J., et al. *Acute and late toxicity of postoperative external irradiation in pT3N0 prostate cancer patients treated within EORTC trial 22911*. Int J Radiat Oncol Biol Phys, 2002. 54(Supple 2): p. S62 abstract 103.

240. Van Cangh, P.J., Richard, F., Lorge, F., Castille, Y., Moxhon, A., Opsomer, R., De Visscher, L., Wese, F.X., Scaillet, P. *Adjuvant radiation therapy does not cause urinary incontinence after radical prostatectomy: results of a prospective randomized study.* J Urol, 1998. 159(1): p. 164-6.
241. Wilder, R.B., Hsiang, J.Y., Ji, M., Earle, J.D., de Vere White, R. *Preliminary results of three-dimensional conformal radiotherapy as salvage treatment for a rising prostate-specific antigen level postprostatectomy.* Am J Clin Oncol, 2000. 23(2): p. 176-80.
242. Han, K.R., Belldegrün, A.S. *Third-generation cryosurgery for primary and recurrent prostate cancer.* Bju International, 2004. 93(1): p. 14-18.
243. Fahmy, W.E., Bissada, N.K. *Cryosurgery for prostate cancer.* Archives of Andrology, 2003. 49(5): p. 397-407.
244. Beerlage, H.P., Thuroff, S., Madersbacher, S., Zlotta, A.R., Aus, G., de Reijke, T.M., de la Rosette, J.J. *Current status of minimally invasive treatment options for localized prostate carcinoma.* Eur Urol, 2000. 37(1): p. 2-13.
245. Rees, J., Patel, B., MacDonagh, R., Persad, R. *Cryosurgery for prostate cancer.* Bju International, 2004. 93(6): p. 710-714.
246. Long, J.P., Bahn, D., Lee, F., Shinohara, K., Chinn, D.O., Macaluso, J.N., Jr. *Five-year retrospective, multi-institutional pooled analysis of cancer-related outcomes after cryosurgical ablation of the prostate.* Urology, 2001. 57(3): p. 518-23.
247. Robinson, J.W., Donnelly, B.J., Saliken, J.C., Weber, B.A., Ernst, S., Rewcastle, J.C. *Quality of life and sexuality of men with prostate cancer 3 years after cryosurgery.* Urology, 2002. 60(2 Suppl 1): p. 12-8.
248. Donnelly, B.J., Saliken, J.C., Ernst, D.S., Ali-Ridha, N., Brasher, P.M., Robinson, J.W., Rewcastle, J.C. *Prospective trial of cryosurgical ablation of the prostate: five-year results.* Urology, 2002. 60(4): p. 645-9.
249. Han, K.R., Cohen, J.K., Miller, R.J., Pantuck, A.J., Freitas, D.G., Cuevas, C.A., Kim, H.L., Lugg, J., Childs, S.J., Shuman, B., Jayson, M.A., Shore, N.D., Moore, Y., Zisman, A., Lee, J.Y., Ugarte, R., Mynderse, L.A., Wilson, T.M., Sweat, S.D., Zincke, H., Belldegrün, A.S. *Treatment of organ confined prostate cancer with third generation cryosurgery: Preliminary multicenter experience.* 2003. 170(4): p. 1126-1130.
250. Bahn, D.K., Lee, F., Badalament, R., Kumar, A., Greski, J., Chernick, M. *Targeted cryoablation of the prostate: 7-year outcomes in the primary treatment of prostate cancer.* Urology, 2002. 60(2 Suppl 1): p. 3-11.
251. De La Taille, A., Benson, M.C., Bagiella, E., Burchardt, M., Shabsigh, A., Olsson, C.A., Katz, A.E. *Cryoablation for clinically localized prostate cancer using an argon-based system: complication rates and biochemical recurrence.* BJU Int, 2000. 85(3): p. 281-6.
252. Koppie, T.M., Shinohara, K., Grossfeld, G.D., Presti, J.C., Jr., Carroll, P.R. *The efficacy of cryosurgical ablation of prostate cancer: the University of California, San Francisco experience.* J Urol, 1999. 162(2): p. 427-32.

253. Aus, G., Abbou C.C, Bolla M, Heidenreich A, van Poppel H, Schmid H-P, Wolff J.M, Zattoni F. *Chapter 10: Experimental Local Treatment of Prostate Cancer*, in *European Association of Urology Guidelines on Prostate Cancer*. 2005. p. 49-53.
254. Thuroff, S., Chaussy, C., Vallancien, G., Wieland, W., Kiel, H.J., Le Duc, A., Desgrandchamps, F., De la Rosette, J., Gelet, A. *High-intensity focused ultrasound and localized prostate cancer: Efficacy results from the European multicentric study*. 2003. 17(8): p. 673-677.
255. Blana, A., Walter, B., Rogenhofer, S., Wieland, W.F. *High-intensity focused ultrasound for the treatment of localized prostate cancer: 5-year experience*. *Urology*, 2004. 63(2): p. 297-300.
256. Huggins, C., Stevens, R.E. Jr, Hodges, C.V. *Studies on prostate cancer. II. The effect of castration on advanced carcinoma of the prostate gland*. *Archives of Surgery*, 1941. 43: p. 209-223.
257. Huggins, C., Hodges, C.V. *Studies on prostatic cancer. I. The effect of castration, of estrogen and of androgen injection on serum phosphatase in metastatic carcinoma of the prostate*. *Cancer Res*, 1941. 1: p. 293-297.
258. Walsh, P.C. *Physiologic basis for hormonal therapy in carcinoma of the prostate*. *Urol Clin North Am*, 1975. 2(1): p. 125-40.
259. Oh, W.K. *The evolving role of estrogen therapy in prostate cancer*. *Clin Prostate Cancer*, 2002. 1: p. 81-89.
260. Scherr, D.S., Pitts, W.R. *The nonsteroidal effects of diethylstilbestrol: The rationale for androgen deprivation therapy without estrogen deprivation in the treatment of prostate cancer*. *Journal of Urology*, 2003. 170(5): p. 1703-1708.
261. Hedlund, P.O., Ala-Opas, M., Brekkan, E., Damber, J.E., Damber, L., Hagerman, I., Haukaas, S., Henriksson, P., Iversen, P., Pousette, A., Rasmussen, F., Salo, J., Vaage, S., Varenhorst, E. *Parenteral estrogen versus combined androgen deprivation in the treatment of metastatic prostatic cancer -- Scandinavian Prostatic Cancer Group (SPCG) Study No. 5*. *Scand J Urol Nephrol*, 2002. 36(6): p. 405-13.
262. Oefelein, M.G., Cornum, R. *Failure to achieve castrate levels of testosterone during luteinizing hormone releasing hormone agonist therapy: the case for monitoring serum testosterone and a treatment decision algorithm*. *J Urol*, 2000. 164(3 Pt 1): p. 726-9.
263. Limonta, P., Montagnani Marelli, M., Moretti, R.M. *LHRH analogues as anticancer agents: pituitary and extrapituitary sites of action*. *Expert Opin Investig Drugs*, 2001. 10(4): p. 709-20.
264. Schally, A.V. *Luteinizing hormone-releasing hormone analogs: their impact on the control of tumorigenesis*. *Peptides*, 1999. 20(10): p. 1247-62.
265. Agarwal, D.K., Costello, A.J., Peters, J., Sikaris, K., Crowe, H. *Differential response of prostate specific antigen to testosterone surge after luteinizing hormone-releasing hormone analogue in prostate cancer and benign prostatic hyperplasia*. *BJU Int*, 2000. 85(6): p. 690-5.
266. Bubley, G.J. *Is the flare phenomenon clinically significant?* *Urology*, 2001. 58(2 Suppl 1): p. 5-9.

267. McLeod, D., Zinner, N., Tomera, K., Gleason, D., Fotheringham, N., Campion, M., Garnick, M.B. *A phase 3, multicenter, open-label, randomized study of abarelix versus leuprolide acetate in men with prostate cancer.* Urology, 2001. 58(5): p. 756-61.
268. Trachtenberg, J., Gittleman, M., Steidle, C., Barzell, W., Friedel, W., Pessis, D., Fotheringham, N., Campion, M., Garnick, M.B. *A phase 3, multicenter, open label, randomized study of abarelix versus leuprolide plus daily antiandrogen in men with prostate cancer.* J Urol, 2002. 167(4): p. 1670-4.
269. Anderson, J. *The role of antiandrogen monotherapy in the treatment of prostate cancer.* Bju International, 2003. 91(5): p. 455-461.
270. Aus, G., Abbou C.C, Bolla M, Heidenreich A, van Poppel H, Schmid H-P, Wolff J.M, Zattoni F. *Chapter 11: Hormonal therapy, in European Association of Urology Guidelines on Prostate Cancer.* 2005. p. 53-69.
271. Tangen, C.M., Faulkner, J.R., Crawford, E.D., Thompson, I.M., Hirano, D., Eisenberger, M., Hussain, M. *Ten-year survival in patients with metastatic prostate cancer.* Clin Prostate Cancer, 2003. 2(1): p. 41-5.
272. Seidenfeld, J., Samson, D.J., Aronson, N., Albertson, P.C., Bayoumi, A.M., Bennett, C., Brown, A., Garber, A., Gere, M., Hasselblad, V., Wilt, T., Ziegler, K. *Relative effectiveness and cost-effectiveness of methods of androgen suppression in the treatment of advanced prostate cancer.* Evid Rep Technol Assess (Summ), 1999(4): p. i-x, 1-246, 11-36, passim.
273. Petrylak, D.P., Tangen, C.M., Hussain, M.H.A., Lara, P.N.J., Jones, J.A., Taplin, M.E., Burch, P.A., Berry, D., Moinpour, C., Kohli, M., Benson, M.C., Small, E.J., Raghavan, D., Crawford, E.D. *Docetaxel and estramustine compared with mitoxantrone and prednisone for advanced refractory prostate cancer.* New England Journal of Medicine, 2004. 351(15): p. 1513-1520.
274. Tannock, I.F., de Wit, R., Berry, W.R., Horti, J., Pluzanska, A., Chi, K.N., Oudard, S., Theodore, C., James, N.D., Turesson, I., Rosenthal, M.A., Eisenberger, M.A. *Docetaxel plus prednisone or mitoxantrone plus prednisone for advanced prostate cancer.* New England Journal of Medicine, 2004. 351(15): p. 1502-1512.
275. Alison, M.R., Poulsom, R., Forbes, S., Wright, N.A. *An introduction to stem cells.* J Pathol, 2002. 197(4): p. 419-23.
276. Till, J.E., McCulloch, E.A. *A direct measurement of the radiation sensitivity of normal mouse bone marrow cells.* Radiat Res, 1961. 14: p. 213-222.
277. Potten, C.S., Lajtha, L.G. *Stem cells versus stem lines.* Ann N Y Acad Sci, 1982. 397: p. 49-61.
278. Becker, A., McCulloch, E.A., Till, J. *Cytological demonstration of the clonal nature of spleen colonies from transplanted mouse cells.* Nature, 1963. 197: p. 452.
279. Cairns, J. *Mutation selection and the natural history of cancer.* Nature, 1975. 255(5505): p. 197-200.
280. Potten, C.S., Owen, G., Booth, D. *Intestinal stem cells protect their genome by selective segregation of template DNA strands.* J Cell Sci, 2002. 115(Pt 11): p. 2381-8.

281. Smith, G.H. *Label-retaining epithelial cells in the mammary gland divide asymmetrically and retain their template DNA strands.* Development, 2005. 132: p. 681-7.
282. Karpowicz, P., Morshead, C., Kam, A., Jervis, E., Ramunas, J., Cheng, V., van der Kooy, D. *Support for the immortal strand hypothesis: neural stem cells partition DNA asymmetrically in vitro.* J Cell Biol, 2005. 170: p. 721-32.
283. Spradling, A., Drummond-Barbosa, D., Kai, T. *Stem cells find their niche.* Nature, 2001. 414(6859): p. 98-104.
284. Fuchs, E., Tumber, T., Guasch, G. *Socializing with the neighbors: stem cells and their niche.* Cell, 2004. 116: p. 769-778.
285. Hamburger, A.W., Salmon, S.E. *Primary bioassay of human tumor stem cells.* Science, 1977. 197(4302): p. 461-3.
286. Pardoll, R., Clarke, M.F., Morrison, S.J. *Applying the principles of stem-cell biology to cancer.* Nat Rev Cancer, 2003. 3: p. 895-902.
287. Al-Hajj, M., Clarke, M.F. *Self-renewal and solid tumor stem cells.* Oncogene, 2004. 23(43): p. 7274-7282.
288. Krivstov, A.V., Twomey, D., Feng, Z.H., Stubbs, M.C., Golub, T.R., Armstrong, S.A. *Transformation from committed progenitor to leukaemia stem cell initiated by MLL-AF9.* Nature, 2006. 442: p. 818-822.
289. Huntly, B.J.P., Shigematsu, H., Deguchi, K., Lee, B.H., Mizuno, S., Duclos, N., Rowan, R., Amaral, S., Curley, D., Williams, I.R., Akashi, K., Gilliland, D.G. *MOZ-TIF2, but not BCR-ABL, confers properties of leukemic stem cells to committed murine hematopoietic progenitors.* Cancer Cell, 2004. 6: p. 587-96.
290. Reya, T., Morrison, S.J., Clarke, M.F., Weissman, I.L. *Stem cells, cancer, and cancer stem cells.* Nature, 2001. 414(6859): p. 105-11.
291. Jordan, C.T., Guzman, M.L., Noble, M. *Mechanisms of disease - Cancer stem cells.* New England Journal of Medicine, 2006. 355(12): p. 1253-1261.
292. Schofield, R. *The relationship between the spleen colony-forming cell and the haemopoietic stem cell.* Blood Cells, 1978. 4(1-2): p. 7-25.
293. Foster, C.S., Dodson, A., Karavana, V., Smith, P.H., Ke, Y. *Prostatic stem cells.* J Pathol, 2002. 197(4): p. 551-65.
294. Potten, C.S., Loeffler, M. *Stem cells: attributes, cycles, spirals, pitfalls and uncertainties. Lessons for and from the crypt.* Development, 1990. 110(4): p. 1001-20.
295. Bjerknes, M., Cheng, H. *Clonal analysis of mouse intestinal epithelial progenitors.* Gastroenterology, 1999. 116(1): p. 7-14.
296. Rochat, A., Kobayashi, K., Barrandon, Y. *Location of stem cells of human hair follicles by clonal analysis.* Cell, 1994. 76(6): p. 1063-73.
297. Schofield, K.P., Rushton, G., Humphries, M.J., Dexter, T.M., Gallagher, J.T. *Influence of interleukin-3 and other growth factors on alpha4beta1 integrin-mediated adhesion and migration of human hematopoietic progenitor cells.* Blood, 1997. 90(5): p. 1858-66.
298. Al-Hajj, M., Wicha, M.S., Benito-Hernandez, A., Morrison, S.J., Clarke, M.F. *Prospective identification of tumorigenic breast cancer cells.* Proceedings of the National Academy of Sciences of the United States of America, 2003. 100(7): p. 3983-3988.

299. Galli, R., Binda, E., Orfanelli, U., Cipelletti, B., Gritti, A., De Vitis, S., Fiocco, R., Foroni, C., Dimeco, F., Vescovi, A. *Isolation and characterization of tumorigenic, stem-like neural precursors from human glioblastoma*. Cancer Research, 2004. 64(19): p. 7011-7021.
300. Kiaris, H., Chatzistamou, I., Trimis, G., Frangou-Plemmenou, M., Pafiti-Kondi, A., Kalofoutis, A. *Evidence for nonautonomous effect of p53 tumor suppressor in carcinogenesis*. Cancer Res, 2005. 65: p. 1627-30.
301. *The Nobel Prize in Physiology or Medicine 2001*. 2001, Nobel Foundation.
302. Israels, E.D., Israels, L.G. *The cell cycle*. Stem Cells, 2001. 19(1): p. 88-91.
303. Bonnet, D. *Haemopoietic stem cells*. J Pathol, 2002. 197: p. 430-440.
304. Ziegler, B.L., Valtieri, M., Porada, G.A., De Maria, R., Muller, R., Masella, B., Gabbianelli, M., Casella, I., Pelosi, E., Bock, T., Zanjani, E.D., Peschle, C. *KDR receptor: a key marker defining hematopoietic stem cells*. Science, 1999. 285(5433): p. 1553-8.
305. Zanjani, E.D., Almeida-Porada, G., Livingston, A.G., al., e. *Human bone marrow CD34⁺ cells engraft in vivo and undergo multilineage expression that includes giving rise to CD34⁺ cells*. Exp Hematol, 1998. 26(353-360).
306. Bhatia, M., Bonnet, D., Murdoch, B., Gan, O.I., Dick, J.E. *A newly discovered class of human hematopoietic cells with SCID-repopulating activity*. Nat Med, 1998. 4(9): p. 1038-45.
307. Shivdasani, R.A., Orkin, S.H. *The transcription control of hematopoiesis*. Blood, 1996. 87(4025-4029).
308. Look, T.A. *Oncogenic transcription factors in human acute leukemias*. Science, 1996. 278: p. 1059-1064.
309. Rabbitts, T.H. *Chrosomal translocations in human cancer*. Nature, 1994. 372: p. 143-145.
310. Robb, L., Lyons, I., Li, R., Hartley, L., Kontgen, F., Harvey, R.P., Metcalf, D., Begley, C.G. *Absence of yolk sac hematopoiesis from mice with a targeted disruption of the scl gene*. Proc Natl Acad Sci U S A, 1995. 92(15): p. 7075-9.
311. Moreau-Gachelin, L., Tavitian, A., Tambourin, P., al., e. *Spi-1 is a putative oncogene in virally induced murine erythroleukemias*. Nature, 1988. 331: p. 277-279.
312. Miwa, H., Beran, M., Saunders, G.F. *Expression of the Wilm's tumor (WT) gene in human leukemia*. Leukemia, 1992. 6: p. 405-408.
313. Thorsteinsdottir, U., Sauvageau, G., Humphries, R.K. *Enhanced in vivo regenerative potential of HOXB4-transduced hematopoietic stem cells with regulation of their pool size*. Blood, 1999. 94(8): p. 2605-12.
314. Sauvageau, G., Thorsteinsdottir, U., Eaves, C.J., Lawrence, H.J., Largman, C., Lansdorp, P.M., Humphries, R.K. *Overexpression of HOXB4 in hematopoietic cells causes the selective expansion of more primitive populations in vitro and in vivo*. Genes Dev, 1995. 9(14): p. 1753-65.
315. Artavanis-Tsakonas, S., Matsuno, K., Fortini, M. *Notch signalling*. Science, 1995. 268: p. 225-232.

316. Karanu, F.N., Murdoch, B., Gallacher, L., Wu, D.M., Koremoto, M., Sakano, S., Bhatia, M. *The notch ligand jagged-1 represents a novel growth factor of human hematopoietic stem cells.* J Exp Med, 2000. 192(9): p. 1365-72.
317. Eaves, A.C., Eaves, C.J. *Maintenance and proliferation control of primitive hemopoietic progenitors in long-term cultures of human marrow cells.* Blood Cells, 1988. 14(2-3): p. 355-68.
318. Bonnet, D., Dick, J.E. *Human acute myeloid leukemia is organized as a hierarchy that originates from a primitive hematopoietic cell.* Nat Med, 1997. 3(7): p. 730-7.
319. Lapidot, T., Sirard, C., Vormoor, J., Murdoch, B., Hoang, T., Caceres-Cortes, J., Minden, M., Paterson, B., Caligiuri, M.A., Dick, J.E. *A cell initiating human acute myeloid leukaemia after transplantation into SCID mice.* Nature, 1994. 367(6464): p. 645-8.
320. Holyoake, T.L., Jiang, X., Drummond, M.W., Eaves, A.C., Eaves, C.J. *Elucidating critical mechanisms of deregulated stem cell turnover in the chronic phase of chronic myeloid leukemia.* Leukemia, 2002. 16(4): p. 549-58.
321. Cobaleda, C., Gutierrez-Cianca, N., Perez-Losada, J., Flores, T., Garcia-Sanz, R., Gonzalez, M., Sanchez-Garcia, I. *A primitive hematopoietic cell is the target for the leukemic transformation in human philadelphia-positive acute lymphoblastic leukemia.* Blood, 2000. 95(3): p. 1007-13.
322. Cox, C.V., Evely, R.S., Oakhill, A., Pamphilon, D.H., Goulden, N.J., Blair, A. *Characterization of acute lymphoblastic leukemia progenitor cells.* Blood, 2004. 104(9): p. 2919-2925.
323. Jordan, C.T. *Unique molecular and cellular features of acute myelogenous leukemia stem cells.* Leukemia, 2002. 16(4): p. 559-62.
324. Larson, R.A., Sievers, E.L., Stadtmauer, E.A., al., e. *Final report of the efficacy and safety of gemtuzumab ozogamicin (Mylotarg) in patients with CD33-positive acute myeloid leukaemia in first recurrence.* Cancer, 2005. 104: p. 1442-52.
325. Hamann, P.R., Hinman, L.M., Hollander, I., Beyer, C.F., Lindh, D., Holcomb, R., Hallett, W., Tsou, H.R., Upeslakis, J., Shochat, D., Mountain, A., Flowers, D.A., Bernstein, I. *Gemtuzumab ozogamicin, a potent and selective anti-CD33 antibody-calicheamicin conjugate for treatment of acute myeloid leukemia.* Bioconjug Chem, 2002. 13(1): p. 47-58.
326. Taussig, D.C., Pearce, D.J., Simpson, C., Rohatiner, A.Z., Lister, T.A., Kelly, G., Luongo, J.L., Danet-Desnoyers, G.A.H., Bonnet, D. *Hematopoietic stem cells express multiple myeloid markers: implications for the origin and targeted therapy of acute myeloid leukemia.* Blood, 2005. 106(13): p. 4086-4092.
327. Deininger, M., Buchdunger, E., Druker, B.J. *The development of imatinib as a therapeutic agent for chronic myeloid leukaemia.* Blood, 2005. 105: p. 2640-53.
328. Graham, S.M., Jorgensen, H.G., Allan, E., Pearson, C., Alcorn, M.J., Richmond, L., Holyoake, T.L. *Primitive, quiescent, Philadelphia-positive stem cells from patients with chronic myeloid leukemia are insensitive to ST1571 in vitro.* Blood, 2002. 99(1): p. 319-25.

329. Cortes, J., O'Brien, S., Kantarjian, H. *Discontinuation of imatinib therapy after achieving a molecular response*. Blood, 2004. 104: p. 2204-5.
330. Guzman, M.L., Neering, S.J., Upchurch, D., Grimes, B., Howard, D.S., Rizzieri, D.A., Luger, S.M., Jordan, C.T. *Nuclear factor-kappaB is constitutively activated in primitive human acute myelogenous leukemia cells*. Blood, 2001. 98(8): p. 2301-7.
331. Xu, Q., Simpson, S.E., Scialla, T.J., Bagg, A., Carroll, M. *Survival of acute myeloid leukaemia cells requires PI3 kinase activation*. Blood, 2003. 102: p. 972-80.
332. Guzman, M.L., Swiderski, C.F., Howard, D.S., Grimes, B.A., Rossi, R.M., Szilvassy, S.J., Jordan, C.T. *Preferential induction of apoptosis for primary human leukemic stem cells*. Proc Natl Acad Sci U S A, 2002. 99(25): p. 16220-5.
333. Xu, Q., Thompson, J.E., Carroll, M. *mTOR regulates cell survival after etoposide treatment in primary AML cells*. Blood, 2005. 106(13): p. 4261-4268.
334. Gage, F.H. *Mammalian neural stem cells*. Science, 2000. 287(5457): p. 1433-8.
335. Reubinoff, B.E., Itsykson, P., Turetsky, T., Pera, M.F., Reinhartz, E., Itzik, A., Ben-Hur, T. *Neural progenitors from human embryonic stem cells*. Nat Biotechnol, 2001. 19(12): p. 1134-40.
336. Reynolds, B.A., Tetzlaff, W., Weiss, S. *A multipotent EGF-responsive striatal embryonic progenitor cell produces neurons and astrocytes*. J Neurosci, 1992. 12(11): p. 4565-74.
337. Reynolds, B.A., Weiss, S. *Generation of neurons and astrocytes from isolated cells of the adult mammalian central nervous system*. Science, 1992. 255(5052): p. 1707-10.
338. Armstrong, R.J., Watts, C., Svendsen, C.N., Dunnett, S.B., Rosser, A.E. *Survival, neuronal differentiation, and fiber outgrowth of propagated human neural precursor grafts in an animal model of Huntington's disease*. Cell Transplant, 2000. 9(1): p. 55-64.
339. Englund, U., Ericson, C., Rosenblad, C., Mandel, R.J., Trono, D., Victorin, K., Lundberg, C. *The use of a recombinant lentiviral vector for ex vivo gene transfer into the rat CNS*. Neuroreport, 2000. 11(18): p. 3973-7.
340. Uchida, N., Buck, D.W., He, D., Reitsma, M.J., Masek, M., Phan, T.V., Tsukamoto, A.S., Gage, F.H., Weissman, I.L. *Direct isolation of human central nervous system stem cells*. Proc Natl Acad Sci U S A, 2000. 97(26): p. 14720-5.
341. Shmelkov, S.V., St Clair, R., Lyden, D., Rafii, S. *AC133/CD133/Prominin-1*. Int J Biochem Cell Biol, 2005. 37: p. 715-9.
342. Vetter, M. *A turn of the helix: preventing the glial fate*. Neuron, 2001. 29(3): p. 559-62.
343. Zhou, Q., Choi, G., Anderson, D.J. *The bHLH transcription factor Olig2 promotes oligodendrocyte differentiation in collaboration with Nkx2.2*. Neuron, 2001. 31(5): p. 791-807.

344. Sun, T., Echelard, Y., Lu, R., Yuk, D.I., Kaing, S., Stiles, C.D., Rowitch, D.H. *Olig bHLH proteins interact with homeodomain proteins to regulate cell fate acquisition in progenitors of the ventral neural tube.* Curr Biol, 2001. 11(18): p. 1413-20.
345. Frisen, J., Lendahl, U. *Oh no, Notch again!* Bioessays, 2001. 23: p. 3-7.
346. Rogister, B., Ben-Hur, T., Dubois-Dalcq, M. *From neural stem cells to myelinating oligodendrocytes.* Mol Cell Neurosci, 1999. 14(4-5): p. 287-300.
347. Wang, S., Sdrulla, A.D., diSibio, G., al., e. *Notch receptor activation inhibits oligodendrocyte differentiation.* Neuron, 1998. 21: p. 63-75.
348. Kennea, N.L., Mehmet, H. *Neural stem cells.* J Pathol, 2002. 197(4): p. 536-50.
349. Shah, N.M., Groves, A.K., Anderson, D.J. *Alternative neural crest cell fates are instructively promoted by TGFbeta superfamily members.* Cell, 1996. 85(3): p. 331-43.
350. Pla, P., Moore, R., Morali, O.G., al., e. *Cadherins in neural crest cell development and transformation.* J Cell Physiol, 2001. 189: p. 121-132.
351. Nakagawa, S., Takeichi, M. *Neural crest emigration from the neural tube depends on regulated cadherin expression.* Development, 1998. 125: p. 2963-2971.
352. Lim, D.A., Tramontin, A.D., Trevejo, J.M., Herrera, D.G., Garcia-Verdugo, J.M., Alvarez-Buylla, A. *Noggin antagonizes BMP signaling to create a niche for adult neurogenesis.* Neuron, 2000. 28(3): p. 713-26.
353. Li, Y., Chen, J., Chopp, M. *Cell proliferation and differentiation from ependymal, subependymal and choroid plexus cells in response to stroke in rats.* J Neurol Sci, 2002. 193(2): p. 137-46.
354. Ignatova, T.N., Kukekov, V.G., Laywell, E.D., Suslov, O.N., Vrionis, F.D., Steindler, D.A. *Human cortical glial tumors contain neural stem-like cells expressing astroglial and neuronal markers in vitro.* Glia, 2002. 39(3): p. 193-206.
355. Singh, S.K., Clarke, I.D., Terasaki, M., Bonn, V.E., Hawkins, C., Squire, J., Dirks, P.B. *Identification of a cancer stem cell in human brain tumors.* 2003. 63(18): p. 5821-5828.
356. Hemmati, H.D., Nakano, I., Lazareff, J.A., Masterman-Smith, M., Geschwind, D.H., Bronner-Fraser, M., Kornblum, H.I. *Cancerous stem cells can arise from pediatric brain tumors.* 2003. 100(25): p. 15178-15183.
357. Taylor, M.D., Poppleton, H., Fuller, C., Su, X.P., Liu, Y.X., Jensen, P., Magdaleno, S., Dalton, J., Calabrese, C., Board, J., MacDonald, T., Rutka, J., Guha, A., Gajjar, A., Curran, T., Gilbertson, R.J. *Radial glia cells are candidate stem cells of ependymoma.* Cancer Cell, 2005. 8: p. 323-335.
358. Singh, S.K., Hawkins, C., Clarke, I.D., Squire, J.A., Bayani, J., Hide, T., Henkelman, R.M., Cusimano, M.D., Dirks, P.B. *Identification of human brain tumour initiating cells.* Nature, 2004. 432(7015): p. 396-401.
359. Vescovi, A.L., Galli, R., Reynolds, B.A. *Brain tumour stem cells.* Nature Reviews Cancer, 2006. 6(6): p. 425-436.
360. Pilkington, G.J. *Cancer stem cells in the mammalian central nervous system.* Cell Prolif, 2005. 38: p. 423-33.

361. Jang, T.C., Litofsky, N.S., Smith, T.W., Ross, A.H., Recht, L.D. *Aberrant nestin expression during ethylnitrosourea-(ENU)- induced neurocarcinogenesis*. *Neurobiology of Disease*, 2004. 15(3): p. 544-552.
362. Almqvist, P.M., Mah, R., Lendahl, U., Jacobsson, B., Hobson, G. *Immunohistochemical detection of nestin in paediatric brain tumours*. *J Histochem Cytochem*, 2002. 50: p. 147-158.
363. Uchida, K., Mukai, M., Okano, H., Kawase, T. *Possible oncogenicity of subventricular zone neural stem cells: Case report*. *Neurosurgery*, 2004. 55(4): p. 977-978.
364. Okano, H., Kawamura, H., Toriya, M., Nakao, K., Shibata, S., Imai, T. *Function of RNA-binding protein Musashi-1 in stem cells*. *Exp Cell Res*, 2005. 306: p. 349-356.
365. DeOme, K.B., Faulkin, L.J.J., Bern, H.A., Blair, P.B. *Development of mammary tumours from hyperplastic alveolar nodules trasplanted into gland-free mammary fat pads of female CH3 mice*. *Cancer Res*, 1959. 19: p. 515-520.
366. Hoshino, K., Gardner, W.U. *Transplantability and life span of mammary gland during serial transplantation in mice*. *Nature*, 1967. 213: p. 193-4.
367. Shackleton, M., Vaillant, F., Simpson, K.J., Stingl, J., Smyth, G.K., Asselin-Labat, M.L., Wu, L., Lindeman, G.J., Visvader, J.E. *Generation of a functional mammary gland from a single stem cell*. *Nature*, 2006. 439(7072): p. 84-88.
368. Stingl, J., Eirew, P., Ricketson, I., Shackleton, M., Vaillant, F., Choi, D., Li, H.I., Eaves, C.J. *Purification and unique properties of mammary epithelial stem cells*. *Nature*, 2006. 439: p. 993-7.
369. Kordon, E.C., Smith, G.H. *An entire functional mammary gland may comprise the progeny from a single cell*. *Development*, 1998. 125: p. 1921-30.
370. Welm, B., Behbod, F., Goodell, M.A., Rosen, J.M. *Isolation and characterization of functional mammary gland stem cells*. *Cell Prolif*, 2003. 36: p. 17-32.
371. Welm, B.E., Tepera, S.B., Venezia, T., Graubert, T.A., Rosen, J.M., Goodell, M.A. *Sca-1(pos) cells in the mouse mammary gland represent an enriched progenitor cell population*. *Dev Biol*, 2002. 245: p. 42-56.
372. Alvi, A.J., Clayton, H., Joshi, C., Enver, T., Ashworth, A., Vivanco, M.M., Dale, T.C., Smalley, M.J. *Functional and molecular characterisation of mammary side population cells*. *Breast Cancer Res*, 2003. 5: p. R1-R8.
373. Dontu, G., Abdallah, W.M., Foley, J.M., Jackson, K.W., Clarke, M.F., Kawamura, M.J., Wicha, M.S. *In vitro propagation and transcriptional profiling of human mammary stem/progenitor cells*. *Genes Dev*, 2003. 17: p. 1253-70.
374. Sleeman, K.E., Kendrick, H., Ashworth, A., Isacke, C.M., Smalley, M.J. *CD24 staining of mouse mammary gland cells defines luminal epithelial, myoepithelial, basal and non-epithelial cells*. *Breast Cancer Res*, 2006. 8: p. R7.
375. Cariati, M., Purushotham, A.D. *Stem cells and breast cancer*. *Histopathology*, 2008. 52: p. 99-107.

376. Ponti, D., Costa, A., Zaffaroni, N., Pratesi, G., Petrangolini, G., Coradini, D., Pilotti, S., Pierotti, M.A., Daidone, M.G. *Isolation and in vitro propagation of tumorigenic breast cancer cells with stem/progenitor cell properties*. Cancer Res, 2005. 65: p. 5506-11.
377. Phillips, T.M., McBride, W.H., Pajonk, F. *The response of CD24(-/low) / CD44 + breast cancer-initiating cells to radiation*. J Natl Cancer Inst, 2006. 98: p. 1777-85.
378. Glinsky, G.V., Berezovska, O., Glinskii, A.B.J.C.I. *Microarray analysis identifies a death-from-cancer signature predicting therapy failure in patients with multiple types of cancer*. J Clin Invest, 2005. 115: p. 1503-21.
379. Abraham, B.K., Fritz, P., McClellan, M., Hauptvogel, P., Athelogou, M., Brauch, H. *Prevalence of CD44+ / CD24- / low cells in breast cancer may not be associated with clinical outcome but may favor distant metastasis*. Clin Cancer Res, 2005. 11: p. 1154-59.
380. Jones, P.H., Watt, F.M. *Separation of human epidermal stem cells from transit amplifying cells on the basis of differences in integrin function and expression*. Cell, 1993. 73: p. 713-724.
381. Morris, R.J., Potten, C.S. *Slowly cycling (label-retaining) epidermal cells behave like clonogenic stem cells in vitro*. Cell Prolif, 1994. 27(5): p. 279-89.
382. Watt, F.M. *Stem cell fate and patterning in mammalian epidermis*. Curr Opin Genet Dev, 2001. 11(4): p. 410-7.
383. Powell, D.W., Mifflin, R.C., Valentich, J.D., Crowe, S.E., Saada, J.I., West, A.B. *Myofibroblasts. II. Intestinal subepithelial myofibroblasts*. Am J Physiol, 1999. 277(2 Pt 1): p. C183-201.
384. Powell, A.J., Darmon, A.J., Gonos, E.S., Lam, E.W., Peden, K.W., Jat, P.S. *Different functions are required for initiation and maintenance of immortalization of rat embryo fibroblasts by SV40 large T antigen*. Oncogene, 1999. 18(51): p. 7343-50.
385. Potten, C.S., Booth, C., Pritchard, D.M. *The intestinal epithelial stem cell: the mucosal governor*. Int J Exp Pathol, 1997. 78(4): p. 219-43.
386. Marshman, E., Booth, C., Potten, C.S. *The intestinal epithelial stem cell*. Bioessays, 2002. 24(1): p. 91-8.
387. Cai, W.B., Roberts, S.A., Potten, C.S. *The number of clonogenic cells in crypts in three regions of murine large intestine*. Int J Radiat Biol, 1997. 71(5): p. 573-9.
388. Korinek, V., Barker, N., Moerer, P., van Donselaar, E., Huls, G., Peters, P.J., Clevers, H. *Depletion of epithelial stem-cell compartments in the small intestine of mice lacking Tcf-4*. Nat Genet, 1998. 19(4): p. 379-83.
389. Booth, C., O'Shea, J.A., Potten, C.S. *Maintenance of functional stem cells in isolated and cultured adult intestinal epithelium*. Exp Cell Res, 1999. 249(2): p. 359-66.
390. Liu, A.Y. *Expression of CD44 in prostate cancer cells*. Cancer Lett, 1994. 76(1): p. 63-9.
391. Wernert, N., Seitz, G., Achtstatter, T. *Immunohistochemical investigation of different cytokeratins and vimentin in the prostate from the fetal period up to adulthood and in prostate carcinoma*. Pathol Res Pract, 1987. 182(5): p. 617-26.

392. Nagle, R.B., Brawer, M.K., Kittelson, J., Clark, V. *Phenotypic relationships of prostatic intraepithelial neoplasia to invasive prostatic carcinoma*. Am J Pathol, 1991. 138(1): p. 119-28.
393. Bostwick, D.G. *Prospective origins of prostate carcinoma. Prostatic intraepithelial neoplasia and atypical adenomatous hyperplasia*. Cancer, 1996. 78(2): p. 330-6.
394. Xue, Y., Smedts, F., Debruyne, F.M., de la Rosette, J.J., Schalken, J.A. *Identification of intermediate cell types by keratin expression in the developing human prostate*. Prostate, 1998. 34(4): p. 292-301.
395. Bonkhoff, H. *Neuroendocrine cells in benign and malignant prostate tissue: morphogenesis, proliferation, and androgen receptor status*. Prostate Suppl, 1998. 8: p. 18-22.
396. di Sant'Agnese, P.A. *Neuroendocrine differentiation in carcinoma of the prostate. Diagnostic, prognostic, and therapeutic implications*. Cancer, 1992. 70(1 Suppl): p. 254-68.
397. di Sant'Agnese, P.A., Cockett, A.T. *Neuroendocrine differentiation in prostatic malignancy*. Cancer, 1996. 78(2): p. 357-61.
398. Bonkhoff, H., Wernert, N., Dhom, G., Remberger, K. *Relation of endocrine-paracrine cells to cell proliferation in normal, hyperplastic, and neoplastic human prostate*. Prostate, 1991. 19(2): p. 91-8.
399. Bonkhoff, H., Stein, U., Remberger, K. *Endocrine-paracrine cell types in the prostate and prostatic adenocarcinoma are postmitotic cells*. Hum Pathol, 1995. 26(2): p. 167-70.
400. Bonkhoff, H., Remberger, K. *Differentiation pathways and histogenetic aspects of normal and abnormal prostatic growth: a stem cell model*. Prostate, 1996. 28(2): p. 98-106.
401. De Marzo, A.M., Meeker, A.K., Epstein, J.I., Coffey, D.S. *Prostate stem cell compartments: expression of the cell cycle inhibitor p27Kip1 in normal, hyperplastic, and neoplastic cells*. Am J Pathol, 1998. 153(3): p. 911-9.
402. Verhagen, A.P., Ramaekers, F.C., Aalders, T.W., Schaafsma, H.E., Debruyne, F.M., Schalken, J.A. *Colocalization of basal and luminal cell-type cytokeratins in human prostate cancer*. Cancer Res, 1992. 52(22): p. 6182-7.
403. Nagle, R.B., Ahmann, F.R., McDaniel, K.M., Paquin, M.L., Clark, V.A., Celniker, A. *Cytokeratin characterization of human prostatic carcinoma and its derived cell lines*. Cancer Res, 1987. 47(1): p. 281-6.
404. Liu, A.Y., True, L.D., LaTray, L., Ellis, W.J., Vessella, R.L., Lange, P.H., Higano, C.S., Hood, L., van den Engh, G. *Analysis and sorting of prostate cancer cell types by flow cytometry*. Prostate, 1999. 40(3): p. 192-9.
405. Ruijter, E.T., Miller, G.J., van de Kaa, C.A., van Bokhoven, A., Bussemakers, M.J., Debruyne, F.M., Ruiter, D.J., Schalken, J.A. *Molecular analysis of multifocal prostate cancer lesions*. J Pathol, 1999. 188(3): p. 271-7.
406. Macintosh, C.A., Stower, M., Reid, N., Maitland, N.J. *Precise microdissection of human prostate cancers reveals genotypic heterogeneity*. Cancer Res, 1998. 58(1): p. 23-8.

407. Sadi, M.V., Barrack, E.R. *Image analysis of androgen receptor immunostaining in metastatic prostate cancer. Heterogeneity as a predictor of response to hormonal therapy.* Cancer, 1993. 71(8): p. 2574-80.
408. Maitland, N.J., Collins, A. *A tumour stem cell hypothesis for the origins of prostate cancer.* Bju International, 2005. 96(9): p. 1219-1223.
409. Bonkhoff, H., Stein, U., Remberger, K. *The proliferative function of basal cells in the normal and hyperplastic human prostate.* Prostate, 1994. 24(3): p. 114-8.
410. Isaacs, J.T., Coffey, D.S. *Etiology and disease process of benign prostatic hyperplasia.* Prostate Suppl, 1989. 2: p. 33-50.
411. English, H.F., Santen, R.J., Isaacs, J.T. *Response of glandular versus basal rat ventral prostatic epithelial cells to androgen withdrawal and replacement.* Prostate, 1987. 11: p. 229-242.
412. English, H.F., Kyprianou, N., Isaacs, J.T. *Relationship between DNA fragmentation and apoptosis in the programmed cell death in the rat prostate following castration.* Prostate, 1989. 15(3): p. 233-50.
413. Cunha, G.R., Hayward, S.W., Wang, Y.Z. *Role of stroma in carcinogenesis of the prostate.* Differentiation, 2002. 70(9-10): p. 473-85.
414. van Leenders, G., Dijkman, H., Hulsbergen-van de Kaa, C., Ruiter, D., Schalken, J. *Demonstration of intermediate cells during human prostate epithelial differentiation in situ and in vitro using triple-staining confocal scanning microscopy.* Lab Invest, 2000. 80(8): p. 1251-8.
415. Hudson, D.L., Guy, A.T., Fry, P., O'Hare, M.J., Watt, F.M., Masters, J.R. *Epithelial cell differentiation pathways in the human prostate: identification of intermediate phenotypes by keratin expression.* J Histochem Cytochem, 2001. 49(2): p. 271-8.
416. Xue, Y., Verhofstad, A., Lange, W., Smedts, F., Debruyne, F., de la Rosette, J., Schalken, J. *Prostatic neuroendocrine cells have a unique keratin expression pattern and do not express Bcl-2: cell kinetic features of neuroendocrine cells in the human prostate.* Am J Pathol, 1997. 151(6): p. 1759-65.
417. Wang, Y., Hayward, S., Cao, M., Thayer, K., Cunha, G. *Cell differentiation lineage in the prostate.* Differentiation, 2001. 68(4-5): p. 270-9.
418. Schalken, J.A., Van Leenders, G. *Cellular and molecular biology of the prostate: Stem cell biology.* Urology, 2003. 62(5A): p. 11-20.
419. Collins, A.T., Maitland, N.J. *Prostate cancer stem cells.* European Journal of Cancer, 2006. 42(9): p. 1213-1218.
420. Sawicki, J.A., Rothman, C.J. *Evidence for stem cells in cultures of mouse prostate epithelial cells.* Prostate, 2002. 50(1): p. 46-53.
421. van Leenders, G.J., Aalders, T.W., Hulsbergen-van de Kaa, C.A., Ruiter, D.J., Schalken, J.A. *Expression of basal cell keratins in human prostate cancer metastases and cell lines.* J Pathol, 2001. 195(5): p. 563-70.

422. Xin, L., Ide, H., Kim, Y., Dubey, P., Witte, O.N. *In vivo* regeneration of murine prostate from dissociated cell populations of postnatal epithelia and urogenital sinus mesenchyme. *Proceedings of the National Academy of Sciences of the United States of America*, 2003. 100: p. 11896-11903.
423. Kinbara, H., Cunha, G.R., Boutin, E., Hayashi, N., Kawamura, J. *Evidence of stem cells in the adult prostatic epithelium based upon responsiveness to mesenchymal inductors*. *Prostate*, 1996. 29(2): p. 107-16.
424. Sugimura, Y., Cunha, G.R., Donjacour, A.A. *Morphogenesis of ductal networks in the mouse prostate*. *Biol Reprod*, 1986. 34: p. 961-971.
425. Cunha, G.R., Donjacour, A.A., Cooke, P.S., Mee, S., Bigsby, R.M., Higgins, S.J., Sugimura, Y. *The endocrinology and developmental biology of the prostate*. *Endocr. Rev.*, 1987. 8: p. 338-362.
426. Tsujimura, A., Koikawa, Y., Salm, S., Takao, T., Coetzee, S., Moscatelli, D., Shapiro, E., Lepor, H., Sun, T.T., Wilson, E.L. *Proximal location of mouse prostate epithelial stem cells: a model of prostatic homeostasis*. *J Cell Biol*, 2002. 157(7): p. 1257-65.
427. Fang, D., Nguyen, T.K., Leishear, K., al., e. *A tumorigenic subpopulation with stem cell properties in melanomas*. *Cancer Res*, 2005. 65: p. 9328-9337.
428. Tokar, E.J., Ancrile, B.B., Cunha, G.R., Webber, M.M. *Stem/progenitor and intermediate cell types and the origin of human prostate cancer*. *Differentiation*, 2005. 73: p. 463-473.
429. Tang, D.G., Patrawala, L., Calhoun, T., Bhatia, B., Choy, G., Schneider-Broussard, R., Jeter, C. *Prostate cancer stem/progenitor cells: Identification, and implications*. *Mol Carcinog*, 2006.
430. Lang, S.H., Stark, M., Collins, A., Paul, A.B., Stower, M.J., Maitland, N.J. *Experimental prostate epithelial morphogenesis in response to stroma and three-dimensional matrigel culture*. *Cell Growth Differ*, 2001. 12(12): p. 631-40.
431. Brown, M.D., Gilmore, P.E., Hart, C.A., Samuel, J.D., Ramani, V.A.C., George, N.J., Clarke, N.W. *Characterization of benign and malignant prostate epithelial Hoechst 33342 side populations*. *The Prostate*, 2007. 67: p. 1384-1396.
432. Richardson, G.D., Robson, C.N., Lang, S.H., Neal, D.E., Maitland, N.J., Collins, A.T. *CD133, a novel marker for human prostatic epithelial stem cells*. *Journal of Cell Science*, 2004. 117(16): p. 3539-3545.
433. Liu, A.Y., True, L.D., LaTray, L., Nelson, P.S., Ellis, W.J., Vessella, R.L., Lange, P.H., Hood, L., van den Engh, G. *Cell-cell interaction in prostate gene regulation and cytodifferentiation*. *Proc Natl Acad Sci U S A*, 1997. 94(20): p. 10705-10.
434. Collins, A.T., Habib, F.K., Maitland, N.J., Neal, D.E. *Identification and isolation of human prostate epithelial stem cells based on alpha(2)beta(1)-integrin expression*. *J Cell Sci*, 2001. 114(Pt 21): p. 3865-72.
435. Naor, D., Sionov, R.V., Ish-Shalom, D. *CD44: structure, function, and association with the malignant process*. *Adv Cancer Res*, 1997. 71: p. 241-319.

436. Hudson, D.L., O'Hare, M., Watt, F.M., Masters, J.R. *Proliferative heterogeneity in the human prostate: evidence for epithelial stem cells.* Lab Invest, 2000. 80(8): p. 1243-50.
437. Miki, J., Furusato, B., Li, H., Gu, Y., Takahashi, H., Egawa, S., Sesterhenn, I.A., McLeod, D.G., Srivastava, S., Rhim, J.S. *Identification of putative stem cell markers, CD133 and CXCR4, in hTERT-immortalized primary nonmalignant and malignant tumor-derived human prostate epithelial cell lines and in prostate cancer specimens.* Cancer Res, 2007. 67: p. 3153-61.
438. Patrawala, L., Calhoun, T., Schneider-Broussard, R., Li, H., Bhatia, B., Tang, S., Reilly, J.G., Chandra, D., Zhou, J., Claypool, K., Coghlan, L., Tang, D.G. *Highly purified CD44(+) prostate cancer cells from xenograft human tumors are enriched in tumorigenic and metastatic progenitor cells.* Oncogene, 2006. 25(12): p. 1696-1708.
439. Avigdor, A., Goichberg, P., Shviti, S., Dar, A., Peled, A., Samira, S., Kollet, O., HersHKoviz, R., Alon, R., Hardan, I., Ben-Hur, H., Naor, D., Nagler, A., Lapidot, T. *CD44 and hyaluronic acid cooperate with SDF-1 in the trafficking of human CD34+ stem/progenitor cells to the bone marrow.* Blood, 2004. 103: p. 2981-2989.
440. Oswald, J., Boxberger, S., Jorgensen, B., Feldmann, S., Ehninger, G., Bornhauser, M., Werner, C. *Mesenchymal stem cells can be differentiated into endothelial cells in vitro.* Stem Cells, 2004. 22(3): p. 377-384.
441. Schwartz, P.H., Bryant, P.J., Fuja, T.J., Su, H.L., O'Dowd, D.K., Klassen, H. *Isolation and characterization of neural progenitor cells from post-mortem human cortex.* Journal of Neuroscience Research, 2003. 74(6): p. 838-851.
442. Gudjonsson, T., Villadsen, R., Nielsen, H.L., Ronnov-Jessen, L., Bissell, M.J., Petersen, O.W. *Isolation, immortalization, and characterization of a human breast epithelial cell line with stem cell properties.* Genes Dev, 2002. 16(6): p. 693-706.
443. Valk-Lingbeek, M.E., Bruggeman, S.W.M., Van Lohuizen, M. *Stem cells and cancer: The polycomb connection.* Cell, 2004. 118(4): p. 409-418.
444. Chambers, I., Smith, A. *Self-renewal of teratocarcinoma and embryonic stem cells.* Oncogene, 2004. 23(43): p. 7150-7160.
445. Beachy, P.A., Karhadkar, S.S., Berman, D.M. *Tissue repair and stem cell renewal in carcinogenesis.* Nature, 2004. 432(7015): p. 324-331.
446. Collins, A.T., Berry, P.A., Hyde, C., Stower, M.J., Maitland, N.J. *Prospective identification of tumorigenic prostate cancer stem cells.* Cancer Research, 2005. 65(23): p. 10946-10951.
447. Goodell, M.A., Brose, K., Paradis, G., Conner, A.S., Mulligan, R.C. *Isolation and functional properties of murine hematopoietic stem cells that are replicating in vivo.* J Exp Med, 1996. 183(4): p. 1797-806.
448. Bunting, K.D. *ABC transporters as phenotypic markers and functional regulators of stem cells.* Stem Cells, 2002. 20(1): p. 11-20.

449. Goodell, M.A., Rosenzweig, M., Kim, H., Marks, D.F., DeMaria, M., Paradis, G., Grupp, S.A., Sieff, C.A., Mulligan, R.C., Johnson, R.P. *Dye efflux studies suggest that hematopoietic stem cells expressing low or undetectable levels of CD34 antigen exist in multiple species.* Nat Med, 1997. 3(12): p. 1337-45.
450. Challen, G.A., Little, M.H. *A side order of stem cells: the SP phenotype.* Stem Cells, 2006. 24: p. 3-12.
451. Kim, M., Morshead, C.M. *Distinct populations of forebrain neural stem and progenitor cells can be isolated using side-population analysis.* J Neuro-sci, 2003. 23: p. 10703-10709.
452. Haraguchi, N., Inoue, H., Tanaka, F., Mimori, K., Utsunomiya, T., Sasaki, A., Mori, M. *Cancer stem cells in human gastrointestinal cancers.* Hum Cell, 2006. 19: p. 24-29.
453. Wulf, G.G., Luo, K.L., Jackson, K.A., al., e. *Cells of the hepatic side population contribute to liver regeneration and can be replenished by bone marrow stem cells.* Haematologica, 2003. 88: p. 368-378.
454. Gussoni, E., Soneoka, Y., Strickland, C.D., Buzney, E.A., Khan, M.K., Flint, A.F., Kunkel, L.M., Mulligan, R.C. *Dystrophin expression in the mdx mouse restored by stem cell transplantation.* Nature, 1999. 401: p. 390-394.
455. Bachrach, E., Li, S., Perez, A.L., Schienda, J., Liadaki, K., Volinski, J., Flint, A., Chamberlain, J., Kunkel, L.M. *Systemic delivery of human micro-dystrophin to regenerating mouse dystrophic muscle by muscle progenitor cells.* Proc Natl Acad Sci U S A, 2004. 101: p. 3581-3586.
456. Addla, S.K., Brown, M.D., Hart, C.A., Ramani, V.A., Clarke, N.W. *Characterization of the Hoechst 33342 side population from normal and malignant human renal epithelial cells.* Am J Physiol Renal Physiol, 2008. 295: p. 680-7.
457. She, J.J., Zhang, P.G., Wang, Z.M., Gan, W.M., Che, X.M. *Identification of side population cells from bladder cancer cells by DyeCycle Violet staining.* Cancer Biol Ther, 2008. 7: p. 1663-8.
458. Bhatt, R.I., Brown, M.D., Hart, C.A., Gilmore, P., Ramani, V.A.C., George, N.J., Clarke, N.W. *Novel method for the isolation and characterisation of the putative prostatic stem cell.* Cytometry Part A, 2003. 54A(2): p. 89-99.
459. Kondo, T., Setoguchi, T., Taga, T. *Persistence of a small subpopulation of cancer stem-like cells in the C6 glioma cell line.* Proc Natl Acad Sci U S A, 2004. 101: p. 781-786.
460. Zhou, S., Schuetz, J.D., Bunting, K.D., Colapietro, A.M., Sampath, J., Morris, J.J., Lagutina, I., Grosveld, G.C., Osawa, M., Nakauchi, H., Sorrentino, B.P. *The ABC transporter Bcrp1/ABCG2 is expressed in a wide variety of stem cells and is a molecular determinant of the side-population phenotype.* Nat Med, 2001. 7: p. 1028-1034.
461. Chaudhary, P.M., Roninson, I.B. *Expression and activity of P-glycoprotein, a multidrug efflux pump, in human hematopoietic stem cells.* Cell, 1991. 66(1): p. 85-94.

462. Patrawala, L., Calhoun, T., Schneider-Broussard, R., Zhou, J.J., Claypool, K., Tang, D.G. *Side population is enriched in tumorigenic, stem-like cancer cells, whereas ABCG2(+) and ABCG2(-) cancer cells are similarly tumorigenic.* Cancer Research, 2005. 65(14): p. 6207-6219.
463. Hirschmann-Jax, C., Foster, A.E., Wulf, G.G., Nuchtern, J.G., Jax, T.W., Gobel, U., Goodell, M.A., Brenner, M.K. *A distinct "side population" of cells with high drug efflux capacity in human tumor cells.* Proceedings of the National Academy of Sciences of the United States of America, 2004. 101(39): p. 14228-14233.
464. Haraguchi, N., Utsunomiya, T., Inoue, H., Tanaka, F., Mimori, K., Barnard, G.F., Mori, M. *Characterization of a side population of cancer cells from human gastrointestinal system.* 2006, 2006. 24: p. 506-13.
465. Harrison, D.E., Lerner, C.P. *Most primitive hematopoietic stem cells are stimulated to cycle rapidly after treatment with 5-fluorouracil.* Blood, 1991. 78(5): p. 1237-40.
466. Summers, Y.J., Heyworth, C.M., de Wynter, E.A., Chang, J., Testa, N.G. *Cord blood G(0) CD34+ cells have a thousand-fold higher capacity for generating progenitors in vitro than G(1) CD34+ cells.* Stem Cells, 2001. 19(6): p. 505-13.
467. Ollai, B.R., Kahane, H., Epstein, J.I. *Can basal cells be seen in adenocarcinoma of the prostate?: an immunohistochemical study using high molecular weight cytokeratin (clone 34betaE12) antibody.* Am J Surg Pathol, 2002. 26(9): p. 1151-60.
468. Bonkhoff, H., Stein, U., Remberger, K. *Multidirectional differentiation in the normal, hyperplastic, and neoplastic human prostate: simultaneous demonstration of cell-specific epithelial markers.* Hum Pathol, 1994. 25(1): p. 42-6.
469. Robinson, E.J., Neal, D.E., Collins, A.T. *Basal cells are progenitors of luminal cells in primary cultures of differentiating human prostatic epithelium.* Prostate, 1998. 37(3): p. 149-60.
470. Potten, C.S., Booth, C., Tudor, G.L., Booth, D., Brady, G., Hurley, P., Ashton, G., Clarke, R., Sakakibara, S., Okano, H. *Identification of a putative intestinal stem cell and early lineage marker; Musashi-1.* Differentiation, 2003. 71(1): p. 28-41.
471. Toda, M., Iizuka, Y., Yu, W., Imai, T., Ikeda, E., Yoshida, K., Kawase, T., Kawakami, Y., Okano, H., Uyemura, K. *Expression of the neural RNA-binding protein Musashi 1 in human gliomas.* Glia, 2001. 34(1): p. 1-7.
472. Ward, R.J., Dirks, P.B. *Cancer stem cells: at the headwaters of tumor development.* Annu Rev Pathol Mech Dis, 2007. 2: p. 175-189.
473. Adams, J.C., Watt, F.M. *Changes in keratinocyte adhesion during terminal differentiation: reduction in fibronectin binding precedes alpha 5 beta 1 integrin loss from the cell surface.* Cell, 1990. 63: p. 425-435.
474. Hotchin, N.A., Kovach, N.L., Watt, F.M. *Functional down-regulation of alpha 5 beta 1 integrin in keratinocytes is reversible but commitment to terminal differentiation is not.* J Cell Sci, 1993. 106(4): p. 1131-1138.
475. Zutter, M.M., Santoro, S.A. *Widespread histologic distribution of the alpha 2 beta 1 integrin cell-surface collagen receptor.* Am J Pathol, 1990. 137: p. 113-20.

476. Zutter, M.M., Painter, A.A., Staats, W.D., Tsung, Y.L. *Regulation of alpha 2 integrin gene expression in cells with megakaryocytic features: a common theme of three necessary elements*. Blood, 1995. 86: p. 3006-14.
477. Zhu, A.J., Haase, I., Watt, F.M. *Signaling via beta1 integrins and mitogen-activated protein kinase determines human epidermal stem cell fate in vitro*. Proc Natl Acad Sci U S A, 1999. 96: p. 6728-33.
478. Mohr, O.L. *Character Changes Caused by Mutation of an Entire Region of a Chromosome in Drosophila*. Genetics, 1919. 4: p. 275-82.
479. Artavanis-Tsakonas, S., Rand, M.D., Lake, R.J. *Notch signaling: cell fate control and signal integration in development*. Science, 1999. 284: p. 770-6.
480. Lowell, S., al., e. *Stimulation of human epidermal differentiation by delta-notch signalling at the boundaries of stem-cell clusters*. Curr Biol, 2000. 10: p. 491-500.
481. Wang, X.D., Leow, C.C., Zha, J.P., Tang, Z.J., Modrusan, Z., Radtke, F., Aguet, M., de Sauvage, F.J., Gao, W.Q. *Notch signaling is required for normal prostatic epithelial cell proliferation and differentiation*. Developmental Biology, 2006. 290(1): p. 66-80.
482. Shou, J., Ross, S., Koeppen, H., de Sauvage, F.J., Gao, W.Q. *Dynamics of notch expression during murine prostate development and tumorigenesis*. Cancer Res, 2001. 61(19): p. 7291-7.
483. Taipale, J., Beachy, P.A. *The Hedgehog and Wnt signalling pathways in cancer*. Nature, 2001. 411(6835): p. 349-54.
484. Karhadkar, S.S., Bova, G.S., Abdallah, N., Dhara, S., Gardner, D., Maitra, A., Isaacs, J.T., Berman, D.M., Beachy, P.A. *Hedgehog signalling in prostate regeneration, neoplasia and metastasis*. Nature, 2004. 431(7009): p. 707-712.
485. Yi, F., Merrill, B.J. *Stem cells and TCF proteins: a role for beta-catenin-independent functions*. Stem Cell Rev, 2007. 3: p. 39-48.
486. Kikuchi, A. *Regulation of B-Catenin signalling in the Wnt pathway*. Biochemical and Biophysical Research Communications, 2000. 268: p. 243-48.
487. Miller, J.R., Moon, R.T. *Signal transduction through beta-catenin and specification of cell fate during embryogenesis*. Genes Dev, 1996. 10: p. 2527-39.
488. Gat, U., DasGupta, R., Degenstein, L., Fuchs, E. *De Novo hair follicle morphogenesis and hair tumors in mice expressing a truncated beta-catenin in skin*. Cell, 1998. 95: p. 605-14.
489. DePinho, R.A., Schreiber-Agus, N., Alt, F.W. *myc family oncogenes in the development of normal and neoplastic cells*. Adv Cancer Res, 1991. 57: p. 1-46.
490. Henriksson, M., Lüscher, B. *Proteins of the Myc network: essential regulators of cell growth and differentiation*. Adv Cancer Res, 1996. 68: p. 109-82.
491. Polakis, P. *Wnt signaling and cancer*. Genes Dev, 2000. 14: p. 1837-51.

492. Verras, M., Brown, J., Li, X.M., Nusse, R., Sun, Z.J. *Wnt3a growth factor induces androgen receptor-mediated transcription and enhances cell growth in human prostate cancer cells*. *Cancer Research*, 2004. 64(24): p. 8860-8866.
493. Joesting, M.S., Perrin, S., Elenbass, B., Fawell, S.E., Rubin, J.S., Franco, O.E., Hayward, S.W., Cunha, G.R., Marker, P.C. *Identification of SFRP1 as a candidate mediator of stromal-to-epithelial signaling in prostate cancer*. *Cancer Research*, 2005. 65(22): p. 10423-10430.
494. Ezoe, S., Matsumara, I., Satoh, Y., Tanaka, H., Kanakura, Y. *Cell cycle regulation in hematopoietic stem/progenitor cells*. *Cell Cycle*, 2004. 3: p. 314-18.
495. Cheng, T., Rodrigues, N., Shen, H., Yang, Y., Dombkowski, D., Sykes, M., Scadden, D.T. *Hematopoietic stem cell quiescence maintained by p21cip1/waf1*. *Science*, 2000. 287(5459): p. 1804-8.
496. Di Cunto, F., Topley, G., Calautti, E., Hsiao, J., Ong, L., Seth, P.K., Dotto, G.P. *Inhibitory function of p21Cip1/WAF1 in differentiation of primary mouse keratinocytes independent of cell cycle control*. *Science*, 1998. 280: p. 1069-72.
497. Coats, S., Flanagan, W.M., Nourse, J., Roberts, J.M. *Requirement of p27Kip1 for restriction point control of the fibroblast cell cycle*. *Science*, 1996. 272: p. 877-80.
498. Guo, Y., Sklar, G.N., Borkowski, A., Kyprianou, N. *Loss of the cyclin-dependent kinase inhibitor p27(Kip1) protein in human prostate cancer correlates with tumor grade*. *Clin Cancer Res*, 1997. 3(12 Pt 1): p. 2269-74.
499. Okano, H., Okabe, M., Taguchi, A., Sawamoto, K. *Evolutionarily conserved mechanisms regulating neural development: lessons from the development of Drosophila peripheral nervous systems*. *Hum Cell*, 1997. 10: p. 139-150.
500. Sakakibara, S., Okano, H. *Expression of neural RNA-binding proteins in the postnatal CNS: implications of their roles in neuronal and glial cell development*. *J Neurosci*, 1997. 17(21): p. 8300-12.
501. Imai, T., Tokunaga, A., Yoshida, T., Hashimoto, M., Mikoshiba, K., Weinmaster, G., Nakafuku, M., Okano, H. *The neural RNA-binding protein Musashi1 translationally regulates mammalian numb gene expression by interacting with its mRNA*. *Mol Cell Biol*, 2001. 21: p. 3888-900.
502. Salm, S.N., Burger, P.E., Coetzee, S., Goto, K., Moscatelli, D., Wilson, E.L. *TGF-beta maintains dormancy of prostatic stem cells in the proximal region of ducts*. *Journal of Cell Biology*, 2005. 170(1): p. 81-90.
503. Kundu, S.D., Kim, I.Y., Yang, T., Doglio, L., Lang, S., Zhang, X., Buttyan, R., Kim, S.J., Chang, J., Cai, X., Wang, Z., Lee, C. *Absence of proximal duct apoptosis in the ventral prostate of transgenic mice carrying the C3(1)-TGF-beta type II dominant negative receptor*. *Prostate*, 2000. 43(2): p. 118-24.
504. Bhowmick, N.A., Chytil, A., Plieth, D., Gorska, A.E., Dumont, N., Shappell, S., Washington, M.K., Neilson, E.G., Moses, H.L. *TGF-beta signaling in fibroblasts modulates the oncogenic potential of adjacent epithelia*. *Science*, 2004. 303: p. 848-851.

505. Bhowmick, N.A., Moses, H.L. *The conditional knock-out of transforming growth factor-beta signaling in the prostate stroma results in prostate intraepithelial neoplasia*. Journal of Urology, 2004. 171(4): p. 109-109.
506. Bruckheimer, E.M., Kyprianou, N. *Bcl-2 antagonizes the combined apoptotic effect of transforming growth factor-beta and dihydrotestosterone in prostate cancer cells*. Prostate, 2002. 53(2): p. 133-42.
507. Yin, A.H., Miraglia, S., Zanjani, E.D., Almeida-Porada, G., Ogawa, M., Leary, A.G., Olweus, J., Kearney, J., Buck, D.W. *AC133, a novel marker for human haemopoietic stem and progenitor cells*. Blood, 1997. 90: p. 5002-5012.
508. Peichev, M., Naiyer, A.J., Pereira, D., Zhu, Z., Lane, W.J., Williams, M., Oz, M.C., Hicklin, D.J., Witte, L., Moore, M.A., Rafii, S. *Expression of VEGFR-2 and AC133 by circulating human CD34(+) cells identifies a population of functional endothelial precursors*. Blood, 2000. 95(952-958).
509. Olempska, M., Eisenach, P.A., Ammerpohl, O., Ungefroren, H., Fandrich, F., Kaltoff, H. *Detection of tumor stem cell markers in pancreatic carcinoma cell lines*. Hepatobiliary Pancreat Dis Int, 2007. 6: p. 92-97.
510. O'Brien, C.A., Pollett, A., Gallinger, S., Dick, J.E. *A human colon cancer cell capable of initiating tumour growth in immunodeficient mice*. Nature, 2007. 445: p. 106-110.
511. Ricci-Vitiani, L., Lombardi, D.G., Pilozzi, E., Biffoni, M., Todaro, M., Peschle, C., al., e. *Identification and expansion of human colon-cancer-initiating cells*. Nature, 2007. 445: p. 111-115.
512. Yin, S., Li, J., Hu, C., Chen, X., Yao, M., Yan, M., Jiang, G., Ge, C., Xie, H., Wan, D., Yang, S., Zheng, S., Gu, J. *CD133 positive hepatocellular carcinoma cells possess high capacity for tumorigenicity*. Int J Cancer, 2007. 120: p. 1444-1450.
513. Bruno, S., Bussolati, B., Grange, C., Collino, F., Graziano, M.E., Ferrando, U. et al. *CD133+ renal progenitor cells contribute to tumor angiogenesis*. Am J Pathol, 2006. 169: p. 2223-2235.
514. Florek, M., Haase, M., Marzesco, A.M., Freund, D., Ehninger, G., Huttner, W.B., al., e. *Prominin-1/CD133, a neural and hematopoietic stem cell marker, is expressed in adult human differentiated cells and certain types of kidney cancer*. Cell Tissue Res, 2005. 319: p. 15-26.
515. Beier, D., Hau, P., Proescholdt, M., Lohmeier, A., Wischhuen, J., Oefner, P.J., Aigner, L., Brawanski, A., Bogdahn, U., Beier, C.P. *CD133+ and CD133- Glioblastoma-derived cancer stem cells show differential growth characteristics and molecular profiles*. Cancer Res, 2007. 67(9): p. 4010-4015.
516. Wang, J., Sakariassen, P.O., Tsinkalovsky, O., Immervoll, H., Boe, S., O., Svendsen, A., Prestegarden, L., Rosland, G., Thorsen, F., Stuhr, L., Molven, A., Bjerkvig, R., Enger, P.O. *CD133 negative glioma cells form tumours in nude rats and give rise to CD133 positive cells*. Int J Cancer, 2008. 122(761-768).

517. Zhang, J.W., Grindley, J.C., Yin, T., Jayasinghe, S., He, X.C., Ross, J.T., Haug, J.S., Rupp, D., Porter-Westpfahl, K.S., Wiedemann, L.M., Wu, H., Li, L.H. *PTEN maintains haematopoietic stem cells and acts in lineage choice and leukaemia prevention*. Nature, 2006. 441(7092): p. 518-522.
518. Yilmaz, O.H., Valdez, R., Theisen, B.K., Guo, W., Ferguson, D.O., Wu, H., Morrison, S.J. *Pten dependence distinguishes haematopoietic stem cells from leukaemia-initiating cells*. Nature, 2006. 441(7092): p. 475-482.
519. Buzzeeo, M.P., Scott, E.W., Cogle, C.R. *The hunt for cancer-initiating cells: a history stemming from leukaemia*. Leukemia, 2007. 21: p. 1619-1627.
520. Wang, S.Y., Gao, J., Lei, Q.Y., Rozengurt, N., Pritchard, C., Jiao, J., Thomas, G.V., Li, G., Roy-Burman, P., Nelson, P.S., Liu, X., Wu, H. *Prostate-specific deletion of the murine Pten tumor suppressor gene leads to metastatic prostate cancer*. Cancer Cell, 2003. 4(3): p. 209-221.
521. Wang, S.Y., Garcia, A.J., Wu, M., Lawson, D.A., Witte, O.N., Wu, H. *Pten deletion leads to the expansion of a prostatic stem/progenitor cell subpopulation and tumor initiation*. Proceedings of the National Academy of Sciences of the United States of America, 2006. 103(5): p. 1480-1485.
522. Finlan, L.E., Hupp, T.R. *p63: the phantom of the tumor suppressor*. Cell Cycle, 2007. 6: p. 1062-71.
523. Keyes, W.M., Mills, A.A. *p63: a new link between senescence and aging*. Cell Cycle, 2006. 5: p. 260-5.
524. Sommer, M., Poliak, N., Upadhyay, S., Ratovitski, E., Nelkin, B.D., Donehower, L.A., Sidransky, D. *DeltaNp63alpha overexpression induces downregulation of Sirt1 and an accelerated aging phenotype in the mouse*. Cell Cycle, 2006. 5: p. 2005-11.
525. Signoretti, S., Waltregny, D., Dilks, J., Isaac, B., Lin, D., Garraway, L., Yang, A., Montironi, R., McKeon, F., Loda, M. *p63 is a prostate basal cell marker and is required for prostate development*. Am J Pathol, 2000. 157(6): p. 1769-75.
526. Ware, J.L. *Prostate cancer progression. Implications of histopathology*. Am J Pathol, 1994. 145(5): p. 983-93.
527. Niu, Y., Xu, Y., Zhang, J., Bai, J., Yang, H., Ma, T. *Proliferation and differentiation of prostatic stromal cells*. BJU Int, 2001. 87(4): p. 386-93.
528. Allen, T.G., Cagle, P.T., Popper, H.H. *Basic concepts of molecular pathology*. Arch Pathol Lab Med, 2008. 132: p. 1551-56.
529. DeRisi, J.L., Iyer, V.R., Brown, P.O. *Exploring the metabolic and genetic control of gene expression on a genomic scale*. Science, 1997. 278: p. 680-6.
530. Brown, T.A. *Genomes*. 1st ed. Vol. 1. 1999, Oxford: BIOS Scientific Publisher Ltd.
531. Fodor, S.P., Read, J.L., Pirrung, M.C., Stryer, L., Lu, A.T., Solas, D. *Light-directed, spatially addressable parallel chemical synthesis*. Science, 1991. 251: p. 767-73.

532. Pease, A.C., Solas, D., Sullivan, E.J., Cronin, M.T., Holmes, C.P., Fodor, S.P. *Light-generated oligonucleotide arrays for rapid DNA sequence analysis*. Proc Natl Acad Sci U S A, 1994. 91: p. 5022-26.
533. Hubbell, E., Liu, W-M., Mei, R. *Robust estimators for expression analysis*. Bioinformatics, 2002. 18: p. 1585-1592.
534. Liu, W.M., Mei, R., Di, X., Ryder, T.B., Hubbell, E., Dee, S., Webster, T.A., Harrington, C.A., Ho, M.H., Baid, J., Smeekens, S.P. *Analysis of high density expression microarrays with signed-rank call algorithms*. Bioinformatics, 2002. 18: p. 1593-9.
535. Chetcuti, A., Margan, S., Mann, S., Russell, P., Handelsman, D., Rogers, J., Dong, Q. *Identification of differentially expressed genes in organ-confined prostate cancer by gene expression array*. Prostate, 2001. 47: p. 132-40.
536. Bull, J.H., Ellison, G., Patel, A., Muir, G., Walker, M., Underwood, M., Khan, F., Paskins, L. *Identification of potential diagnostic markers of prostate cancer and prostatic intraepithelial neoplasia using cDNA microarray*. Br J Cancer, 2001. 84: p. 1512-19.
537. Luo, J., Duggan, D.J., Chen, Y., Sauvageot, J., Ewing, C.M., Bittner, M.L., Trent, J.M., Isaacs, W.B. *Human prostate cancer and benign prostatic hyperplasia: molecular dissection by gene expression profiling*. Cancer Res, 2001. 61: p. 4683-8.
538. Luo, J., Dunn, T., Ewing, C., Sauvageot, J., Chen, Y., Trent, J., Isaacs, W. *Gene expression signature of benign prostatic hyperplasia revealed by cDNA microarray analysis*. Prostate, 2002. 51(3): p. 189-200.
539. Dhanasekaran, S.M., Barrette, T.R., Ghosh, D., Shah, R., Varambally, S., Kurachi, K., Pienta, K.J., Rubin, M.A., Chinnaiyan, A.M. *Delineation of prognostic biomarkers in prostate cancer*. Nature, 2001. 412: p. 822-6.
540. Welsh, J.B., Sapinoso, L.M., Su, A.I., Kern, S.G., Wang-Rodriguez, J., Moskaluk, C.A., Frierson, H.F., Hampton, G.M. *Analysis of gene expression identifies candidate markers and pharmacological targets in prostate cancer*. Cancer Res, 2001. 61: p. 5974-8.
541. Brooks, J.D. *Microarray analysis in prostate cancer research*. Curr Opin Urol, 2002. 12: p. 395-99.
542. Singh, D., Febbo, P.G., Ross, K., Jackson, D.G., Manola, J., Ladd, C., Tamayo, P., Renshaw, A.A., D'Amico, A.V., Richie, J.P., Lander, E.S., Loda, M., Kantoff, P.W., Golub, T.R., Sellers, W.R. *Gene expression correlates of clinical prostate cancer behavior*. Cancer Cell, 2002. 1(2): p. 203-9.
543. Pascal, L.E., Deutsch, E.W., Campbell, D.S., Korb, M., True, L.D., Liu, A.Y. *The urologic epithelial stem cell database (UESC) – a web tool for cell type-specific gene expression and immunohistochemistry images of the prostate and bladder*. BMC Urology, 2007. 7: p. 19.
544. Chakrabarti, R., Robles, L.D., Gibson, J., Muroski, M. *Profiling of differential expression of messenger RNA in normal, benign, and metastatic prostate cell lines*. Cancer Genet Cytogenet, 2002. 139(2): p. 115-25.

545. Perez-Iratxeta, C.P., Palidwor, G., Porter, C.J., Sanche, N.A., Huska, M.R., Suomela, B.P., Muro, E.M., Krzyzanowski, P.M., Hughes, E., Campbell, P.A., Rudnicki, M.A., Andrade, M.A. *Study of stem cell function using microarray experiments*. FEBS Letters, 2005. 579: p. 1795-1801.
546. Birnie, R., Bryce, S.D., Roome, C., Dussupt, V., Droop, A., Lang, S.H., Berry, P.A., Hyde, C.F., Lewis, J.L., Stower, M.J., Maitland, N.J., Collins, A.T. *Gene expression profiling of human prostate cancer stem cells reveals a pro-inflammatory phenotype and the importance of extracellular matrix interactions*. Genome Biology, 2008. 9: p. R83.
547. Shepherd, C.J., Rizzo, S., Ledaki, I., Davies, M., Brewer, D., Attard, G., de Bono, J., Hudson, D.L. *Expression profiling of CD133+ and CD133- epithelial cells from human prostate*. Prostate, 2008. 68: p. 1007-1024.
548. Yashiro, Y., Bannai, H., Minowa, T., Yabiku, T., Miyano, S., Osawa, M., Iwama, A., Nakauchi, H. *Transcriptional profiling of hematopoietic stem cells by high-throughput sequencing*. Int J Hematol, 2008. Epub ahead of print.
549. Behbod, F., Xian, W., Shaw, C.A., Hilsenbeck, S.G., Tsimelzon, A., Rosen, J.M. *Transcriptional profiling of mammary gland side population cells*. Stem Cells, 2006. 24(4): p. 1065-1074.
550. Cui, X.Y., Guo, Y.J., Yao, H.R. *[Analysis of microRNA in drug-resistant breast cancer cell line MCF-7/ADR]*. Nan Fang Yi Ke Da Xue Xue Bao, 2008. Epub ahead of print.
551. Huang, D., Gao, Q., Guo, L., Zhang, C., Wei, J., Li, H., Jing, W.J., Han, X., Shi, Y., Shih Hsin, L. *Isolation and Identification of Cancer Stem-like Cells in Esophageal Carcinoma Cell Lines*. Stem Cells Dev, 2008. Epub ahead of print.
552. Mitsutake, N., Iwao, A., Nagai, K., Namba, H., Ohtsuru, A., Saenko, V., Yamashita, S. *Characterization of side population in thyroid cancer cell lines: cancer stem-like cells are enriched partly but not exclusively*. Endocrinology, 2007. 148: p. 1797-803.
553. Chiba, T., Kita, K., Zheng, Y.W., Yokosuka, O., Saisho, H., Iwama, A., Nakauchi, H., Taniguchi, H. *Side population purified from hepatocellular carcinoma cells harbors cancer stem cell-like properties*. Hepatology, 2006. 44(1): p. 240-251.
554. Rose, A., Xu, Y., Chen, Z.X., Fan, Z.B., Stamey, T.A., McNeal, J.E., Caldwell, M., Peehl, D.M. *Comparative gene and protein expression in primary cultures of epithelial cells from benign prostatic hyperplasia and prostate cancer*. Cancer Letters, 2005. 227(2): p. 213-222.
555. Montironi, R., Filho, A.L., Santinelli, A., Mazzucchelli, R., Pomante, R., Colanzi, P., Scarpelli, M. *Nuclear changes in the normal-looking columnar epithelium adjacent to and distant from prostatic intraepithelial neoplasia and prostate cancer. Morphometric analysis in whole-mount sections*. Virchows Arch, 2000. 437(6): p. 625-34.
556. Masters, J.R., Kane, C., Yamamoto, H., Ahmed, A. *Prostate cancer stem cell therapy: hype or hope?* Prostate Cancer and Prostatic Diseases, 2008.
557. Kaighn, M.E., Narayan, K.S., Ohnuki, Y., Lechner, J.F., Jones, L.W. *Establishment and characterization of a human prostatic carcinoma cell line (PC-3)*. Invest Urol, 1979. 17: p. 16-23.

558. Martin, G.R., Evans, M.J. *Differentiation of clonal lines of teratocarcinoma cells: formation of embryoid bodies in vitro*. Proc Natl Acad Sci U S A, 1975. 72: p. 1441-5.
559. Martin, G.R., Wiley, L.M., Damjanov, I. *The development of cystic embryoid bodies in vitro from clonal teratocarcinoma stem cells*. Dev Biol, 1977. 61: p. 230-44.
560. Brady, G., Barbara, M., Iscove, N.N. *Representative in vitro cDNA amplification from individual hemopoietic cells and colonies*. Meth Mol Cell Biol, 1990. 2: p. 17-25.
561. Iscove, N.N., Barbara, M., Gu, M., Gibson, M., Modi, C., Winegarden, N. *Representation is faithfully preserved in global cDNA amplified exponentially from sub-picogram quantities of mRNA*. Nat Biotechnol, 2002. 20: p. 940-943.
562. Gentleman, R.C., Carey, V.J., Bates, D.M., Bolstad, B., Dettling, M., Dudoit, S., Ellis, B., Gautier, L., Ge, Y., Gentry, J. et al. *Bioconductor: open software development for computational biology and bioinformatics*. Genome Biol, 2004. 5: p. R80.
563. Wilson, C.L., Miller, C.J. *Simpleaffy: a BioConductor package for Affymetrix Quality Control and data analysis*. Bioinformatics, 2005. 21: p. 3683-5.
564. Liu, W.M., Mei, R., Di, X., Ryder, T.B., Hubbell, E., Dee, S., Webster, T.A., Harrington, C.A., Ho, M.H., Baid, J. et al. *Analysis of high density expression microarrays with signed-rank call algorithms*. Bioinformatics, 2002. 18: p. 1593-9.
565. Schroeder, A., Mueller, O., Stocker, S., Salowsky, R., Leiber, M., Gassmann, M., Lightfoot, S., Menzel, W., Granzow, M., Ragg, T. *The RIN: an RNA integrity number for assigning integrity values to RNA measurements*. BMC Molecular Biology, 2006. 7: p. 3.
566. Smyth, G.K. *Linear models and empirical bayes methods for assessing differential expression in microarray experiments*. Stat Appl Genet Mol Biol, 2004. 3: p. Article 3.
567. Smyth, G.K. *Limma: linear models for microarray data*. Bioinformatics and Computational Biology Solutions using R and Bioconductor, ed. R. Gentleman, et al. 2005, New York: Springer.
568. Keselman, H.J., Cribbie, R., Holland, B. *Controlling the rate of Type I error over a large set of statistical tests*. Br J Math Stat Psychol., 2002. 55: p. 27-39.
569. Benjamini, Y., Hochberg, Y. *Controlling the false discovery rate: a practical and powerful approach to multiple testing*. J. R. Stat. Soc., 1995. 57: p. 289-300.
570. Benjamini, Y., Hochberg, Y. *On the adaptive control of the false discovery rate in multiple testing with independent statistics*. J. Edu. Behav. Stat., 2000. 25: p. 60-83.
571. Weissman, I.L. *Stem cells: units of development, units of regeneration, and units in evolution*. Cell, 2000. 100(1): p. 157-68.
572. Hadnagy, A., Gaboury, L., Beaulieu, R., Balicki, D. *SP analysis may be used to identify cancer stem cell populations*. Exp Cell Res, 2006. 312: p. 3701-10.
573. Fuchs, E., Segre, J.A. *Stem cells: a new lease on life*. Cell, 2000. 100(1): p. 143-55.

574. Smalley, M.J., Clarke, R.B. *The mammary gland "side population": a putative stem/progenitor cell marker?* J Mammary Gland Biol Neoplasia, 2005. 10: p. 37-47.
575. Inowa, T., Hishikawa, K., Takeuchi, T., Kitamura, T., Fujita, T. *Isolation and potential existence of side population cells in adult human kidney.* International Journal of Urology, 2008. 15: p. 272-275.
576. Oates, J.E., Grey, B.R., Samuel, J.D., Addla, S.K., Brown, M.D., Clarke, N.W. *Hoechst 33342 stem cell identification is a conserved and unified mechanism in urological cancers.* BJUI, 2007. 99 Suppl 4: p. 2-15.
577. Benchaouir, R., Rameau, P., Decraene, C., Dreyfus, P., Israeli, D., Pietu, G., Danos, O., Garcia, L. *Evidence for a resident subset of cells with SP phenotype in the C2C12 myogenic line: a tool to explore muscle stem cell biology.* Experimental Cell Research, 2004. 294(1): p. 254-268.
578. Affymetrix. *GeneChip® Expression Analysis - Data Analysis Fundamentals.* 2008.
579. Camargo, F.D., Chambers, S.M., Drew, E., McNagny, K.M., Goodell, M.A. *Hematopoietic stem cells do not engraft with absolute efficiencies.* Blood, 2006. 107: p. 501-7.
580. Parmar, K., Sauk-Schubert, C., Burdick, D., Handley, M., Mauch, P. *Sca(+)/CD34(-) murine side population cells are highly enriched for primitive stem cells.* Experimental Hematology, 2003. 31(3): p. 244-250.
581. NuGEN. *A study of WT-Ovation™ Amplification Performance.* 2006.
582. Wick, N., Saharinen, P., Saharinen, J., Gurnhofer, E., Steiner, C.W., Raab, I., Stokic, D., Giovanoli, P., Buchsbaum, S., Burchard, A., Thurner, S., Alitalo, K., Kerjaschki, D. *Transcriptomal comparison of human dermal lymphatic endothelial cells ex vivo and in vitro.* Physiol Genomics, 2007. 28: p. 179-92.
583. De Minicis, S., Seki, E., Uchinami, H., Kluwe, J., Zhang, Y., Brenner, D.A., Schwabe, R.F. *Gene expression profiles during hepatic stellate cell activation in culture and in vivo.* Gastroenterology, 2007. 132: p. 1937-46.
584. Ginsberg, S.D. *RNA amplification strategies for small sample populations.* Methods, 2005. 37: p. 229-37.
585. Barker, C.S., Griffin, C., Dolganov, G.M., Hanspers, K., Yang, J.Y., Erle, D.J. *Increased DNA microarray hybridization specificity using sscDNA targets.* BMC Genomics, 2005. 6: p. 57.
586. Wilson, C.L., Pepper, S.D., Hey, Y., Miller, C.J. *Amplification protocols introduce systematic but reproducible errors into gene expression studies.* Biotechniques, 2004. 36: p. 498-506.
587. Linton, K.M., Hey, Y., Saunders, E., Jeziorska, M., Denton, J., Wilson, C.L., Swindell, R., Dibben, S., Miller, C.J., Pepper, S.D., Radford, J.A., Freemont, A.J. *Acquisition of biologically relevant gene expression data by Affymetrix microarray analysis of archival formalin-fixed paraffin-embedded tumours.* Br J Cancer, 2008. 98: p. 1403-14.
588. Dontu, G., Liu, S.L., Wicha, M.S. *Stem cells in mammary development and carcinogenesis - Implications for prevention and treatment.* Stem Cell Reviews, 2005. 1(3): p. 207-213.

589. Morrison, S.J., Wandycz, A.M., Hemmati, H.D., Wright, D.E., Weissman, I.L. *Identification of a lineage of multipotent hematopoietic progenitors*. Development, 1997. 124: p. 1929-1939.
590. Morrison, S.J., Weissman, I.L. *The long-term repopulating subset of hematopoietic stem cells is deterministic and isolatable by phenotype*. Immunity, 1994. 1: p. 661-673.
591. van Leenders, G.J., Schalken, J.A. *Stem cell differentiation within the human prostate epithelium: implications for prostate carcinogenesis*. BJU Int, 2001. 88 Suppl 2: p. 35-42; discussion 49-50.
592. Shmelkov, S.V., Butler, J.M., Hooper, A.T., Hormigo, A., Kushner, J., Milde, T., St.Clair, R., Baljevic, M., White, I., Jin, D.K., Chadburn, A., Murphy, A.J., Valenzuela, D.M., Gale, N.W., Thurston, G., Yancopoulos, G.D., D'Angelica, M., Kemeny, N., Lyden, D., Rafii, S. *CD133 expression is not restricted to stem cells, and both CD133+ and CD133- metastatic colon cancer cells initiate tumors*. J Clin Invest, 2008. [Epub ahead of print] doi:10.1172/JCI34401.
593. Oates, J.E., Grey, B.R., Addla, S., Swann, R., Hart, C.A., Brown, M.D., Clarke, N.W. *CD133 is a marker for early proliferative cells but not cancer stem-cells in Renal Cell carcinoma*. BJU Int, 2008. 101(Suppl 5): p. 43.

